MODELING AND MANAGEMENT OF WATER QUANTITY AND QUALITY IN COLD-CLIMATE PRAIRIE WATERSHEDS

A Thesis Submitted to the College of

Graduate Studies and Research

In Partial Fulfillment of the Requirements

For the Degree of Doctor of Philosophy

In the

Department of Civil and Geological Engineering

University of Saskatchewan

Saskatoon

By

Balew A. Mekonnen

PERMISSION TO USE

In presenting this thesis in partial fulfilment of the requirements for a Postgraduate degree from the University of Saskatchewan, I agree that the Libraries of this University may make it freely available for inspection. I further agree that permission for copying of this thesis in any manner, in whole or in part, for scholarly purposes may be granted by my supervisors, and in their absence, by the Head of the Civil and Geological Engineering Department or the Dean of the College of Engineering. It is understood that any copying or publication or use of this thesis or parts thereof for financial gain shall not be allowed without my written permission. It is also understood that due recognition shall be given to me and to the University of Saskatchewan in any scholarly use which may be made of any material in this thesis.

Requests for permission to copy or to make other use of material in this thesis in whole or part should be addressed to:

Head of the Department of Civil and Geological Engineering
University of Saskatchewan
Saskatoon, Saskatchewan
Canada, S7N 5A9

ABSTRACT

Saskatchewan's surface and ground water sources are vital to life in the province, not only as the supply of safe drinking water for the residents, but also as a key driver of economic activity. The Qu'Appelle and Assiniboine River Basins are among the highly valued water resources in the province as they supply water for more than one-third of the population of Saskatchewan and contain a chain of eight lakes that are major recreational and economically valued resources in the region. The health of several watersheds within these highly valued river basins is being degraded by intensive agricultural and other developmental activities. The decision making processes for sustainable water management in these watersheds is stunted by limited observed field data. As a result, for Saskatchewan watersheds in general, and the Qu'Appelle and Assiniboine River Basins in particular, a better understanding is required of the type, extent and sources of pollutant loadings, and effects of potential alternative management practices may have to mitigate water quality problems.

Modeling approaches that have the capacity to analyze the quantity and quality of water resources, identify existing and potential watershed stressors, and quantify the relative importance of best management options are therefore needed. With the intention of helping decision makers in the province, this thesis focuses on developing an eco-hydrological model, which is suitable for Canadian prairie watersheds and capable of simulating the long term effects of land management practices. Following a review of several models, the Soil and Water Assessment Tool (SWAT) has been selected for this study.

In order to achieve the objectives, the SWAT model has been modified to suit site specific characteristics of the Canadian prairies. The first such modification was to incorporate the numerous landscape depressions that vary in storage capacity into SWAT. This was done by

representing depression storage heterogeneity using a probability distribution using an algorithm called “Probability Distributed Landscape Depressions (PDLD)”. The modified model, called SWAT-PDLD, was tested over two prairie watersheds: the Assiniboine and Moose Jaw watersheds. An improved simulation for streamflow was achieved for both case study watersheds as compared to the original SWAT lumped storage approach.

The other modification to SWAT was the incorporation of seasonally varying soil erodibility due to the cold climate conditions. This was done using a sediment module with a time variant soil erodibility factor that allows the value of soil erodibility to vary between seasons. The modified SWAT-PDLD along with seasonally varying soil erodibility was tested for sediment export simulation for the same two case study watersheds: the Assiniboine and Moose Jaw watersheds. Results show an improved sediment simulation for both case study watersheds when seasonally varying soil erodibility factors are considered as compared to the original SWAT model sediment module, which uses annual values of soil erodibility. The modified model was also used to simulate phosphorous and nitrogen export from the Assiniboine watershed and a satisfactory model performance was obtained.

In addition, the developed model was used to assess the impacts of three different management practices on the export of pollutants for the Assiniboine watershed. The scenarios considered were conservation tillage, a cover crop, and filter strips. Model results show that both the filter strips and cover crops decreased sediment, phosphorous, and nitrogen export, while conservation tillage increased phosphorous export in the study watershed.

Finally, the study investigated the different sources of modeling uncertainty for the developed model. Parameter as well as precipitation, observed discharge, and model structure uncertainty of the SWAT-PDLD model was evaluated. Parameter uncertainty was quantified

using three different techniques that include GLUE, ParaSol, and SUFI-2. Model structure uncertainty was assessed using a framework that combines the Bayesian Model Averaging (BMA) and Shuffled Complex Evolution (SCE). Results suggest that ignoring either input error or model structure uncertainty will lead to unrealistic model simulations and incorrect uncertainty bounds. The study also shows that prediction uncertainty bounds, posterior parameter distribution, and final parameter values vary between methods.

ACKNOWLEDGMENTS

My ultimate gratitude goes to my supervisors, Dr. Kerry Anne Mazurek and Dr. Gordon Putz, for giving me the opportunity to pursue my dream in watershed modeling. Their invaluable guidance has been epic in helping me grow as a student and an independent researcher. Throughout the course of this dissertation, Drs. Mazurek and Putz challenged me to be better, supported me to move forward, and encouraged me to strive for excellence. Their critical appraisal and suggestions have been priceless at every stage of this research. It is simply impossible to thank Drs. Mazurek and Putz enough for their countless insight, tremendous encouragement, and boundless patience. I would like to extend my acknowledgement to my advisory committee members Dr. Doug Milne, Dr. Howard Wheater, Dr. Jim Kells, and Dr. Warren Helgason for their valuable suggestions and feedback. Their input impacted my academic growth in numerous ways. I would take this opportunity to thank all past and present members of hydraulics lab for being friendly and positively touching my life in so many ways. Particularly, I thank Dale Pavier for showing me the way to hydraulics lab and helping me in many ways.

I want to take this opportunity to thank Lemlem and her family, Dr. Paulos and his family, Dr. Samson and his family, Dr. Nigatu and Azeb, for making my stay in Saskatoon happy and feeling home.

My special thanks goes to my parents, my wife, my daughter, my sisters, and my little brother for your special support, encouragements, and making me feel important. I would like to thank my Mother-In-Law, Ayehush, as she has been the person who has been there for us on all the most important days of our lives.

TABLE OF CONTENTS

LIST OF TABLES

LIST OF FIGURES

LIST OF ABBREVIATIONS

AAFC	Agriculture and Agri-Food Canada
AGNPS	Agricultural Nonpoint Source Pollution Model
AGWA	Automated Geospatial Watershed Assessment
ANN	Artificial Neural Network
AnnAGNPS	Agricultural Non-Point Source Pollution Model
ARS	Agricultural Research Service
BMA	Bayesian Model Averaging
BMP	Best Management Practice
CAEDYM	Computational Aquatic Ecosystem Dynamics Model
CDED	Canadian Digital Elevation Data
CHRM	Cold Regions Hydrological Model
CH3D-IMS	Curvilinear-grid Hydrodynamics 3D-Integrated Modeling System
CH3D-SED	Curvilinear Hydrodynamics 3D-Sediment Transport
CLASS	Canadian Land Surface Scheme
CMAS	Circular Map Accuracy Standard
CN	Curve Number
DIAS/IDLMAS	Dynamic Information Architecture System/Integrated Dynamic Landscape Analysis and Modeling System
DEM	Digital Elevation Model
DWSM	Dynamic Watershed Simulation Model
ECOMSED	Estuary and Coastal Ocean Model with Sediment Transport
EFDC	Environmental Fluid Dynamics Code
EM	Expectation Maximization
EPA	Environmental Protection Agency
EPIC	Erosion Productivity Impact Calculator
ESRI	Environmental Systems Research Institute
GLUE	Generalized Likelihood Uncertainty Estimation
HRU	Hydrologic Response Unit
HSPF	Hydrological Simulation Program Fortran

HYDAT	Hydrometric Database
GCDC	Gridded Climate Dataset for Canada
GIS	Geographic Information System
GISPLM	GIS-Based Phosphorus Loading Model
GLEAMS	Groundwater Loading Effects of Agricultural Management Systems
GLLVHT	Generalized, Longitudinal-Lateral-Vertical Hydrodynamic and Transport
GSSHA	Gridded Surface Subsurface Hydrologic Analysis
GWLF	Generalized Watershed Loading Functions
HEC-6	Scour and Deposition in Rivers and Reservoirs
HEC-6T	Sedimentation in Stream Networks
HEC-HMS	Hydraulic Engineering Center-Hydrologic Modeling System
HEC-RAS	Hydrologic Engineering Center-River Analysis System
HSCTM-2D	Hydrodynamic, Sediment, and Contaminant Transport Model
HSPF	Hydrologic Simulation Program—FORTRAN
HRU	Hydrologic Response Unit
KINEROS2	Kinematic Runoff and Erosion Model, v2
LH-OAT	Latin Hypercube Sampling-One Factor at a Time method
LSPC	Loading Simulation Program in C++
MCM	Mercury Cycling Model
MESH	Modélisation Environmentale Communautaire – Surface and Hydrology
MUSIC	Model for Urban Stormwater Improvement Conceptualization
MUSLE	Modified Universal Soil Loss Equation
NSE	Nash and Sutcliffe Efficiency
NSERC	Natural Sciences and Engineering Research Council of Canada
NTDB	National Topographic Database
NTS	National Topographic System
P8-UCM	Program for Predicting Polluting Particle Passage through Pits, Puddles, and Ponds–Urban Catchment Model
ParaSol	Parameter Solution
PBIAS	Percent Bias
PCSWMM	Stormwater Management Model

PDLD	Probability Distributed Landscape Depressions
PFRA	Prairie Farm Rehabilitation Administration
PGC – BMP	Prince George's County Best Management Practice Module
PPR	Prairie Pothole Region
QUAL2E	Enhanced Stream Water Quality Model
REMM	Riparian Ecosystem Management Model
RMSE	Root Mean Square Error
RUSLEFAC	Revised Universal Soil Loss Equation Application in Canada
SCS	Soil Conservation Service
SCE-UA	Shuffled Complex Evolution-Uncertainty Analysis
SED3D	Three-Dimensional Numerical Model of Hydrodynamics and Sediment Transport in Lakes and Estuaries
SLAMM	Source Loading and Management Model
SLC	Soil Landscapes of Canada
SLURP	Simple Lumped Reservoir Parametric
SPARROW	SPAtially Referenced Regression On Watershed Attributes
SSE	Sum of Squared Errors
STDEV	Standard Deviation
STORM	Storage, Treatment, Overflow, Runoff Model
SUFI	Sequential Uncertainty FItting
SWAT	Soil and Water Assessment Tool
SWA	Saskatchewan Watershed Authority
SWMM	Storm Water Management Model
THREATS	The Healthy River Ecosystem AssessmenT System
US	United States
USGS	United States Geological Survey
USLE	Universal Soil Loss Equation
USDA	United States Department of Agriculture
USEPA	United States Environmental Protection Agency
VIC	Variable Infiltration Capacity
WAMView	Watershed Assessment Model with an ArcView Interface

WARMF	Watershed Analysis Risk Management Framework
WASP	Water Quality Analysis Simulation Program
WEB	Watershed Evaluation of Best Management Practices
WEPP	Water Erosion Prediction Project
WinHSPF	Interactive Windows Interface to HSPF
WMS	Watershed Modeling System
XP-SWMM	Stormwater and Wastewater Management Model

CHAPTER 1 INTRODUCTION

1.1 Background

Agriculture is the root of Saskatchewan's economy and accounts for over one-third of the province's total exports. The province is the leading producer and exporter of several crops in the world. In fact, over 40 percent of Canada's farmland totaling more than 60 million acres is found in the Province of Saskatchewan of which approximately 33 million acres of agricultural land is used for crop production each year (Government of Saskatchewan 2015). As agriculture is the dominant economic force in the province, a massive change of land use to cultivation has occurred in the region since the time of the European settlement (Crumpton and Goldsborough 1998). According to Statistics Canada (2011), the amount of fertilized land in the province has increased by nearly 400% between 1971 and 2006. There are also ongoing plans to further increase agricultural activity in the region (Saskatchewan Ministry of Agriculture 2013).

However, ongoing intensive agricultural activities together with other resource development activities are causing environmental problems in Saskatchewan. Past incidents of frequent fish kills in the Qu'Appelle River Basin are indicators of degraded water quality in the region (Allan et al. 1980; Hall et al. 1999; Qu'Appelle Basin Study Board. 1972). Such local effects are observed throughout several watersheds within the province (Dube et al. 2011). The 2010 Saskatchewan Watershed Authority's (SWA) State of the Watershed Report (Davies and Hanley 2010) revealed that the health of several watersheds in the Province were impacted. According to this report, the health of four out of twenty-nine watersheds that were assessed were environmentally impacted, while majority of the remaining watersheds were stressed and only few were healthy (Davies and Hanley 2010). According to SWA, a watershed is impacted if

it has shown a degradation or change in the function and services it provides. Among the impacted watersheds were the Moose Jaw River, Wascana Creek, Quill Lakes, and Assiniboine River.

The main stressors for these impacted watersheds are nutrient loadings (Davies and Hanley 2010). Nutrients are naturally derived from weathering and leaching from rocks and soils (Whitehead 2006). However, inputs of nutrients to aquatic ecosystems can be significantly enhanced by human activities, resulting in nutrient enrichment (Chambers et al. 2001; Withers and Lord 2002; Smith and Schindler 2009). The enrichment of bodies of fresh water by inorganic plant nutrients (such as nitrate and phosphate) is called eutrophication (Lawrence and Jackson, 1998). Eutrophication can cause an increase in the abundance of algae and aquatic plants in the receiving water bodies (Smith et al. 1999; Withers and Lord 2002; Smith and Schindler 2009). The environmental consequences of eutrophication are more serious than nuisance increases in plant growth alone (Smith et al. 1999; Chambers et al. 2001). This is because eutrophication of receiving water bodies can result in decreased species diversity and dominant biota changes, increased plant and animal biomass, increased turbidity, increased rate of sedimentation, anoxic conditions, higher treatment costs for drinking water, a health risk for humans, and losses of the services that these systems provide (USEPA 1996; Chambers et al. 2001; Armstrong 2002; Whitehead 2006).

Nutrient sources can be broadly classified as originating from either point or non-point sources, with the relative contribution of each varying between river basins (Ongley 1996). Unlike for point sources (such as sewage effluents), non-point source loadings (such as the run-off from agricultural land) come from diffuse sources and therefore do not have discrete identifiable input locations (Novotny 2003). In Saskatchewan watersheds, the major sources of

nutrients are attributed to agricultural inputs (such as fertilizer, manure, and pesticides), wetland loss, and soil erosion (Davies and Hanley 2010).

Phosphorus and nitrogen are nutrients that are commonly measured in water quality and of most concern because of their primary role as food for phytoplankton (algae) and aquatic plants in water bodies (Novotny and Olem 1994; Withers and Lords 2002; Whitehead 2006). For both phosphorous and nitrogen, inputs to fresh waters in Canadian prairies come principally from diffuse sources (particularly agriculture), while point sources (usually urban wastewater) contribute only a small amount (Chambers et al. 2001). For instance, point source contributions of phosphorous and nitrogen in the Assiniboine watershed are only about 1.9 and 2.1 % respectively to the overall nutrient load (Armstrong 2002). Both phosphorous and nitrogen occur in both dissolved and particulate forms and can be exported to receiving water bodies either in surface or subsurface flows (Withers and Lords 2002; Novotny 2003). Surface loads include dissolved nitrogen and phosphorous in overland runoff or nutrients absorbed to particulates resulting from sediment erosion, while the subsurface loads occur from dissolved nitrogen and phosphorous in groundwater (Heathwaite et al. 2000; Withers and Lords 2002).

In the past, there have been some strategies in place to improve water quality degradation in the province. These control measures were often directed at point source pollution. For instance, the city of Moose Jaw diverted all of its sewage to agricultural land in 1987 (Hall et al. 1999). However, the diversion of sewage to agricultural land did not show a significant improvement of water quality except for the decrease in total phosphorous load (Hall et al. 1999). This was likely due to the fact that the source of pollution is not from a single point source, as such a sewage system but rather from multiple sources in the catchment including agricultural runoff, municipal and industrial wastewaters, and seepage from septic systems.

Nutrient loadings into water bodies can be reduced by implementing effective management practices. However, the effectiveness of a management practice needs to be evaluated prior to its implementation. Accurate estimation of the movement of nutrients across a watershed is required in order to evaluate the effectiveness of such a management practice. However, the Province of Saskatchewan in many cases has limited observed data of water quality. In this regard, eco-hydrologic models can be an efficient method for these watersheds as it can provide information that is continuous over time and space about watershed processes with relatively a low cost. Hydrologic models can also be helpful in predicting future scenarios of nutrient loadings to water bodies. Such capability is in particularly important for evaluation of proposed changes in water and or nutrient management before they are implemented.

This study therefore was carried out to adapt, calibrate, and validate an eco-hydrological model for Saskatchewan watersheds to help the decision making processes of water management problems in the province. However, modeling these watersheds is very difficult as these watersheds fall within the Canadian Prairie Pothole Region, in which the runoff generation occurs under the existence of numerous landscape depressions that vary in storage capacity and have dynamic connectivity to one another. This leads to a dynamic contributing area to streamflow, which invalidates the application of conventional hydrological models that require a basin's contributing area to be a fixed value (Shook et al. 2013). In addition, these watersheds exhibit a cold region hydrology (Pomeroy et al. 2007). In this region, hydrological responses (flow and contaminants) are highly affected by the cold-climate conditions such as snow melt and accumulation, runoff over a frozen ground, infiltration into partially or totally frozen soil processes, and frequent freeze-thaw cycles (Granger et al. 1984; Gray and Landine 1988; van Vliet and Hall 1991; McConkey et al. 1997; Han et al. 2010). Furthermore, uncertainty of the

developed model for the study watersheds needs to be quantified in order to assess the reliable of the model.

1.2 Research Objectives

The broad aim of this research is to develop streamflow and pollutants loading modeling framework for dealing with flooding, erosion, water quality, and other water resources related problems under cold-climate prairie watershed conditions. The specific objectives are the following:

1. To develop a streamflow modeling framework for the cold-climate prairie watersheds in Southern Saskatchewan;
2. To develop a sediment export modeling framework for the cold-climate prairie watersheds in Southern Saskatchewan;
3. To further evaluate the developed streamflow and sediment modeling framwork for nutrients export simulation from a cold-climate prairie watershed in Southern Saskatchewan;
4. To apply the developed modeling framework to investigate the effect of changing agricultural management practices on water quality in a cold-climate prairie watershed in Southern Saskatchewan; and
5. To estimate the different sources of uncertainty of the developed model of the study watersheds.

1.3 Scope of the Thesis

This study will use modeling using the existing data to estimate streamflow, sediment, nitrogen, and phosphorous export in the Qu'Appelle and Assiniboine River basins in the Province of Saskatchewan. The scope of this research is confined to selecting a suitable method,

identifying limitations of the selected method for cold-climate prairie watersheds, conceptualization and formulation of new technique to improve identified limitations, incorporation of new conceptualizations into the selected method, testing capability of the modified method in simulating watershed processes (flow, sediment, nitrogen, and phosphorous) for large area cold-climate Canadian prairie watersheds, assessing impacts of agricultural practices on water quality variables, and assessing the major sources of uncertainty of the developed method.

1.4 Content of the Thesis

This thesis is organized with the first, second, and last chapters focusing on the general introduction, literature review, and conclusions, respectively. The remaining four chapters are organized in accordance with the research objectives. After the introduction (Chapter 1), this thesis starts with a literature review (Chapter 2). Chapter 3 addresses the first objective, namely streamflow model development and evaluation. Chapter 4 addresses the second objective that is sediment export simulation model development and evaluation. Chapter 5 addresses the third and fourth objectives that are development and evaluation of nutrient simulation model and scenario analysis, respectively. Chapter 6 address the fifth objective that is investigation the different sources of modeling uncertainty. This is a manuscript style thesis that the contribution of the thesis are documented in four papers.

1.5 References

Allan, R.J., Williams, J.D., Josh, R., and Warwick, W.F. 1980. Historical changes and relationship to internal loading of sediment phosphorus forms in hypertrophic Prairie Lakes. Journal of Environmental Quality, **9**(2): 199–206.

Armstrong, N. 2002. Assiniboine river water quality study nitrogen and phosphorus dynamics May 2001 to May 2002. Water Quality Management Section, Water Branch. Manitoba Conservation, Manitoba Conservation Report No. 2002-10, Manitoba.

Chambers, P.A., Guy, M., Roberts, E., Charlton, M., Kent, R., Gagnon, C., Grove, G., and Foster, N. 2001. Nutrients and their impact on the Canadian environment. Agriculture and Agri-Food Canada, Environment Canada, Fisheries and Oceans Canada, Health Canada and Natural Resources Canada, Technical report, Hull, Quebec, 241p.

Crumpton, W.G., and Goldsborough, L.G. 1998. Nitrogen transformation and fate in prairie wetlands. Great Plains Research, **8**(1): 57–72.

Davies, H., and Hanley, P.T. 2010. 2010 State of the watershed report. Saskatchewan Watershed Authority, Science, Information and Monitoring Stewardship Division, Regina, Saskatchewan, Canada, 39 pp.

Dube, M., Nadorozny, N., and Squires, A. 2011. Development of the Healthy River Ecosystem AssessmenT System (THREATS) for integrated change assessments of water quality in Canadian watersheds. In: Lundqvist J, editor. On the water front: Selections from the 2010 World Water Week in Stockholm. Stockholm, Sweden. Stockholm International Water Institute: p 32–41.

Government of Saskatchewan. 2015. Statistics: Who knew – Agriculture in Saskatchewan. Accessed 20 October 2015, http://www.agriculture.gov.sk.ca/Default.aspx?DN=7b598e42–c53c–485d–b0dd–e15a36e2785b

Granger, R.J., Gray, D.M., and Dyck, G.E. 1984. Snowmelt infiltration to frozen prairie soils. Canadian Journal of Earth Science, **21**(6): 669–677.

Gray, D.M., and Landine, P.G. 1988. An energy–budget snowmelt model for the Canadian Prairies. Canadian Journal of Earth Sciences, **25**(8): 1292–1303.

Hall, R.I., and Leavitt, P.R. 1999. Effects of agriculture, urbanization, and climate on water quality in the northern Great Plains. Limnology and Oceanography, **44**(3–2): 739–756.

Han, C.W., Xu, S.G., Liu, J.W., and Lian, J.J. 2010. Nonpoint–source nitrogen and phosphorous behaviour and modelling in cold-climate: A review. Water Science and Technology, **62**(10): 2277–2285.

Heathwaite, A.L., and Dils, R.M. 2000. Characterising phosphorus loss in surface and subsurface hydrological pathways. Sci Total Environ, 251/252: 523–538.

Lawrence, E., Jackson, A.R.W., and Jackson, J.M. 1998. Eutrophication, in Longman Dictionary of Environmental Science. London, England, Addison Wesley Longman Limited, p. 144-145.

McConkey, B.G., Nicholaichuk, W., Steppuhn, H., and Reimer, C.D. 1997. Sediment yield and seasonal soil erodibility for semiarid cropland in western Canada. Can. J. Soil Sci., **77**(1): 33–40.

Novotny, V. 2003. Basic concepts of diffuse pollution. water quality: diffuse pollution and watershed management. John Wiley & Sons Inc., Hoboken, NJ, 104-133.

Novotny, V. and Olem, H. 1994. Water quality, prevention, identification, and management of diffuse pollution. Van Nostrand Reinhold, New York.

Ongley, E. 1996. Control of water pollution from Agriculture. FOA irrigation and drainage paper 55. Food & Agriculture Organization of United Nations. Rome, Italy.

Pomeroy, J.W., Gray, D.M., Brown, T., Hedstrom, N.M., Quinton, W., Granger, R.J., and Carey, S. 2007. The Cold Regions Hydrological Model (CRHM), a platform for basing process representation and model structure on physical evidence. Hydrological Processes, **21**(19): 2650–2667.

Qu'Appelle Basin Study Board. 1972. Report of the Qu'Appelle basin study board. Technical report, Queen's Printer, Regina, Saskatchewan, Canada.

Saskatchewan Ministry of Agriculture. 2013. Plans and annual reports: Plan for 2014-15, Government of Saskatchewan, Regina, Saskatchewan, Canada.

Smith V.H., and Schindler, D.W. 2009. Eutrophication science: where do we go from here? Trends in Ecology and Evolution, 24**(4)**: 2001-2007.

Smith, V.H., Tilman, G.D., and Nekola, J.C. 2009. Eutrophication: impacts of excess nutrient inputs on freshwater, marine, and terrestrial ecosystems. Environmental Pollution, 100**(1–3)**: 179–196.

Statistics Canada. 2011. Fertilized land area in Canada by ecozone, selected years, 1971 to 2006. Accessed 20 October 2015, http://www.statcan.gc.ca/pub/16-201-x/2009000/t235-eng.htm

US EPA. 1996. Environmental Indicators of Water Quality in the United States (US EPA 841-R-96-02). Office of Water (4503F), US Government Printing office, Washington, D.C.

van Vliet, L.J.P., and Hall, J.W. 1991. Effects of two crop rotations on seasonal runoff and soil loss in the Peace River region. Can. J. Soil Sci., **71**(4): 533–544.

Whitehead, J. 2006. Integrated catchment scale model of a lowland eutrophic lake and river system. PhD Thesis, Cranfield University, Silsoe Institute of Water and Environment, Norfolk, UK.

CHAPTER 2 LITERATURE REVIEW ON MODEL SELECTION

2.1 Introduction

This chapter reviews the literature pertinent to the different approaches to water quality modeling. The review was conducted to establish the current state of knowledge in water quantity and quality modeling approaches, as well as to describe the procedure followed to select the appropriate model for this study. Further, a brief description and detailed background information are given about the selected model.

2.2 Modeling Approaches

Watershed models vary in many ways including the time step, the spatial scale, whether the model simulates single events or on a continuous basis, and how different watershed processes are computed (Pike 1995; Singh 1995; Merritt et al. 2006). They have been classified in numerous ways in the literature (e.g. Clarke 1973; Freeze and Harlan 1969; Wheater et al. 1993; Leavesley 1994; Refsgaard 1996; Chappell 2005; Merritt et al. 2003). In general, watershed modeling approaches fall into two main categories depending on how the physical processes are represented in the model: empirical (or statistical) or process based (or mechanistic) (Riecken et al. 1995; Cherry et al. 2008; Al-Amin et al. 2013). It should be noted that many models have both empirical and mechanistic components, however it is possible to classify most models according to whether the model is based more strongly in either empiricism or theory.

2.2.1 Empirical models

Empirical models, also called black-box models (Willems 2000; Nor et al. 2007), are based primarily on the analysis of observations and try to characterize response from observed

datasets (Singh 1988; Wheater et al. 1993; Merritt et al. 2003). They use mathematical equations derived from concurrent input and output time series and not from the physical processes of the watershed (Singh 1988; Jajarmizadeh et al. 2012; Devi et al. 2015). They are generally the simplest of all model types and have less computational time requirements (Shoemaker et al. 1997; Merritt et al. 2003; Devi et al. 2015). These models are generally based on the assumption of stationarity (i.e., the underlying conditions remain unchanged), which restricts such a model from being applied for predicting the effects of watershed change or to other regions (Leavesley 1994; Shoemaker et al. 1997; Merritt et al. 2003; Devi et al. 2015). In addition, for water quality modeling they require intensive observed nutrient datasets for parameter calibration and pattern identification. For areas with limited water quality data, the potential for success of this modeling approach is limited.

The most commonly used empirical models include regression models (e.g., Osborne and Wiley 1988; Hainly and Kahn 1996; Smith et al. 1997), nutrient budget (e.g., Brouwer 1998; Vagstad et al. 2004; Oenema et al. 2005), and export coefficients (e.g., Johnes 1996; Mattikalli and Richards 1996; Liu et al. 2009). While each of these approaches is capable of estimating the nutrient load in a stream, the ability to estimate the source of the nutrients varies from no consideration of the source to the prediction of non-point source contributions from individual land uses (Cherry et al. 2008).

Recently, the capabilities of empirical modeling have greatly expanded following developments in computational intelligence, in particular in the area of machine learning (Solomatine et al. 2009). Some of the newer techniques include neural networks, fuzzy rule-based systems and genetic algorithms (Solomatine et al. 2009; Devi et al. 2015). The field which

encompasses these new approaches is called data-driven modelling (DDM) (Solomatine et al. 2009; Devi et al. 2015).

2.2.2 Process-based models

Process-based (or mechanistic) watershed models attempt to simulate a complete system and quantify the processes that constitute it, which include the detailed processes representing runoff and pollutant generation and transport (Brinkmann 1985; Cherry et al. 2008; Al-Amin and Abdul-Aziz 2013). Unlike empirical models, mechanistic models attempt to mathematically describe, with varying complexity, the underlying physical and chemical processes in a watershed. Mechanistic models therefore are relatively complex (Min et al. 2011). Because they can have an internal structure that explicitly represents an understanding of underlying causal mechanisms, they are more likely to be successful at predicting changes in a watershed (Min et al. 2011). These models range from conceptual approaches that use simplified depictions of hydrological processes, to more complex physically-based approaches that model the individual hydrological, geological, biological, and chemical processes using the theoretical equations. In reality, however, there is no a fully physically-based model available for use due to lack of knowledge about all process details or a lack of input information to perform a physical and detailed simulation. For instance, the SWAT model, which is among the operational process-based models, can be considered as conceptual or physically based model depending on input data availability. It can be used as a physically-based model if sub-hourly input data is available, in which the Green and Ampt method of runoff prediction method can be implemented. But, the model can be used as a conceptual model if sub-hourly data is not available and it uses the Curve Number method to estimate surface runoff.

Depending on how watershed processes and parameters are spatially represented, mechanistic models can be categorized as either lumped or distributed (Merritt et al. 2003). Lumped models simulate hydrological processes by taking a watershed as a single unit. They use average values to represent various processes over an entire watershed in order to obtain an overall output at the basin outlet (Rosso 1992). These models are based on the assumption of uniform conditions throughout the system (Riecken 1995). Such models generally do not account for the spatial distribution of the following: (1) the input variables such as rainfall; (2) the parameters characterizing physical processes such as hydraulic conductivity; and (3) the output variables such as streamflow (Clarke 1973; Singh 1988; Singh 1995). Examples of such models are the Stanford Watershed Model (SWM) (Crawford and Linsley 1996), the Generalized Watershed Loading Functions (GWLF) (Haith et al. 1992), and Groundwater Loading Effects of Agricultural Management Systems (GLEAMS) (Leonard et al. 1987).

In contrast, distributed models explicitly account for the spatial variability of watershed hydrological processes. Distributed models can be further categorized as semi or fully distributed based on the approach implemented to incorporate spatial heterogeneity. Semi-distributed hydrological models are those models that subdivide the watershed into different sub-watersheds within which lumped calculations are performed. Examples of semi-distributed models are the Soil and Water Assessment Tool (SWAT) model (Arnold et al. 1998), which is based on the identification of similar hydrologic units (Hydrological Response Units (HRUs)), TOPMODEL (Beven and Kirkby 1979), which is based on the conceptual definition of topographic units, and the WATFLOOD model (Kouwen 1988), which is based on grouping similar HRUs called Group Response Units (GRUs). On the other hand, fully distributed models make use of grids or finite-elements to represent spatial heterogeneity where numerical solutions to the governing

physical equations are performed. The SHE (Système Hydrologique Européen) model (Abbot et al. 1986a, 1986b) is an example of a fully distributed model, after which spatial distribution of catchment parameters, rainfall input and hydrological response is achieved in the horizontal through the representation of the catchment by an orthogonal grid network and in the vertical by a column of horizontal layers at each grid square. It uses a 3D groundwater model, a 2D diffusive wave approximation for overland flow, and a 1D full dynamic component for river flow (Abbot et al. 1986b). Other examples of fully distributed models are the Areal Non-Point Source Watershed Environment Response Simulation model ANSWERS (Beasley et al. 1985) and hydrological modeling system MIKE SHE (Graham and Butts 2005). Fully distributed models generally require more information and usually contain more parameters than do lumped models (Singh 1995). They are time-consuming to set up and generation of results need considerable computer resources, which often prevent the realization of fully distributed models for large area watershed applications (Arnold et al. 1998; Jajarmizadeh et al. 2012). Singh (1988) and Arnold et al. (1998) suggested that semi-distributed models are generally able to provide useful results efficiently and economically for water management problems.

2.3 Model Selection Procedure

Considering the range of models increasingly available in the literature, model selection is becoming more difficult (Beven 2012). To choose a model to meet the needs of the current study, the following selection process was used. The procedure consists of four main steps: (1) identification of the selection criteria; (2) preparation of a list of candidate models; (3) evaluation of the candidate models according to the selection criteria; and (4) selection of the model.

2.3.1 Model selection criteria

To meet the objectives of the present study, the following were set as the major requirements that the candidate model should fulfill:

- The model should be able to test different agricultural best management practices (and ideally also be suitable for climate change assessments for future use). Thus, process based models are of prime interest in this research.
- The model should be able to simulate both watershed and instream processes.
- The research sites are located in Canadian prairies that is dominated by agricultural activities. Therefore, the model should be suitable for agricultural areas and be able to address snow processes and issues related to frozen soils.
- The model should be able to simulate generation and transport of flow, sediment, nitrogen, and phosphorous. It would be also advantageous if it had the potential for modeling other water quality parameters.
- The modeling approach must consider both point and non-point sources. Non-point source pollution from agricultural activities is important in the Province of Saskatchewan. Point sources such as sewage are also contributing in the study watersheds.
- The model should be able to perform continuous simulations. Since the aim of the research is to assess long term effects of management practices, it is better to use a continuous simulation rather than event based approaches.
- The model should be able to simulate water management operations. The study watersheds are highly controlled.
- The model should be computationally efficient for large area watersheds as the study watersheds are large.

- The model should be based on readily available input data. Data scarcity is a problem for the study watersheds.
- The model should be in the public domain so that the source code can be freely accessed for potential modifications to suit specific catchment characteristics.
- Preferably, the model should be user friendly and have up to date documentation.

2.3.2 List of candidate models

This review of available models primarily focuses on public domain models though some commercial models are also included if they are published. The review includes models that have been listed by the United States Environmental Protection Agency (USEPA) (Shoemaker et al. 2005), as well as other models that have been applied in the study watersheds. Table 2–1 provides a summary of potential models that have been identified and assessed for this study. The potential models range from simple pollutant loading models to complex fully distributed process-based models. As shown in Table 2-1, a total of 74 different models have been considered and evaluated to be used as a potential model for the current study.

Table 2–1 Summary of available water quality models (adapted from Shoemaker et al. 2005).

Model	Full model name	Source	Watershed processes	In-stream processes	Empirical	Process-based	BMP
AGNPS	Agricultural Non-point Source Pollution Model	USDA-Agricultural Research Service (USDA-ARS)	✓	–	–	✓	✓
AGWA	Automated Geospatial Watershed Assessment	USDA-ARS	✓	–	–	✓	✓
AnnAGNPS	Annualized Agricultural Nonpoint Source Pollution Model	USDA-ARS	✓	–	–	✓	✓
ANSWERS2000	Areal Non-Point Source Watershed Environment Response Simulation-2000	Theo Dillaha – Virgina Tech	✓	✓	–	✓	✓

✓ Supported – Not supported

Table 2–1 Summary of available water quality models (continued).

Model	Full model name	Source	Watershed processes	In-stream processes	Empirical	Process-based	BMP
AQUATOX		USEPA	–	✓	–	✓	–
CAEDYM	Computational Aquatic Ecosystem Dynamics Model	University of Western Australia	–	✓	–	✓	–
CANWET	Canadian ArcView Nutrient and Water Evaluation Tool	Greenland International Consulting Inc.	✓	✓	-	✓	✓
CCHE1D		University of Mississippi	–	✓	–	✓	–
CE-QUAL-ICM/TOXI		US Army Corps of Engineers (USACE)	–	✓	–	✓	–
CE-QUAL-R1		USACE	–	✓	–	✓	–
CE-QUAL-RIV1		USACE	–	✓	–	✓	–
CE-QUAL-W2		USACE	–	✓	–	✓	–
CH3D-IMS	Curvilinear-grid Hydrodynamics 3D— Integrated Modeling System	University of Florida, Department of Civil and Coastal Engineering	–	✓	–	✓	–
CH3D-SED	Curvilinear Hydrodynamics 3D—Sediment Transport	USACE	–	✓	–	✓	–
CHRM	Cold Regions Hydrological Model	U of Saskatchewan, Hydrology	✓	✓	–	✓	✓
DELFT3D	–	WL | Delft Hydraulics	–	✓	–	✓	–
DIAS/IDLMAS	Dynamic Information Architecture System/Integrated Dynamic Landscape Analysis and Modeling System	Argonne National Laboratory	✓	–	–	✓	✓
DRAINMOD		North Carolina State University	✓	–	–	✓	✓
DWSM	Dynamic Watershed Simulation Model	Illinois State Water Survey	✓	✓	–	✓	✓
ECOMSED	Estuary and Coastal Ocean Model with Sediment Transport	HydroQual, Inc.	–	✓	–	–	✓
EFDC	Environmental Fluid Dynamics Code	EPA and Tetra Tech, Inc.	–	✓	–	–	✓
EPIC	Erosion Productivity Impact Calculator	Texas A&M University—Texas Agricultural Experiment Station		–	–	✓	✓
FHWA	Federal Highway Administration Model		✓	–	✓	–	–
GISPLM	GIS-Based Phosphorus Loading Model	College of Charleston, Stone Environmental, and Dr. William Walker (for Vermont DEC)	✓	-	–	✓	✓
GLEAMS	Groundwater Loading Effects of Agricultural Management Systems	USDA-ARS		–	–	✓	✓
GLLVHT	Generalized, Longitudinal-Lateral-Vertical Hydrodynamic and Transport	J.E. Edinger Associates, Inc.	✓	✓	–	✓	–
HEC-6T	Sedimentation in Stream Networks	USACE	–	✓	–	✓	–
HEC-HMS	Hydraulic Engineering Center Hydrologic Modeling System	USACE	✓	–	–	✓	–
HEC-RAS	Hydrologic Engineering Center River Analysis System	USACE	–	–	–	✓	–

✓ Supported – Not supported

Table 2–1 Summary of available water quality models (continued).

Model	Full model name	Source	Watershed processes	In-stream processes	Empirical	Process-based	BMP
HSCTM-2D	Hydrodynamic, Sediment, and Contaminant Transport Model	USEPA	–	✓	–	✓	–
HSPF	Hydrologic Simulation Program—FORTRAN	USEPA	✓	✓	–	✓	✓
KINEROS2	Kinematic Runoff and Erosion Model, v2	USDA-ARS	✓	–	–	✓	✓
LSPC	Loading Simulation Program in C++	EPA and Tetra Tech, Inc.	✓	✓	–	✓	✓
MCM	Mercury Cycling Model	Tetra Tech, Inc		✓	–	✓	–
Mercury Loading Model	Watershed Characterization System—Mercury Loading Model	USEPA	✓	–	–	✓	–
MESH	Modélisation Environmentale Communautaire - Surface and Hydrology	Environment Canada	✓	✓	–	✓	–
MIKE 11		Danish Hydraulic Institute	–	✓	–	✓	–
MIKE 21		Danish Hydraulic Institute	–	✓	–	✓	–
MIKE SHE		Danish Hydraulic Institute	✓	–	–	✓	✓
MINTEQA2	Metal Speciation Equilibrium Model for Surface and Ground Water	USEPA	–	✓	–	✓	–
MUSIC	Model for Urban Stormwater Improvement Conceptualization	Monash University, Cooperative Research Center for Catchment Hydrology	✓	–	–	✓	✓
P8-UCM	Program for Predicting Polluting Particle Passage through Pits, Puddles, and Ponds—Urban Catchment Model	Dr. William Walker	✓	–	–	✓	✓
PCSWMM	Stormwater Management Model	Computational Hydraulics Int.	✓	✓	–	✓	✓
PGC – BMP	Prince George's County Best Management Practice Module	Prince George's County, MD	–	–	–	✓	✓
QUAL2E	Enhanced Stream Water Quality Model	USEPA	–	✓	–	✓	–
QUAL2K	–	Dr. Steven Chapra, EPA TMDL Toolbox	–	✓	–	✓	–
REMM	Riparian Ecosystem Management Model	USDA-ARS	–	–	–	✓	✓
RMA-11		Resource Modelling Associates	–	✓	–	✓	✓
SED2D		USACE	–	✓	–	✓	✓
SED3D	Three-Dimensional Numerical Model of Hydrodynamics and Sediment Transport in Lakes and Estuaries	USEPA	–	✓	–	✓	✓
SHETRAN		University of Newcastle (UK)	✓	✓	–	✓	✓
SLAMM	Source Loading and Management Model	University of Alabama	✓	–	✓	–	–
SLOSS-PHOSPH	Simplified Pollutant Yield Approach	USEPA	✓	–	✓	–	–

✓ Supported – Not supported

Table 2–1 Summary of available water quality models (continued).

Model	Full model name	Source	Watershed processes	In-stream processes	Empirical	Process-based	BMP
SPARROW	SPAtially Referenced Regression On Watershed Attributes	USGS	✓	–	✓	–	–
STORM	Storage, Treatment, Overflow, Runoff Model	USACE (Mainframe version), Dodson & Associates, Inc. (PC version)	✓	–	–	✓	✓
SWAT	Soil and Water Assessment Tool	USDA-ARS	✓	✓	–	✓	✓
SWMM	Storm Water Management Model	USEPA	✓	✓	–	✓	✓
Toolbox	TMDL Modeling Toolbox	USEPA	✓	✓	–	✓	✓
TOPMODEL		Lancaster University (UK), Institute of Environmental and Natural Sciences	✓	–	–	✓	–
USGS Regression Method	US Geological Survey Regression Method	USGS	✓	–	✓	–	–
USEPA Screening Procedures	US Environmental Protection Agency Screening Procedures	USEPA	✓	–	✓	–	–
WAMView	Watershed Assessment Model with an ArcView Interface	Soil and Water Engineering Technology, Inc. (SWET) and EPA	✓	✓	–	✓	✓
WARMF	Watershed Analysis Risk Management Framework	Systech Engineering, Inc.	✓	✓	–	✓	✓
WASP	Water Quality Analysis Simulation Program	USEPA	–	✓	–	✓	–
Watershed	Watershed		✓	–	✓	–	–
WEPP	Water Erosion Prediction Project	USDA-ARS	✓	–	–	✓	✓
WinHSPF	Interactive Windows Interface to HSPF	USEPA	✓	✓	–	✓	✓
WMS	Watershed Modeling System (Version 7.0)	Environmental Modeling Systems, Inc.	✓	✓	–	✓	✓
WMM	Watershed Management Model		✓	–	✓	–	–
XP-SWMM	Stormwater and Wastewater Management Model	XP Software, Inc.	✓	✓	–	✓	✓

✓ Supported – Not supported

2.3.3 Model comparison and selection

From the list of models (Table 2–1), simple methods that include SLAMM, SPARROW, EPA Screening Procedures, USGS Regression Method, SLOSS-PHOSPH, FHWA, and WMM are not suitable for evaluating potential changes in pollutant loadings due to changes in management practices (such as tillage practices, nutrient management, and buffer strips). Furthermore, such methods require intensive measured in-stream water quality data; however,

there is limited data at the study sites. Therefore, these models appear to fail to meet the minimum criteria for this study and therefore were removed from further consideration. In addition, from the list of process-based models considered for the study, P8-UCM, PCSWMM, STORM, SWMM, and XP-SWMM are mainly developed for urban areas. These models are not suitable for agricultural areas, which is the dominant land use in the current study watershed. Therefore, P8-UCM, PCSWMM, STORM, SWMM, and XP-SWMM models also were not considered further as a potential model for this study.

Furthermore, from the list of process-based models considered by the USEPA (Table 2–1), AQUATOX, CEADYM, CCHE1D, CE-QUAL-ICM/TOXI, CE-QUAL-R1, CE-QUAL-RIV1, CE-QUAL-W2, CH3D-IMS, CH3D-SED, DELFT3D, ECOMSED, EFDC, EPIC, GLEAMS, GLLVHT, HEC-6, HEC-6T, HEC-RAS, HSCTM-2D, MCM, MIKE 11, MIKE 21, MINTEQA2, PFC-BMP, QUAL2E, QUAL2K, REMM, RMA-11, SED2D, SED3D, and WASP are mainly developed for receiving water bodies and do not simulate watershed processes. As these models do not simulate watershed processes, they were not considered further as a potential model for this study. In contrast, other models such as AGNPS, AGWA, AnnAGNPS, DIAS/DLMAS, DRAINMOD, GISPLM, GSSHA, GWLF, HEC-HMS, KINEROS2, Mercury Loading Model, MUSIC, SLAMM, TOPOMODEL, and WEPP are able to simulate watershed processes, but they do not simulate in-stream processes. As a result, these models were not considered further.

Both AGNPS and ANSWERS2000 are event-based models (USEPA 1997); thus, they were excluded from the short list since the model needs to perform continuous simulations for long term effects assessments. They are also fully distributed models and hence they are not suitable for large area watershed applications due to longer computational time requirements.

Furthermore, ANSWERS is unable to simulate point source pollution (USPEA 1997) and does not simulate snow pack and snowmelt processes.

Some other models such as DWSM, LSPC, SHETRAN, Toolbox, WARMF, WinHSPF, and WMS do not have a fully developed land management practices module, and in particular, rural land management practices. For instance, DWSM, LSPC, SHETRAN, Toolbox, and WinHSPF were not able to simulate scenarios due to wetlands management while WARMF and WMS were not able to simulate vegetative practices. Irrigation practices and tile drains are among the rural land management practice that are not being simulated by DWSM, LSPC, SHETRAN, Toolbox, WARMF, WinHSPF, and WMS. Therefore, these models were not considered for further evaluation as a potential model for this study.

Both the CHRM and MESH models are used frequently in the Province of Saskatchewan to predict streamflow. However, a water quality component for these models has not yet been fully developed. These models therefore do not simulate all required water quality parameters. In addition, the source code of these models is not available in the public domain. Currently, the MESH model does not include water management practices such as water abstractions for irrigation or other purposes and agricultural management practices (Nazemi and Wheater 2015a, 2015b).

MIKE SHE is commercial software and the source code is not freely available. The model does not have a well-developed management practices module. In addition, MIKE SHE is a fully distributed model and may not be computationally efficient for large area watershed applications. Similarly, WAMView simulates at a sub-daily time step and hence may not be computationally efficient for long term simulation. In addition, it is difficult to get input datasets at a sub-daily time step for the study watersheds.

SWAT and HSPF appear to be similarly suitable models for this study and need to be evaluated further to choose between them. However, HSPF does not simulate rural land management operations such as irrigation practices and tile drains. In addition, HSPF has limitations in simulating some management scenarios, which include detention basin, infiltration practices, vegetative practices, wetlands, and other structural practices. HSPF runs at a sub-daily time step, which may be difficult to do using the input datasets from the study watersheds. Furthermore, HSPF is relatively not user friendly and has no interface for input data preparation (USEPA 1997). On the other hand, SWAT runs on both sub-daily and daily time steps, is suitable for agricultural watersheds, has well developed management scenario modules (including detention basin, infiltration practices, wetlands, other structural practices, etc.), and simulates a wide range of agricultural practices (including irrigation practices, tile drains, nutrient control management, vegetative practices, agricultural conservation practices, etc.). As a result, it appears that the SWAT model is the most suitable model for this particular study.

In general, the SWAT model is among the most widely applied eco-hydrological models throughout the world (Gassman et al. 2007). The wider applicability is driven by the numerous advantages of the SWAT that include its modularity, computational efficiency, ability to predict long-term impacts as a continuous model, ability to use readily available global datasets, multiple geographic information system (GIS) interface tools, other supporting software, online resources of supporting documents, availability of reliable user and developer support, incorporation of a wide range of watershed management practices, simulation of several processes including, but not limited to, sediment, nutrient, pesticide, and bacterial, and open access status of the source code (Gassman et al. 2010).

2.4 Soil and Water Assessment Tool (SWAT)

2.4.1 SWAT model

The Soil and Water Assessment Tool (SWAT) is a continuous watershed simulation model that operates on a daily and sub-daily time step (Gassman et al. 2007). It is a process-based model (Shoemaker et al. 2005), which was developed in the early 1990s by the United States Department of Agriculture- Agricultural Research Service (USDA-ARS) Grassland, Soil and Water Research Laboratory in Temple, Texas (Arnold et al. 1998). The model was developed with the aim of modeling the long term effect of agricultural practices in large un-gauged basins (Arnold et al. 1998). It is an integrated eco-hydrological model that simulates surface runoff, lateral flow, percolation, crop growth, irrigation, groundwater flow, water management, agricultural practices, reach routing, sediment, nutrient, metal, mercury, bacteria, and pesticide loading among other features (Neitsch et al. 2011). The model has undergone continual review and expansion of capabilities since it was created (Gassman et al. 2007; 2010).

2.4.2 SWAT's modeling approach

SWAT models a watershed by sub-dividing it into sub-basins that are further divided into Hydrologic Response Units (HRUs) (Neitsch et al. 2011). Hydrologic Response Units are unique combinations of land use, soil, and slope within a sub-basin. Following watershed discretization and definition of HRUs, SWAT simulates the hydrological processes in two major phases: land and routing phase (Neitsch et al. 2011). In the land phase, a water balance equation is applied at the HRU level for both flow and water quality variables.

In modeling hydrology, surface runoff for each HRU is computed using either the modified curve number method (CN) (USDA Soil Conservation Service 1972) or the Green-Ampt method (Green and Ampt 1911). Potential evapotranspiration for each HRU is estimated

using one of three different methods that include the Penman-Monteith (Monteith 1965), Priestley-Taylor (Priestley and Taylor 1972), and Hargreaves (Hargreaves et al. 1985) approaches. Actual evaporation from soils and transpiration from plants is estimated separately as described by Ritchie (1972). A linear storage of up to ten soil layers can be considered for the percolation component. The rate of percolation is governed by the hydraulic conductivity and available water capacity of each layer. A kinematic storage model is used to simulate the lateral subsurface flow. The shallow aquifer, which is connected to the streamflow, is recharged by percolation from root zone recharges (Arnold et al. 1998).

In modeling sediment, SWAT estimates sediment generation at the HRU level. The sediment yield from surface runoff is estimated using the modified Universal Soil Loss Equation (MUSLE) (Williams 1975). Snow cover may reduce erosive power of rainfall and runoff. Thus, an adjustment for snow cover is incorporated in the algorithm and also additional lag factor is added in the model for sub-basins with time of concentration is greater than one day. SWAT model also calculates the amount of sediment contributed by groundwater and lateral flow. This is estimated as shown in Equation 2.1.

$$SED_L = \frac{(Q_L + Q_{GW}) * A_{HRU} * CON_{SED}}{1000} \qquad (2.1)$$

where SED_L is the sediment loading in the lateral and groundwater flow (metric tons), Q_L is the lateral flow for a given day (mm H2O), Q_{GW} is the groundwater flow for a given day (mm H2O), A_{HRU} is the area of the HRU (km^2) and CON_{SED} is the concentration of sediment in lateral and groundwater flow (mg/L).

In simulating nutrients, SWAT considers several forms of nitrogen and phosphorous, and tracks the movement and transformation of them in the watershed. In the soil, transformation of nitrogen and phosphorous is controlled by the nitrogen and phosphorous cycles (Neitsch et al.

2011). SWAT models nitrogen by conceptualizing the nitrogen cycle in soil as five different pools with two being inorganic (ammonium and nitrate) and three being organic (active, stable, and fresh) (see Figure 2–1) (Neitsch et al. 2011). The model simulates movement between nitrogen pools including mineralization, decomposition/immobilization, nitrification, plant uptake, denitrification, and ammonia volatilization. The model simulates the mass balance of each pool in the soil at the HRU level. As per the current SWAT framework, the nitrogen cycle uses fertilizers, precipitation, and nitrification as its source while it is reduced by denitrification, plant uptake and removal by flow (surface, groundwater and interflow). Details of soil nitrogen processes are described in the model's theoretical documentation (Neitsch et al. 2011). Similarly, the SWAT model represents the phosphorous cycle using six pools (see Figure 2–2). Three of the pools are characterized as mineral phosphorous and the remaining three as organic phosphorus (Neitsch et al. 2011). Transformations of soil phosphorus between the six pools are regulated by mineralization, decomposition, and immobilization. As per the current SWAT framework of the phosphorous cycle, the phosphorous cycle uses fertilizer, manure wastes, wastes, and sludge as its source while it is reduced by plant uptake and removal by flow (surface, groundwater and interflow). Details of soil phosphorous processes are also described in the model's theoretical documentation (Neitsch et al. 2011). Once the output (flow and water quality variables such as sediment, nitrogen and phosphorous) from each HRU is determined, the sub-basin output is calculated as the weighted sum of the output from all HRUs within the sub-basin. The area of the HRU is used as a weighting factor during calculation of the output from the sub-basin as shown in Equation 2.2 below:

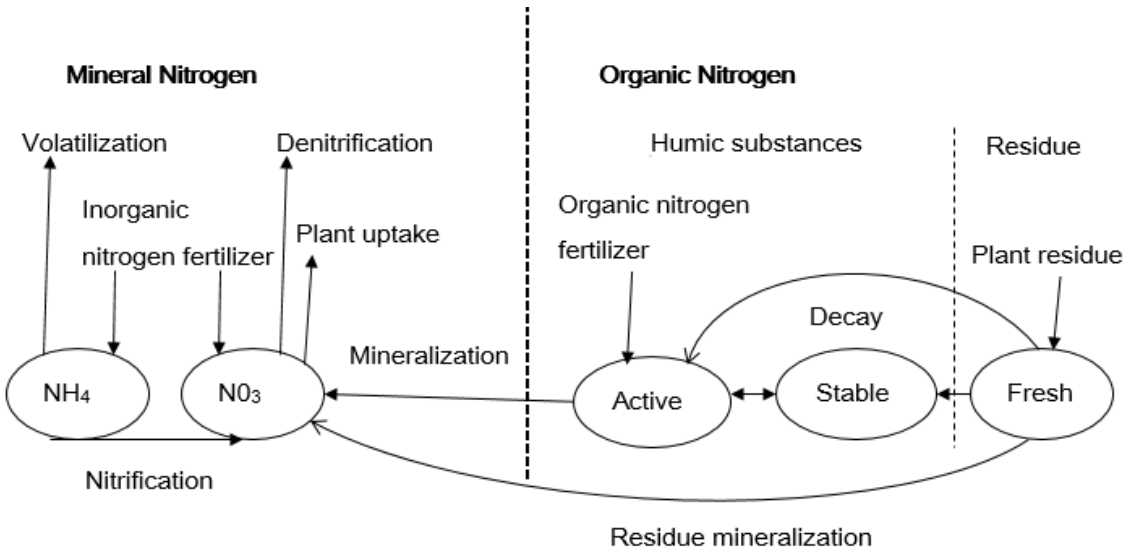

Figure 2– 1 SWAT modeling approach of nitrogen cycle in the soil (Adapted from Neitsch et al. (2011)).

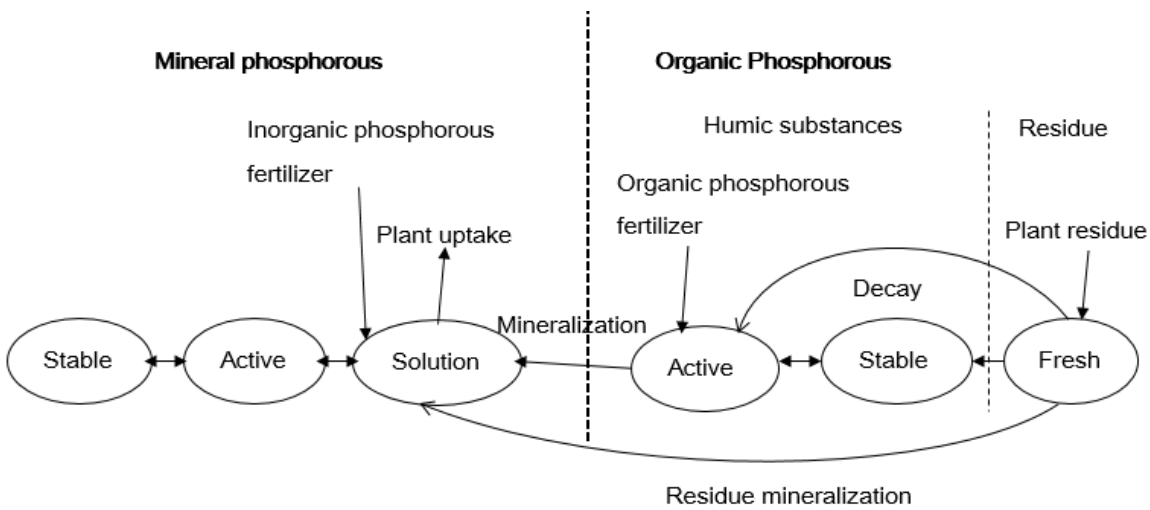

Figure 2– 2 SWAT modeling approach of phosphorous cycle in the soil (Adapted from Neitsch et al. (2011)).

$$out_{sub} = \frac{\sum_{i=1}^{n} out_{HRUi} * Area_{HRUi}}{sub_{area}} \qquad (2.2)$$

where n is the number of $HRUs$ in the sub-basin, out_{HRUi} is the output from $HRUi$, out_{sub} is the output from the sub-basin, $Area_{HRUi}$ is the area of $HRUi$, and sub_{area} is the area of the sub-basin.

Once the yield from each sub-basin is determined, the routing phase continues and controls movement of water, sediment, nutrients and pesticides through the channel and water impoundments (such as wetlands) to the outlet of the watershed. For flow, the routing phase is performed using either the Muskingum (Cunge 1969) or Variable storage (Williams 1969) routing methods. The flow routing approach that controls water flows downstream also considers the following: the water loss due to evaporation and transmission; water utilization for agricultural or human purposes; flow supplemented by the fall of rain directly on the stream and addition of water from point source discharges; and transfer of water to or from other sub-basins or outside of the watershed. For the sediment routing phase, sediment deposition and stream bed degradation are simulated by SWAT. The routing phase of nitrogen and phosphorous is controlled by the QUAL2E algorithm, which includes the in-stream transformations, integration of all contributions of the watershed model to the river, and contribution of point sources (Griensven 2002).

2.4.3 Review of SWAT model applications

The Soil and Water Assessment Tool (SWAT) model (Arnold et al. 1998) has emerged as one of the most widely used water quality watershed models to solve a wide range of problems (Gassman et al. 2007, 2010). The model has been applied throughout the world and a review by Gassman et al. (2010) identified over 600 peer-reviewed journal papers related to the SWAT model.

The SWAT model also has been extensively applied across Canada (e.g. Singh et al. (2005); Liu et al. (2007); Michaud et al. (2007); Watson et al. (2008); Ahmed et al. (2010); Chikhaoui et al. (2010); Levesque et al. (2010); Rahman et al. (2010); Troin and Caya (2013); Fu et al. (2014); Watson and Putz (2014)). More importantly, SWAT model has also been used within the Canadian prairies as well. Shrestha et al. (2012) applied SWAT to estimate future climate change impacts on nitrogen and phosphorous export form the upper Assiniboine watershed in Saskatchewan. Though Shrestha et al. (2012) did not incorporate landscape depressions in the study watershed, they reported a satisfactory model performance of SWAT for streamflow. However, this came at the expense of forcing parameter values outside recommended limits. Conversely, unsatisfactory results have been reported by Chanasyk et al. (2003) while using SWAT for Canadian prairie watersheds. Chanasyk et al. (2003) applied the SWAT model over three small watersheds that varied from 1.5 to 226 ha in Saskatchewan, Canada. They found model performance based upon Nash & Sutcliffe efficiency (NSE) (defined in detail in the next chapter) that ranges from -35.7 to -0.005. The poor NSE values are likely because the version of SWAT model used did not consider runoff over a frozen ground and infiltration into frozen soil. Storage in landscape depressions was also not considered during model development.

With the intention of incorporating storage due to landscape depressions, Wang et al. (2008) developed the hydrologic equivalent wetland concept within SWAT and reported an improved streamflow simulation for prairie watersheds. However, this modeling approach of simulating individual wetlands is not computationally feasible for large area watersheds with numerous landscape depressions. This modified SWAT model was also used by Yang et al. (2008, 2010) to evaluate the water quality and quantity benefits of wetland restoration in

restoration on peak streamflow and sediment export in the Broughton's Creek watershed in south-western Manitoba. SWAT has also been used to model whole watersheds within the Province of Alberta by Abbaspour et al. (2010). They reported poor SWAT model performance at several model calibration sites within the province because of input data limitation about control structures (such as reservoirs) and model structure limitation to handle potholes (Faramarzi et al. 2015).

Furthermore, SWAT is being used by Agriculture and Agri-Food Canada (AAFC) in the Watershed Evaluation of Beneficial Management Practices (WEBs) project. The WEB project was initiated in 2004 with the aim of investigating the economic and environmental performances of BMPs in nine watersheds across Canada (AAFC 2015). SWAT together with other models have been selected as a watershed model for the project to evaluate beneficial land management practices (BMPs) (AAFC 2015). SWAT is used as the primary hydrologic model used alone or in conjunction with other models in most of the WEBS projects, which is seven out of the nine WEBs. The seven watersheds in the WEBs project using SWAT include watersheds in Nova Scotia, New Brunswick, Ontario, British Columbia, Alberta, Manitoba, and the Pipestone Creek watershed in Saskatchewan.

As noted in the Introduction section, the study watersheds fall within the Canadian prairies, where most conventional watershed models such as SWAT have had a limited success in simulating watershed processes. This is mainly because runoff and pollutant generation and transport occurs under the existence of numerous landscape depressions that vary in storage capacity within a watershed. Additionally, there is complex freeze-thaw cycles. Like many other models, the current SWAT model is using a lumped storage module, which aggregates landscape depressions together and represented them by a single synthetic storage, to simulate depressions

storage. Such an approach does not represent the actual processes of depression-dominated watersheds, which contains numerous landscape depressions that vary in storage capacity.

In terms of modeling the cold-climate hydrology of Canadian prairie watersheds, SWAT has been through a continuous modification to include a snow module and this has been successfully applied to simulate streamflow in cold-climate watersheds (e.g., Wang and Melesse 2005; Watson and Putz 2014). This has added simulation of surface runoff over a frozen ground as well as partially or fully frozen soil infiltration in the recent version of SWAT (SWAT2009) (Neitsch et al. 2011). The frozen soil is incorporated by adjusting the curve number for frozen top soil layer and ceasing water movement (percolation and lateral flow) of a frozen soil layer. In SWAT modeling, a soil layer is considered as frozen if its temperature drops below $0^{o}C$ (Neitsch et al. 2011). Despite the progress of SWAT model development for streamflow simulation over cold-climate watersheds, little has been done with SWAT about sediment and nutrient export in cold-climate watersheds (Han et al. 2010). Though several laboratory and field studies reported the significance of cold-climate conditions such as the freeze-thaw cycles on sediment and nutrient mobilization and transport (e.g., Kirby and Mehuys 1987; Coote et al. 1988; Wall et al. 1988; van Vliet and Hall 1991; McConkey et al. 1997; Ferrick and Gatto 2005; Dagesse 2013), conceptualization and incorporation of such processes into SWAT model is not considered for the current version of SWAT model (SWAT2009).

Therefore, the following are two important research questions that need to be considered while developing SWAT model for the study watersheds: (1) how should the current SWAT model version be modified to accommodate heterogeneity in storage capacity of the numerous landscape depressions that exist within a watershed for large area watershed application for the Canadian prairie watersheds? and (2) how should the current SWAT model version be further

modified to consider sediment and nutrient generation processes in cold-climate conditions for large area watershed application for Canadian prairie watersheds?

2.5 References

Abbaspour, K.C., Fararnarzi, M., and Rouholahnejad, E. 2010. Hydrological modeling of Alberta using SWAT model. Alberta Water Research Institute, Calgary, AB.

Abbott, M.B., Bathurst, J.C., Cunge, J.A., O'Connell, P.E., and Rasmussen, J. 1986. An Introduction to the European Hydrological System – Système Hydrologique Européen, SHE, 1: history and philosophy of a physically–based, distributed modelling system. Journal of Hydrology, **87(1–2)**: 45–59.

Agriculture and Agri-Food Canada (AAFC). 2015. Watershed Evaluation of Beneficial Management Practices. Viewed 20 October 2015, http://www.agr.gc.ca/eng/?id=1338479161231

Ahmad, H.M.N. 2010. Modeling hydrology and nitrogen export for the Thomas Brook watershed with SWAT. M.Sc. thesis, Dalhousie University, Halifax, NS.

Al-Amin, S., and Abdul-Aziz, O.I. 2013. Challenges in mechanistic and empirical modelling of stormwater: review and perspectives. Irrigation and Drainage, **62(S2)**: 20–28.

Arnold, J.G., Srinivasan, R., Muttiah, R.S., and Williams, J.R. 1998. Large-area hydrologic modeling and assessment: Part I Model development, Journal of American Water Resources Association, **34(1)**: 73–89.

Beasley, D.B., Huggins, L.F., and Monke E.J. 1980. ANSWERS: A model for watershed planning. Transactions of the ASAE, **234**: 938–944.

Beven, K.J. 2012, Rainfall–runoff modelling: The Primer, 2nd Edition, Wiley–Blackwell, Chichester, UK.

Beven, K.J. and Kirkby, M.J. 1979. A physically based variable contributing area model of basin hydrology. Hydrological Sciences Bulletin, **241**: 43–69.

Booty, W., and Benoy, G. 2009. Multi-criteria review of nonpoint source water quality models for nutrients, sediments, and pathogens. Water Qual. Res. J. Can., **44(4)**: 365–377.

Brinkmann, W.L.F. 1985. Urban stormwater pollutants: sources and loadings. Geo Journal, **11(3)**: 277–283.

Brouwer, F. 1998. Nitrogen balances at farm level as a tool to monitor effects of agri-environmental policy. Nutrient Cycling in Agroecosystems, **52**(2-3): 303–308.

Chanasyk, D.S., Mapfumo, E., Willms, W. 2003. Quantification and simulation of surface runoff from fescue grassland watersheds. Agricultural Water Management, **592**: 137–153.

Chappell, N.A. 2005. Modelling tropical forest watersheds: setting realistic goals. ETFRN News, **45**: 25–28.

Cherry, K. A., Shepherd, M., Withers, P. J. A., and Mooney, S. J. 2008. Assessing the effectiveness of actions to mitigate nutrient loss from agriculture: A review of methods. Science of the Total Environment, **406(1)**: 1–23.

Chikhaoui, M., Gombault, C., Madramootoo, C., Michaud, A., and Beaudin, I. 2010. Assessment of climate change impact on the subsurface drainage flow in the Pike river watershed using the SWAT model. Proceedings, International Drainage Symposium with CIGR and CSBE/SCGAB, ASABE, Québec City, QC.

Clarke, R.T. 1973. A review of some mathematical models used in hydrology, with observations on their calibration and use. Journal of Hydrology, **19(1)**: 1–20.

Coote, D.R, Malcolm–McGovern, C.A., Wall, G.J., Dickinson, W.T., and Rudra, R.P. 1988. Seasonal variation of erodibility indices based on shear strength and aggregate stability in some Ontario soils. Can. J. Soil Sci., **68**: 105–416.

Crawford, N.H., and Linsley, R.K. 1966. Digital simulation in hydrology: Stanford Watershed model IV. Tech. Rep. 39, Stanford Univ., Palo Alto, Calif.

Cunge, J.A. 1969. On the subject of a flood propagation computation method Musklngum method. Journal of Hydraulic Research, **7(2)**: 205–230.

Dagesse, D.F. 2013. Freezing cycle effects on water stability of soil aggregates. Can. J. Soil Sci., **93**: 473–483.

Devi, G.K., Ganasri, B.P. and Dwarakish, G.S. 2015. A review on hydrological models. Aquatic Procedia, 4: 1001–1007.

Faramarzi, M., Srinivasan, R., Iravani, M., Bladon, K.D. Abbaspour, K.C, Zehnder, A.J.B., and Goss, G.G. 2015. Setting up a hydrological model of Alberta: Data discrimination analyses prior to calibration. Environmental Modelling & Software, **74**: 48–65.

Ferrick, M.G., and Gatto, L.W. 2005. Quantifying the effect of a freeze–thaw cycle on soil erosion: laboratory experiments. Earth Surf. Process. Landforms, **30**: 1305–1326.

Freeze, R.A., and Harlan, R.L. 1969. Blueprint for a physically-based, digitally-simulated hydrologic response model. Journal of Hydrology, **9(3)**: 237–258.

Fu, C., James, A.L., and Yao, H. 2014. SWAT-CS: Revision and testing of SWAT for Canadian Shield catchments. Journal of Hydrology, **511**: 719–735.

Gassman, P.W., Reyes, M.R., Green, C.H., and Arnold, J.G. 2007. The soil and water assessment tool: historical development, applications, and future research directions. Trans. ASABE, **50(4)**: 1211–1250.

Gassman, P.W., Arnold, J.G., Srinivasan, R., and Reyes, M. 2010. The worldwide use of the SWAT Model: Technological drivers, networking impacts, and simulation trends, in: Proceedings of the Watershed Technology Conference, 21–24 February, American Society

of Agricultural and Biological Engineers, Earth University, Costa Rica, St. Jospeh, MI, 2010.

Graham, D.N. and Butts, M.B. 2005. Flexible integrated watershed modeling with MIKE SHE. Watershed Models, V.P. Singh and D.K. Frevert, eds., CRC Press, 245–272.

Green, W.H. and Ampt, G.A. 1911. Studies on soil physics, 1. The flow of air and water through soils. Journal of Agricultural Sciences, **4**: 11–24.

Griensven, A.V. 2002. Developments towards integrated water quality modelling for river basins. PhD thesis, Department of Hydrology and Hydraulic Engineering, Vrije Universiteit Brussel, Brussel, Belgium.

Hainly, R.A., and Kahn, J.M. 1996. Factors affecting herbicide yields in the Chesapeake Bay watershed, Water Resour. Bull., **32**: 965–984.

Han, C.W., Xu, S.G., Liu, J.W., and Lian, J.J. 2010. Nonpoint–source nitrogen and phosphorous behaviour and modelling in cold climate: a review. Water Science and Technology, **62(10)**: 2277–2285.

Hargreaves, G.L., Hargreaves, G.H., and Riley, J.P. 1985. Agricultural benefits for Senegal River Basin. Journal of Irrigation and Drainage Engineering, **111(2)**: 113–124.

Haith, D.A., Mandel, R., and Wu, R.S. 1992. GWLF–Generalized Watershed Loading Functions, version 2.0 user's manual. Cornell University, Department of Agricultural Engineering, Ithaca, NY.

Jajarmizadeh, M., Harun, S. and Salarpour, M. 2012. A review on theoretical consideration and types of models in hydrology. Journal of Environmental Science and Technology, **5(5)**: 249–261.

Johnes, Penny J. 1996. Evaluation and management of the impact of land use change on the nitrogen and phosphorus load delivered to surface waters: the export coefficient modelling approach. Journal of Hydrology, **183(3)**: 323–349.

Kirby, P.C., and Mehuys, G.R. 1987. Seasonal variation of soil erodibilities in southwestern Quebec. J. Soil Water Cons., **42**: 2ll–215.

Kouwen, N. 1988. WATFLOOD: A microcomputer–based flow forecasting system based on real–time weather data. Can. Water. Resour. J., **13**: 62–77.

Leavesley, G.H. 1994. Modeling the effects of climate change on water resources-a review. Climatic Change, **28(1-2)**: 159–177.

Leonard, R.A., Knisel, W.G., and Still, D.A. 1987. GLEAMS: Groundwater loading effects of agricultural management systems. Transactions of the American Society of Agricultural Engineers, **30**: 1403–1418.

Levesque, E., Anctil, F., Van Griensven, A.N.N., and Beauchamp, N. 2008. Evaluation of streamflow simulation by SWAT model for two small watersheds under snowmelt and rainfall. Hydrological Sciences Journal, **53(5**): 961–976.

Liu, R.M., Yang, Z.F., Shen, Z.Y., Yu, S.L., Ding, X.W., Wu, X., and Liu, F. 2009. Estimating nonpoint source pollution in the upper Yangtze River using the export coefficient model, remote sensing, and geographical information system. Journal of Hydraulic Engineering, **135(9)**: 698–704.

Liu, Y., Yang, W., and Wang, X. 2007. GIS-based integration of SWAT and REMM for estimating water quality benefits of riparian buffers in agricultural watersheds. Transactions of the ASAE, **50(5)**: 1549–1563.

Mattikalli, N.M. and Richards, K.S. 1996. Estimation of surface water quality changes in response to land use change: application of the export coefficient model using remote sensing and geographical information system. Journal of Environmental Management, **48(3):** 263–282.

McConkey, B.G., Nicholaichuk, W., Steppuhn, H., and Reimer, C.D. 1997. Sediment yield and seasonal soil erodibility for semiarid cropland in western Canada. Can. J. Soil Sci., **77**: 33–40.

Mekonnen, M.A., Wheater, H.S., Iresona, A.M., Spence, C., Davison, B., and Pietroniro, A. 2014. Towards an improved land surface scheme for prairie landscapes. Journal of Hydrology, **511**: 105–116.

Merritt, W.S., Letcher, R.A., and Jakeman, A.J. 2003. A review of erosion and sediment transport models. Environmental Modeling Software, **18**: 761–799.

Michaud, A., Beaudin, I., Deslandes, J., Bonn, F., and Madramootoo, C. 2007. SWATpredicted influence of different landscape and cropping system alterations on phosphorus mobility within the Pike River watershed of south-western Quebec. Canadian Journal of Soil Science, **87(3)**: 329–344.

Min, J.H., Paudel, R. and Jawitz, J.W., 2011. Mechanistic biogeochemical model applications for Everglades restoration: a review of case studies and suggestions for future modeling needs. Critical Reviews in Environmental Science and Technology, **41(S1)**: 489–516.

Monteith, J.L. 1965. Evaporation and the environment. In the state and movement of water in living organisms. 19th Symposia of the Society for Experimental Biology. Cambridge University Press, London, UK, p. 205–234.

Nazemi, A., and Wheater, H.S. 2015a. On inclusion of water resource management in Earth system models–Part 1: Problem definition and representation of water demand. Hydrology and Earth System Sciences, **19(1)**: 33–61.

Nazemi, A., and Wheater, H.S. 2015b. On inclusion of water resource management in Earth system models–Part 2: Representation of water supply and allocation and opportunities for improved modeling. Hydrology and Earth System Sciences, **19(1)**: 63–90.

Neitsch S.L., Arnold, J.G., Kiniry, J.R., and Williams, J.R. 2011. Soil and Water Assessment Tool theoretical documentation: Version 2005, Grassland, Soil and Water Research Laboratory, Blackland Research Center, Temple, TX.

Nor, N.I., Harun, S., and Kassim, A.H. 2007. Radial basis function modeling of hourly streamflow hydrograph. Journal of Hydrologic Engineering, **12(1)**: 113–123.

Oenema, O., van Liere, L., and Schoumans, O. 2005. Effects of lowering nitrogen and phosphorus surpluses in agriculture on the quality of groundwater and surface water in the Netherlands. Journal of Hydrology, **304(1)**: 289–301.

Osborne, L.L., and Wiley, M.J. 1988. Empirical relationships between land use/cover and stream water quality in an agricultural watershed, J. Environ. Manage., **26**: 9–27.

Pike, R.G. 1995. Current limitations of hydrologic modeling in B.C.: An Examination of the HSPF, TOPMODEL, UBCWM and DHSVM Hydrologic Simulation Models, B.C. Data Resources and Hydrologic-Wildfire Impact Modeling. MSc Thesis, Department of Geography, University of Victoria, BC, Canada.

Priestley, C.H.B., and Taylor, R.J. 1972. On the assessment of surface heat flux and evaporation using large–scale parameters. Monthly Weather Review, **100**: 81–92.

Rahman, M., Bolisetti, T., and Balachandar, R. 2010. Effect of climate change on low-flow conditions in the Ruscom river watershed, Ontario. Transaction of the American Society of Agricultural and Biological Engineers, **52(3)**: 1521–1532.

Refsgaard, JC. 1996. Terminology, modelling protocol and classification of hydrological model codes. In: Distributed Hydrological Modelling. Eds. Abbott, M. B., and Refsgaard, J. C. Kluwer Academic Publishers, Netherlands. **2**: 17–40.

Riecken, S. 1995. A compendium of water quality models. British Columbia Environment, Water Quality Branch, Government of British Columbia, BC.

Ritchie, J.T. 1972. A model for predicting evaporation from a row crop with incomplete cover. Water Resources Research, **8**: 1204–1213.

Rosso, R. 1992. An introduction to spatially distributed modeling of basin response. p.3-30. In Advances in Distributed Hydrology. Rosso, R., Peano, A., Becchi, I., and Bemporad, G. (eds.). Water Resources Publications, Colorado.

Shoemaker, L., Lahlou, M., and Bryer, M. 1997. Compendium of tools for watershed assessment and TMDL development. Watershed Branch, Assessment and Watershed Protection Division, Office of Wetlands, Oceans, and Watershed, United States Environmental Protection Agency, Washington, DC.

Shrestha, R.R., Dibike, Y.B., and Prowse, T.D. 2012. Modeling climate change impacts on hydrology and nutrient loading in the upper Assiniboine catchment. J. American Water Resour. Assoc., **48(1)**: 74–89.

Singh, V.P. 1988. Hydrologic Systems, Vol. 1. Rainfall-Runoff Modeling. Prentice Hall, Inc. Englewood Cliffs, New Jersey.

Singh, V.P. 1995. Watershed Modeling - Chapter 1. p.1-21. In computer models of watershed hydrology. V.P. Singh (ed.). Water Resources Publications, Colorado.

Singh, A., Rudra, R., and Yang, W. 2005. Adapting SWAT for riparian wetlands in an Ontario watershed. 3rd International SWAT Conference, Zurich, Switzerland, 123-131.

Smith, R.A., Schwarz, G.E. and Alexander, R.B. 1997. Regional interpretation of water-quality monitoring data, Water Resour. Res., **33**: 2781–2798.

Solomatine, D., See, L.M. and Abrahart, R.J. 2009. Data-driven modelling: concepts, approaches and experiences. In Practical hydroinformatics (pp. 17-30). Springer Berlin Heidelberg.

Tiessen, K.H.D., Elliott, J.A., Yarotski, J., Lobb, D.A., Flaten, D.N., and Glozier, N.E. 2010. Conventional and Conservation Tillage: Influence on Seasonal Runoff, Sediment, and Nutrient Losses in the Canadian Prairies. J. Environ. Qual., **39**: 964–980.

Troin, M., and Caya, D. 2013. Evaluating the SWAT's snow hydrology over a Northern Quebec watershed. Hydrological Processes, **28(4)**: 1858–1873.

USDA Soil Conservation Service. 1972. National engineering handbook section 4 hydrology. Chapters 4–10. Washington, DC: U.S. Government Printing Office.

United States Environmental Protection Agency USEPA. 1997. Compendium of tools for watershed assessment and TMDL development. Office of Wetlands, Oceans, and Watersheds, Washington, DC. 244p.

Vagstad, N., Stålnacke, P., Andersen, H.E., Deelstra, J., Jansons, V., Kyllmar, K., Loigu, E., Rekolainen, S., and Tumas, R. 2004. Regional variations in diffuse nitrogen losses from agriculture in the Nordic and Baltic regions. Hydrology and Earth System Sciences Discussions, **8(4)**: 651–662.

van Vliet, L.J.P., and Hall, J.W. 1991. Effects of two crop rotations on seasonal runoff and soil loss in the Peace River region. Can. J. Soil Sci., **71**: 533–544.

Wall, G.J., Dickinson, W.T., Rudra, R.P., and Coote, D.R. 1988. Seasonal soil erodibility variation in southwestern Ontario. Can. J. Soil Sci., **68**: 417–424.

Wang, X., and Melesse, A.M. 2005. Evaluation of the SWAT models snowmelt hydrology in a northwestern Minnesota watershed. Trans. ASAE, **484**: 1359–1376.

Wang, X., Yang, W., and Melesse, A.M. 2008. Using hydrologic equivalent wetland concept within SWAT to estimate streamflow in watersheds with numerous wetlands. Trans. ASAE, **51(1)**: 55–72.

Watson, B.M., McKeown, R.A., Putz, G., and MacDonald, J.D. 2008. Modification of SWAT for modelling streamflow from forested watersheds on the Canadian Boreal Plain. Journal of Environmental Engineering and Science, **7(S1)**: 145–159.

Watson, B.M., and Putz, G. 2014. Comparison of Temperature–Index snowmelt models for use within an operational water quality model. Journal of Environmental Quality, **43**: 1, 199–207.

Wheater, H.S., Jakeman, A.J., Beven, K.J. 1993. Progress and directions in rainfall-runoff modelling. In: Jakeman, A.J., Beck, M.B., McAleer, M.J. (Eds.), Modelling Change in Environmental Systems. John Wiley and Sons, Chichester, pp. 101–132.

Williams, J.R. 1969. Flood routing with variable travel time or variable storage coefficients. Transactions of the ASAE, **12(1)**: 100–103.

Willems, P. 2000. Probabilistic modeling of emission receiving surface waters. Ph.D. Thesis, Faculty of Engineering, Katholieke Universiteit, Leuven, Belgium.

Yang, W., Wang, X., Gabor, S., Boychuk, L., and Badiou, P. 2008. Water quantity and quality benefits from wetland conservation and restoration in the Broughton's Creek Watershed, Ducks Unlimited Canada, Regina, SK.

Yang, W., Wang, X., Liu, Y., Gabor, S., Boychuk, L., and Badiou, P. 2010. Simulated environmental effects of wetland restoration scenarios in a typical Canadian prairie watershed. Wetlands Ecology and Management, **18(3)**: 269–279.

CHAPTER 3 INCORPORATING LANDSCAPE DEPRESSION HETEROGENEITY INTO THE SOIL AND WATER ASSESSMENT TOOL (SWAT) USING A PROBABILITY DISTRIBUTION

This chapter is a research paper in the Hydrological Processes Journal.

Citation: Mekonnen, B.A., Mazurek, K.A., and Putz, G. (2016). Incorporating landscape depression heterogeneity into the Soil and Water Assessment Tool (SWAT) using a probability distribution. Hydrological Processes, DOI: 10.1002/hyp.10800.

The document has been reformatted from the original version for inclusion in the thesis though no content has changed from the published version.

Contribution of the Ph.D. candidate

The contribution of the Ph.D. candidate for the work in this chapter includes the following: identification of limitation of the current modeling schemes for prairie hydrology; conceptualization and formulation of the Probability Distributed Landscape Depressions (PDLD) module to represent the numerous landscape depressions; integration of the PDLD algorithm into SWAT, customization of the SWAT model database such as crop and soil characteristics for Canadian conditions; input data preparation and SWAT model setup; and testing model performance and results analysis. The second and third authors (the Ph.D. supervisors) provided advice on various aspects of the work. The text of the published manuscript was drafted by the candidate with the second and third authors offering critical review and editorial guidance.

Contribution of this chapter to the overall study

The general objective of this thesis is developing a water quantity and quality model and perform scenario analysis under the conditions of a cold climate prairie watershed. This chapter contributes to the general theme by focusing on the streamflow simulation aspects of the research, which is the first step towards attaining the general objective. Considering the strong influence of streamflow on water quality simulation, it is important to accurately estimate streamflow for better simulation of water quality variables. For accurate simulation of streamflow, it is important to identify limitations of the current model and upgrade it to suit the conditions seen in the study watersheds (Canadian prairie, cold-climate, depression-dominated watershed). This was done by developing SWAT-PDLD modeling framework that allows depression storage heterogeneity representation in SWAT model. In this model, a probability distribution is used to describe landscape depressions storage heterogeneity. The resulting developed model is an improvement over the lumped approach for handling landscape depressions found in the original SWAT model. The modified model (SWAT-PDLD) was applied over two large area prairie watersheds. In this chapter, the improvement in predicting streamflow achieved by the modified model is compared against the lumped storage approach found in the original SWAT model. The modified SWAT-PDLD model was found to be a better streamflow simulation tool.

3.1 Abstract

Modelling the hydrology of North American Prairie watersheds is complicated due to the existence of numerous landscape depressions that vary in storage capacity. The Soil and Water Assessment Tool (SWAT) is a widely applied model for long term hydrological simulations in watersheds dominated by agricultural land uses. However, several studies show that the SWAT

model has had limited success in handling prairie watersheds. In past works using SWAT, landscape depression storage heterogeneity has largely been neglected or lumped. In this study, a probability distributed model of depression storage is introduced into the SWAT model to better handle landscape storage heterogeneity. The work utilizes a probability density function to describe the spatial heterogeneity of the landscape depression storages that was developed from topographic characteristics. The integrated SWAT-PDLD model is tested using datasets for two prairie depression dominated watersheds in Canada: the Moose Jaw River watershed, Saskatchewan; and the Assiniboine River watershed, Saskatchewan. Simulation results were compared to observed streamflow using graphical and multiple statistical criterions. Representation of landscape depressions within SWAT using a probability distribution (SWAT-PDLD) provides improved estimations of streamflow for large prairie watersheds in comparison to results using a lumped, single storage approach.

3.2 Introduction

The Soil and Water Assessment Tool (SWAT) (Arnold et al. 1998) is a widely used, semi-distributed physically based hydrological model that has been applied in many types of watersheds (Gassman et al. 2007). It was initially developed for large area agricultural watersheds (Arnold et al. 1998) by the Agricultural Research Service of the US Department of Agriculture (Gassman et al. 2007). Although the Canadian prairie region has widespread agricultural activity and is highly productive (Stewart 2006; Stewart et al. 2009; Kissinger and Rees 2009), there has been some difficulty in applying the SWAT model to this region (Chanasyk et al. 2003; Mekonnen et al. 2015). The problems are due to the existence of numerous landscape depressions (Eulis et al. 1999) that have a significant influence on runoff and infiltration processes in the region (Hayashi et al. 2003; Hayashi et al. 2004). For instance,

about 67 percent of the Assiniboine River watershed at Kamsack drains into depressions before entering the stream course (Godwin and Martin 1975).

These landscape depressions are largely the result of glaciation events and extend through both Canada and the United States (Tiner 2003). The landscape depressions are often called ‘sloughs’ or ‘potholes’ (Woo and Rowsell 1993; Hayashi et al. 2003). The heterogeneity in storage in the depressions and the dynamic connectivity between depressions result in a dynamic contributing area in depression-dominated watersheds (Shaw et al. 2011).

For a single depression, the water budget includes precipitation on the water surface, surface runoff from the uplands, evapotranspiration, surface outflow (overflow) when a depression is filled beyond capacity, and groundwater flow (Woo and Rowsell 1993; Winter and Woo 1990; Hayashi et al. 1998; Fang and Pomeroy 2008). More specifically, landscape depressions in Canadian prairie region watersheds receive the majority of their water budget input from snowmelt runoff and direct precipitation on the depression (Hayashi et al. 1998; Labaugh et al. 1998). In this region, 30-60% of winter precipitation on upland areas is transmitted into landscape depressions during snowmelt runoff (Hayashi et al. 1998). The large contribution of snowmelt runoff is because of the reduced infiltration capacity of frozen soils (Granger et al. 1984; Gray and Landine 1988; van der Kamp et al. 2003). In a prairie watershed, evapotranspiration and lateral flow of shallow groundwater driven by evapotranspiration are the dominant pathways by which water leaves the depressions (Woo and Roswell 1993; van der Kamp and Hayashi 2009). The influence of deep groundwater exchange on the water budget of the depressions is minimal because of the low hydraulic conductivity of the deeper underlying tills (van der Kamp and Hayashi 2009). According to Linsley et al. (1949), for a watershed where the surface depressions vary in size, the smallest depressions will begin to overflow before

larger depressions that are still being filled, thus initiating runoff. Deep depressions reach their storage capacity more slowly and less often than shallow ones and can retain water longer after rainfall (Beven 2012).

There have been some attempts to model the depression storage processes in the North American prairie region but these have generally been for plot scale or small watersheds by describing the processes occurring for individual depressions using a detailed physically-based model (Su et al. 2000; Pomeroy et al. 2007; Fang and Pomeroy, 2008; Shook et al. 2013; Chu et al. 2013). For instance, Su et al. (2000), Pomeroy et al. (2007), and Fang and Pomeroy (2008) tried to simulate the water budget for an individual closed wetland. Shook et al. (2013) used a fully distributed model to model the fluxes in depressions on three small watersheds and compared the results to a parameterized model (Pothole Cascade model) using LIDAR and Satellite data to define the depressions. Chu et al. (2013) used a physically-based distributed model and tried to simulate landscape depression water balance on a plot scale by extracting geometries of individual depressions also from detailed LiDAR data.

A potential alternate approach for handling depression storage heterogeneity was proposed by Ullah and Dickinson (1979), who found that the storage capacity of depressions in the Canadian prairie region followed a probability distribution. Abedini (1998) followed this idea and noted that the probability distributed models being used to describe heterogeneity in soil moisture storage (e.g., Moore and Clarke 1981; Moore 1985; 2007; Bell et al. 2007; Bell et al. 2009; Noto 2014) could be used in a modelling approach for depression storage heterogeneity. In the laboratory and at plot scale, Abedini (1998) simulated streamflow from depression dominated surfaces. More recently, a similar approach was implemented by Mekonnen et al. (2014), who used a probability distributed model within the Modélisation Environmentale

Communautaire - Surface and Hydrology (MESH) model to simulate the runoff generation from landscape depressions for a small portion of the headwaters of the Assiniboine Watershed in Saskatchewan (Canada) (1939 km^2). However, they did not attempt to quantify the parameters of the probability distribution used to describe storage capacity based upon the topography of the watershed. Furthermore, though they reported an improved simulation during model calibration period, they did not validate the model due to data limitations. Probability distributed models have often been promoted as an extension of semi-distributed models to represent a spatial distribution of storage capacities in a watershed (Beven 2012).

For much larger watersheds in the region, SWAT has often been applied (e.g, Sophocleous et al. 1999; Almendinger et al. 2012; Shrestha et al. 2012; Mekonnen et al. 2015). However, in past application of the SWAT model, the influences of multiple landscape depressions are often either neglected or lumped. For example, Shrestha et al. (2012) assumed the entire watershed area was contributing to the watershed outlet for all events. However, Sophocleous et al. (1999) treated the depressions as if they never contribute runoff (i.e. they were treated as permanent non-contributing areas). In an attempt to take into account some of the depression dynamics, in some studies the individual depressions were aggregated and represented with a single lumped storage per sub-basin to use SWAT's surface depression module for simulating the fill and spill processes (e.g., Almendinger et al. 2012; Mekonnen et al. 2015). Although the latter approach improves model simulation of streamflow, this type of approach does not consider the heterogeneity of storage capacity on the landscape (Wang et al. 2008; Yang et al. 2010). The problem is then how should SWAT be modified to accommodate spatial variations in landscape depression storages?

Some attempts have been made to incorporate landscape depressions storage heterogeneity into SWAT. Wang et al. (2008), followed by Yang et al. (2010), developed a routine to simulate the processes occurring for each individual depression. Similar approaches, using a cascade of multiple reservoirs, have been implemented recently to simulate flood occurance in karst endorheic areas (Iacobellis et al. 2015) and for the Jinsha River and three Gorges cascade reservoirs in the Changjiang River basin of China (Zhou et al. 2015). However, modelling many depressions individually for a very large watershed can be difficult because of the computational demands and need for input data to characterize each depression, which may number in the many thousands. For large watersheds, the probability distributed approach appears to be more feasible.

The focus of this study is to incorporate heterogeneity of landscape depressions storage into the SWAT model using a probability distribution approach in large area watershed modelling. The Soil and Water Assessment Tool (SWAT) was selected for this study because of its wide application (Gassman et al. 2007), suitability for agriculture dominated watersheds (Neitsch et al. 2011), and free access to the source code (Neitsch et al. 2011). For the current study, a probability distribution is incorporated into the SWAT model surface depression routine. This adaptation of the model allows for consideration of the spatial variability of depression storage capacities within a sub-basin. Therefore, the parameter for storage capacity in the probability distribution has also been allowed to vary between sub-basins based on topographic characteristics. The proposed model is calibrated and validated over two depression dominated watershed outlets in the Moose Jaw and Assiniboine River basins in Saskatchewan, Canada. These watersheds are located within the northern glaciated prairie region of North America where numerous landscape depressions of varying sizes exist (Hayashi et al. 2003).

In the paper, three model setup approaches are compared for the prediction of streamflow in the study watersheds. The three model setups considered are the following: (1) assumption of no depression occurrence in the watersheds; (2) simulation of depressions using the semi-distributed algorithm (lumped approach); and (3) use of a probability distributed algorithm within a semi-distributed model to simulate multiple depressions.

3.3 The SWAT Model Description

The Soil and Water Assessment Tool (SWAT) is a continuous physically-based semi-distributed hydrological model that simulates the various hydrological processes of a watershed including water, sediment, and pollutant yields (Arnold et al. 1998). SWAT simulates the hydrological cycle of a watershed by partitioning it into a number of sub-basins that are further grouped into Hydrological Response Units (HRUs) (Arnold et al. 1998). HRUs are non-spatially specific lumped areas within a sub-basin that are comprised of unique combinations of land cover, soil type, and slope (Neitsch et al. 2011).

Water balance computations are performed at the HRU level and hydrological processes are computed separately for each HRU of the sub-basin. Surface runoff is computed using either the modified Curve Number Method (CN) (SCS: USDA Soil Conservation Service 1972) or Green-Ampt methods (Green and Ampt 1911). The SWAT model uses a temperature-index method to predict snowmelt (Neitsch et al. 2011). Potential evapotranspiration is estimated using one of three different methods that include Hargreaves (Hargreaves et al. 1985), Priestley-Taylor (Priestley and Taylor 1972), and Penman-Monteith (Monteith 1965). The actual evaporation from soils and plants is estimated by the method described in Ritchie (1972). Baseflow is modelled by partitioning groundwater into a two aquifer system (shallow and deep) (Arnold et al. 1998). The contributions of each HRU are then accumulated to represent water yield to the

main channel within a sub-basin. Water export is then routed to the outlet of the sub-basin. Routing is performed based on either the variable storage coefficient method (Williams 1969) or the Muskingum routing method (Cunge 1969).

The model has been through several modifications to simulate cold climate hydrology. These include incorporation of seasonally variable snowmelt rate (Fontaine et al. 2002), sub-dividing each sub-basin into 10 elevation bands (Fontaine et al. 2002), and modification of the curve number value for frozen soil conditions to enhanced surface runoff and reduced infiltration (Tolston and Shoemaker 2007). Since the watersheds studied in the present work are in a cold climate, the recent version of SWAT model (SWAT2009) with the above described modifications has been used for the current work.

The SWAT model provides several modules that potentially might be used to simulate landscape depressions including Pothole, Pond, and Wetland (capitalized here to denote SWAT-specific tools) (Neitsch et al. 2011). In the Pothole conceptualization, which is developed by Du et al. (2005), the routine does not allow contribution of upland runoff from other HRUs within a sub-basin. In reality, the landscape depressions in the prairie watersheds may receive water from different HRUs (e.g., Almendinger et al. 2014). On the other hand, Pond and Wetland allow runoff contribution from any HRUs within a sub-basin. Pond and Wetland rely on similar conceptualization of depression dynamics (either one could be used). As these modules, Pond and Wetland, consider runoff contribution from multiple HRUs, they have been often implemented to represent landscape depressions in past modeling works (e.g.,Kiesel et al. 2010; Almendinger et al. 2012). Furthermore, unlike the Wetland and Pond routines, water quality variable simulation is not yet included in the Pothole routine (Neitsch et al. 2011). In this work,

therefore, the Pond routine was used for comparison to the results generated by a probability distributed approach to describe the landscape depressions.

3.4 Probability Distributed Model Development

3.4.1 Water balance in a depression

For the development of the probability distributed model for implementation into SWAT, the water balance in a single depression must first be described. As noted above, the depression takes up water from precipitation and upland runoff generated from its contributing areas and loses water through evapotranspiration and seepage. The difference between these inputs and outputs either fills or empties the depression. When the net input exceeds the available storage in the depression, the depression will spill and therefore generate runoff. The generated runoff will join the sub-basin stream network and will then be routed through it. This runoff generation behaviour for an individual depression may be expressed mathematically as:

$$Q = \begin{cases} P + Q_{\mathrm{u}} - E - I - (c - S) & \text{for} \quad P + Q_{\mathrm{u}} > c - S + E + I \\ 0 & \text{for} \quad P + Q_{\mathrm{u}} \leq c - S + E + I \end{cases} \tag{3.1}$$

where P is the precipitation, Q_{u} is the runoff into the landscape depression from the upland within the sub-basin, E is evapotranspiration, I is seepage from the depression, c is the storage capacity of the depression, S is water in the depression, and Q is the resulting direct runoff generated from the depression over the time interval considered. Each of these quantities is expressed as a volume per surface area of the depression and is calculated on a daily increment in SWAT.

Over an entire sub-basin, the runoff generation principle at every depression may be similarly described, each depression differing from another only with regard to its storage

capacity. The total runoff generated from the landscape depressions will be the cumulative runoff generated from the individual depressions.

3.4.2 Quantification of depression storage

Next, following a similar methodology used for soil storage by Moore (1985, 2007) and for landscape depressions by Abedini (1999), landscape depressions within a sub-basin are conceptualized as consisting of a population of storages of varied capacity following a probability density function $f(c)$. The storage capacity c of a depression is the volume of the depression divided by its surface area. Considering storage capacity as a random variable, C, the probability of storage values in the size range c to $c+dc$, $P(c \le C \le c+dc)$, can be formulated using the probability density function, $f(c)$, as shown below:

$$P(c \le C \le c+dc) = \int_{c}^{c+dc} f(c)dc \tag{3.2}$$

The cumulative distribution function of storage capacity is defined using the density function as:

$$F(c) = P(C \le c) = \int_{-\infty}^{c} f(c)dc \tag{3.3}$$

where $F(c)$ is the cumulative distribution function. The probability density function, $f(c)$, varies with the type of probability distribution selected, from which different cumulative distribution functions can be derived.

To determine the form of the probability density function for the storage capacity of landscape depressions for the watersheds of interest, terrain analysis was performed. The terrain analysis was carried out using ArcGIS10. The Digital Elevation Model (DEM), which was used in terrain analysis, was obtained from the GeoBase Canada (GeoBase Canada, 2007) with a grid resolution of 18 m and vertical resolution of 1 m. The variables that were estimated from the Digital Elevation Model (DEM) analysis included the portion of upland areas contributing into

landscape depressions (used for the SWAT modelling) and depression geometries (volume, surface area, and depth). Figure 3-1 shows the frequency distribution for the capacity (volume per surface area) of depressions for the two case study watersheds (i.e. Moose Jaw and Assiniboine River watersheds). It is seen in Figure 3-1 that both the Pareto and exponential distributions can be used to represent the variation of both depression capacity in these watersheds. For the Moose Jaw River watershed, the correlation coefficients R^2 between the terrain analysis data for depression capacity and the fitted theoretical distributions are 0.78 and 0.80 for the exponential and Pareto distributions respectively. Similarly, the correlation coefficients for the Assiniboine River watershed were found to be 0.76 and 0.77 for the exponential and Pareto distributions. Because the improvement in fit to the data using the Pareto distribution was small compared to the exponential distribution and the exponential distribution has fewer parameters, the exponential distribution was used to describe depression storage capacity variation for the current work.

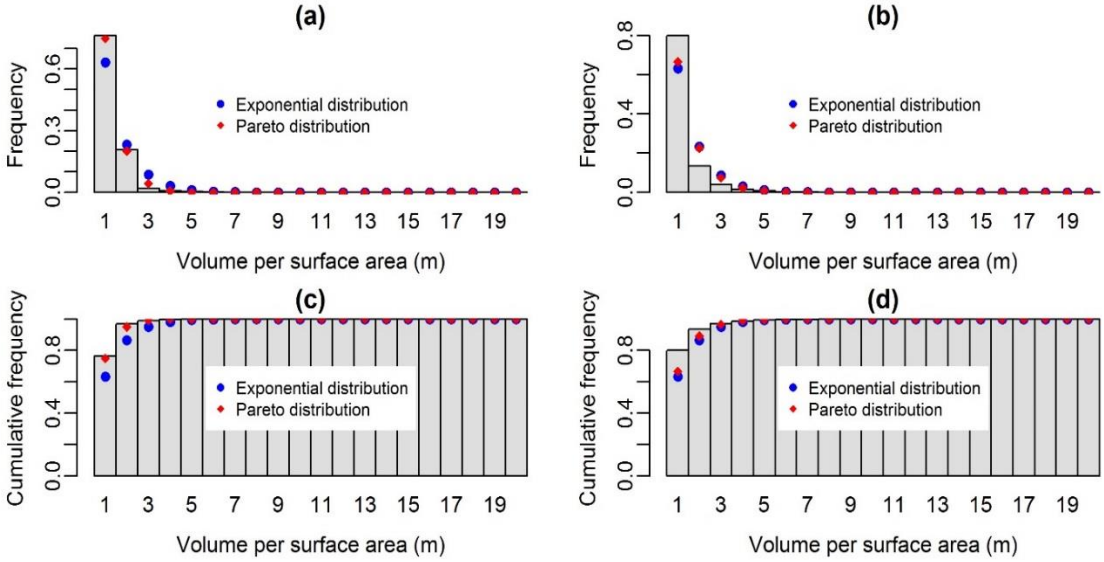

Figure 3–1 Theoretical probability distributions fitted for landscape depression storage capacity: (a) and (c) Moose Jaw River watershed; (b) and (d) Assiniboine River watershed.

Following the expression of cumulative probability distribution presented in Equation (3.4), the cumulative distribution of the one parameter exponential distribution function can be specifically defined as:

$$F(c) = 1 - \exp\left(\frac{-c}{\bar{c}}\right) \tag{3.4}$$

where $\bar{c}$ is the mean storage capacity, which was also determined directly from the terrain analysis.

3.4.3 Basic equations in probability distributed landscape depressions

In developing the method for incorporating landscape depressions into the SWAT model, the type of interaction between the individual depressions must be represented. The nature of this interaction can be either interacting or non-interacting (Moore 1985). Herein, we describe and utilize the interacting neighbouring storage approach because past works (e.g. Rosenberry and Winter 1997; Leibowitz and Vining 2003) reported surface water connectivity between depressions in the Canadian prairie region. In this configuration, there will be equal distribution of water input into the depressions. Additionally, all depressions with a storage capacity greater than C^*, called the critical capacity, will have an equal amount (volume per surface area) of water stored in the depressions equal to C^*. Those depressions with a storage capacity less than C^* are full to their capacity (as depicted in Figure 3-2) and cannot contain more water. Therefore, landscape depressions with storage capacity less than C^* are generating runoff. The proportion of the landscape depressions with a storage capacity less than or equal to C^* can be described by $\text{prob}(c \le C^*) = F(C^*)$.

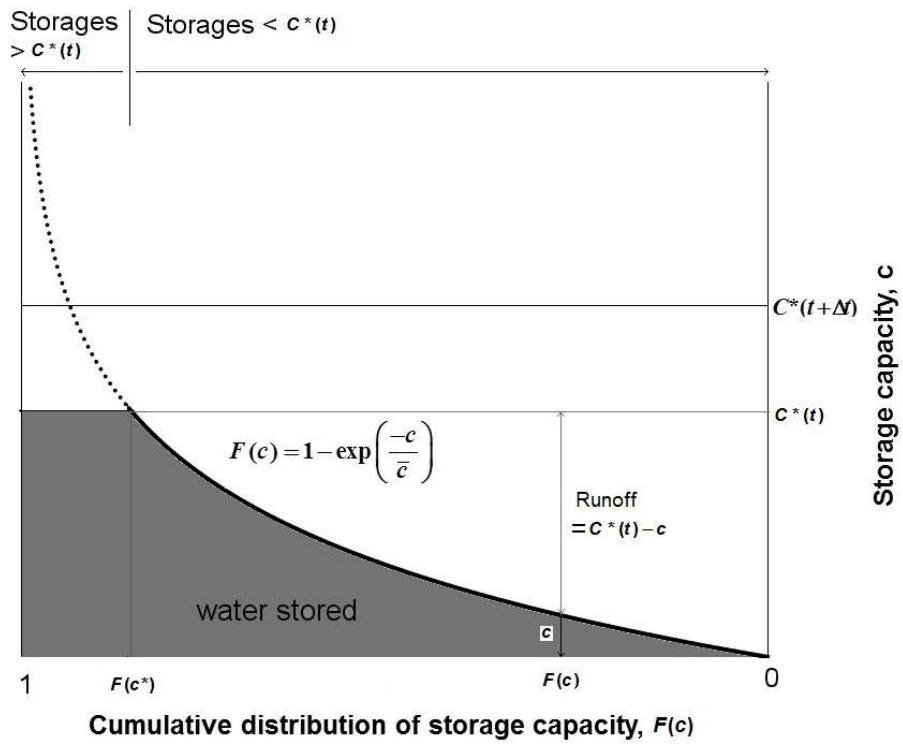

Figure 3–2 The distribution of storage capacity and its relationship to water stored, critical capacity, and over spill runoff generation from landscape depressions.

Considering Figure 3–2, the total water stored in the depressions at a particular time (Figure 3–2, Gray area), is the sum of water stored in depressions that are full (depressions with a capacity less than the critical capacity) and the water stored in part-full depressions (depressions with a capacity greater than the critical capacity). This storage is given by:

$$S(t) = \int_0^{C^*(t)} cf(c)dc + C^*(t)\int_{C^*(t)}^{\infty} f(c)dc \qquad (3.5)$$

The first term in the right hand side of Equation (3.5) represents the water stored in the full depressions while the second term represents water stored in the part-full depressions. Making use of the general result:

$$\int_0^{C^*(t)} cf(c)dc = C^*(t)\,\mathrm{F}(\mathrm{C}^*) - \int_0^{C^*(t)} \mathrm{F}(c)dc$$

and incorporating the relation $\int_{C^*(t)}^{\infty} f(c)dc = 1 - F(\mathrm{C}^*)$ into Equation (3.5) followed by some re-arrangements, the total water stored in depressions, $S(t)$, and critical capacity, $C^*(t)$, at a particular time can be related as follows:

$$S(t) = \int_0^{C^*(t)} (1 - F(c))dc \tag{3.6}$$

Since the exponential distribution was selected to describe the variation of the capacity of the depressions, $F(c)$ can be described using Equation (3.4). By combining Equation (3.4) and Equation (3.6) the storage $S(t)$ can be re-written as:

$$S(t) = \int_0^{C^*(t)} \left(-\exp\left(\frac{-c}{\bar{c}} \right) \right) dc \tag{3.7}$$

Integration of Equation (3.7) gives the following relation:

$$S(t) = \bar{c}\left(1 - \exp\left(\frac{-C^*(t)}{\bar{c}} \right) \right) \tag{3.8}$$

The value of critical storage capacity at any time t, $C^*(t)$, is obtained by solving for $C^*(t)$ within Equation (3.8); that is:

$$C^*(t) = -\bar{c}\ln\left(1 - \frac{S(t)}{\bar{c}} \right) \tag{3.9}$$

For a net water input to the depressions of $\pi\Delta t$, expressed as a total volume of water per total surface area of the depressions, occurring during the time interval ($t, t + \Delta t$), the critical capacity, $C^*(t + \Delta t)$, will increase over $C^*(t)$ by $\pi\Delta t$, or

$$C^*(t + \Delta t) = C^*(t) + \pi\Delta t \tag{3.10}$$

as illustrated in Figure 3-2. For the increased critical capacity, $C^*(t+\Delta t)$, the corresponding stored water over the landscape depressions at $t+\Delta t$, $S(t+\Delta t)$, can be computed using Equation (3.11) as follows:

$$S(t+\Delta t) = \bar{c}\left(1-\exp\left(\frac{-C^*(t+\Delta t)}{\bar{c}}\right)\right) \tag{3.11}$$

The direct runoff, $R(t,t+\Delta t)$, generated from the landscape depressions within a sub-basin during the time interval (t, $t+\Delta t$) then can be computed:

$$R(t,t+\Delta t) = \pi\Delta t - \left(S(t+\Delta t) - S(t)\right) \tag{3.12}$$

An initial condition must be assumed or estimated for the amount of water stored in the landscape depressions, $S(0)$, at the beginning of a model simulation using the above described Probability Distributed Landscape Depressions (PDLD) algorithm in order for the calculations to proceed.

3.5 SWAT and Probability Distributed Landscape Depressions Integration

The probability distributed landscape depressions (PDLD) algorithm was coded into the Soil and Water Assessment Tool (SWAT) as an alternative to the existing SWAT model pond/wetland algorithm. Figure 3–3 shows a conceptualization of how landscape depressions are represented in the PDLD approach as compared to the existing SWAT Pond module. For both cases, within the SWAT model the surface runoff generation from each HRU within a sub-basin is calculated using the Curve Number method. Part of the runoff generated from each HRU will then be intercepted by the pond(s), while the remaining portion will directly discharge into the stream network. The amount of water directed to the depression storage within a sub-basin is calculated based on the contributing area of the depressions, which was determined from the DEM analysis using the depression analysis routine within the ArcHydro Tools (ESRI 2011)

available for ArcGIS Desktop 10 (v. 10.0). This is a fixed value for each sub-basin. However, each sub-basin in the study watershed has a different storage capacity that is similarly determined from DEM analysis.

The Pond module in SWAT, uses a lumped storage routine that allows only a maximum of one pond per sub-basin (see Figure 3-3a). This means that all the water directed to depression storage is stored in this single virtual pond. On the other hand, the PDLD algorithm uses a distributed storage routine that allows a sub-basin to contain multiple storages with varying storage capacities (see Figure 3-3b). The PDLD configuration therefore can represent a large number of depressions such as those seen in a prairie watershed.

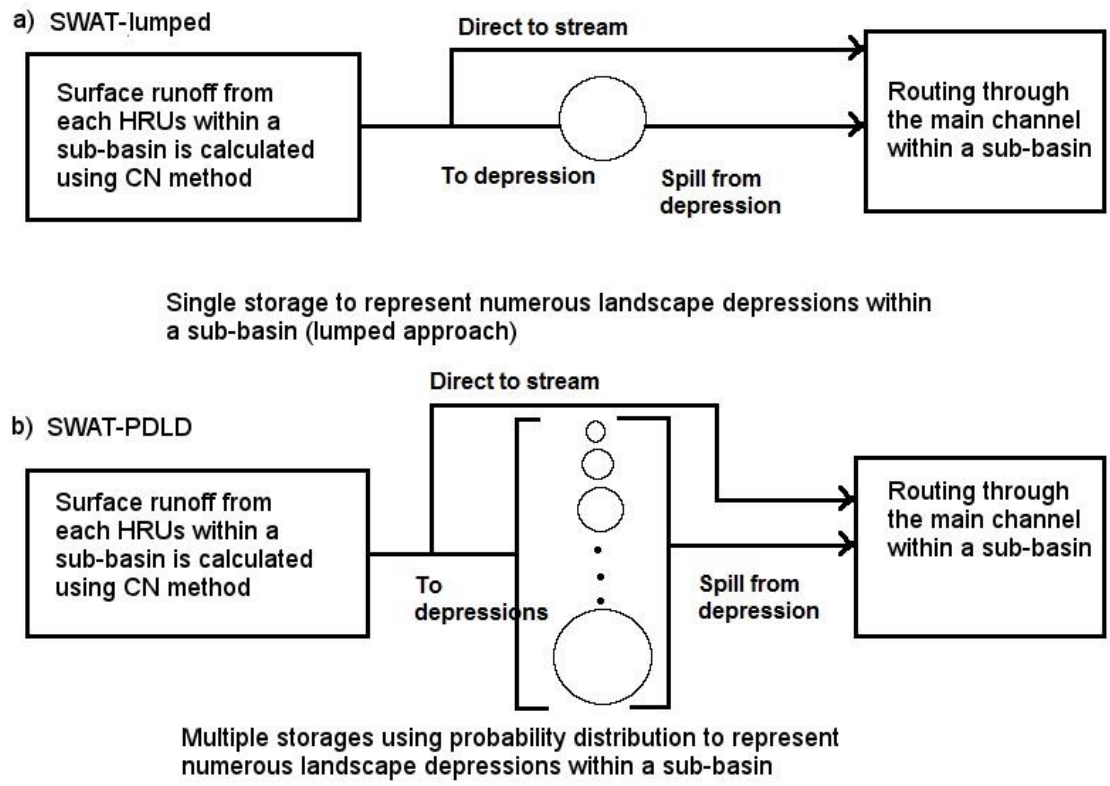

Figure 3–3 The Soil and Water Assessment Tool (SWAT) modelling system linked with the probability distributed model for the prairie hydrology.

3.6 Study Areas and Data

3.6.1 Study areas

To test the capability of the SWAT model to simulate depressions, a study was conducted on two prairie watersheds within the Moose Jaw River and Assiniboine River basins, which are located in the Province of Saskatchewan, Canada (shown in Figure 3-4).

The Assiniboine River basin covers an area of about 17 300 km^2 in Saskatchewan. The watershed is located within two major physiographic regions that include the Saskatchewan Plains and the Saskatchewan Uplands (Saskatchewan Watershed Authority 2005). In the Assiniboine River basin, the gauging station at Kamsack (Water Survey Canada gauging station number: 05MD004) was selected for evaluation of the three model setups. The Kamsack gauging station (05MD004) is located at Latitude 51o33’53’’ N and Longitude 101o54’48’’ W. The watershed outlet at Kamsack has a gross drainage area of 13 000 km2 of which only 4 320 km2 is effective area. Effective area is defined according to Godwin and Martin (1975) who give that the effective area as areas that are contributing for the 1:2 year return period storm. The majority of land in this watershed is used for agriculture (58%), mainly for crop production. Black chernozemic soils that are high in organic matter cover almost 70% of the basin. The topography varies between 428 and 718 m above mean sea level. The mean annual temperature in the basin is about 1°C and the mean annual precipitation is 450 mm per year, with 27 percent as snowfall. Most streamflow, about 63 percent, occurs during April and May from snowmelt (Saskatchewan Watershed Authority 2005).

The Moose Jaw River basin has a gross drainage area of 9 230 km2, however only 3 470 km2 is considered as effective area (Godwin and Martin 1975). The Moose Jaw River is a major tributary of the Qu’Appelle River. A gauging station near Burdick (Water Survey Canada

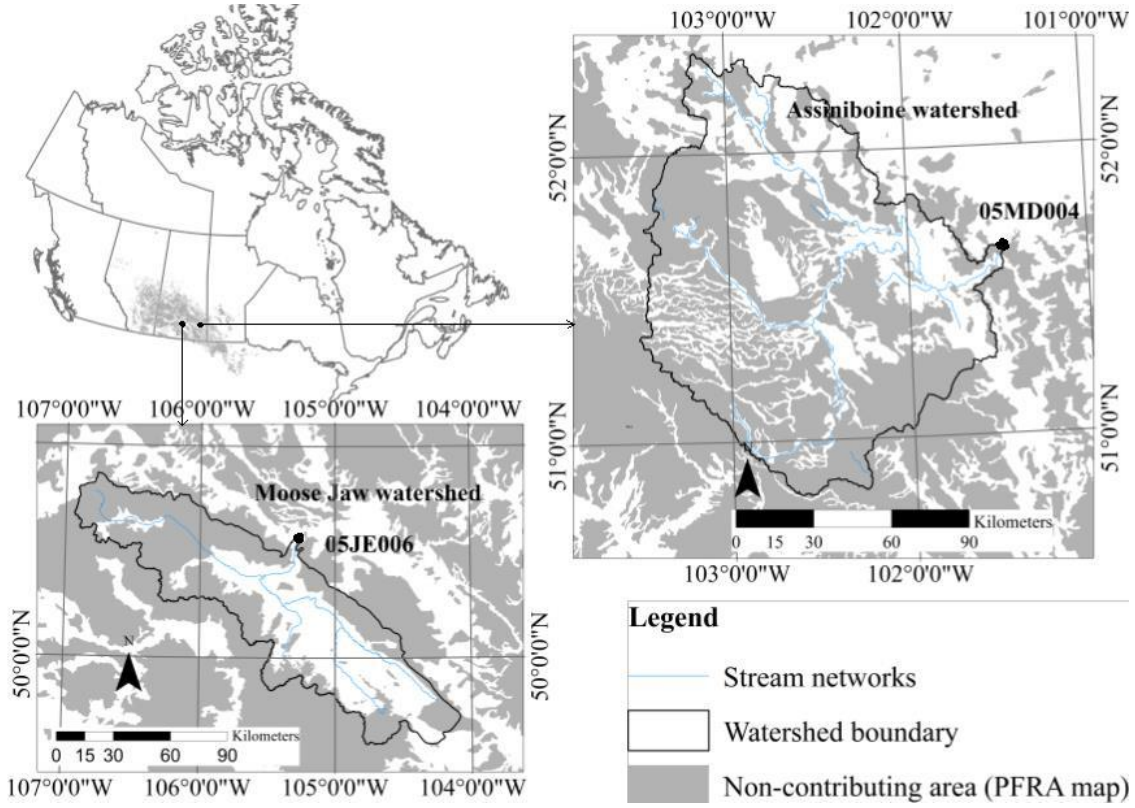

Figure 3–4 The prairie pothole region and location of the study watersheds within the Assiniboine and Moose Jaw River Basins in Saskatchewan, Canada.

gauging station number: 05JE006) was used for evaluation of the model. The gauging station is located at 50º24’1.2” N and 105º23’52.3”W. Similar to the Assiniboine River watershed (described above), the majority of the land in this watershed is used for agriculture (70%), mainly for crop production. The topography of the Moose Jaw River watershed varies between 536 and 877 m above mean sea level. The watershed is located in an area of diverse soil types ranging from heavy clay soils in the East to gravelly sandy soils in the West. Frozen soils and wind redistribution of snow develop over the winter, and snowmelt runoff normally occurs in the early spring with the peak basin streamflow usually happening in the second half of April. The

30-year (1971-2000) mean annual precipitation at Moose Jaw is 365 mm, of which 115.5 mm occurs mostly as snow in winter; the 30-year annual average air temperature at Moose Jaw is 4°C (Environment Canada 2009).

3.6.2 Land cover, topographic and soil data

The SWAT model requires several categories of spatial input data including the land cover, digital elevation model, and soil data. Detailed land cover data was obtained from the LCC200V database in GeoBase Canada (GeoBase Canada 2009). The land cover data were prepared through vectorization of raster thematic data originating from classified Landsat 5 and Landsat 7 ortho-images with the Circular Map Accuracy Standard (CMAS) of 30 meters and is distributed as 1:250 000 scale National Topographic System (NTS) tiles. The topographic data for the study areas were obtained from the GeoBase Canada website (GeoBase Canada 2007). The source for the DEM data was provincial data sets where possible. When provincial data was not available, the 1:50, 000 National Topographic Data Base were used as source materials. Depending on the latitude, the grid resolution varied from 8 to 23 m with a vertical resolution of 1 m. For the study watershed, the grid resolution was about 18 m. The third spatial input data for the SWAT model is the soil map. Soil data at a resolution of 1:1 000 000 was obtained from Soil Landscapes of Canada (SLC) that is found in the Agriculture and Agri-Food Canada database (Soil Landscapes of Canada Working Group 2007).

3.6.3 Meteorological and flow data

Gridded climate data derived from the Gridded Climate Dataset for Canada (GCDC) (Hutchinson et al. 2009) were used as forcing data for hydrologic modelling. The gridded datasets were employed instead of the relatively sparse climate station observation data because of their more detailed spatial coverage. The suitability of such data for this region is supported

by the work of Shrestha et al. (2012), who demonstrated that the Soil and Water Assessment Tool (SWAT) could be suitably calibrated in the Assiniboine watershed, which is a case study watershed for this study, using gridded data. The Gridded Climate Dataset for Canada (GCDC) consists of daily precipitation measurements and maximum and minimum air temperature data south of 60°N latitude in Canada for the period 1961-2003 (Hutchinson et al. 2009). The dataset is based on daily Environment Canada climate station observations interpolated at 10 km spatial resolution using a thin-plate smoothing spline-surface fitting method. Flow data was extracted from the Hydrometric Database (HYDAT) for the two streamflow gauging stations mentioned above.

3.7 Model Setup, Calibration and Evaluation Criteria

3.7.1 Model setup and calibration methodology

The hydrologic model was setup using the ArcSWAT interface for SWAT2009 (Neitsch et al. 2011). Using the ArcSWAT interface, the DEM was used to discretize the watersheds into sub-basins and create stream networks for the study watersheds. The land use and soil data were then imported and processed to define HRUs. Three modelling approaches were tested in this study. In the first approach, the SWAT model was setup in such a way that all the watershed area is contributing to the outlet of the watershed for all events. The second approach was setup to simulate landscape depressions using the SWAT pond algorithm, i.e. a single storage per sub-basin (lumped approach). The third approach was to simulate hydrological processes of landscape depressions using the PDLD algorithm (SWAT-PDLD: SWAT with Probability Distributed Landscape Depressions).

Following input data preparation for the three model setups, parameters that strongly influence the land and the channel routing phases of the hydrological cycle were identified using

a sensitivity analysis, which was performed with the Latin hypercube sampling-one factor at a time procedure (van Griensven et al. 2006). Once the most sensitive parameters had been selected (Table 3-1), an automatic calibration was performed using the robust Shuffled Complex Evolution-Uncertainty Analysis algorithm at the outlet of the two watersheds. The aim of the automatic calibration procedure is to minimize the sum of squared errors (SSE):

$$\mathrm{SSE} = \sum_{i=1}^{n} \left(\hat{Q} - Q_i \right)^2 \tag{3.13}$$

where $\hat{Q}$ is the simulated streamflow and Q_i is the observed streamflow at time i and n is total number of observed data points.

The available measured data was sub-divided into calibration and validation periods. For the station at Kamsack, these were data from 1992 to 1995 and 1996 to1999, respectively. For the station at Moose Jaw, these were data from 1992 to 1997 and 1998 to 2002, respectively. To pre-condition the model, the two year period of 1990 and 1991 was used as a warm-up period. The warm-up period minimizes the potential adverse effect of poorly estimated initial state variables such as soil water content (Zhang et al. 2008).

Herein, the simulation was allowed to start at the end of April and the initial water stored was assumed to be same as the total storage capacity of depressions within the sub-basin. This was assumed because all depressions are expected be at full capacity by this time due to spring snowmelt, which is a major prairie hydrological event capable of causing surface runoff.

Table 3–1 Parameters selected for SWAT model automatic calibration and resulting optimum values for the three model setups: 'no depressions' approach (Case-1), single lumped storage approach (Case-2), and PDLD approach (Case-3).

Parameter	Parameter default value	Range of optimization		Optimum parameter values for Assiniboine River watershed			Optimum parameter values for Moose Jaw River watershed		
		Min	Max	Case 1	Case 2	Case 3	Case 1	Case 2	Case 3
CN2[a, b]	Varies	-10	+10	-7.11	3.36	-2.00	-8.00	-2.53	-3.64
ESCO[a, b]	0.90	0	1	0.41	0.82	0.80	0.62	0.52	0.56
SURLAG[a, b]	4	0	10	0.50	1.31	1.00	0.70	1.43	1.00
ALPHA_BF[a, b]	0.048 day	0	1	0.55	0.23	0.34	0.70	0.33	0.49
SFTMP[b]	1°C	-5	+5	-2.1	-1.21	-0.64	-2.4	-3.20	-4.94
SMTMP[b]	0.5°C	-5	+5	-0.5	-4.20	-3.29	2.7	-3.33	-2.25
SMFMX[b]	4.5 mm $^{o}C^{-1}$ d^{-1}	0	7	4.0	3.22	2.15	6.9	2.72	2.55
SMFMN[b]	4.5 mm $^{o}C^{-1}$ d^{-1}	0	7	0.6	1.10	0.23	2.5	0.97	0.94
TIMP[b]	1	0	1	0.3	0.21	0.05	0.12	0.08	0.01
SNOCOVMX[b]	1 mm	0	500	195	150	225	195	98	121
SNO50COV[b]	0.5	0	1	0.22	0.10	0.02	0.09	0.13	0.02
SMAX[b]	varies	-0.2	+0.2	-	-	0.13	-	-	0.09
CH_N[a, b]	0.014	0	0.065	0.065	0.06	0.04	0.06	0.06	0.05

[a] Ranked within the first five most sensitive parameter based on the sensitivity analysis of current study.

[b] Parameters that were identified as calibration parameters in previously published SWAT models.

3.7.2 Model performance evaluation

Three statistics were used to evaluate model performance: the Nash & Sutcliffe efficiency index (NSE: Nash and Sutcliffe, 1970); the Coefficient of Determination (R^2); and the Root Mean Square Error (RMSE). To determine how well the simulation versus the observed data fits a 1:1 line, the Nash and Sutcliffe efficiency index (NSE) was used. This was calculated by Equation (3.14) below:

$$\mathrm{NSE} = 1 - \frac{\mathrm{SSE}}{\sum_{i=1}^{n}\left(\bar{Q} - Q_i\right)^2} \tag{3.14}$$

where $\bar{Q}$ is the average observed streamflow. To describe the co-linearity of simulated to observed data, the Coefficient of Determination (R^2) was used, where:

$$R^2 = \left(\frac{\sum_{i=1}^{n}(Q_i - \bar{Q})(\hat{Q}_i - \bar{\hat{Q}})}{\sqrt{\sum_{i=1}^{n}(Q_i - \bar{Q})^2}\sqrt{\sum_{i=1}^{n}(\hat{Q} - \bar{\hat{Q}})^2}} \right)^2 \tag{3.15}$$

Finally, the amount of error associated with the simulated streamflow values in units of streamflow was assessed using the Root Mean Square Error (RMSE):

$$\text{RMSE} = \sqrt{\frac{\sum_{i=1}^{n}(Q_i - \hat{Q}_i)^2}{n}} \tag{3.16}$$

3.8 Results and Discussion

3.8.1 Calibrated parameters

In Table 3–1 the calibrated parameters, their default, upper and lower bounds, and optimized values are listed. A total of 13 parameters were considered for optimization. The calibrated parameters include SCS curve number (CN2), soil evaporation compensation factor (ESCO), surface runoff lag coefficient (SURLAG), baseflow factor for bank storage (ALPHA_BF), snowfall temperature (SFTMP), snowmelt base temperature (SMTMP), maximum melt factor (SMFMX), minimum melt factor (SMFMN), snowpack temperature lag factor (TIMP), areal snow coverage threshold at 100% (SNOCOVMX), areal snow coverage threshold at 50% (SNO50COV), maximum storage capacity (SMAX), and Manning n for the main channel (CH_N). The parameters were adjusted to have values within the recommended ranges. It was observed that final parameter values vary between modelling approaches. For instance, the SCS runoff curve number (CN2) was set to the lower bound of the optimization range under ‘no depressions’ modelling approach, which is much lower than the other two modelling approaches. The reduced value of CN2 under the ‘no depression’ modelling approach may be because the study area is dominated by a large number of depressions that significantly affect the runoff processes.

3.8.2 Model performance comparisons

Model performance was initially assessed through visual inspection of the simulated versus observed hydrographs. Average monthly hydrographs at Kamsack (Assiniboine River) and near Burdick (Moose Jaw River) gauging stations are presented in Figures 3–5 and 3–6 respectively. It is seen that a poor fit is observed for the first approach using a standard SWAT model setup (with the assumption of no depressions on the landscape). In particular, the peaks are highly over-estimated. Model performance was significantly improved over the first case for both the second (SWAT-lumped) and third (SWAT-PDLD) approaches. Both the SWAT-lumped and SWAT-PDLD models produce simulated hydrographs that are representative of the observed average monthly streamflow for the two watersheds during the calibration and validation periods. Specifically, the timing and duration of peaks are well simulated by both models. However, the SWAT-lumped model tends to under-predict the larger peaks (e.g., the peaks in 1995 at Kamsack and in 1994, 1996 and 1997 near Burdick) in comparison to the SWAT-PDLD model.

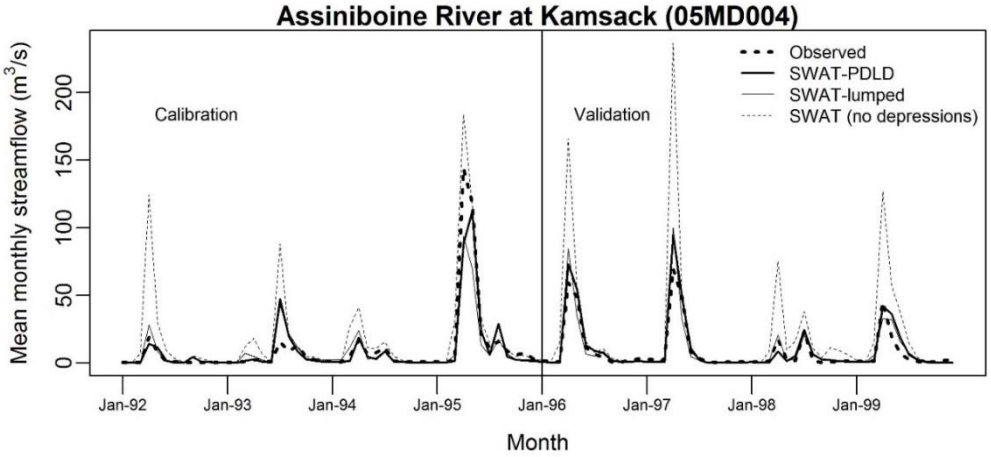

Figure 3–5 Average monthly hydrographs for Assiniboine River at Kamsack during calibration and validation periods using three model configurations: SWAT-lumped (with a single depression), SWAT-PDLD, and SWAT with no depression model setup.

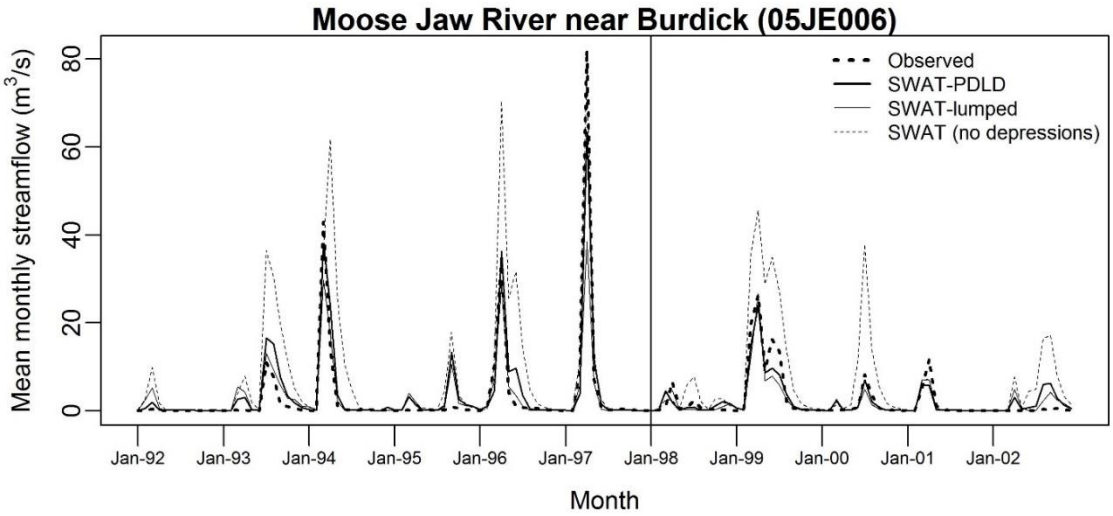

Figure 3–6 Average monthly hydrographs for Moose Jaw River near Burdick during calibration and validation periods using three model configurations: SWAT-lumped (with a single depression), SWAT-PDLD (with multiple depressions), and SWAT (with no depression) model setup.

In addition to average monthly plots, daily observed and simulated hydrographs at Kamsack (Assiniboine River) and Burdick (Moose Jaw River) are presented in Figures 3–7 to 3–10. The daily streamflow is generally well simulated by the SWAT-PDLD and SWAT-lumped models for both watersheds (Figures 3–7 and 3–8). The magnitude, timing and duration of most of the peak flows are reasonably represented by both models. As a weakness for both models, they were unable to simulate the very large peak in 1995 at Kamsack (Figure 3–7). In examining Figure 3–8, it is seen that there is a tendency to under-estimate major peaks near Burdick by the SWAT-lumped model (e.g., peaks in the years of 1994, 1996, and 1997). The SWAT-probability distributed landscape depression (SWAT-PDLD) model does better in simulating those major peaks on the Moose Jaw River near Burdick in comparison to the SWAT-lumped model. The consistent under-estimation of high flows by SWAT-lumped is also observed on flow duration curve plot (Figures 3–9 and 3–10).

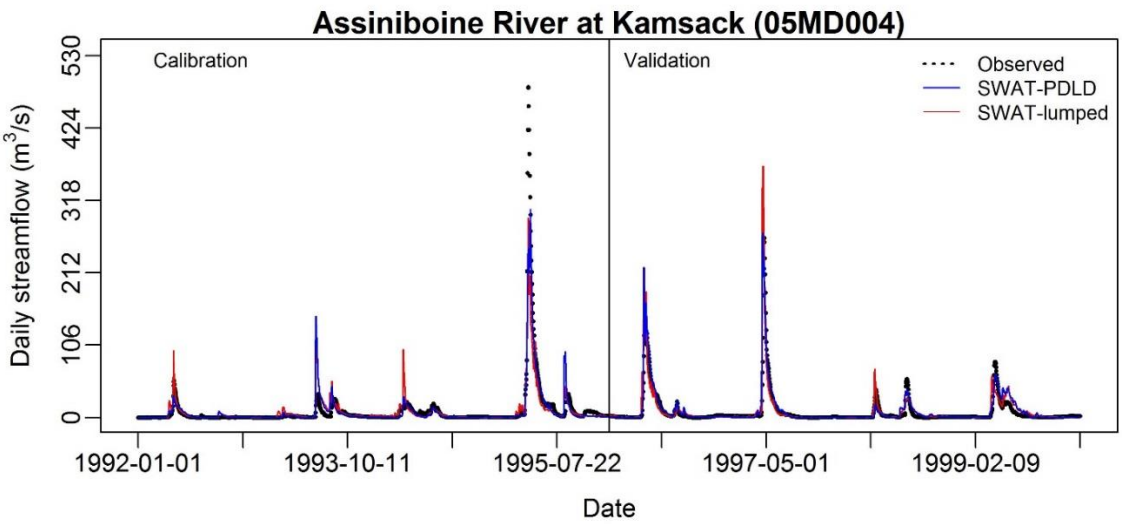

Figure 3–7 Daily hydrographs of the SWAT-lumped and SWAT-PDLD models for Assiniboine River at Kamsack during calibration and validation periods.

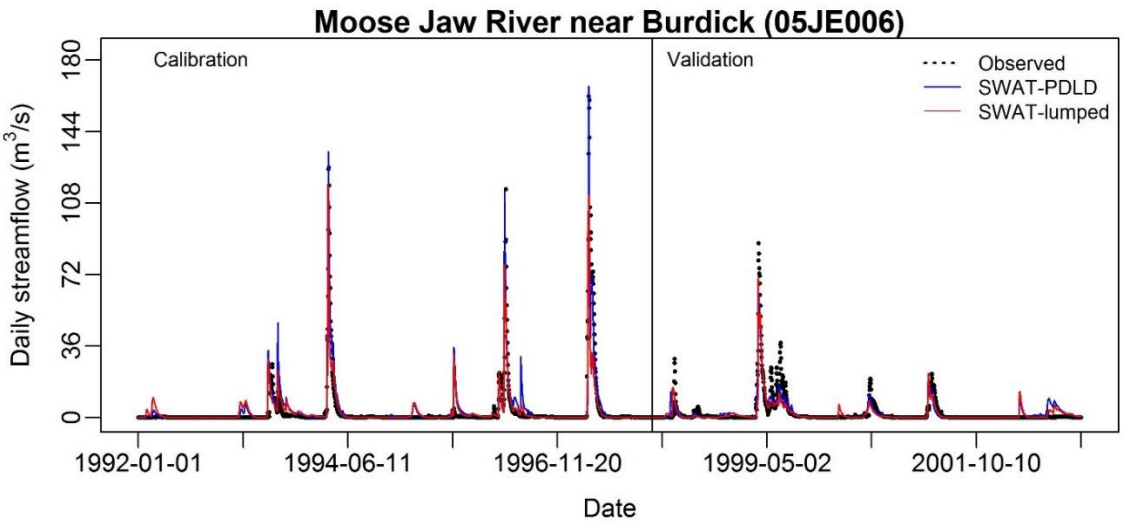

Figure 3–8 Daily streamflow hydrographs of the SWAT-lumped and SWAT-PDLD models for Moose Jaw River near Burdick: both calibration and validation periods.

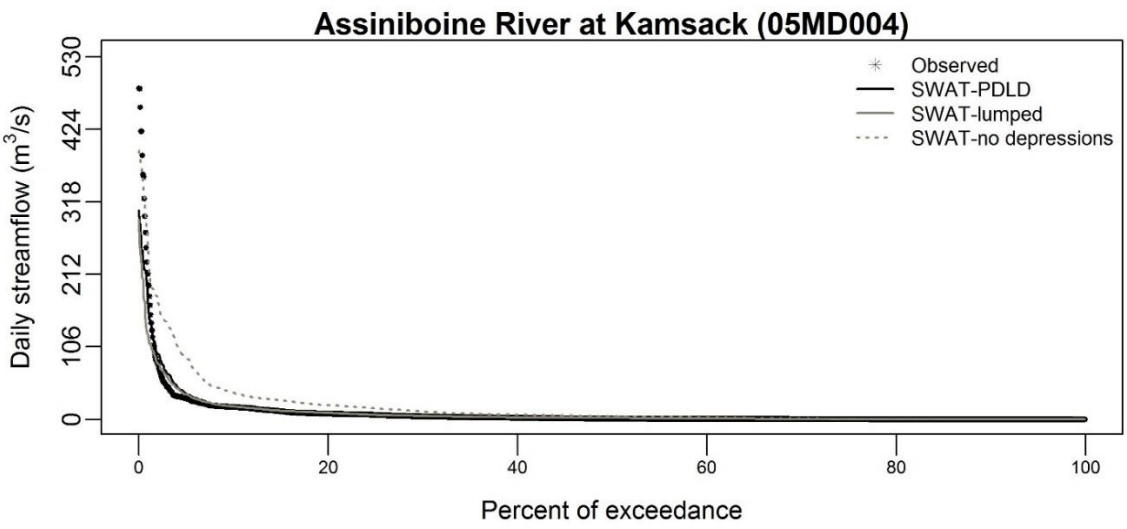

Figure 3–9 Duration curves of the observed, SWAT-PDLD, SWAT-lumped, and SWAT with no depressions models for Assiniboine River at Kamsack.

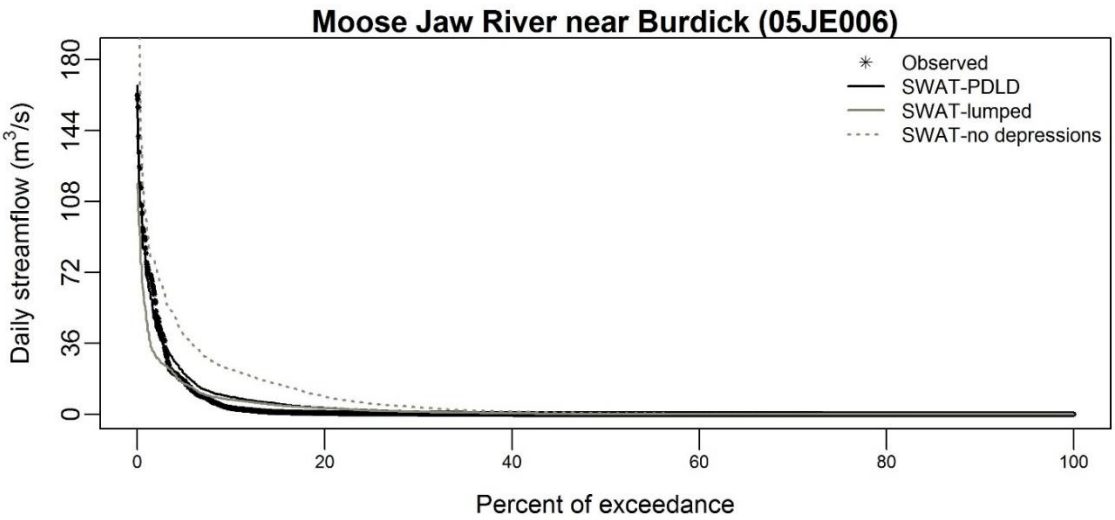

Figure 3–10 Duration curves of the observed, SWAT-PDLD, SWAT-lumped, and SWAT with no depressions models for Moose Jaw River near Burdick.

Trends of long term average mean monthly streamflow were also assessed. Figures 3–11 and 3–12 present the observed and simulated average mean monthly streamflow over the calendar year (i.e., calendar monthly averages over the complete calibration and validation period) at Kamsack and near Burdick, respectively. The first approach (SWAT with the assumption of no depressions) tends to overestimate the long-term average mean monthly

streamflow. In particular, this approach significantly overestimates the peak flows from spring snowmelt and summer rainstorms because the model does not consider water storage in the depressions that would attenuate the peak flows. On the other hand, the observed monthly averages are generally well represented by both the SWAT-lumped (with single depression) and SWAT-PDLD (with multiple depressions) model predictions. Though both models simulate satisfactorily, the SWAT-PDLD model still provides better performance in matching the average spring runoff flows.

Model performance was also evaluated through multiple statistical metrics. Table 3-2 summarizes results of model evaluation using statistical metrics for average monthly streamflow prediction. Model performance for the monthly streamflow prediction (Table 3–2) was rated based on the scheme presented by Moriasi et al. (2007). In this scheme, models are rated as "very good" for NSE>0.75, "good" for 0.65<NSE≤0.75, "satisfactory" for 0.5<NSE≤0.65, and "unsatisfactory" for NSE≤0.5. Appling these rating criteria for the current study, monthly streamflow prediction capability of the first approach (model set up with the assumption of no depressions) is rated as "unsatisfactory" during the calibration and validation periods. On the other hand, monthly streamflow prediction capability of both the SWAT-lumped and SWAT-PDLD models at Kamsack and Moose Jaw gauging stations can be rated as "very good" during the calibration and validation periods (see Table 3–2).

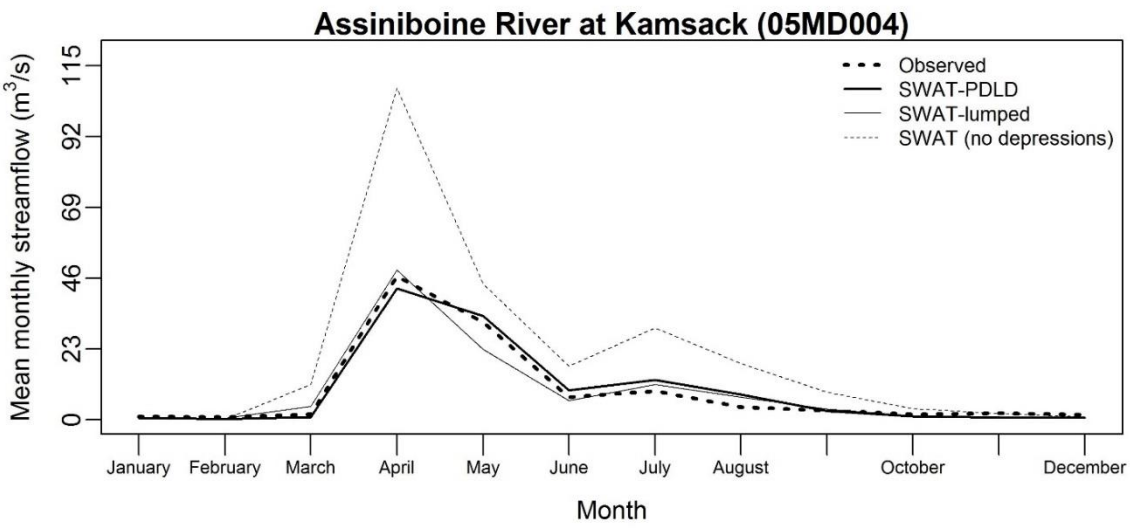

Figure 3–11 Monthly average observed and modelled Assiniboine River flows for the period of January 1992 – December 1999 at Kamsack.

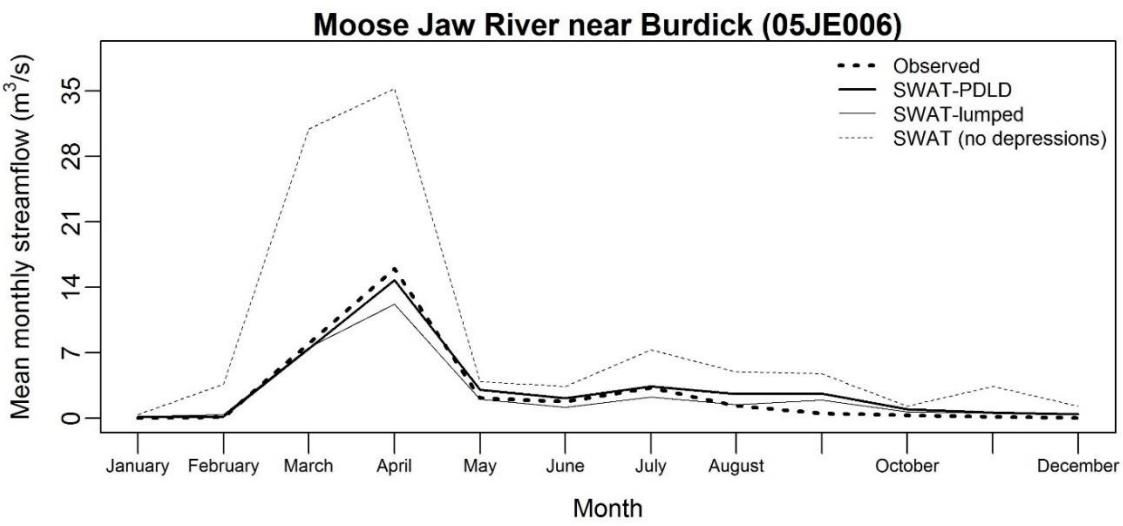

Figure 3–12 Monthly average observed and modelled Moose Jaw River flows near Burdick for the period of January 1992 – December 2002.

Table 3–2 Measures of model performance for monthly streamflow simulation during calibration and validation periods.

Model	Location	Model performance of monthly streamflow: calibration (validation)			
		NSE	R^2	RMSE	NSE Performance rating
SWAT (No depression)	Kamsack	0.37 (-2.00)	0.80 (0.86)	26.93 (28.98)	Unsatisfactory* (Unsatisfactory*)
	Burdick	-0.80(-2.10)	0.87 (0.66)	15.58 (12.77)	Unsatisfactory* (Unsatisfactory*)
SWAT-lumped	Kamsack	0.81 (0.80)	0.87 (0.87)	10.82 (7.40)	Very good* (Very good*)
	Burdick	0.76 (0.84)	0.84 (0.86)	5.74 (2.94)	Very good* (Very good*)
SWAT-PDLD	Kamsack	0.86 (0.89)	0.88 (0.95)	8.84 (5.60)	Very good* (Very good*)
	Burdick	0.90 (0.89)	0.91 (0.91)	3.67 (2.46)	Very good* (Very good*

*NSE performance rating is based on criteria set by Moriasi et al. (2007).

Examining the details of the statistical parameters (i.e., NSE, R^2 and RMSE), the SWAT-PDLD model predicts monthly streamflow better than the SWAT-lumped model during the calibration as well as the validation period for both watersheds (see Table 3–2). For instance at Kamsack on the Assiniboine River the SWAT-PDLD model improved monthly streamflow prediction from 0.81 to 0.86 and 0.80 to 0.89 for the NSE statistical parameter during the calibration and validation period, respectively. Similar analysis of model performance for the second watershed (Moose Jaw) revealed that the SWAT-PDLD model prediction of monthly streamflow is improved over the SWAT-lumped model predictions. More specifically, the monthly streamflow prediction at Moose Jaw near Burdick is improved from 0.76 to 0.90 and 0.84 to 0.89 for NSE during calibration and validation periods, respectively.

Model performance was further assessed for daily streamflow prediction capability (see Table 3–3). Model performance for this daily streamflow prediction was rated based on the scheme presented by Van Liew et al. (2007). In this scheme, models are rated as “good” for NSE>0.75, “satisfactory” for 0.36<NSE≤0.75, and “unsatisfactory” for NSE≤0.36. Following these rating criteria, daily streamflow prediction capability of the first approach (model setup with the assumption of no depressions) is rated as “unsatisfactory” in all cases except at Kamsack station during calibration period.

Table 3–3 Measures of model performance for daily streamflow simulation during calibration and validation periods.

Model	Location	Model performance of daily streamflow: calibration (validation)			
		NSE	R^2	RMSE	NSE performance rating
SWAT (No depression)	Kamsack	0.39 (-3.29)	0.71 (0.43)	30.05 (48.73)	Satisfactory** (Unsatisfactory**)
	Burdick	-3.08 (-6.50)	0.76 (0.48)	28.59 (22.05)	Unsatisfactory** (Unsatisfactory**)
SWAT-lumped	Kamsack	0.76 (0.50)	0.82 (0.65)	18.97 (16.69)	Good** (Satisfactory**)
	Burdick	0.69 (0.76)	0.72 (0.78)	7.82 (3.91)	Satisfactory** (Good**)
SWAT-PDLD	Kamsack	0.79 (0.72)	0.85 (0.79)	17.60 (12.37)	Good** (Satisfactory**)
	Burdick	0.79 (0.81)	0.79 (0.81)	6.49 (3.49)	Good** (Good**)

** NSE performance rating is based on criteria set by van Liew et al. (2007).

On the other hand, both SWAT-lumped and SWAT-PDLD models are rated as satisfactory and above. In general both the SWAT-lumped and SWAT-PDLD models are able to representatively simulate the daily streamflow near Burdick and at Kamsack gauging stations. Details of statistical metrics (Table 3–3), however, revealed that the SWAT-PDLD performed better than the SWAT-lumped model for both watersheds during the calibration as well as validation periods.

3.8.3 Discussion

Watersheds with a large number of landscape depressions with scarce data on their physiography are difficult to model. Therefore assumptions and simplifications need to be made to incorporate depression storage into the SWAT model.

One typical assumption used in previous studies that have attempted to use SWAT to model streamflow generated from depression-dominated landscapes on the Canadian prairies is to assume ‘no landscape depressions’. In the current work when SWAT was used with all areas contributing it was seen that the model consistently overestimated streamflow (with daily NSE

values in the range of -6.5 to 0.39). This poor modeling result is similar to previous works where that assumption was used. For example, Chanasyk et al. (2003) applied the SWAT model over three watersheds that varied from 1.5 to 226 ha in Saskatchewan, Canada. They found model performance based upon NSE that ranges from -35.7 to -0.005. On the other hand, Shrestha et al. (2011) reported satisfactory model performance in a prairie watershed (NSE= 0.65) with a similar modelling approach (no depressions). However, this comes at the expense of forcing parameter values outside of the recommended limits. In their study, they assigned a value of 0.11 to the Manning's n for the main channel parameter, which is much higher than the recommended range (which is below 0.065 for natural streams) (Arnold et al. 2012). In addition, they reduced the curve number values by 13% from default values. In the case of Shrestha et al. (2011), the reduced curve number affects the surface runoff generated and the increased Manning's n values would act to slow water flow through the main channel. Similar behavior of parameter values were observed under the current study with the assumption of no depressions. For instance, the SCS curve numbers under the assumption of no depressions tend have values lower than model setups for both study watersheds that account for the presence of surface depressions.

Another typical assumption is that the numerous depressions can be represented by a single lumped storage. With the use of a single lumped storage to simulate depressions for each sub-basin (using the Pond routine in SWAT), the daily NSE values in the current study did improve to give values of 0.76 and 0.69 for the Assiniboine and Moose Jaw watersheds respectively. However, this modelling approach tends to underestimate most of the peak flows. Similar behaviours were observed by Wang et al. (2008). As explained by Wang et al. (2008), the underestimation using the single lumped storage approach is due to inappropriate representation of the numerous depressions that vary in storage capacity within a prairie

watershed. Further improvement of model performance is achieved by incorporating the numerous depressions storage heterogeneity into the SWAT model using a probability distributed model (PDLD). It was seen that the distributed PDLD approach improves streamflow simulation for the study watersheds. All model performance statistical metrics that were used in the current study showed improved simulations of streamflow by the new SWAT-probability distributed landscape depressions modelling framework in comparison to the single lumped storage approach.

3.9 Conclusion

Landscape depressions have a significant influence on flow processes in depression dominated watersheds. Depressions are numerous and vary in storage capacity at a watershed scale. This study shows improved simulation can be achieved by incorporating landscape depressions heterogeneity into the SWAT model. In particular, the current study presents a probability distributed landscape depressions (PDLD) algorithm that was developed to represent multiple landscape depressions that can exist within a prairie watershed. The PDLD algorithm considers the spatial variability of depression storage capacity using a probability distribution function. The PDLD algorithm was integrated into the SWAT model as a modelling framework referred to as SWAT-PDLD. The depression storage algorithm in the SWAT model (lumped approach) cannot represent multiple landscape depressions of differing storage capacity that can exist within a sub-basin. The two models, SWAT with lumped storage enabled and the SWAT-PDLD, were evaluated for streamflow prediction capability using visual inspection of hydrographs and multiple statistical metrics.

Model performance was evaluated at daily and monthly time scales for two different watersheds in the Canadian prairie region: the Moose Jaw River near Burdick, Saskatchewan and

the Assiniboine River at Kamsack, Saskatchewan. Visual comparisons of the observed and predicted hydrographs showed that both daily and monthly streamflow were satisfactorily simulated by both models (SWAT-lumped and SWAT-PDLD) unlike the approach with an assumption of no depressions. Further assessment of the two models reveal that streamflow is better simulated by the SWAT-PDLD model as compared to the SWAT-lumped routine with or without the storage algorithm engaged for both watersheds. In particular, peak flows are better represented by the SWAT-PDLD model. The results of the study also show that all statistical measures of model performance for prediction of streamflow are improved for the SWAT-PDLD model. In general it is concluded that integration of the new PDLD algorithm into the SWAT model improves its streamflow prediction capability in a depression dominated watershed.

3.10 Acknowledgments

The authors would like to thank the Province of Saskatchewan Go Green Fund for financial support for this work and the Natural Sciences and Engineering Research Council of Canada (NSERC) in terms of Discovery Grants to the second author. The data used in this study were provided by Agriculture and Agri-Food Canada (precipitation, temperature, and soil data), GeoBase Canada (DEM and land cover data), and Environment Canada (streamflow data: HYDAT). The authors would also like to thank Dr. Monique Dube for her initial work in the developing the broader project in which this work was part.

3.11 References

Abedini, M.J. 1998. On depression storage, it's modelling and scale, Ph.D. thesis, Department of Water Resources Engineering, University of Guelph, Guelph, Canada.

Almendinger, J.E., Murphy, M.S., Ulrich, J.S. 2012. Use of the Soil and Water Assessment Tool to scale sediment delivery from field to watershed in an agricultural landscape with topographic depressions. Journal of Environmental Quality, **43**(1): 9–17.

Arnold, J.G., Srinivasan, R., Muttiah, R.S., Williams, J.R. 1998. Large-area hydrologic modeling and assessment: Part I Model development. J. American Water Resour. Assoc., **34**(1): 73–89.

Bell, V.A., Kay, A.L., Jones, R.G., Moore, R.J. 2007. Use of a grid-based hydrological model and regional climate model outputs to assess changing flood risk. International Journal of Climatology, **27**(12): 1657–1671.

Bell, V.A., Kay, A.L., Jones, R.G., Moore, R.J., Reynard, N.S. 2009. Use of soil data in a grid-based hydrological model to estimate spatial variation in changing flood risk across the UK. Journal of Hydrology, **377** (3-4): 335–350.

Beven, K.J. 2012. Rainfall-Runoff Modelling: The Primer, 2nd Edition, Wiley-Blackwell, Chichester, UK.

Chanasyk, D.S., Mapfumo, E., Willms, W. 2003. Quantification and simulation of surface runoff from fescue grassland watersheds. Agricultural Water Management, **59**(2): 137–153.

Choi, W., Kim, S.J., Rasmussen, P.F., Moore, A.R. 2009. Use of the North American Regional Reanalysis (NARR) for hydrological modelling in Manitoba. Canadian Water Resources Journal, **34**(1):17–36.

Chu, X., Yang, J., Chi, Y., Zhang, J. 2013. Dynamic puddle delineation and modeling of puddle-to-puddle filling-spilling-merging-splitting overland flow processes. Water Resources Research, **49**(6): 3825–3829.

Cunge, L.A. 1969. On the subject of a flood propagation method (Muskingum method). J. Hydraulic Research, **7**(2): 205–230.

Environment Canada. 2009. Canadian climate normals 1971-2000. Accessed on Sep. 10, 2011. http://www.climate.weatheroffice.ec.gc.ca/climate_normals/index_e.html.

ESRI (Environmental Systems Research Institute). 2011. Arc hydro tools: Tutorial, version 2.0. Environmental Systems Research Institute, Redlands, CA.

Euliss, Jr, N.H., Mushet, D.M., Wrubleski, D.A. 1999. Wetlands of the Prairie Pothole Region: invertebrate species composition, ecology, and management. Batzer, D.P., Rader, R.B. and Wissinger, S.A., eds. Invertebrates in Freshwater Wetlands of North America: Ecology and Management, Chapter 21. John Wiley & Sons, New York. Jamestown, ND: Northern Prairie Wildlife Research Center Online. Accessed on Jan. 15, 2013. http://www.npwrc.usgs.gov/resource/wetlands/pothole/index.htm.

Fang, X., Pomeroy, J.W. 2008. Drought impacts on Canadian prairie wetland snow hydrology. Hydrological Processes, **22**(15): 2858–2873.

Fontaine, T.A., Cruickshank, T.S., Arnold, J.G., Hotchkiss, R.H. 2002. Development of a snowfall–snowmelt routine for mountainous terrain for the soil water assessment tool (SWAT). Journal of Hydrology, **262**(1–4): 209–223.

Gassman, P.W., Reyes, M.R., Green, C.H., Arnold, J.G. 2007. The Soil and Water Assessment Tool: historical development, applications, and future research directions. Trans. ASABE, **50**(4): 1211–1250.

GeoBase Canada. 2007. Canadian Digital Elevation Data, Level 1 Product Specifications. Government of Canada Natural Resources, Canada Centre for Topographic Information, Sherbrooke, Quebec, Canada.

GeoBase Canada. 2009. Land Cover, circa 2000-Vector data product specifications: Edition 1.0. Centre for Topographic Information, Earth Sciences Sector, Natural Resources Canada, Sherbrooke, Quebec, Canada.

Godwin, R.B., Martin, F.R. 1975. Calculation of Gross and Effective Drainage Areas for the Prairie Provinces, Canadian Hydrology Symposium, (p. 5), Winnipeg.

Granger, R.J., Gray, D.M., Dyck, G.E. 1984. Snowmelt infiltration to frozen prairie soils. Canadian Journal of Earth Science, **21**(6): 669–677.

Gray, D.M., Landine, P.G. 1988. An energy-budget snowmelt model for the Canadian Prairies. Canadian Journal of Earth Sciences, **25**(8): 1292–1303.

Green, W.H., Ampt, G.A. 1911. Studies on soil physics-1: The flow of air and water through soils. J. Agric. Sci., **4**: 11–24.

Hargreaves, G.L., Hargreaves, G.H., Riley, J.P. 1985. Agricultural benefits for Senegal River Basin. J. Irrig. Drain. Eng., **111**(2): 113–124.

Hayashi, M., Quinton, W.L., Pietroniro, A., Gibson, J.J. 2004. Hydrologic functions of wetlands in a discontinuous permafrost basin indicated by isotopic and chemical signatures. Journal of Hydrology, **296**(1–4): 81–97.

Hayashi, M., van der Kamp, G., Schmidt, R. 2003. Focused infiltration of snowmelt water in partially frozen soil under small depressions. Journal of Hydrology, **270**(3–4): 214–229.

Hayashi, M., van der Kamp, G., Rudolph, D.L. 1998. Water and solute transfer between a prairie wetland and adjacent uplands: 1. Water balance. Journal of Hydrology, **207**(1–2): 42–55.

Hutchinson, M.F., McKenney, D.W., Lawrence, K., Pedlar, J.H., Hopkinson, R.F., Milewska, E., Papadopol, P. 2009. Development and Testing of Canada-Wide Interpolated Spatial Models of Daily Minimum–Maximum Temperature and Precipitation for 1961-2003. Journal of Applied Meteorology and Climatology, **48**: 725–741.

Iacobellis, V., Castorani, A., Di Santo, A.R., Gioia, A. 2015. Rationale for flood prediction in karst endorheic areas. Journal of Arid Environments, **112**: 98–108.

Kiesel, J., Fohrer, N., Schmalz, B., White, M.J. 2010. Incorporating landscape depressions and tile drainages of a northern German lowland catchment into a semi-distributed model. Hydrological Processes, **24**(11): 1472–1486.

Kissinger, M., Rees, W.E. 2009. Footprints on the prairies: Degradation and sustainability of Canadian agricultural land in a globalizing world. Ecological Economics, 68(8–9): 2309–2315.

Labaugh, W.L., Winter, T.C., Rosenberry, D.O. 1998. Hydrologic functions of prairie wetlands. Great Plains Research, **8**(spring): 17–37.

Leibowitz, S.G., Vining, K.C. 2003. Temporal connectivity in a prairie pothole complex. Wetlands, **23**(1): 13–25.

Linsley, R.K., Kohler, M.A., Paulus, J.L. 1949. Applied hydrology, McGraw-Hill: New York.

Mekonnen, B.A., Nazemi, A., Mazurek, K.A., Elshorbagy, A., Putz, G. 2015. Hybrid modelling approach to prairie hydrology: Fusing data-driven and process-based hydrological models. Hydrological Sciences Journal, **60**(9): 1473–1489.

Mekonnen, M.A., Wheater, H.S., Iresona, A.M., Spence, C., Davison, B., Pietroniro, A. 2014. Towards an improved land surface scheme for prairie landscapes. Journal of Hydrology, **511**: 105–116.

Moore, R.J. 1985. The probability-distributed principle and runoff production at point and basin scales. Hydrological Sciences Journal, **30**(2): 273–297.

Moore, R.J. 2007. The PDM rainfall-runoff model. Hydrology and Earth System Sciences, **11**(1): 483–499.

Moore, R.J., Clarke, R.T. 1981. A distribution function approach to rainfall runoff modelling. Water Resources Research, **17**(5): 1367–1382.

Monteith, J.L. 1965. Evaporation and the environment: In The state and movement of water in living organisms, Proc. 19th Symp. Swansea, UK, Society of Experimental Biology, Cambridge University Press.

Moriasi, D.N., Arnold, J.G., Van Liew, M.W., Bingner, R.L., Harmel, R.D., Veith, T.L. 2007. Model evaluation guidelines for systematic quantification of accuracy in watershed simulations. Trans. ASABE, **50**(3): 885–900.

Nash, J.E., Sutcliffe, J.V. 1970. River flow forecasting through conceptual models. Part I: A discussion of principles. Journal of Hydrology, **10**(2): 282–290.

Neitsch, S.L., Arnold, J.G., Kiniry, J.R., Williams, J.R. 2011. Soil and Water Assessment Tool theoretical documentation: Version 2005, Grassland, Soil and Water Research Laboratory, Blackland Research Center, Temple, TX.

Noto, L.V. 2014. Exploiting the topographic information in a PDM - based conceptual hydrological model. Journal of Hydrological Engineering, **19**(6): 1173–1185.

Pomeroy, J.W., Gray, D.M., Brown, T., Hedstrom, N.M., Quinton, W., Granger, R.J., Carey, S. 2007. The Cold Regions Hydrological Model, a platform for basing process representation and model structure on physical evidence. Hydrological Processes, **21**(19): 2650–2667.

Priestley, C.H.B., Taylor, R.J. 1972. On the assessment of surface heat flux and evaporation using large-scale parameters. Mon. Weather Rev., **100**(2): 81–92.

Ritchie, J.T. 1972. A model for predicting evaporation from a row crop with incomplete cover. Water Resources Research, 8(5): 1204–1213.

Rosenberry, D.O., Winter, T.C. 1997. Dynamics of water-table fluctuations in an upland between two prairie-pothole wetlands in North Dakota. Journal of Hydrology, 191(1–4): 266–289.

Saskatchewan Watershed Authority (SWA). 2005. Background report: Assiniboine River watershed, Regina, Technical committee, 123 pp.

SCS (Soil Conservation Service). 1972. National engineering handbook, Section 4: Hydrology, SCS, USA.

Shaw, D.A, van der Kamp, G., Conly, F.M., Pietroniro, A., Martz, L. 2011. The Fill-Spill Hydrology of prairie wetland complexes during drought and deluge. Hydrological Processes, **26**(20): 3147–3156.

Shook, K., Pomeroy, J.W., Spence, C., Boychuk, L. 2013. Storage Dynamics simulations in prairie wetland hydrology models: evaluation and parameterization. Hydrological Processes, **27**(13): 1875–1889.

Shrestha, R.R., Dibike, Y.B., Prowse, T.D. 2012. Modeling Climate Change Impacts on Hydrology and Nutrient Loading in the Upper Assiniboine Catchment. J. American Water Resour. Assoc., **48**(1): 74–89.

Shrestha, R.R., Dibike, Y.B., Prowse, T.D. Modelling of climate-induced hydrologic changes in the Lake Winnipeg watershed. Journal of Great Lakes Research, **38**: 83–94.Soil Landscapes of Canada Working Group. 2007. Soil Landscapes of Canada v3.1.1,

Agriculture and Agri-Food Canada, Digital Map and Database at 1:1 Million Scale, http://sis.agr.gc.ca/cansis/nsdb/slc/v3.1.1/intro.html.

Sophocleous, M.A., Koelliker, J.K., Govindaraju, R.S., Birdie, T., Ramireddygari, S.R., Perkins, S.P. 1999. Integrated numerical modeling for basin-wide water management: The case of the Rattlesnake Creek basin in south-central Kansas. Journal of Hydrology, **214**(1–4): 179–196.

Stewart, B. 2006. Measures and causes of productivity growth in Prairie agriculture. MSc thesis, University of Alberta.

Stewart, B., Veeman, T.S., Unterschultz, J. 2009. Crops and livestock productivity growth in the Prairies: The impacts of technical change and scale. Canadian Journal of Agricultural Economics, **57**(3): 379–394.

Su, M., Stolte, W.J., van der Kamp, G. 2000. Modelling Canadian prairie wetland hydrology using a semi-distributed streamflow model. Hydrological Processes, **14**(14): 2405–2422.

Tiner, R.W. 2003. Geographically isolated wetlands of the United States. Wetlands, 23(3): 494–516.

Tolson, B.A., Shoemaker, C.A. 2007. Cannonsville reservoir watershed SWAT2000 model development, calibration, and validation. Journal of Hydrology, **337**(1-2): 68–86.

Ullah, W., Dickinson, W.T. 1979. Quantitative description of depression storage using a digital surface model, II. Characteristics of surface depressions. Journal of Hydrology, **42**(1–2): 77–90.

van der Kamp, G., Hayashi, M. 2009. Groundwater-wetland ecosystem interaction in the semiarid glaciated plains of North America. Hydrogeology Journal, **17**(1): 203–214.

van der Kamp, G., Hayashi, M., Gallen, D. 2003. Comparing the hydrology of grassed and cultivated catchments in the semi-arid Canadian prairies. Hydrological Processes, **17**(3): 559–575.

van Liew, M.W., Arnold, J.G., Garbrecht, J.D. 2003. Hydrologic Simulation on agricultural watersheds choosing between two models. Trans. ASABE, **46**(6): 1539–1551.

van Griensven, A., Meixner, T., Grunwald, S., Bishop, T., Di Luzio, M., Srinivasan, R. 2006. A global sensitivity analysis method for the parameters of multi-variable watershed models. Journal of Hydrology, **324**(1–4): 10–23.

Wang, X., Yang, W., Melesse, A.M. 2008. Using hydrologic equivalent wetland concept within SWAT to estimate streamflow in watersheds with numerous wetlands. Trans. ASAE, **51**(1): 55–72.

Williams, J.R. 1969. Flood routing with variable travel time or variable storage coefficients. Trans. ASAE, **12**(1): 100−103.

Winter, T.C., Woo, M.K. 1990. Hydrology of lakes and wetlands. In The Geology of North America, Vol. 0-1, Surface Water Hydrology, 159-87. Boulder, CO: The Geological Society of America.

Woo, M.K., Rowsell, R.D. 1993. Hydrology of a prairie slough. Journal of Hydrology, **146**(1–4): 175–207.

Yang, W., Wang, X., Liu, Y., Gabor, S., Boychuk, L., Badiou, P. 2010. Simulated environmental effects of wetland restoration scenarios in a typical Canadian prairie watershed. Wetlands Ecology and Management, **18**(3): 269–279.

Zhang, X., Srinivasan, R., Debele, B., Hao, F. 2008. Runoff simulation of the headwaters of the Yellow River using the SWAT model with three snowmelt algorithms. J. American Water Resour. Assoc., 44(1): 48–61.

Zhou, Y., Guo, S., Xu, C., Liu, P., Qin, H. 2015. Deriving joint optimal refill rules for cascade reservoirs with multi-objectives evaluation. Journal of Hydrology, **524**: 166–181.

CHAPTER 4 SEDIMENT EXPORT MODELING IN COLD CLIMATE PRAIRIE WATERSHEDS

This chapter is a case study paper in the Journal of Hydrologic Engineering.

Citation: Mekonnen, B.A., Mazurek, K.A., and Putz, G. (2016). Sediment export modelling in cold climate prairie watersheds. Journal of Hydrologic Engineering, DOI: 10.1061/(ASCE)HE.1943–5584.0001336.

The document has been reformatted from the original version for inclusion in the thesis though no content has changed from the published version.

Contribution of the PhD candidate

The contribution of the Ph.D. candidate to this paper includes the following: identification of the limitations of the current SWAT model for sediment simulation under cold-climate conditions; conceptualization of sediment generation processes in a cold climate and incorporation into the SWAT model; evaluation and comparison study between the modified and original SWAT model for sediment export simulation over two cold climate prairie watersheds; and analysis of results. The second and third authors (the Ph.D. supervisors) provided advice on various aspects of the work. The text of the published manuscript was drafted by the candidate with the second and third authors (the Ph.D. supervisors) offering critical review and editorial guidance.

Contribution of this chapter to the overall study

With the broad aim of a developing flow and pollutant loadings estimator for Canadian prairie watersheds, this Chapter contributes to the general theme by focusing on the sediment simulation aspects of this research, which serves as the second step towards attaining the general objective. This work is a continuation from the previous Chapter and mainly focuses on modification and evaluation of the SWAT–PDLD streamflow modeling framework for sediment export simulation. Accurate estimation of sediment export is important for better simulation of nutrient export as nutrient movement can also occur attached to sediments. Therefore, it is important to simulate sediment export appropriately following streamflow but prior to simulating other pollutants.

Accordingly, this work, as part of the overall objectives, mainly focuses on developing a sediment simulation model for the study watersheds. This was carried out by conceptualizing sediment generation processes by season. In particular, this was addressed by allowing seasonally varying soil erodibility factors. Accordingly, the original sediment module of SWAT, Modified Universal Soil Loss Equation (MUSLE), that uses annual values of the soil erodibility factor, was modified to incorporate seasonal variability of soil erodibility. The modified sediment module of SWAT–PDLD was applied over two large area prairie watersheds. The predictions in sediment yield achieved by the modified model are compared with those produced from the sediment module found in the original SWAT model. The modified SWAT–PDLD with seasonally varying soil errodiblity model was found to be a better sediment yield simulation tool.

4.1 Abstract

Non–point source pollution is a critical problem in Canadian prairie watersheds. However, sediment mobilization and export are poorly represented in existing models for these

watersheds. The poor representation is partly because the hydrology of the region is highly influenced by the existence of numerous dynamically–connected landscape depressions that vary in storage capacity and because of the complex freeze–thaw cycles in the region. The objective of this research was to improve sediment export simulation modelling in these cold climate prairie watersheds by incorporating a probability distribution function of depression storage capacity and a seasonally varying soil erodibility factor into the Soil and Water Assessment Tool (SWAT) model. The probability distribution function is used to represent the variation in storage capacity of the numerous depressions, whereas the seasonally varied soil erodibility factor is used to account for changes in erodibility as the soil freezes and thaws. Results from two case study watersheds confirm an improvement in sediment export predictions when varying storage capacity is represented and the sediment loss routine includes seasonally varying soil erodibility.

4.2 Introduction

The introduction of agriculture in the late 1800s and early 1900s increased sedimentation in water bodies in Canadian Prairie watersheds (Wall et al. 1995; de Boer et al. 2005; Koroluk and de Boer 2007). There are ongoing plans to further increase agricultural activity in the region (Saskatchewan Ministry of Agriculture 2013). Not only can sediment itself degrade water quality, but it also carries other pollutants to the water body (Koroluk 2000; Koroluk and de Boer 2007). Accurate estimation of streamflow and sediment export is important for predicting potential adverse impacts of anthropogenic activities and for guiding the management of water resources systems to mitigate environmental effects.

Simulation of hydrological processes on the prairie landscape, however, remains challenging due to the numerous landscape depressions that store water and vary in storage capacity. The North American Prairie Region, which covers a vast area of West–Central Canada

and the North–Central United States, is characterized by low relief landscapes dotted with millions of depressional wetlands called potholes or sloughs that are largely the result of glaciation events (Winter and Woo, 1990; Euliss et al. 1999). Depressional wetlands play an important environmental role because they attenuate flooding and serve as traps for sediment and nutrients (Koroluk 2000; Du et al. 2005; Almendinger et al. 2012).

For a single landscape depression, the water budget includes precipitation on the water surface, surface runoff from the uplands, evapotranspiration, surface outflow (overflow) when a depression is filled beyond capacity, and groundwater flow (Woo and Rowsell 1993; Winter and Woo 1990; Hayashi et al. 1998; Fang and Pomeroy 2008). This "fill and spill" mechanism of a depression is reasonably straightforward to implement into a hydrological model for a single depression. However, streamflow and sediment export processes over a large prairie watershed area occur in the presence of the millions of landscape depressions. The response of the watershed in the presence of these numerous depressions is complex. It is highly dependent on topographic details of the landscape, including the pothole geometry and location and connectivity between the potholes (van der Kamp and Hayashi 2009; Shaw et al. 2011). The heterogeneity in storage in the depressions and the dynamic connectivity between depressions result in a dynamic contributing area in prairie watersheds (Shaw et al. 2011).

For streamflow prediction in large–area prairie watersheds, a potential approach to handle the landscape depressions was suggested by Ullah and Dickison (1979), who proposed that a probability distribution could be used to account for the variability in storage on the landscape. Abedini (1998) followed this idea and tested, at plot and laboratory scale, the probability–distributed models being used to describe heterogeneity in soil moisture storage (e.g., Moore 1985; 2007) to model runoff produced in a landscape with depressions. Such approach has then

been successfully applied, in larger areas, to represent the surface depressional storage distribution of the upper Kolyma River basin in the permafrost region of Russia (the catchment area is 99,400 km^2) (Kuchment et al. 2000). Similarly, Mekonnen et al. (2014) implemented a probability–distributed model for depression storage in the Modélisation Environmentale Communautaire – Surface and Hydrology (MESH) model (a grid–based model using Grouped Hydrological Response Units) for predicting streamflow in a small watershed (1939 km^2). Recently, Mekonnen et al. (2016) have incorporated a probability–distribution model into the Soil and Water Assessments Tool (SWAT) in order to handle the landscape depressions for streamflow prediction in two large–area prairie watersheds in Saskatchewan, Canada: the Assiniboine River Basin (watershed area of 1300 km^2); and the Moose Jaw River Basin (watershed area of 9320 km^2). They reported good results for streamflow simulation based on several statistical parameters and improved streamflow simulation over the case of aggregated depression storage into a single storage for each hydrological response unit. However, the applicability of such conceptualization so far has not been tested for sediment export prediction.

In considering the sediment budget for a cold–climate, prairie watershed with depressions, sediment is mobilized from open fields. Some portion of that sediment directly reaches the watershed outlet. However, much of the sediment is trapped within the watershed (Lane et al. 1997). Sediment is detained whenever runoff velocity is low enough to deposit the suspended sediment (Kleiss 1996; Lane et al. 1997). For the depressions in particular, it has been demonstrated that the depressions in the prairie region are sediment sinks (Koroluk 2000; Almendinger et al. 2012). The wetlands forming in these depressions are often regarded as hydrologically–closed basins because they do not have permanent surface inflow or outflow (Parsons et al. 2004). Landscape depressions also modify the movement of water through a

watershed by lowering the peak flow and volume of flood discharges, reducing sediment carrying capacity (Kleiss 1996; Neitsch et al. 2011).

Sediment mobilization and export from cold–climate watersheds are expected to be higher during the snowmelt period (Aldrich and Slaughter 1983; Dickinson et al. 1975; van Vliet and Hall 1991; McConkey et al. 1997). This is because of increased soil erodibility during freeze–thaw cycles (Kirby and Mehuys 1988; Wall et al. 1988), increased surface runoff enhanced by reduced infiltration in frozen or partially–frozen soils (Granger et al. 1984; Gray et al. 2001), and the longer duration of the snowmelt–runoff period as compared to individual rainfall–runoff events (Tiessen et al. 2010). Freeze–thaw cycles are thought to reduce the erosion resistance of the soil as the ice that forms in soil voids during freezing pushes the soil grains apart (Ferrick and Gatto 2005; Dagesse 2013; Edwards 2013). This reduced erosion resistance has been seen in laboratory measurements of the erodibility of frozen soils (e.g., Coote et al. 1988; Wall et al. 1988; Ferrick and Gatto, 2005; Dagesse, 2013), as well as in field experiments (e.g., Kirby and Mehuys 1987; van Vliet and Hall 1991; McConkey et al. 1997). The increased soil erodibility during freeze–thaw has been taken into account in the handbook of RUSLEFAC (Revised Universal Soil Loss Equation Application in Canada), which suggests the soil erodibility factor should be corrected by a factor of two to take into account the increase in erodibility during thawing conditions (Wall et al. 2002). However, most hydrological models used to predict soil export in cold–climate watersheds do not use seasonally adjusted erodibility coefficients (e.g., Yang et al. 2009; Tiessen et al. 2010).

The aim of this study is to adapt and test the applicability of the Soil and Water Assessment Tool (SWAT) for sediment export simulation from cold–climate, depression–dominated prairie watersheds. Several other watershed models exist that can simulate sediment

processes on a watershed scale, such as the Agricultural Non–Point Source Pollution Model (AnnAGNPS) (Geter and Theurer 1998) and the Hydrological Simulation Program Fortran (HSPF) (Donigian et al. 1984). However, SWAT was selected because of its suitability for large–area agricultural watersheds (Gassman et al. 2007), its freely available source code that will permit adaptation (Neitsch et al. 2011), the existence of an extensive manual (e.g., Neitsch et al. 2011), and its GIS interface (di Luzio et al. 2002). To simulate streamflow in a depression–dominated watershed, the modified version of SWAT proposed by Mekonnen et al. (2016), which calculates runoff from landscape depressions based on the available storage capacity of a depression and considers storage variations across the watershed using a probability distribution, was used. This model is called SWAT–Probability Distribution Landscape Depression (SWAT–PDLD). Additionally, to account for the seasonal variability of soil erodibility due to the freeze–thaw process, SWAT–PDLD is further adapted for cold climate conditions by incorporating seasonally varying soil erodibility. The adapted model is applied and tested over two cold–climate, depression–dominated Canadian prairie watersheds: the Assiniboine and Moose Jaw River watersheds in Saskatchewan, Canada.

4.3 Case Studies

4.3.1 Watershed descriptions

The Assiniboine River Basin drains areas in Eastern Saskatchewan and Western Manitoba and terminates at the Red River in Winnipeg (shown in Figure 4–1). The portion of the watershed within the province of Saskatchewan covers an area of about 17,300 km^2. The Kamsack gauging station (05MD004) (51º33’53’’N latitude and 101º54’48’’ W longitude) on the Assiniboine River was used to test the SWAT–PDLD model’s capability to simulate sediment export. Measured daily flow and daily sediment load datasets for the Assiniboine River

at Kamsack were obtained from the Hydrometric Database (HYDAT) of the Water Survey of Canada. The watershed to the Kamsack gauging station has a gross drainage area of 13,000 km^2 of which about 4,320 km^2 is considered as effective area following the definition of Godwin and Martin (1975). Godwin and Martin (1975) define the effective area as that portion of the watershed contributing to the main stream for a 1:2 year return period storm. The elevation in the watershed ranges from 718 m in the southwest and northwest part of the watershed to 428 m near the Kamsack gauging station. The mean annual temperature and precipitation is about 1°C and 450 mm per year, respectively. Sixty–three percent of the total streamflow is generated from snowmelt runoff during April and May (Saskatchewan Watershed Authority 2005). The watershed is predominantly agricultural consisting of annual crops (62%), pasture and range grass (25%), and forest (11%) (Olthof et al. 2008). The predominant soils are generally characterized as Black Chernozemic soils (70%) (Saskatchewan Watershed Authority 2005).

Daily flow and daily sediment data from the Moose Jaw River Basin gauging station near Burdick (50˚24’1.2” N latitude and 105˚23’52.3”W longitude; Station No. 05JE006) was also used to test the SWAT–PDLD model (Figure 4–1). The Moose Jaw River watershed to the Burdick gauging station has a gross drainage area of 9,230 km^2 of

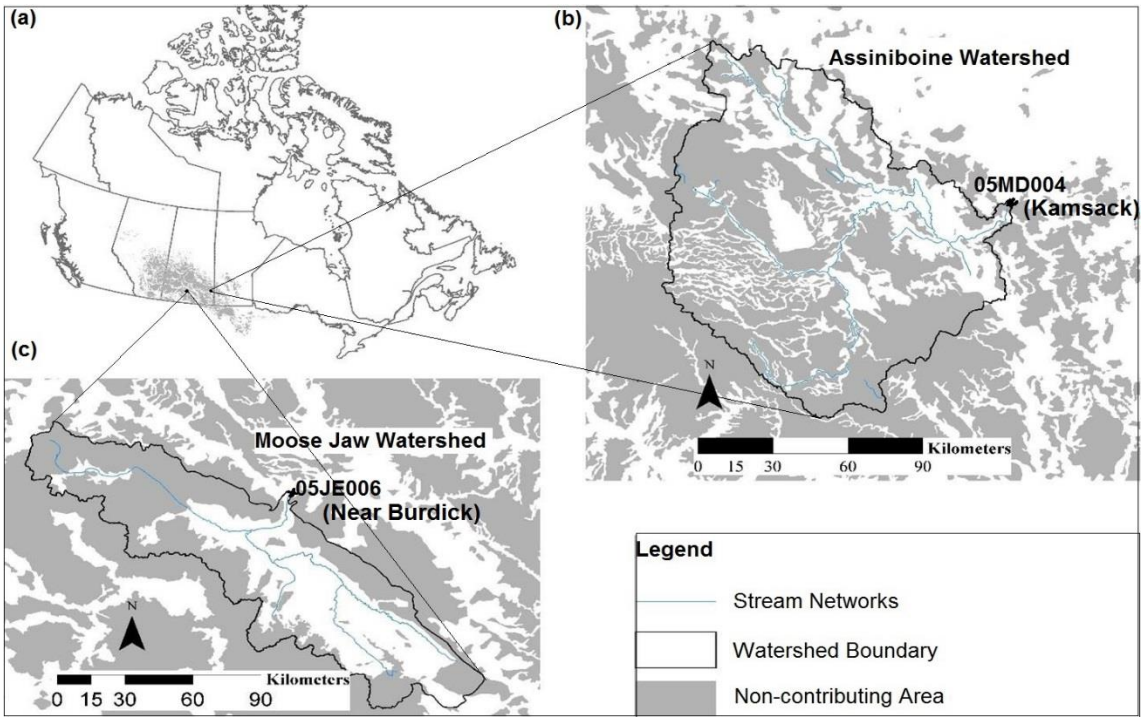

Figure 4–1 The prairie pothole region and location of the case study areas within the Assiniboine and Moose Jaw River Basins in Canada: a) Canada, b) Assiniboine watershed, and c) Moose Jaw watershed.

which about 3,470 km^2 is considered effective drainage area (Godwin and Martin 1975). The elevation of the watershed ranges from 877 m in the southwest region of the watershed to 395 m in the central region near Burdick. According to Environment Canada (2009), the mean annual precipitation at Moose Jaw is 365 mm and annual average air temperature at is 4˚C. Similar to the Assiniboine River, most of the streamflow in the Moose Jaw River at Burdick comes from snowmelt occurring in the early spring. The watershed is predominantly agricultural consisting of annual crops (71%), pasture and range grass (21%), and forest (4%) (Olthof et al. 2008). The soil in the watershed varies from heavy clay soils in the east to gravelly sandy soils in the west (Saskatchewan Watershed Authority 2005).

4.3.2 Seasonality of soil erodibility in the study watersheds

To show the influence of seasonality on soil erodibility in the study watersheds, the sediment load in the Assiniboine and Moose Jaw Rivers were plotted against streamflow for data segmented into periods, as seen in Figures 4–2 and 4–3. The periods designated as follows: Period 1 was taken as November 1 to March 15th; Period 2 included March 16 to March 31st; Period 3 included April 1 to April 30th; and Period 4 was taken as May 1 to October 31st. The period designations were done to match the previous work by McKonkey et al. (1997), who divided their observations of soil erodibility in nearby field–scale experiments (near Swift Current, Saskatchewan) into these seasons based on the characteristics of runoff generation during those periods. In Period 1, runoff was due to snowmelt over frozen ground. In Period 2, runoff occurred due to snowmelt over partially–frozen soil. In Period 3, in areas where there is no snow, the soil is thawed, and in areas with snow, the soil is thawing. In Period 4, there is no snow and the soil is thawed.

In Figure 4–2, for the Assiniboine watershed for Periods 1 and 2 that have a similar range of flow, it is seen that the partially–frozen soils in Period 2 produce higher sediment loads for a given streamflow than during the winter Period 1. Similarly, Period 3 (with some partially–frozen soils) and thawing tends to produce more sediment than in Period 4, when there is a summer condition, for a similar range in streamflow. Figure 4–2 thus indicates that some differences in erodibility of the soils exist for the different periods. Similar results are seen for the Moose Jaw watershed in Figure 4–3.

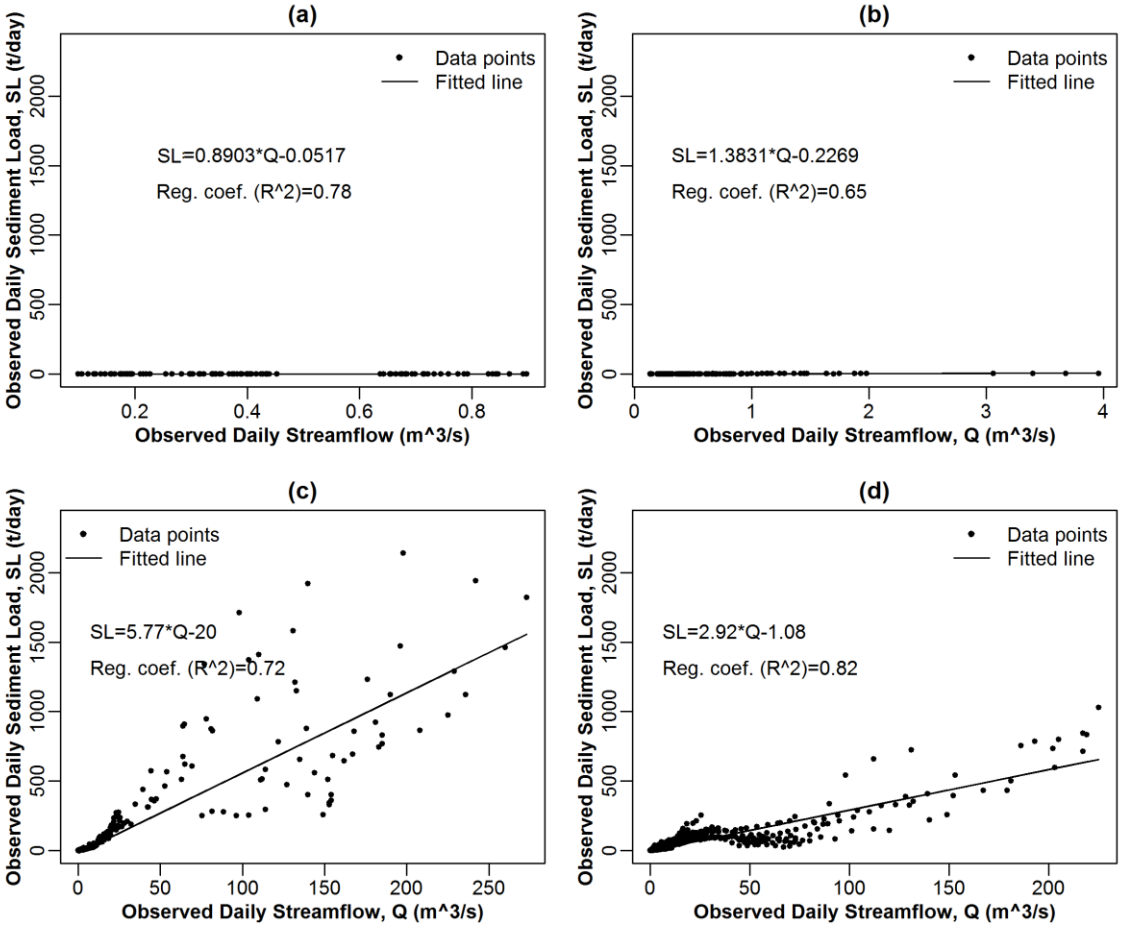

Figure 4–2 Daily flow and sediment load relationship for the Assiniboine River at Kamsack: (a) Period 1: 1 November–15 March, (b) Period 2: 16 March–31 March, (c) Period 3: 1 April–30 April, and (d) Period 4: 1 May–30 October.

The differences in production of sediment load during different periods presented in Figure 4–2 and 4–3 support the results of previous research on the seasonality of soil erodibility in cold–climate watersheds (Aldrich and Slaughter 1983; Dickinson et al. 1975; van Vliet and Hall 1991; McConkey et al. 1997). In the Swift Current watershed, also in Southern Saskatchewan and with similar climatic conditions to the study watersheds, McConkey et al. (1997) investigated the seasonality of soil erodibility in cold climate by measuring the sediment loads produced from three fields with areas of 4.66, 4.86, and 5.06 ha. They conducted measurements over a period of 31 years between 1962 to 1992 and divided the year into four

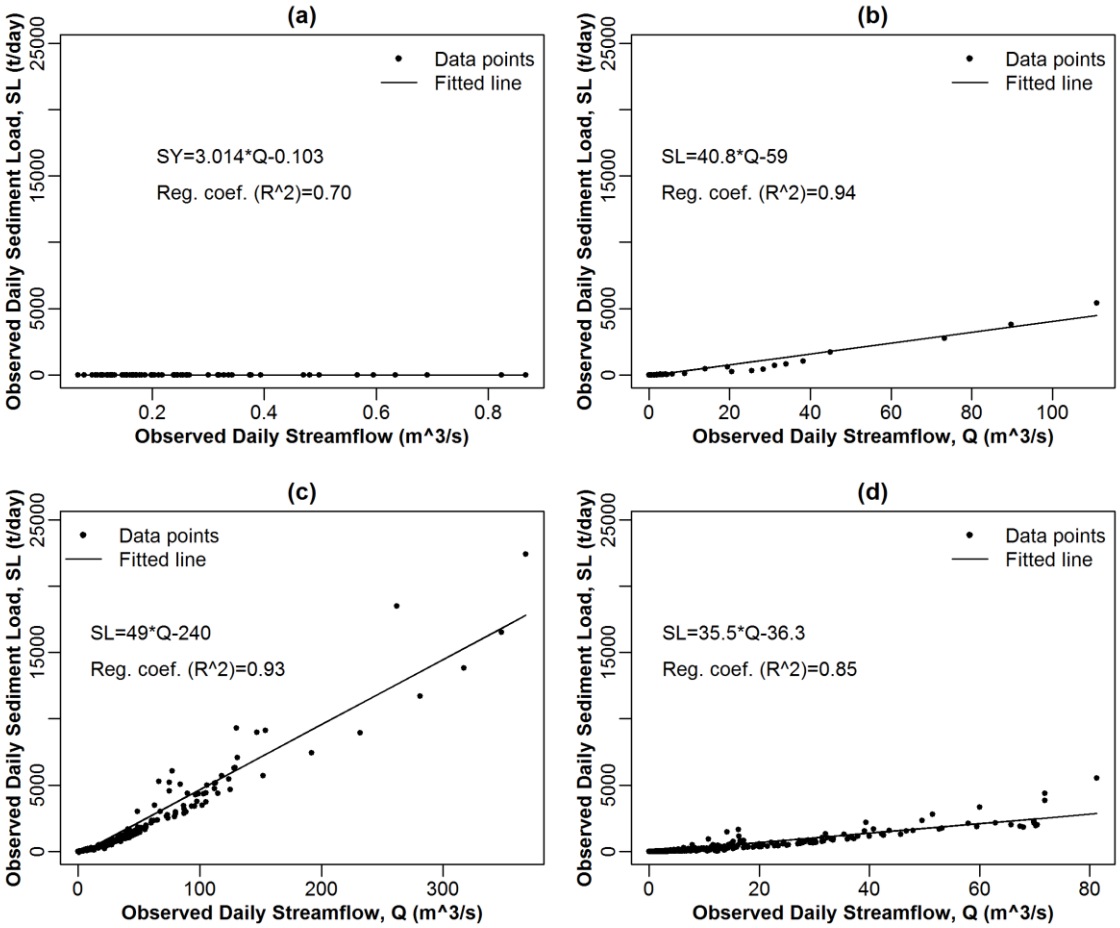

Figure 4–3 Daily flow and sediment load relationship for the Moose Jaw River near Burdick: (a) Period 1: 1 November–15 March, (b) Period 2: 16 March–31 March, (c) Period 3: 1 April–30 April, and (d) Period 4: 1 May–30 October.

periods based on general characteristics of runoff generation as discussed above. They determined the soil erodibility (for the Modified Universal Soil Loss Equation) for Periods 1 to 4 to be 0.021, 0.060, 0.096, and 0.051 Mg h MJ–1 mm–1, respectively. The summer (Period 4) value for erodibility matched the value from the common nomograph used for finding soil erodibility (Wischmeier and Smith 1978). The recognition of the need for using the nomograph K factor for the summer and varying the soil erodibility for other periods is also made in the RUSLE (Renard et al. 1994) and RUSLEFAC (Wall et al. 2002). McConkey et al. (1997) suggested the relative weighting of ratio of the soil erodibility (K) for a given season to that in

the summer should be 0.41 1.18, and 1.9 for Period 1, Period 2, and Period 3. McConkey et al. (1997) also confirmed that these relative K follow the pattern of seasonally weighted K's for a nearby location in the United States. Similar weightings for K are also recommended in the RUSLEFAC handbook (Revised Universal Soil Loss Equation Application in Canada) (Wall et al. 2002). Therefore, these weightings were used in the current modeling work. The erodibility of the soils for the summer for the study watersheds was determined using the nomographs provided in Wischmeier and Smith (1978).

4.4 Model Description and Input Data Requirements

4.4.1 SWAT model description

The Soil and Water Assessment Tool (SWAT: Arnold et al. 1998) is a physically based semi–distributed model that can operate on different time steps including daily and/or sub–daily (Neitsch et al. 2011). As a semi–distributed model, SWAT implements a Hydrological Response Units (HRUs) based approach to represent heterogeneity of land–use, soil type, and slope within a sub–basin. The SWAT model utilizes a water balance approach, which is calculated at the HRU level.

For the water budget for each HRU, the model simulates precipitation, surface runoff, infiltration, evapotranspiration, lateral flow, groundwater flow, deep aquifer recharge, and soil moisture storage. Daily or sub–daily precipitation (both rainfall and snowfall) data is imported for each HRU. For snow, the model uses the temperature–index method to predict snowmelt. Surface runoff and infiltration amounts for each HRU can be estimated using either the curve number method (Soil Conservation Service 1972) or Green and Ampt method (Mein and Larson 1973). The curve number method was used for the current work. Three different techniques are available in SWAT to estimate potential evapotranspiration, including the Hargreaves

(Hargreaves et al. 1985), Priestley–Taylor (Priestley and Taylor 1972), and Penman–Monteith (Monteith 1965) methods. For this study, the Hargreaves method was used. The model then calculates the actual evaporation from soils and plants following the Ritchie (1972) procedure. The infiltrated water that percolates through each soil layer is modeled in SWAT using a storage routing technique (Arnold et al. 1998). The SWAT model simulates the groundwater system by partitioning groundwater into a two–aquifer system (shallow and deep) (Arnold et al. 1998). Following estimation of the water budget for each HRU, the water yield at a sub–basin level is estimated as a weighted sum of yields from all HRUs within a sub–basin. The water yield generated from a sub–basin is then routed through a river channel following either the variable storage (Williams 1969) or the Muskingum routing method (Cunge 1969) procedures. Herein, the variable storage method was used.

Soil erosion from each HRU is quantified using the Modified Universal Soil Loss Equation (MUSLE) (Williams 1975) and the estimated surface runoff. The Modified Universal Soil Loss Equation differs from the standard Universal Soil Loss Equation in that it uses the runoff hydrograph rather than rainfall energy to estimate erosive power of individual runoff events, given by:

$$S = 11.8(QqA_{hru})^{0.56} K * LS * C * P * CFRG \tag{4.1}$$

where S = sediment export on a given day (metric tons), Q = surface runoff volume (mm H_2O ha^{-1}), q = peak runoff rate (m^3 s^{-1}), A_{hru} = area of the HRU (ha), K = soil erodibility factor, LS = topographic factor, C = cover and management factor , P = supporting practice factor, and $CFRG$ = coarse fragment factor. As noted, herein the SWAT model was modified to allow

seasonality of the soil erodibility factor, K, in order to simulate cold climate watershed sediment export.

The mobilized sediment from the landscape is lagged and routed through grassed waterway, vegetative filter strips, and water bodies such as wetlands, if available, before reaching the main channel (Neitsch et al. 2011). The sediment reaching the main channel then will be routed through the main channel of a sub–basin by considering both deposition and erosion processes. These are determined by comparing the maximum concentration of sediment that can be transported by the water, $CONC_{sed,ch,mx}$, with the concentration of sediment in the reach at the beginning of the time step, $CONC_{sed,ch,i}$. The maximum concentration of sediment that can be carried by water is estimated as follows:

$$CONC_{sed,ch,mx} = c_{sp} * v_{ch,pk}^{spexp} \tag{4.2}$$

where $CONC_{sed,ch,mx}$ = the maximum concentration of sediment that can be transported by the water (ton/m^3), c_{sp} = a coefficient calibrated by the user, $v_{ch,pk}$ = the peak channel velocity (m/s), and $spexp$ = an exponent calibrated by the user, which normally varies between 1 and 2. The peak channel velocity, $v_{ch,pk}$, is calculated as follows:

$$v_{ch,pk} = \frac{q_{ch,pk}}{A_{ch}} = \frac{prf * q_{ch}}{A_{ch}} \tag{4.3}$$

where $q_{ch,pk}$ = the peak flow rate (m^3/s), A_{ch} =the cross–sectional area of flow, prf =the peak rate adjustment factor (a calibrated quantity), and q_{ch} =the daily average flow rate (m^3/s).

For Eq. (4.2), if $CONC_{sed,ch,i} > CONC_{sed,ch,mx}$ deposition is the dominant process in the reach segment and the net amount of sediment deposited is determined using:

$$SED_{dep} = (CONC_{sed,ch,i} - CONC_{sed,ch,mx}) * V_{ch} \quad (4.4)$$

where SED_{dep} = the amount of sediment deposited in the reach segment (metric tons), and V_{ch} = the volume of water in the reach segment (m^3). On the other hand, if $CONC_{sed,ch,i} < CONC_{sed,ch,mx}$, degradation is the dominant process in the reach segment and the net amount of sediment re–entrained is calculated as:

$$SED_{\text{deg}} = (\text{CONC}_{sed,ch,mx} - CONC_{sed,ch,i}) * V_{ch} * K_{ch} * C_{ch} \quad (4.5)$$

where SED_{deg} = the amount of sediment reetrained in the reach segment (metric tons), K_{ch} = the channel erodibility factor (cm/h/Pa), and C_{ch} = the channel cover factor.

4.4.2 SWAT–PDLD model

A probability–distributed model was used to account for the heterogeneity in storage of the landscape depressions in the study watersheds. In this model, the water budget for a single landscape depression considers input from precipitation and upland areas and losses through evapotranspiration and seepage; the difference between these inputs and outputs either fills or empties the depression. The depression will spill and therefore generate runoff when the net input exceeds the available storage in the depression. In this conceptualization, storage capacity of landscape depressions is an important variable that governs the outflow from the depressions. The total runoff generated from the landscape depressions over the entire sub–basin is estimated as the cumulative overspill runoff generated from the individual depressions. Detailed descriptions of the probability–distributed model formulations are given in Moore and Clarke (1981) Moore (1985; 2007) Bell et al. (2007) Bell et al. (2009) Noto (2013) and many others for soil moisture storage applications and Abedini (1999), Mekonnen et al. (2014), Mekonnen et al.

(2016) with respect to the landscape depressions application. Herein, only the most important equations to such a formulation for depression storage are briefly described.

Let the total water stored in the depressions over the entire sub–basin, at a particular time be $S(t)$. As demonstrated by Moore (1985; 2007) and Abedini (1999), $S(t)$ and the dynamic critical capacity, $C*(t)$, can be related as follows:

$$S(t) = \int_0^{C*(t)} cf(c)dc + C*(t)\int_{C*(t)}^{\infty} f(c)dc \tag{4.6}$$

where c = the storage capacity, and $f(c)$ = the probability density function that describes the distribution of storage capacity across the landscape. The critical storage capacity, $C*(t)$, separates the storages that are completely full and over spilling from those still filling at a particular time. The first term in the right side of Eq. (4.6) represents the water stored in depressions which are full and contributing. The second term in the right side of Eq. (4.6) represents the water stored in depressions that are not at full capacity and do not start contributing for the current conditions. It has been demonstrated (Moore 1985; 2007; Abedini 1999) that the water storage at time t, $S(t)$ is equal to:

$$S(t) = \int_0^{C*(t)} (1 - F(c))dc \tag{4.7}$$

where $F(c)$ is the cumulative $f(c)$.

For this study, the probability density functions to be used for each watershed were determined using the DEM data for the watersheds. ArcGIS was used to quantify the depression geometries across each watershed. Then, the storage capacity of each depression was plotted by frequency of occurrence. The probability density function was then fitted to this data so that an expression of the variation of capacity across the watershed could be found. Both the Pareto and exponential distributions were evaluated for the study watersheds with close results for the

correlation coefficients by Mekonnen et al. (2016). The exponential distribution was selected because of its relative simplicity (a one parameter function) as compared to the Pareto distribution. The cumulative exponential distribution is expressed as follows:

$$F(c) = 1 - \exp\left(\frac{-c}{\bar{c}}\right) \tag{4.8}$$

where $\bar{c}$ is the mean storage capacity. This mean or average storage capacity is calculated for each sub–basin and Eq. (4.8) is applied to represent the distribution of storage capacity across each sub–basin.

The value of the critical storage capacity at any time t, $C^*(t)$, is obtained by combining Eqs. (4.7) and (4.8) then integrating and solving for $C^*(t)$, where:

$$C^*(t) = -\bar{c}\ln\left(1 - \frac{S(t)}{\bar{c}}\right) \tag{4.9}$$

For a net water input to the depressions of $\pi\Delta t$ occurring during the time interval ($t, t+\Delta t$), the critical capacity, $C^*(t+\Delta t)$, will increase over $C^*(t)$ by $\pi\Delta t$. For the increased critical capacity, $C^*(t+\Delta t)$, the corresponding stored water over the landscape depressions at $t+\Delta t$, $S(t+\Delta t)$, can be computed as:

$$S(t+\Delta t) = \bar{c}\left(1 - \exp\left(\frac{-C^*(t+\Delta t)}{\bar{c}}\right)\right) \tag{4.10}$$

The direct runoff, $R(t, t+\Delta t)$, generated from the landscape depressions within a sub–basin during the time interval ($t, t+\Delta t$) then can be computed:

$$R(t, t+\Delta t) = \pi\Delta t - \left(S(t+\Delta t) - S(t)\right) \tag{4.11}$$

An initial condition must be assumed or estimated for the amount of water stored in the landscape depressions, $S(0)$, at the beginning of a model simulation using the above described

Probability Distributed Landscape Depressions (PDLD) algorithm in order for the calculations to proceed. The initial condition used at the start of the warm up period for the model was that during the spring snowmelt period the depressions were all at full capacity.

4.4.3 Input data requirements

The spatial data required for use in the model include land cover, topographic, and soils data. The land cover data was obtained from the GeoBase Canada database (http://www.geobase.ca/) and was prepared through vectorization of raster thematic data originating from classified Landsat 5 and Landsat 7 ortho–images. The land cover data is available at a scale of 1:250,000. The DEM of the case study basins were obtained from the GeoBase Canada website (http://www.geobase.ca/) at a scale of 1:50,000. Detailed soil data at a resolution of 1:1,000,000 along with soil properties used in the SWAT model (version 2009) were obtained from the Agriculture and Agri–Food Canada database (Soil Landscapes of Canada Working Group 2007).

Gridded daily temperature (minimum and maximum) and precipitation data was used as the meteorological input data for the SWAT model (version 2009). The Gridded Climate Dataset for Canada (Hutchinson et al. 2009) was obtained from Agriculture and Agri–Food Canada. This dataset covers south of 60°N latitude in Canada for the period 1961–2003 and was prepared through interpolation of observations from Environment Canada using a thin–plate smoothing spline–surface fitting method at a 10 km spatial resolution. Choi et al. (2009) demonstrated the suitability of gridded climate data to calibrate a hydrologic model in a prairie environment.

4.5 Model Setup and Evaluation

4.5.1 Model setup

To setup the model for the study watersheds, input databases including the weather generator parameters and soil characteristic databases were customized for Canadian Prairie conditions. Input files for the case study watersheds were then prepared using the ArcSWAT interface. ArcSWAT was used to discretize the study watersheds into sub–basins based on topographic features and further sub–divided into multiple Hydrological Response Units (HRUs) by overlaying the land–use, soil, and slope characteristics. Following input data preparation, two model setups were implemented. The first model setup used the SWAT–PDLD algorithm and an annual value for soil erodibility based on the values given in Wischmeier and Smith (1978) (called Setup 1: SWAT–PDLD with Annual K). The second model setup (called SWAT–PDLD with Seasonal K) used the SWAT–PDLD algorithm but allowed the soil erodibility factor to vary between seasons by utilizing the weighting factor values of soil erodibility and seasons identified by McConkey et al. (1998) as described above.

4.5.2 Model calibration and validation

To identify the parameters that strongly influence the hydrology in the study watersheds as well as sediment generation and transport parameters, a sensitivity analysis that was performed using the Latin Hypercube Sampling–One Factor at a Time method (LH–OAT: van Griensven et al. 2006). Following the identification of these sensitive parameters, model calibration was carried out in two steps. First, flow parameters were adjusted to best represent flow processes. This calibration process was performed using the Shuffled Complex Evolution–Uncertainty Analysis (SCE–UA) algorithm. Then, the sediment calibration parameters were optimized, using the same SCE–UA algorithm, keeping the flow parameters fixed. Streamflow

was calibrated first because runoff strongly influences the sediment generation. In addition, measurement uncertainty was assumed to be less for the flow data since the sediment data available from the gauging stations were sparse as compared to the flow measurements. This step by step calibration process has also been implemented by several other researchers including Santhi et al. (2001), Grizzetti et al. (2003), White and Chaubey (2005), and Abbaspour et al. (2007).

Observed daily discharge data from the Assiniboine River at Kamsack and Moose Jaw River near Burdick hydrometric stations were used for the flow calibration. Four years of flow data (1992–1995) were used for model calibration and another four years of flow data (1996–1999) for model validation at the Kamsack gauging station. Similarly, five years of flow data (1992–1997) were used for model calibration and an additional five years of flow data (1998–2002) for model validation at the Moose Jaw River near Burdick gauging station. Furthermore, two years of model warm–up period were allowed prior to model calibration for both watersheds so as to reduce uncertainty associated with initial conditions.

For the calibration for sediment, the challenge for the study watersheds was the limited frequency of sediment load measurements and period of coverage. For instance, the Water Survey of Canada had terminated sediment data collection in the study watersheds in 1983. Consequently, sediment data is available only in the period of 1970 to 1983 and limited to spring and summer time. Calibration and validation were performed by comparing the simulated sediment load with observations corresponding to the dates when observation data were available (mostly available for spring and summer periods). A total of 980 observations of sediment loading over four years (1972–1975) and 979 observations over four years (1976–1979) were used for calibration and validation, respectively, for the Assiniboine River watershed (Kamsack

gauging station). Similarly, sediment data consisting of 1238 observations over the years 1972–1977 were used to calibrate the model for the Moose Jaw River watershed. Additional sediment data consisting of 385 observations over the years 1978–1983 were used to validate the model for the Moose Jaw River watershed. Prior to the model calibration and validation periods, two years of model input data and warm–up period were allowed to reduce uncertainty associated with initial conditions. Therefore, because of data limitations, the flow and sediment calibrations were performed over different periods. A similar methodology had to be implemented by Santhi et al. (2001) while calibrating SWAT for a large river basin in the USA (Bosque River Watershed). Thus, the model's performance at simulating streamflow was assessed for the sediment calibration and validation periods. It was seen that the model had good performance during these periods as shown by the results.

4.5.3 Model performance evaluation

Quantitative evaluation of model performance for daily time step simulations was assessed using a range of statistical metrics that include the Nash & Sutcliffe efficiency index (NSE) (Nash and Sutcliffe 1970), Percent Bias (PBIAS) (Gupta et al. 1999), and the ratio of the root mean square error to the standard deviation of measured data (RSR) (Singh et al. 2005).

The Nash & Sutcliffe efficiency index (NSE) was used to evaluate how well the simulation data versus the observed data fits a 1:1 line as follows:

$$\text{NSE} = 1 - \frac{\sum_{i=1}^{n}\left(\hat{Q}_i - Q_i\right)^2}{\sum_{i=1}^{n}\left(\bar{Q} - Q_i\right)^2} \tag{4.12}$$

where $\hat{Q}_i$ is the simulated streamflow, Q_i is the observed streamflow at time i, n is total number of data points, and $\bar{Q}$ is the average observed streamflow.

To measure the average tendency of the predicted data to be smaller or larger than the observed data Percent Bias (PBIAS) was used (Gupta et al. 1999). PBIAS is calculated using:

$$\text{PBIAS} = \frac{\sum_{i=1}^{n}\left(Q_i - \hat{Q}_i\right)*100}{\sum_{i=1}^{n} Q_i} \tag{4.13}$$

Finally, a standardized version of the root mean square error (RSR) was used following Singh et al. (2005). The RSR is the ratio of the root mean square error (RMSE) to the standard deviation (STDEV_o) of the measured data set. The RSR is formulated as follows:

$$\text{RSR} = \frac{\text{RMSE}}{\text{STDEV}_o} = \frac{\sqrt{\sum_{i=1}^{n}\left(Q_i - \hat{Q}_i\right)^2}}{\sqrt{\sum_{i=1}^{n}\left(Q_i - \overline{Q}\right)^2}} \tag{4.14}$$

4.6 Results and Discussion

4.6.1 Calibrated parameters

For the model, the calibrated parameters for streamflow are the curve number, soil evaporation compensation factor, surface runoff lag coefficient, baseflow factor, snowfall temperature, snowmelt base temperature, maximum melt factor, minimum melt factor, snowpack temperature lag factor, areal snow coverage threshold at 100%, areal snow coverage threshold at 50%, maximum storage capacity, and Manning's n for the main channel (Table 4–1).

The calibrated parameters for predictions of sediment yield in the study watersheds are the peak rate adjustment factor for sediment, linear parameter for maximum sediment re–entrained, exponent parameter for sediment re–entrained, USLE (Universal Soil Loss Equation) support practice, channel erodibility factor, and channel cover factor. These parameters are listed in Table 4–1 with their calibrated values.

Table 4–1 Parameters selected for SWAT–PDLD model automatic calibration and resulting optimum values.

Parameter description	Default value	Range		Optimum Values	
		Min	Max	Kamsack	Moose Jaw
Streamflow parameters					
SCS runoff curve number (CN2)	Varies	–10	+10	–2.00	–3.64
Soil evaporation compensation factor (ESCO)	0.90	0	1	0.80	0.56
urface runoff lag coefficient (SURLAG)	4	0	10	1.00	1.00
Baseflow factor for bank storage (ALPHA_BF)	0.048 day	0	1	0.34	0.49
Snowfall temperature (SFTMP)	1ºC	–5	+5	–0.64	–4.94
Snowmelt base temperature (SMTMP)	0.5ºC	–5	+5	–3.29	–2.25
Maximum melt factor (SMFMX)	4.5 mm $^{o}C^{-1}$ /d	0	7	2.15	2.55
Minimum melt factor (SMFMN)	4.5 mm $^{o}C^{-1}$ /d	0	7	0.23	0.94
Snowpack temperature lag factor (TIMP)	1	0	1	0.05	0.01
Areal snow coverage threshold at 100% (SNOCOVMX)	1 mm	0	500	225	121
Areal snow coverage threshold at 50% (SNO50COV)	0.5	0	1	0.02	0.02
Maximum storage capacity (SMAX)	Varies	–0.2	+0.2	+0.13	+0.09
Manning *n* for the main channel (CH_N)	0.014	0	0.05	0.04	0.05
Sediment parameters					
Peak rate adjustment factor for sediment (PRF)	1.0	0	2	0.87	0.9
Linear parameter for maximum sediment reentrained (SPCON)	0.001	0.0001	0.01	0.0008	0.005
Exponent parameter for sediment reentrained (SPEXP)	1.0	0	1.5	1.29	1.0
USLE support practice (USLE_P)	1.0	0	1.0	1.00	1.00
Channel erodibility factor (CH_COV1)	0	0	1.0	0.94	0.82
Channel cover factor (CH_COV2)	0	0	1.0	0.92	0.72

4.6.2 Modeling streamflow

As noted, the model was calibrated and validated for streamflow in the periods of 1992 to 1995 and 1996–1999 for the Assiniboine River at Kamsack. For the Moose Jaw River near Budick, the calibration and validation periods of 1992–1997 and 1998–2002 were used. The simulation results for these periods are presented for each watershed in Figures 4–4 and 4–5. Table 4–2 gives the statistical metrics for these simulations. It is seen that the timing of streamflow is well represented by the model and the evaluation metrics show good model performance. The model captures most of the peak flows on both watersheds, which is important to correctly predict sediment export. However, the model tends to underestimate the1995 streamflow peak at Kamsack (Figure 4–4). In general, the modified model (SWAT–PDLD) is well able to capture the dynamics of the basin streamflow response for both watersheds (daily NSE=0.72 during calibration and validation periods).

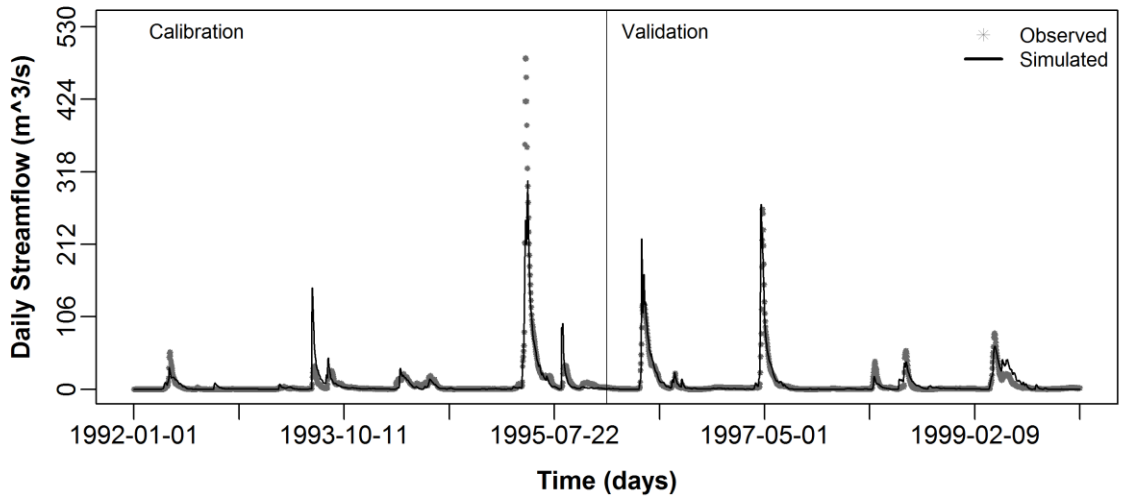

Figure 4–4 Observed and predicted daily streamflow for the Assiniboine River at Kamsack during the calibration and validation periods.

Prior to modeling sediment export, since the model was not calibrated for streamflow during the same period, the performance of the model for streamflow simulation during the time period selected for simulation of sediment export was assessed. The statistical metrics for model performance are given in Table 4–3 and show good model performance.

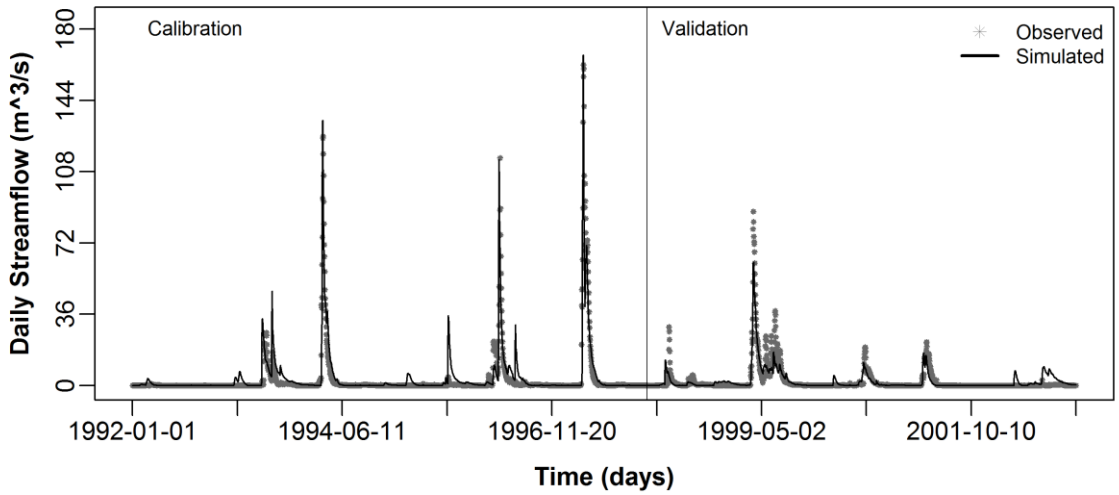

Figure 4–5 Observed and predicted daily streamflow for the Moose Jaw River near Burdick during the calibration and validation periods.

Table 4–2 Model performance for simulation of streamflow calibration and validation.

	Period	Location	NSE	PBIAS	RSR
Calibration	1992–1995	Kamsack	0.79	9.3	0.46
	1992–1997	near Burdick	0.78	–23	0.51
	1996–1999	Kamsack	0.72	–17	0.53
Validation	1998–2002	near Burdick	0.81	17	0.43

4.6.3 Modeling sediment export

Figures 4–6 to 4– 9 show model performance results for daily sediment export prediction. In general, both setups (SWAT–PDLD with annual *K* and seasonal *K*) satisfactorily simulate the temporal trend of sediment export from the case study watersheds. However, a relative comparison between the two model setups reveals improved sediment export prediction by the SWAT–PDLD with seasonal *K* set–up compared to the SWAT–PDLD with annual K set–up. For instance, the NSE varies from 0.42 to 0.60 and 0.53 to 0.83 for SWAT–PDLD with annual and seasonal K respectively (see Table 4–3). The SWAT–PDLD with annual *K* model tends to under predict sediment export on both case study watersheds, in particular during spring peaks. Considering the good agreement between the observed and simulated streamflow, the plant and snow cover and/or erodibility are the factors that need to be better represented in sediment module for improved sediment export simulation. In the study watershed, crops are often planted at the end of May, which is well beyond the freeze-thaw period (April 1 to April 30th) and hence due not have as such a significant impact on sediment generation process during the freeze-thaw period. The other cover factor is the snow cover impact on sediment generation. Fortunately, impacts of snow cover on sediment generation processes are already incorporated into the sediment module for recent versions of SWAT (SWAT2009 and later). Therefore, it appears that the soil erodibility is the main factor that need to be improved to improve sediment export simulation in cold-climate watersheds. In this study, sediment export prediction is improved when seasonal variability of soil erodibility is incorporated using the SWAT–PDLD with

seasonal *K* model. In general, the current research shows improved sediment export predictions from two case study watersheds when seasonal variability of soil erodibility factor is incorporated into the model (SWAT–PDLD with seasonal *K*). Although the simulation results are improved, the SWAT–PDLD with seasonal *K* results still tends to under predict for some peaks, particularly sediment export in the Assiniboine watershed during the 1976 and 1979 spring periods (see Figure 4–7).

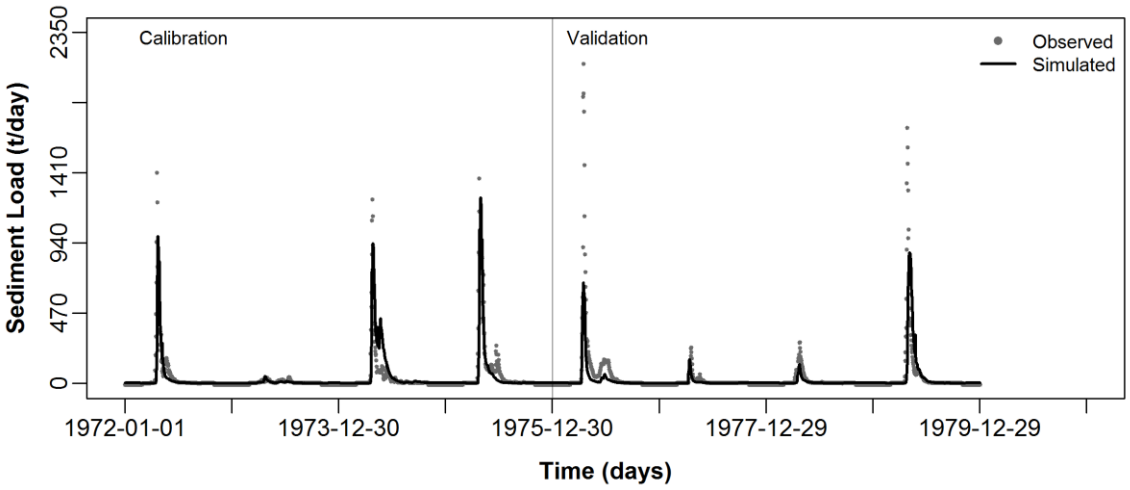

Figure 4–6 Observed and simulated daily sediment export for the Assiniboine River at Kamsack using SWAT–PDLD with annual *K* (annual soil erodibility).

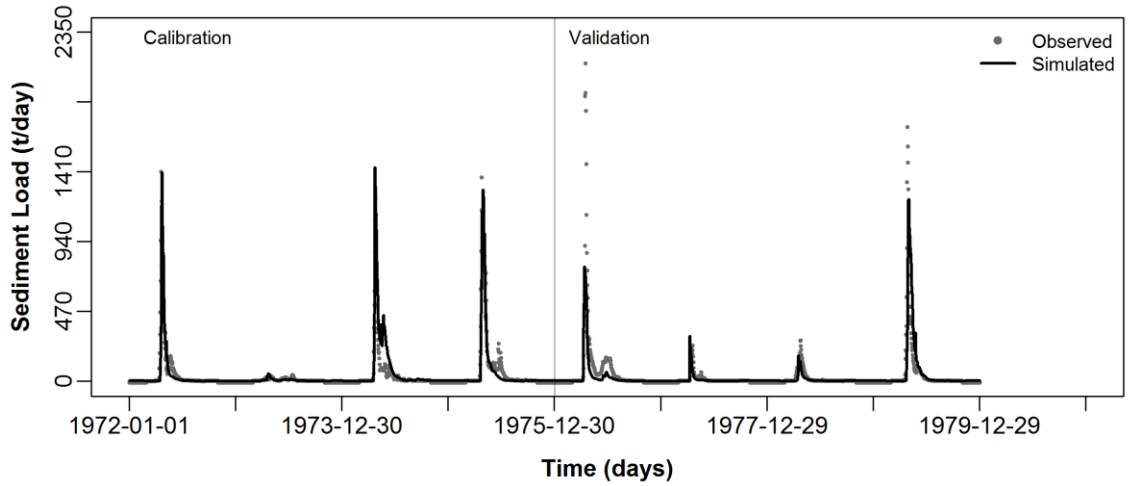

Figure 4–7 Observed and simulated daily sediment export for the Assiniboine River at Kamsack using SWAT–PDLD with seasonal *K* (seasonally varying soil erodibility).

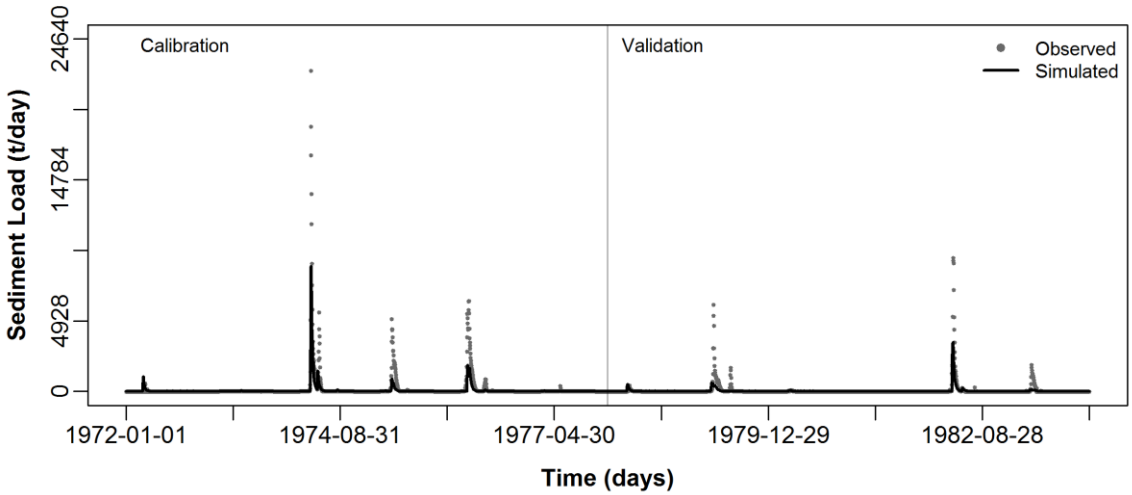

Figure 4–8 Observed and simulated daily sediment export for the Moose Jaw River near Burdick using SWAT–PDLD with annual *K* (annual soil erodibility).

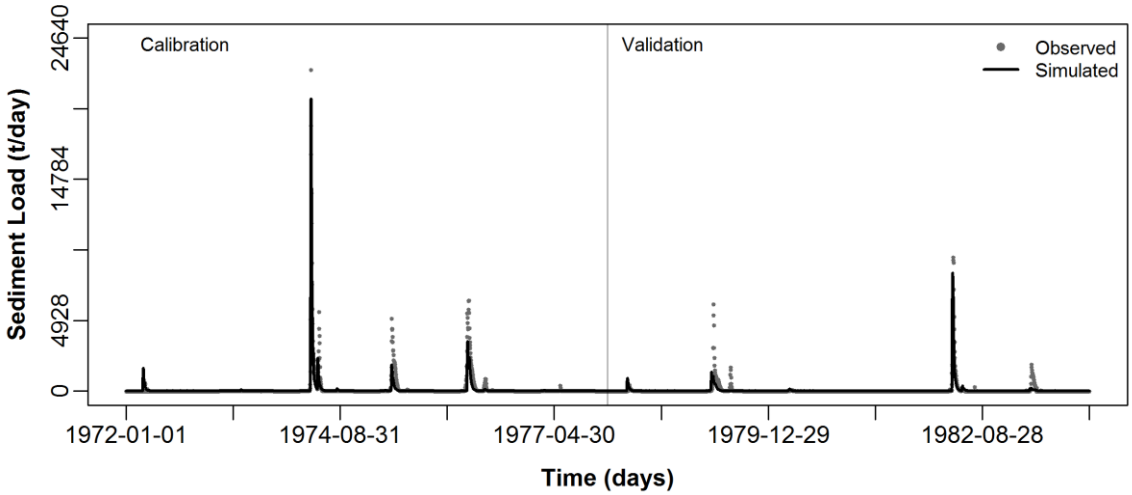

Figure 4–9 Observed and simulated daily sediment export for the Moose Jaw River near Burdick using SWAT–PDLD with seasonal *K* (seasonally varying soil erodibility).

Table 4–3 Model performance for simulation of streamflow and sediment yield: calibration (validation).

	Model	Location	Model performance: calibration (validation)		
			NSE	PBIAS	RSR
Flow	SWAT–PDLD	Kamsack	0.65(0.62)	–38(–34)	0.58(0.61)
		near Burdick	0.75(0.68)	–23(–39)	0.49(0.55)
Sediment	SWAT–PDLD annual *K*	Kamsack	0.56(0.45)	3.0(42)	0.66(0.74)
		near Burdick	0.60(0.42)	62(64)	0.63(0.77)
	SWAT–PDLD seasonal *K*	Kamsack	0.61(0.53)	–9.4(31)	0.62(0.68)
		near Burdick	0.83(0.54)	35(38)	0.42(0.69)

Note:
- The calibration and validation periods for Assiniboine River at Kamsack are 1972–1975 and 1976–1979 respectively.
- The calibration and validation periods for Moose Jaw River near Burdick are 1972–1977 and 1978–1983 respectively.

The tendency for under prediction by both models may be attributed to unaccounted for management practices in these agricultural watersheds. The model used in the present study assumes that for every year, there is a crop cover in agricultural areas. However, as described by van Kooten et al. (1989), it is a common practice to leave agricultural fields as a fallow for some years because of economic reasons. Such a practice can cause increased soil erosion because of the higher exposure of uncovered fields to erosion generation (van Kooten and Furtan 1987;

Campbell et al. 1993). Therefore, model performance might be further improved by incorporating detailed management practices of the case study watersheds for the simulation periods although no such data is available.

Further assessment of sediment export prediction capability was carried out using a seasonally segmented sediment loading datasets. Four seasons were used for data segmentation including fall, winter, spring, and summer (see Table 4–4). The two model set–ups, SWAT–PDLD with annual and seasonal *K*, were then evaluated for sediment export simulation capability for each season (see Table 4–4, Figures 4–10 and 4–11). The SWAT–PDLD with seasonal *K* simulates sediment export better than the SWAT–PDLD with annual *K* on both case study watersheds (see Figures 4–10 and 4–11). More specifically, the SWAT–PDLD with seasonal *K* outperformed the SWAT–PDLD with annual *K* during the spring and summer seasons. In particular, the SWAT–PDLD with seasonal *K* highly outperformed SWAT–PDLD with annual *K* during the spring season (see Table 4–4, Figures 4–10 and 4–11). The improved performance is mainly because the freeze–thaw process that leads to higher soil erodibility occurs during spring time. On the other hand, the SWAT–PDLD with seasonal and annual *K* simulates the fall sediment export equally well (see Table 4–4). It is difficult to evaluate the two models set–ups during the winter season because of limited observed data for the season (see Table 4–4).

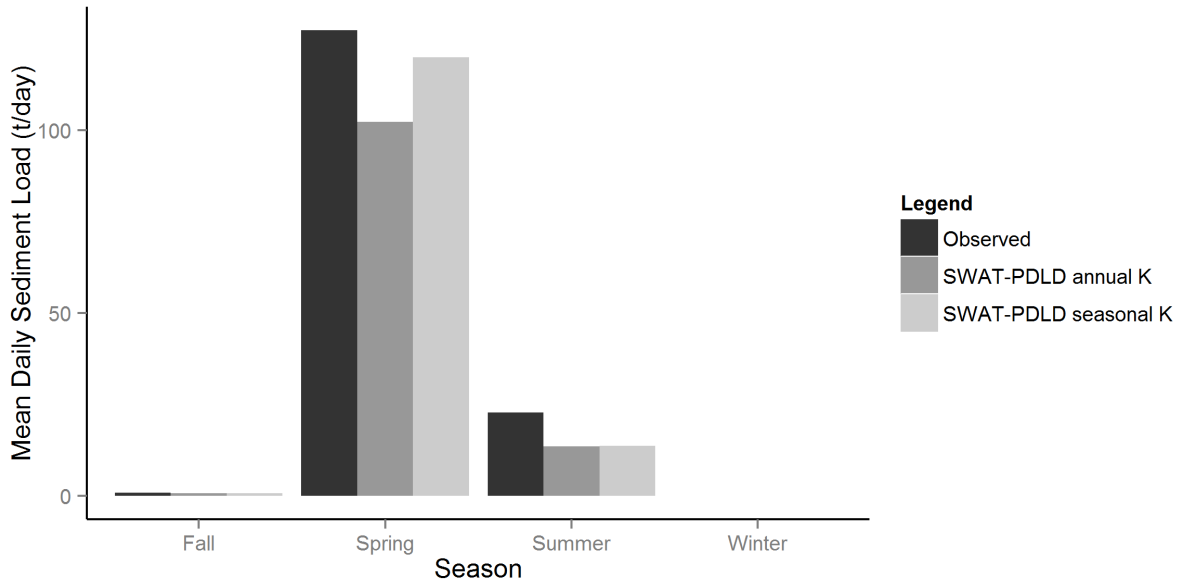

Figure 4–10 Seasonally segmented predicted and observed sediment export for the Assiniboine River at Kamsack.

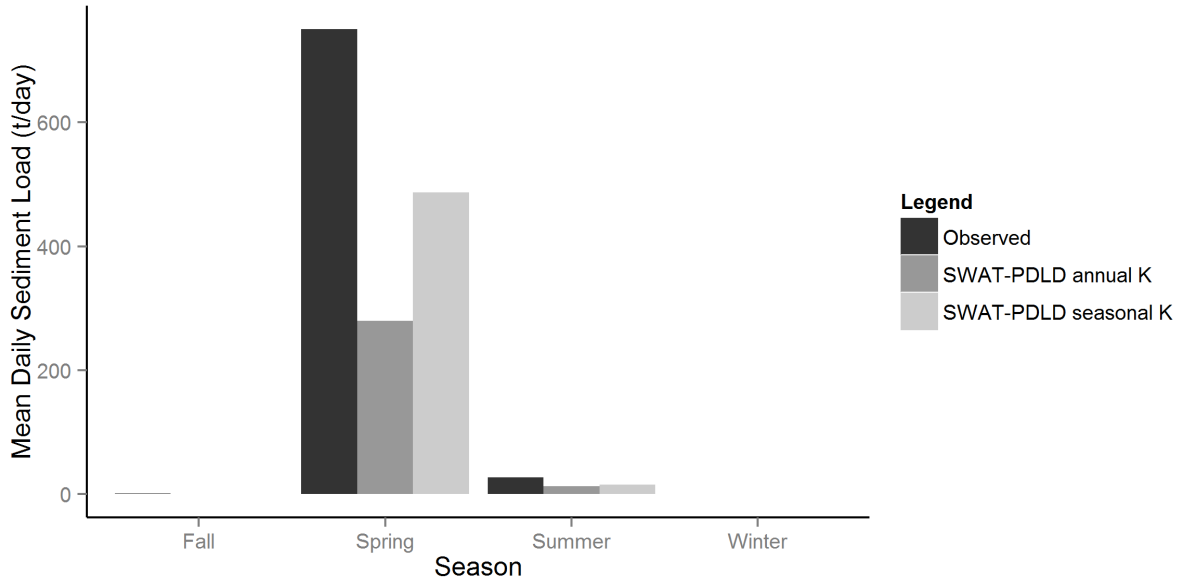

Figure 4–11 Seasonally segmented predicted and observed sediment export for the Moose Jaw River near Burdick.

Table 4–4 Model performance for simulation of seasonal sediment export.

Season	Months	Location	Mean daily sediment yield (tons per day)		
			Observed	Simulated (SWAT–PDLD annual *K*)	Simulated (SWAT–PDLD seasonal *K*)
Fall	September, October, and November	Kamsack	0.94	0.76	0.77
		near Burdick	0.73	0.46	0.48
Winter	December, January, and February	Kamsack	*	0.10	0.10
		near Burdick	*	0.03	0.03
Spring	March, April, and May	Kamsack	127.4	102.3	120.0
		near Burdick	750.3	279.8	486.9
Summer	June, July, and August	Kamsack	22.9	13.6	13.8
		near Burdick	26.9	12.9	15.5

* No observed data for the specified season.

4.7 Conclusion

Sediment export predictions from cold climate Canadian Prairie watersheds has been challenging because of the numerous landscape depressions and variability in sediment generation processes. Prior modeling with seasonally segmented data analysis revealed the seasonality of runoff–sediment export relationships in both watersheds. In this research, seasonal variability of soil erodibility was incorporated into the SWAT–PDLD model and a comparison study between annual and seasonally varying values of soil erodibility factor was carried out. The two model set–ups were evaluated for two prairie case study watersheds (i.e. Assiniboine and Moose Jaw River watersheds). Graphical plots and statistical measures revealed that both model set–ups reproduce the temporal variation of sediment export from the case study watersheds. However, sediment export prediction capability is significantly improved and observed data replicated better when seasonal variability of soil erodibility was considered for cold climate Canadian prairie watershed conditions. In addition, model performance evaluations were conducted for seasonally segmented datasets. The results show that the SWAT–PDLD

model with seasonally varying soil erodibility outperformed the SWAT–PDLD model with annual soil erodibility factor in particular during the spring runoff periods (i.e., during the freeze–thaw cycle). In general, it is found necessary to take into account both the seasonal variability of soil erodibility and the presence of landscape depressions while modeling sediment export from cold climate Canadian prairie watersheds.

As a final remark, it is important to note that seasonality of soil erodibility is incorporated using a fixed date in identifying each season. Therefore, future research should focus on incorporation of climatic variables in identifying each season as the beginning and ending date of each season varies between years.

4.8 Acknowledgments

The authors would like to thank the Province of Saskatchewan Go Green Fund for financial support for this work and the Natural Sciences and Engineering Research Council of Canada (NSERC) in terms of Discovery Grants to the second authors. The authors would also like to thank Dr. Monique Dube and Dr. Nicole Nadorozny for making available the datasets from different sources.

4.9 References

Abbaspour, K.C., Yang, J., Maximov, I., Siber, R., Bogner, K., Mieleitner, J., Zobrist, J., and Srinivasan, R. 2007. Modelling hydrology and water quality in the pre–alpine/alpine Thur watershed using SWAT. Journal of Hydrology, **333**(2–4): 413–430.

Abedini, M.J. 1998. On depression storage, its modelling and scale. Ph.D. thesis, Department of Water Resources Engineering, University of Guelph, Guelph, Canada.

Aldrich, J.W., and Slaughter, C.W. 1983. Soil erosion on subarctic forest slopes. Journal of Soil Water Conservation, **38**(2): 115–118.

Almendinger, J.E, Murphy, M.S., and Ulrich, J.S. 2012. Use of the Soil and Water Assessment Tool to scale sediment delivery from field to watershed in an agricultural landscape with topographic depressions. Journal of Environmental Quality, **43**(1): 9–17.

Arnold, J.G., Srinivasan, R., Muttiah, R.S., and Williams, J.R. 1998. Large-area hydrologic modeling and assessment: Part I Model development. J. American Water Resour. Assoc., **34**(1): 73–89.

Bell, V.A., Kay, A.L. Jones, R.G., and Moore, R.J. 2007. Use of a grid–based hydrological model and regional climate model outputs to assess changing flood risk. International Journal of Climatology, **27**(12): 1657–1671.

Bell, V.A., A.L. Kay, R.G. Jones, R.J. Moore, and N.S. Reynard. 2009. Use of soil data in a grid–based hydrological model to estimate spatial variation in changing flood risk across the UK. Journal of Hydrology, **377** (3–4): 335–350.

Campbell, C.A., Moulin, A.P., Curtin, D., Lafond, G.P., and Townley–Smith, L. 1993. Soil aggregation as influenced by cultural practices in Saskatchewan: I. Black Chernozemic soils. Can. J. Soil Sci., **73**(4): 579–595.

Chanasyk, D.S., Mapfumo, E., and Willms, W. 2003. Quantification and simulation of surface runoff from fescue grassland watersheds. Agricultural Water Management, **59**(2): 137–153.

Choi, W, Kim, S.J., Rasmussen, P.F., and Moore, A.R. 2009. Use of the North American Regional Reanalysis for Hydrological Modelling in Manitoba. Canadian Water Resources Journal, **34**(1): 17–36.

Cunge, L.A. 1969. On the subject of a flood propagation method (Muskingum method). J. Hydraulic Research, **7**(2): 205–230.

Coote, D.R., Malcolm–McGovern, C.A., Wall, G.J., Dickinson, W.T., and Rudra, R.P. 1988. Seasonal variation of erodibility indices based on shear strength and aggregate stability in some Ontario soils. Can. J. Soil Sci., **68**(2): 105–416.

Dagesse, D.F. 2013. Freezing cycle effects on water stability of soil aggregates. Can. J. Soil Sci. **93**(4): 473–483.

De Boer, D.H., Hassan, M.A., MacVicar, B., and Stone, M. 2005. Recent (1999–2003) Canadian research on contemporary processes of river erosion and sedimentation, and river mechanics. Hydrological Processes, **19**(1): 265–283.

Di Luzio, M., Srinivasan, R., Arnold, J.G., and Neitsch, S.L. 2002. ArcView Interface for SWAT2000 user's guide. USDA Agricultural Research Service; Blacklands Research and Extension Center BRC Rep. 02–07; Grassland, Soil, and Water Research Laboratory GSWRL Report 02–03; and Texas Water Resources Institute TWRI Report TR–193.

Dickinson, W.T., Scott, A., and Wall, G. 1975. Fluvial sedimentation in Southern Ontario. Can. J. Earth Sci., **12**(11): 1813–1819.

Donigian, A.S. Jr., Imhoff, J.C., Bicknell, B.R., and Kittle, J.L. Jr. 1984. Application Guide for the Hydrological Simulation Program–FORTRAN. USEPA Environmental Research Lab, Athens, GA.

Du, B., Arnold, J.G., Saleh, A., and Jaynes D.B. 2005. Development and application of SWAT to landscapes with tiles and potholes. Trans. ASAE, **48**(3): 1121–1133.

Edwards, L.M. 2013. The effects of soil freeze-thaw on soil aggregate breakdown and concomitant sediment flow in Prince Edward Island: A review. Can. J. Soil Sci., **93**(4): 459–472.

Environment Canada. 2009. Canadian climate normals 1971–2000. Accessed on Dec. 10, 2011, http://www.climate.weatheroffice.ec.gc.ca/climate_normals/index_e.html.

ESRI (Environmental Systems Research Institute). 2011. Arc hydro tools: Tutorial, version 2.0. Environmental Systems Research Institute, Redlands, CA.

Euliss, N.H. Jr., Mushet, D.M., and Wrubleski, D.A. 1999. Wetlands of the Prairie Pothole Region: Invertebrate Species Composition, Ecology, and Management. Pages 471–514 in Batzer, D.P., Rader, R.B. and Wissinger, S.A., eds. Invertebrates in Freshwater Wetlands of North America: Ecology and Management, Chapter 21. John Wiley & Sons, New York. Jamestown, ND: Northern Prairie Wildlife Research Center Online, Accessed on Mar 20, 2011, http://www.npwrc.usgs.gov/resource/wetlands/pothole/index.htm.

Fang, X., and Pomeroy, J.W. 2008. Drought impacts on Canadian prairie wetland snow Hydrology. Hydrological Processes, **22**(15): 2858–2873.

Ferrick , M.G., and Gatto, L.W. 2005. Quantifying the effect of a freeze–thaw cycle on soil erosion: laboratory experiments. Earth Surf. Process. Landforms, **30**(10): 1305–1326.

Gassman P.W., Reyes, M.R., Green, C.H., and Arnold, J.G. 2007. The soil and water assessment tool: historical development, applications, and future research directions. Trans. ASABE, **50**(4): 1211–1250.

Geter, W.F., and Theurer, F.D. 1998. AnnAGNPS-RUSLE sheet and rill erosion. In Proc. 1st Federal Interagency Hydrologic Modeling Conference, vol. 1: 1-17 to 1-24. Washington, D.C.: Interagency Advisory Committee on Water Data, Subcommittee on Hydrology.

Godwin, R.B., and Martin, F.R. 1975. Calculation of Gross and Effective Drainage Areas for the Prairie Provinces. Canadian Hydrology Symposium, (p. 5), Winnipeg, Manitoba, Canada.

Granger, R.J., Gray, D.M., and Dyck, G.E. 1984. Snowmelt infiltration to frozen Prairie soils. Can. J. Earth Sci., **21**(6): 669–677.

Gray, D.M., Toth, B., Zhao, L., Pomeroy, J.W., and Granger, R.J. 2001. Estimating areal snowmelt infiltration into frozen soils. Hydrological processes, **15**(16): 3095–3111.

Grizzetti, B., Bouraoui, F., Granlund, K., Rekolainen, S., and Bidoglio, G. 2003. Modelling Diffuse Emission and Retention of Nutrients in the Vantaanjoki Watershed (Finland) Using the SWAT Model. Ecological Modelling, **169**(1): 25–38.

Gupta, H.V., Sorooshian, S., and Yapo, P.O. 1999. Status of automatic calibration for hydrologic models: Comparison with multilevel expert calibration. J. Hydrol. Eng., **4**(2): 135–143.

Hargreaves, G.L., Hargreaves, G.H., and Riley, J.P. 1985. Agricultural benefits for Senegal River Basin. J. Irrig. Drain. Eng., **111**(2): 113–124.

Hayashi, M., van der Kamp, G., and Rudolph, D.H. 1998. Water and solute transfer between a prairie wetland and adjacent uplands: 1. Water balance. Journal of Hydrology, **207**(1–2): 42–55.

Hutchinson, M.F., McKenney, D.W., Lawrence, K., Pedlar, J.H., Hopkinson, R.F., Milewska, E., and Papadopol, P. 2009. Development and Testing of Canada–Wide Interpolated Spatial Models of Daily Minimum–Maximum Temperature and Precipitation for 1961–2003. Journal of Applied Meteorology and Climatology, **48**: 725–741.

Kiesel, J., Fohrer, N., Schmalz, B., and White, M.J. 2010. Incorporating landscape depressions and tile drainages of a northern German lowland catchment into a semi–distributed model. Hydrological Processes, **24** (11): 1472–1486.

Kirby, P.C., and Mehuys, G.R. 1987. Seasonal variation of soil erodibilities in southwestern Quebec. J. Soil Water Cons., **42**(3): 2ll–215.

Kleiss, B.A. 1996. Sediment retention in a bottomland hardwood Wetland in eastern Arkansas. Wetlands, **16**(3): 321–333.

Koroluk, S.L. 2000. Prairie wetland and sediment: a record of the recent past. MSc Thesis, Department of Geography, University of Saskatchewan, Saskatoon, Canada.

Koroluk, S.L., and de Boer, D.H. 2007. Land use change and erosional history in a lake catchment system on the Canadian prairies. Catena, **70**(2): 155–168.

Kuchment, L.S., Gelfan, A.N., and Demidov, V.N. 2000. A distributed model of runoff generation in the permafrost regions. Journal of Hydrology, **240**(1–2): 1–22.

Lane, L.J., Hernandez, M., and Nichols, M. 1997. Processes controlling sediment yield from watersheds as functions of spatial scale. Environmental Modelling and Software, **12**(4): 355–369.

Leibowitz, S.G., and Vining, K.C. 2003. Temporal connectivity in a prairie pothole complex. Wetlands, **23**(1): 13–25.

McConkey, B.G., Nicholaichuk, W., Steppuhn1, H., and Reimer, C.D. 1997. Sediment yield and seasonal soil erodibility for semiarid cropland in western Canada. Can. J. Soil Sci., **77**(1): 33–40.

Mein, R.G., and C.L. Larson. 1973. Modeling infiltration during a steady rain. Water Resources Research, **9**(2): 384–394.

Mekonnen, B.A., Nazemi, A., Mazurek, K.A., Elshorbagy, A., and Putz, G. 2015. Hybrid modelling approach to prairie hydrology: Fusing data–driven and process–based hydrological models. Hydrological Sciences Journal, **60**(9): 1473–1489.

Mekonnen, M.A., Wheater, H.S., Iresona, A.M., Spence, C., Davison, B., and Pietroniro, A. 2014. Towards an improved land surface scheme for prairie landscapes. Journal of Hydrology, **511**: 105–730 116.

Moore, R.J. 1985. The probability–distributed principle and runoff production at point and basin scales. Hydrological Sciences Journal, **30**(2): 273–297.

Moore, R.J. 2007. The PDM rainfall–runoff model. Hydrology and Earth System Sciences, **11**(1): 483–499.

Moore, R.J., and Clarke, R.T. 1981. A distribution function approach to rainfall runoff modelling. Water Resources Research, **17**(5): 1367–1382.

Monteith, J.L. 1965. Evaporation and the environment: In The State and Movement of Water in Living Organisms. Proc. 19th Symp. Swansea, UK, Society of Experimental Biology, Cambridge University Press.

Nash, J.E., and Sutcliffe, J.V. 1970. River flow forecasting through conceptual models. Part I: A discussion of principles. Journal of Hydrology, **10**(3): 282–290.

Neitsch, S.L., Arnold, J.G., Kiniry, J.R., and Williams, J.R. 2011. Soil and Water Assessment Tool theoretical documentation: Version 2005. Grassland, Soil and Water Research Laboratory, Blackland Research Center, Temple, TX.

Noto L.V. 2014. Exploiting the topographic information in a PDM – based conceptual hydrological model. Journal of Hydrological Engineering, **19**(6): 1173-1185.

Olthof, I., Latifovic, R., and Pouliot, D. 2008. Circa–2000 Northern Land Cover of Canada. Earth Sciences Sector, Canada Centre for Remote Sensing, Natural Resources Canada.

Parsons, D.F, Hayashi, M. and van der Kamp, G. 2004. Infiltration and solute transport under a seasonal wetland: bromide tracer experiments in Saskatoon, Canada. Hydrological Processes, 18(11): 2011–2027.

Priestley, C.H.B., and Taylor, R.J. 1972. On the assessment of surface heat flux and evaporation using large–scale parameters. Mon. Weather Rev., **100**: 81–92.

Renard, K.G., Foster, G.R., Weesies, G.A., McCool, D.K., and Yoder, D.C. 1994. Predicting soil erosion by water: A guide to conservation planning with the revised universal soil loss equation (RUSLE). Agric. Handbook 703. US Department of Agriculture, Washington, DC.

Ritchie, J.T. 1972. A model for predicting evaporation from a row crop with incomplete cover. Water Resources Research, **8**(5): 1204–1213.

Rosenberry, D.O., and Winter, T.C. 1997. Dynamics of water–table fluctuations in an upland between two prairie–pothole wetlands in North Dakota. Journal of Hydrology, **191**(1–4): 266–289.

Santhi, C., Srinivasan, R., Arnold, J.G., and Williams, J.R. 2006. A modeling approach to evaluate the impacts of water quality management plans implemented in a watershed in Texas. Environmental Modelling & Software, **21**(8): 1141–1157.

Saskatchewan Ministry of Agriculture. 2013. Plan for 2014–2015. Government of Saskatchewan, Regina, SK, Canada.

Saskatchewan Watershed Authority. 2005. Background report: Assiniboine River watershed. Regina, Technical committee 123 pp.

Shaw, D.A., van der Kamp, G., Conly, M., F.M., Pietroniro, A., and Martz, L. 2011. The Fill–Spill hydrology of prairie wetland complexes during drought and deluge. Hydrological Processes, **26**(20): 3147–3156.

Singh, J., Knapp, H.V., Arnold, J.G., and Demissie, M. 2005. Hydrologic modeling of the Iroquois River watershed using HSPF and SWAT. J. American Water Resources Assoc., **41**(2): 361–375.

Soil Conservation Service. 1972. National Engineering Handbook, Section 4: Hydrology. Soil Conservation Service, USA.

Soil Landscapes of Canada Working Group. 2007. Soil Landscapes of Canada v3.1.1. Agriculture and Agri–Food Canada, Digital Map and Database at 1:1 Million Scale. Accessed on Mar. 20, 2011, http://sis.agr.gc.ca/cansis/nsdb/slc/v3.1.1/intro.html.

Shrestha, R.R., Dibike, Y.B., Prowse, T.D. 2012. Modeling Climate Change Impacts on Hydrology and Nutrient Loading in the Upper Assiniboine Catchment. J. American Water Resour. Assoc., **48**(1): 74–89.

Tiessen, K.H.D., Elliott, J.A., Yarotski, J., Lobb, D.A., Flaten, D.N., and Glozier, N.E. 2010. Conventional and Conservation Tillage: Influence on Seasonal Runoff , Sediment, and Nutrient Losses in the Canadian Prairies. J. Environ. Qual., **39**(3): 964–980.

Ullah, W., and Dickinson, W.T. 1979. Quantitative description of depression storage using a digital surface model, II. Characteristics of surface depressions. Journal of Hydrology, **42**(1–2): 77–90.

van der Kamp, G., and Hayashi, M. 2009. Groundwater–wetland ecosystem interaction in the semiarid glaciated plains of North America. Hydrogeology Journal, **17**(1): 203–214.

van Liew, M.W., Arnold, J.G., and Garbrecht, J.D. 2003. Hydrologic Simulation on agricultural watersheds choosing between two models." Trans. ASABE, **46**(6): 1539–1551.

van Griensven, A., Meixner, T., Grunwald, S., Bishop, T., Di Luzio, M., and Srinivasan, R. 2006. A global sensitivity analysis method for the parameters of multi–variable watershed models. Journal of Hydrology, **324**(1–4): 10–23.

van Kooten, G.C., and Furtan, W.H. 1987. A review of issues pertaining to soil deterioration in Canada. Cdn. J. of Agric. Economics, **35**(1): 33–54.

van Kooten, G.C., Weisensel, W.P., and de Jong, E. 1989. Estimating the costs of soil erosion in Saskatchewan. Cdn. J. of Agric. Economics, **37**(1): 63–75.

van Vliet, L.J.P., and Hall, J.W. 1991. Effects of two crop rotations on seasonal runoff and soil loss in the Peace River region. Can. J. Soil Sci., **71**(4): 533–544.

Wall, G.J., Pringle, E.A., Padburt, G.A., Rees, H.W., Tajeck, J., van Vliet, L.J.P., Stushnoff, C.T., Eilers, R.G., and Cossette, J.M. 1995. Erosion. In: Acton, D. F., and L. J. Gregorich (Eds.), The Health of Our Soils: Toward Sustainable Agriculture in Canada. Publication 1906/E, Centre for Land and Biological Resources research." Research Branch, Agriculture and Agri–Food Canada, pp. 61–76.

Wall, G.J., Coote, D.R., Pringle, E.A., and Shelton, I.J. (editors). 2002. RUSLEFAC — Revised Universal Soil Loss Equation for Application in Canada: A Handbook for Estimating Soil

Loss from Water Erosion in Canada. Research Branch, Agriculture and Agri–Food Canada. Ottawa. Contribution No. AAFC/AAC2244E. 117 pp.

Wall, G.J., Dickinson, W.T., Rudra, R.P., and Coote, D.R. 1988. Seasonal soil erodibility variation in southwestern Ontario. Can. J. Soil Sci., **68**(2): 417–424.

Wang, X., Yang, W., and Melesse, A.M. 2008. Using hydrologic equivalent wetland concept within SWAT to estimate streamflow in watersheds with numerous wetlands. Trans. ASAE, **51**(1): 55–72.

White, K.L., and Chaubey, I. 2005. Sensitivity analysis, calibration, and validations for a multisite and multivariable swat model. Journal of the American Water Resources Association, **41**(5): 1077–1089.

Wischmeier, W.H., and Smith, D.D. 1978. Predicting rainfall erosion losses. Agric. Handbook 537. US Department of Agriculture, Washington, DC.

Williams, J.R. 1975. Sediment–yield prediction with universal equation using runoff energy factor. In: Present and prospective technology for predicting sediment yield and sources. Proceedings of the sediment–yield workshop, USDA Sedimentation Lab., Oxford, MS, November 28–30 1972. ARS–S–40.

Williams, J. R. 1969. Flood routing with variable travel time or variable storage coefficients. Trans. ASAE, **12**(1): 100–103.

Winter, T.C., and Woo, M.K. 1990. Hydrology of lakes and wetlands. In The Geology of North America, Vol. 0–1, Surface Water Hydrology 159–87. Boulder, CO: The Geological Society of America.

Woo, M.K., and Rowsell, R.D. 1993. Hydrology of a prairie slough. Journal of Hydrology, **146**: 175–207.

Yang, W., Wang, X., Liu, Y., Gabor, S., Boychuk, L., and Badiou, P. 2009. Simulated environmental effects of wetland restoration scenarios in a typical Canadian prairie watershed. Wetlands Ecology and Management, **18**(3): 269–279.

CHAPTER 5 MODELING OF NUTRIENT EXPORT AND EFFECTS OF MANAGEMENT PRACTICES IN A COLD-CLIMATE PRAIRIE WATERSHED: ASSINIBOINE RIVER WATERSHED, CANADA

This chapter has been submitted as a research paper to the Journal of Agricultural Water Management.

Citation: Mekonnen, B.A., Mazurek, K.A., and Putz, G. (2016). Modeling of nutrient export and effects of management practices in a cold-climate prairie watershed: Assiniboine river watershed, Canada. Journal of Agricultural Water Management (submitted).

The document has been reformatted from the original version for inclusion in the thesis though no content has changed from the submitted version.

Contribution of the PhD candidate

The contribution of the PhD candidate to the research presented in this chapter is extending the application of the developed model for nutrient (phosphorous and nitrogen) export simulation. Model development, calibration, validation, and uncertainty analysis for nutrient export simulation, as well as application of the model to assess impacts of management practices on nutrients export, were carried out by the candidate. The candidate also drafted the manuscript. The second and third authors provided advice on various aspects of the work as well as critical review and editorial guidance of the manuscript.

Contribution of this chapter to the overall study

In line with the broad goal of this dissertation, which is developing flow and pollutants export simulation tool to assess impacts of anthropogenic activities on pollutant export, this section of the thesis contributes to the general theme by focusing on nutrient (nitrogen and phosphorous) simulation together with assessment of impacts of management practices on pollutant export aspects of the research. This Chapter, therefore, is an extension of the previous Chapter and it mainly focuses on extending the developed model for nutrient export simulation and use it as a tool to assess impacts of management practices on sediment and nutrient export.

5.1 Abstract

Non-point source pollution due to agricultural activities is an important problem that has been threatening water resources in Canadian prairie watersheds. The development of strategies to prevent nutrient loss depends on the quantification of nutrient mobilization and transport across a watershed. Integrated eco-hydrological models can play an important role in this regard. However, current model applicability to cold-climate Canadian prairie watersheds is limited due to the complex dynamics of nutrient export under the existence of numerous landscape depressions and freeze-thaw cycles. The aim of this study was to evaluate an eco-hydrological model for nutrient export prediction and assess the impacts of management practices for a cold-climate prairie watershed. To achieve the objectives, a new version of the SWAT model called SWAT-PDLD, which combines SWAT and a Probability Distributed Landscape Depressions (PDLD) model, along with a seasonally varying soil erodibility factor, was applied to a Canadian prairie watershed (the Assiniboine River Watershed, Saskatchewan, Canada). The PDLD module is used to simulate the effect of the numerous landscape depressions that exist in these watersheds on streamflow, whereas a seasonally varying soil erodibility factor is used to take

into account seasonal variation of sediment and nutrient generation due to the cold climate conditions. Model calibration and uncertainty analysis were performed using the Sequential Uncertainty FItting (SUFI-2). The study shows that the SWAT-PDLD model with seasonally varying soil erodibility simulates the daily nutrient export in a cold prairie watershed satisfactorily as confirmed by both graphical plots and statistical measures. A sensitivity analysis of sub-watershed discretization revealed that the streamflow is relatively insensitive to sub-watershed discretization but it did affect sediment and nutrient export. Importantly, the model shows that both filter strips and cover crops decreased sediment, phosphorous, and nitrogen export, while conservation tillage increased phosphorous export in the study watershed. However, precaution should be taken for filter strips as the current filter strips module does not consider factors related to the frozen soil condition in the study watershed. Therefore, the current model result for filter strips is based on assumptions that may limit the validity of the conclusions.

5.2 Introduction

Environmental problems due to increased non-point source pollution such as nutrient loadings are a problem of global importance (Chambers et al. 2001; Newham et al. 2004; De and Bezuglov, 2006; Santhi et al. 2006). Canadian prairie watersheds are not exceptions, if not worse, as agriculture is a dominant economic force that has led to a large-scale change of land use to cultivation (Crumpton and Goldsborough 1998; Assiniboine Watershed Stewardship Association 2000; Huel et al. 2000; Statistics Canada 2011). According to Statistics Canada (2011), the amount of fertilized, cultivated land in the Canadian prairies has increased by nearly 400% between 1971 and 2006. With this increase in agricultural activity, excess inputs of nutrients into waterbodies have been observed on the Canadian prairies. For instance, Bourne et

al. (2002) indicated that increases in nitrogen and phosphorous loads, 13% and 10% respectively, have occurred in Lake Winnipeg during the period between 1973–1999.

Nutrients are essential elements required for plant growth, however, excessive inputs of nutrients into an aquatic ecosystem can lead to significant negative impacts on water quality. Eutrophication is among the many environmental problems caused by excessive nutrient enrichment as evidenced by frequent fish kills in Canadian prairie lakes such as The Lake of the Prairies and Lake Winnipeg (Hall and Leavitt 1999; Chambers et al. 2001; Jones and Armstrong 2001; Saskatchewan Watershed Authority 2005; Lake Winnipeg Stewardship Board 2006; Salvano et al. 2009). In fact, eutrophication frequency and severity is showing an increasing trend in Canadian prairie watersheds (Hall and Leavitt 1999; Chambers et al. 2001; Dube et al. 2011). Furthermore, increased agricultural activities proposed by the Saskatchewan Ministry of Agriculture (Saskatchewan Ministry of Agriculture 2013) and expected future climate change (Shrestha et al. 2012) have the potential to further worsen water quality degradation in the region.

In order to guide the development of an appropriate remediation strategy, information about how nutrient export processes are occurring across a watershed is required (Panagopoulos et al. 2012). Simulation models can play an important role in quantifying nutrient loss and export processes (e.g., Zhang and Jørgensen 2005; Elshorbagy and Ormsbee 2006; Barlund et al. 2007; Dong et al. 2014). A wide range of nutrient loss and export models have been developed and applied to different watersheds (Merritt et al. 2003; Borah and Bera 2003; Booty and Benoy 2009). Each model was initially developed for a specific region and goal, and differed from other models in complexity, data requirements, and spatial and temporal resolution (Merritt et al. 2003). However, modeling nutrient export from Canadian prairie watersheds remains difficult.

Much of the difficulty of this problem is because the landscape is dominated by numerous landscape depressions (potholes) that vary in storage capacity and have a dynamic connectivity (Shaw et al. 2011; Shook et al. 2013). Also as a result, there are numerous non-contributing areas to streamflow in the region (Godwin and Martin 1975; Shaw et al. 2011; Shook et al. 2013). The dynamic connectivity between landscape depressions leads to dynamic non-contributing areas, which invalidates most conventional models that assume a fixed contributing area (Shook et al. 2013).

In considering a single depression, the major components of the water budget include precipitation on the water surface, surface runoff from uplands, evapotranspiration, surface outflow (overflow) when a depression is filled beyond capacity, and groundwater flow (Woo and Rowsell 1993; Winter and Woo 1990; Hayashi et al. 1998; Fang and Pomeroy 2008). The most significant input to the prairie landscape depression water budget is upland snowmelt, which is vital for the existence of wetlands because summer precipitation is exceeded by evapotranspiration (Hayashi et al. 1998; Labaugh et al. 1998; Fang and Pomeroy 2008). The other inputs include precipitation directly on the depression and surface runoff during intense rainfall events (Hayashi et al. 1998; Labaugh et al. 1998; Fang and Pomeroy 2008). Evapotranspiration and lateral flow of shallow groundwater driven by evapotranspiration are the main pathway for water leaving the depressions (Woo and Roswell 1993; van der Kamp and Hayashi 2009). However, the influence of deep groundwater exchange on the water budget of the depressions is limited due to the low hydraulic conductivity of the deeper underlying tills (van der Kamp and Hayashi 2009).

In considering the nutrient budget, for a prairie watershed with depressions nutrients are mobilized from open fields. Some portion of these nutrients directly reaches the watershed

outlet. However, in the prairie watershed much are trapped, transformed, and stored in the depressions (Neely and Baker 1989; Johnston 1991; van der Valk and Jolly 1992; Crumpton and Goldsborough 1998; Murkin 1998). Nutrients in the depression water can be exchanged to the atmosphere (nitrogen only), sediment-interstitial water, and living and dead biomass through biogeochemical processes (Crumpton and Goldsborough 1998; Brunet 2011). Several past studies demonstrated that depressions in the prairie region are nutrient sinks (Neely and Baker 1989; Crumpton et al. 1993; Moraghan 1993; Reddy et al. 1999; Birgand et al. 2007).

The other challenge in modeling a Canadian prairie watershed is that it exhibits a cold-climate hydrology (Pomeroy et al. 2007). The hydrological processes in the region are highly influenced by snow accumulation and melt, runoff over frozen ground, infiltration into frozen or partially frozen soil, and freeze-thaw processes. The majority of the runoff occurs over a few weeks in the spring when the melt rate of the snowpack exceeds the reduced infiltration rate to frozen soils (Granger et al. 1984; Gray and Landine 1988). The mobilization and transport of pollutants, such as sediment and nutrients, are also influenced by the cold-climate conditions (Deelstra et al. 2009; Han et al. 2010). Several studies show that pollutant mobilization and export are higher during the snowmelt period (e.g., McConkey et al. 1997). This is mainly because of the increased soil erodibility during freeze-thaw cycles (Wall et al. 1988), increased surface runoff enhanced by reduced infiltration in frozen or partially-frozen soils (Gray et al. 2001), and the longer duration of the snowmelt-runoff period as compared to individual rainfall-runoff events (Tiessen et al. 2010). As noted by Han et al. (2010), however, most hydrological models do not consider the seasonality of nutrient generation.

With respect to modeling of Canadian prairie watersheds, there is much research on how to handle the thousands of landscape depressions that may exist within a watershed (Abedini

1998; Su et al. 2000; Pomeroy et al. 2007; Fang and Pomeroy 2008; Wen et al. 2011; Shrestha et al. 2012; Mekonnen et al. 2014; Mekonnen et al. 2015; Mekonnen et al. 2016a; 2016b). An approach that uses a probability distribution to model dynamic storage on the landscape is increasing in use for large-area watersheds (e.g., Abedini 1998; Mekonnen et al. 2014; Mekonnen et al. 2016a). The Soil and Water Assessment Tool (SWAT) was recently modified to consider landscape depression storage heterogeneity using this probability distribution approach (with the algorithm called "Probability Distributed Landscape Depressions" (PDLD)) (Mekonnen et al. 2016a). The upgraded SWAT model, called SWAT-PDLD, calculates runoff from landscape depressions based on the available storage capacity of a depression and considers storage capacity variations across the watershed. SWAT-PDLD was tested in simulating the daily streamflow for two Canadian prairie watersheds (the Assiniboine and Moose Jaw River watersheds Saskatchewan, Canada) and showed improved performance over the lumped synthetic storage approach used in the existing version of SWAT (Mekonnen et al. 2016a). Additionally, the SWAT-PDLD was modified to include seasonally varying soil erodibility parameters, which showed good performance in simulating sediment export in the same watersheds (Mekonnen et al. 2016b). The goal of the latter study was to better replicate variations in soil erodibility between frozen, thawing, and unfrozen soils as observed by McConkey et al. (1997).

The objectives of this study are the following: (1) to evaluate the applicability of the SWAT-PDLD model with seasonally varying soil erodibility for nutrient export simulation in a Canadian prairie watershed (the Assiniboine River watershed, Saskatchewan, Canada); and (2) to assess the potential impacts of several agricultural management practices on nutrient export in this watershed using SWAT-PDLD. In order to achieve the objectives, the SWAT-PDLD model

was applied in simulating nutrient export in the Assiniboine watershed. Model calibration and uncertainty analyses of SWAT-PDLD were done using a Sequential Uncertainty FItting algorithm (SUFI-2) (Abbaspour et al. 2004). Model performance was evaluated using both multiple statistical criterions and graphical plots. In addition, a sensitivity analysis was performed to evaluate the influences of sub-watershed discretization level. Finally, the impacts of three different management practices on phosphorous and nitrogen export for the study watershed are assessed. The management practices evaluated are filter strips, a change in tillage practice to conservation tillage, and planting red clover as a cover crop.

5.3 Materials and Methods

5.3.1 Study area

The modelling study was conducted on the Assiniboine River watershed, Saskatchewan, Canada (see Fig. 5–1). The Assiniboine River and its tributaries drain areas in eastern Saskatchewan and western Manitoba in Canada (Saskatchewan Watershed Authority 2005). The watershed at the Kamsack gauging station (see Fig. 5–1) has a gross drainage area of 13,000 km^2 of which about 4,320 km^2 is considered as effective drainage area following the definition of Godwin and Martin (1975). Godwin and Martin (1975) defined the effective drainage area as that contributing into the main stream for the 1:2 year return period flood. The mean elevation of the watershed is about 537 m above mean sea level. The lowest point is 428 m above mean sea level, which is located at the Kamsack gauging station; and the highest point is 718 m above sea level, which is in the upland of the northern headwater. Close to 90% of the watershed area lies below 600 m elevation and only 0.1% above 700 m. The topography is gently to moderately undulating, with the steeper slopes along the Assiniboine River and a relatively level topography

of the Assiniboine Plains throughout most of the watershed (Saskatchewan Watershed Authority 2005).

The watershed exhibits cold region hydrology, which is characterized by long and cold winters, snow accumulation, snowmelt, frozen ground, and freeze and thaw cycles (Fang and Pomeroy 2008). The mean annual temperature in the basin is about 1°C. The normal frost-free season duration is from 90 to 110 days (102 at Kamsack). The mean annual precipitation for the watershed is 450 mm per year, of which about 74 percent of the precipitation occurs as rainfall and the remaining 26 percent is snowfall (Assiniboine Watershed Stewardship Association 2000). The average daily discharge at Kamsack is 8.3 m^3/s for the period of 1944-2011, with a minimum value of 0 m^3/s and a maximum value of 484 m^3/s (HYDAT 2014).

In the watershed, agriculture is the dominant economic activity, with grain farms and livestock operations located throughout. Close to 58% of the land within the watershed is used for agricultural activities and mostly for annual crops. In addition, 17% is covered by grassland and forages. The dominant soil type is black chernozemic that has generally developed under native grassland vegetation and is high in organic matter. The black chernozemic soil covers close to 70% of the watershed (Saskatchewan Watershed Authority 2005).

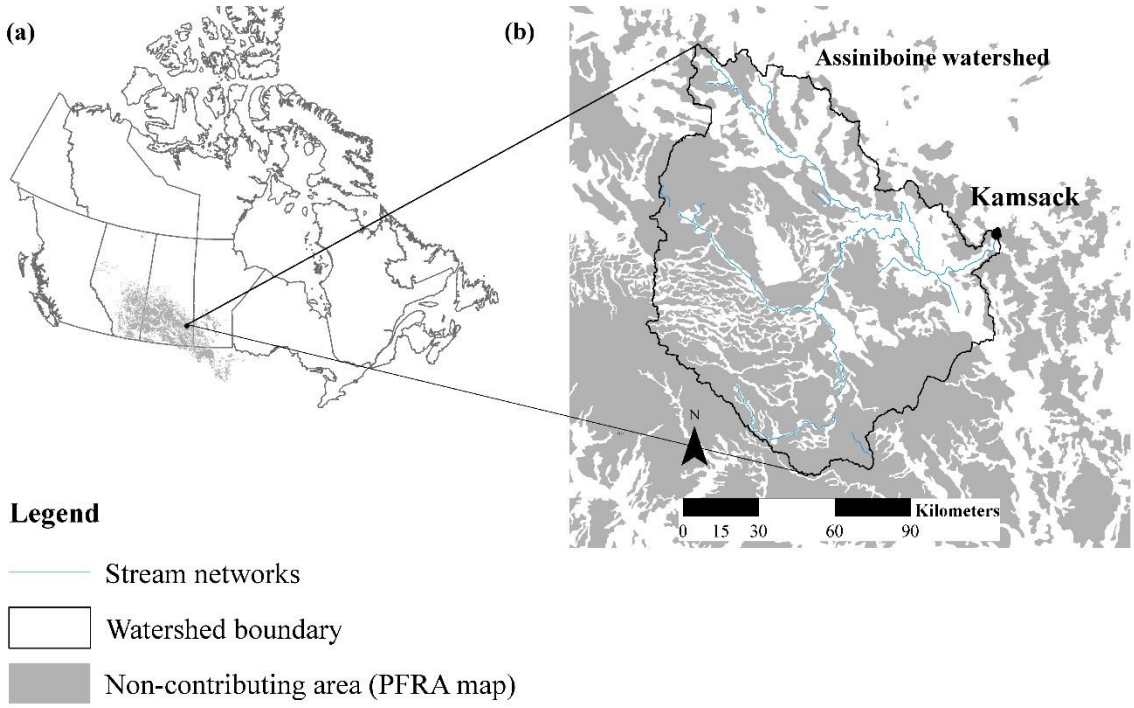

Figure 5–1 The Assiniboine River watershed (a) within Canada and (b) upstream of the Kamsack gauging station.

5.3.2 SWAT model description

The Soil and Water Assessment Tool (SWAT) (Arnold et al. 1998) is a continuous processes based semi-distributed model that simulates the various hydrological and water quality processes of a watershed (Neitsch et al. 2011). As described in Neitsch et al. (2011), SWAT simulates hydrological processes by partitioning a watershed into a number of sub-watersheds that are further grouped into Hydrological Response Units (HRUs). Watershed processes such as surface runoff, evapotranspiration, infiltration, sediment yield, nutrient cycles, crop growth and management practices are simulated for each HRU and then weighted for the sub-basin. The simulated flow, sediment, and nutrients from each sub-basin are then routed through the river channel using the variable storage (Williams 1969) or Muskingum routing method (Cunge 1969).

Surface runoff from daily rainfall or snowmelt estimated with a temperature-index method (Neitsch et al. 2011) is computed using either the Curve Number Method (CN) (SCS: USDA Soil Conservation Service 1972) or Green-Ampt method (Green and Ampt 1911). A provision for estimating runoff from frozen soil is also included in such a way that if the temperature in a particular soil layer reaches less than or equal $0^{o}C$, no percolation is allowed through that layer. Potential evapotranspiration is estimated using one of three different methods that include Hargreaves (Hargreaves et al. 1985), Priestley-Taylor (Priestley and Taylor 1972), and Penman-Monteith (Monteith 1965). The actual evapotransration from soils and plants is estimated as described by Ritchie (1972).

For each HRU the soil profile is sub-divided into multiple layers (maximum 10) that support soil-water processes. The processes considered for each soil layer include infiltration, evaporation, plant uptake, lateral flow, and percolation to lower layers. Downward flow through each soil layer occurs when the field capacity of a soil layer is exceeded and the layer below is not saturated. Percolation from the bottom of the soil profile recharges the shallow aquifer, which contributes to return flow and deep aquifer recharge. Groundwater flow contribution to total streamflow, also called return flow or baseflow, is simulated by routing a shallow aquifer storage component to the stream (Neitsch et al. 2011).

Sediment yield is estimated for each HRU with the Modified Universal Soil Loss Equation (MUSLE) (Williams and Berndt 1977). MUSLE uses the runoff hydrograph rather than rainfall energy to estimate erosive power of individual runoff events. Sediment yield from each sub-basin is then routed though the main channel. The sediment routing in the channel model considers channel degradation and deposition processes.

Nutrient cycles (both nitrogen and phosphorous) in the SWAT model are simulated at the HRU level. Details of the nutrient cycle representations are described by Neitsch et al. (2011). As nutrient inputs, the model takes into consideration natural sources such as organic matter mineralization, N-fixation, wet deposition of nitrate, and anthropogenic contributions such as fertilizer applications (diffuse sources) and wastewater from treatment plants (point sources). The in-stream water quality modelling is based on QUAL2E (Brown and Barnwell 1987).

In addition, SWAT also has the capability to simulate conservation practices such as filter strips that remove pollutants before reaching nearby water bodies (Neitsch et al. 2011).

5.3.3 SWAT-PDLD model description

SWAT-PDLD is a modified form of the SWAT model in which landscape depressions and cold climate condition influences are considered. Unlike the original SWAT model that uses a lumped storage approach, the SWAT-PDLD model uses a probability distribution module called Probability Distributed Landscape Depressions (PDLD) to take into account storage capacity heterogeneity of the numerous landscape depressions. The SWAT-PDLD model has been previously tested for two Canadian prairie watersheds (the Assiniboine and Moose Jaw River watersheds) to simulate streamflow (Mekonnen et al. 2016a) and sediment export (Mekonnen et al. 2016b).

The PDLD module considers the water budget for a single depression as an input from precipitation and upland areas and losses through evapotranspiration and seepage (Equation (5.1)). The depression will spill and therefore generate runoff when the net input exceeds the available storage in the depression. The water budget of a single depression can be formulated as:

$$Q = \begin{cases} P + Q_{\mathrm{u}} - E - I - (c - S) & \text{for} \quad P + Q_{\mathrm{u}} > c - S + E + I \\ 0 & \text{for} \quad P + Q_{\mathrm{u}} \leq c - S + E + I \end{cases} \tag{5.1}$$

where P = precipitation; Q_{u} = runoff into the depression from upland areas within the sub-basin; E = evapotranspiration; I = seepage from the depression; c = the storage capacity of the depression; S = water stored in the depression; and Q = resulting direct runoff generated from the depression over the time interval considered.

The PDLD module calculates the total runoff generated from all the landscape depressions as the cumulative overspill runoff generated from the individual depressions. In such a conceptualization, the proportion of depressions that are taken to be spilling is calculated from a probability distribution describing the variation in storage capacity within the sub-basin. Considering field measurement studies showing surface water connectivity in the prairies (e.g. Rosenberry and Winter 1997; Leibowitz and Vining 2003), the depressions are treated as if they interact, which means that water is redistributed among the depressions. Under such conditions, all depressions with a storage capacity greater than the critical capacity, $C^*(t)$, will have an equal amount of water stored in the depressions equal to $C^*(t)$. Those depressions with a storage capacity less than $C^*(t)$ are full to their capacity and cannot contain more water but instead will spill and therefore contribute runoff to the main stream. Therefore, the total water stored in the depressions at a particular time, $S(t)$ is the sum of water stored in depressions that are full (depressions with a capacity less than the critical capacity) and the water stored in part-full depressions (depressions with a capacity greater than the critical capacity). This total water stored in the landscape depressions within a sub-basin is given by:

$$S(t) = \int_0^{C^*(t)} c f(c) dc + C^*(t) \int_{C^*(t)}^{\infty} f(c) dc \tag{5.2}$$

where C = the storage capacity; $C*(t)$ =the dynamic critical capacity; and $f(c)$ = the probability density function that describes the distribution of storage capacity across the landscape. The critical storage capacity, $C*(t)$, separates the storages that are completely full and over spilling from those still filling at a particular time. The first term in the right side of Equation (5.2) represents the water stored in depressions which are full and contributing. The second term in the right side of Equation (5.2) represents the water stored in depressions that are not at full capacity and do not start contributing for the current conditions. Making use of the general result:

$$\int_0^{C*(t)} cf(c)dc = C*(t)\,\mathrm{F}(\mathrm{C}*) - \int_0^{C*(t)} \mathrm{F}(c)dc$$

and incorporating the relation $\int_{C*(t)}^{\infty} f(c)dc = 1 - F(\mathrm{C}*)$ followed by some re-arrangements, Equation (5.2) can be re-formulated as follows:

$$S(t) = \int_0^{C*(t)} (1 - F(c))dc \tag{5.3}$$

where $F(c)$ = the cumulative $f(c)$.

For this study, the probability density function to be used for the watershed was determined using digital elevation data analysis. ArcGIS was used to quantify the depression geometries across the watershed. Then, the storage capacities of the depressions were plotted by frequency of occurrence. A probability density function was then fitted to this data so that an expression of the variation of capacity across the watershed could be found. An exponential distribution was selected because of its relative simplicity (a one parameter function) with a satisfactorily fit to the data as shown in Mekonnen et al. (2016a). The cumulative exponential distribution is expressed as follows:

$$F(c) = 1 - \exp\left(\frac{-c}{\bar{c}}\right) \tag{5.4}$$

where $\overline{c}$ = the mean storage capacity. The mean or average storage capacity was calculated for each sub-basin.

The value of the critical storage capacity at any time, *t*, *C*(t)*, is obtained by combining Equations (5.2) and (5.3) then integrating and solving for $C*(t)$, where:

$$C*(t) = -\overline{c}\ln\left(1-\frac{S(t)}{\overline{c}}\right) \tag{5.5}$$

For a net water input to the depressions of $\pi\Delta t$ occurring during the time interval (*t, t*+Δt), the critical capacity, $C*(t+\Delta t)$, will increase over $C*(t)$ by $\pi\Delta t$. For the increased critical capacity, $C*(t+\Delta t)$, the corresponding stored water over the landscape depressions at $t+\Delta t$, $S(t+\Delta t)$, can be computed as:

$$S(t+\Delta t) = \overline{c}\left(1-\exp\left(\frac{-C*(t+\Delta t)}{\overline{c}}\right)\right) \tag{5.6}$$

The direct runoff, $R(t,t+\Delta t)$, generated from the landscape depressions within a sub-basin during the time interval (t, $t+\Delta t$) then can be computed:

$$R(t,t+\Delta t) = \pi\Delta t - \left(S(t+\Delta t) - S(t)\right) \tag{5.7}$$

An initial condition must be assumed or estimated for the amount of water stored in the landscape depressions, $S(0)$, at the beginning of a model simulation using the above described Probability Distribution of Landscape Depressions (PDLD) algorithm in order for the calculations to proceed. The initial condition assumed at the start of the warm up period for the model run was that during the spring snowmelt period the depressions were all at full capacity.

The PDLD algorithm was used to modify the “Ponds” routine within SWAT that is used to represent depressions (Mekonnen et al. 2016a, 2016b). Unlike the ‘Pond” routine that allows only a single depression per sub-basin in the original SWAT model, the PDLD module

represents the numerous depressions that exist within a sub-basin. In fact, SWAT provides three specific tools for simulating landscape depressions including “Potholes”, “Ponds”, and “Wetlands”. In the original SWAT model, the Potholes routine only captures flow from individual HRUs, whereas Ponds and Wetlands are capture flow from any number of different HRUs within a sub-basin. The Pond routine was selected for modification with the PDLD algorithm because depressions in prairie watersheds capture flow from any number of different HRUs and therefore, which better approximates the behaviors in these watersheds.

5.3.4 Seasonality of sediment and nutrient export

Several studies have shown seasonality of sediment and nutrient export under cold-climate conditions in Canadian prairie watersheds (e.g., Coote et al. 1988; Wall et al. 1988; McConkey et al. 1997). Seasonality of sediment export from the Assiniboine River watershed was also confirmed by past works (e.g., Mekonnen et al. 2016b). For cold-climate Canadian conditions, the relative weighting of the ratio of the soil erodibility factor (K) for a given season to that in the summer (Period 4: May 1 to October 31st) was determined to be 0.41 1.18, and 1.9 for Period 1 (November 1 to March 15th), Period 2 (March 16 to March 31st), and Period 3 (April 1 to April 30th) repectively (McConkey et al. 1997). These relative K also follow the pattern of seasonally weighted K’s for a nearby location in the United States (McConkey et al. 1997). Similar weightings for K are also recommended in the RUSLEFAC handbook (Revised Universal Soil Loss Equation Application in Canada) (Wall et al. 2002). The weighting factor of soil erodibility was used to incorporate seasonality of sediment export into the SWAT-PDLD model (Mekonnen et al. 2016b). Unlike the original SWAT model, which uses an annual value of soil erodibility, the value of soil erodibility is allowed to vary between the four seasons. As demonstrated by Mekonnen et al. (2016b), consideration of soil erodibility factor seasonality

improves sediment prediction capability of conventional models that often assume an annual value of soil erodibility (Mekonnen et al. 2016b). Seasonality of erodibility then is important to consider since nutrients such as phosphorous tend to move in attachment with sediment.

5.3.5 SWAT-PDLD model input data requirements

The basic datasets used to develop the model input files are topography, soil, land use and climatic data. The Digital Elevation Model (DEM) of the study watershed was obtained from the GeoBase Canada website (http://www.geobase.ca/) (GeoBase Canada 2007) at a scale of 1:50,000. Similarly, the land cover data was obtained from the GeoBase Canada database (http://www.geobase.ca/) (GeoBase Canada 2009). The data was prepared through vectorization of raster thematic data originating from Landsat 5 and Landsat 7 ortho-images and is available at a scale of 1:250,000. The soil data, at a resolution of 1:1,000,000 along with soil properties used in the SWAT-PDLD model, were obtained from the Agriculture and Agri-Food Canada database (Soil Landscapes of Canada Working Group 2007).

Daily gridded climate data including temperature (minimum and maximum) and precipitation was used as input meteorological data for the SWAT model. The Gridded Climate Dataset for Canada (Hutchinson et al. 2009) was obtained from Agriculture and Agri-Food Canada. This dataset covers south of 60°N latitude in Canada for the period 1961-2003 and was prepared through interpolation of observations from Environment Canada using a thin-plate smoothing spline-surface fitting method at a 10 km spatial resolution.

The major sources of surface water pollution in the watershed are agriculture and livestock operations, while effluent from sewage treatment facilities and stormwater runoff also contribute to pollution (Saskatchewan Watershed Authority 2005). Fertilizer and manure application rates were obtained from Saskatchewan Watershed Authority (Saskatchewan

Watershed Authority 2010). According to the Saskatchewan Watershed Authority (2010), the rate of fertilizer application in the Assiniboine watershed ranges between 45.51 to 60.29 and 8.51 to 10.50 kg/ha of nitrogen and phosphorous respectively. More than 80% of fertilizer application occurs during crop planting, while the remaining 20% is applied during other growing periods (Flaten 2013). The amount of manure applied over the Assiniboine watershed ranges between 1098 to 1628 kg/ha. Of this total amount of manure, 55% was produced by beef cows, followed by calves (17%), heifers (9%), steers (5%), pigs (4%), bulls (3%), dairy cows (2%), poultry (1%), and others (1%) (Saskatchewan Watershed Authority 2010). In the Assiniboine River watershed, the dominate tillage practice (more than 60%) was conventional tillage for many years but the proportion of conventional tillage has decreased and has been replaced by conservation tillage since 1995 (Awada et al. 2014; The Encyclopedia of Saskatchewan 2015). Crops are generally planted in May and harvested in September (West Coast Seeds, 2015). In considering the cropping pattern of Saskatchewan, there is no uniformity of cropping pattern across the watershed. However, the crop type distribution in Saskatchewan is dominated by cereal crops that cover more than 60% of agricultural areas while the remaining areas are used for fallow practices and other crops such as oil seeds and pulses based on survey data of Agriculture & Agri-Food Canada's (AAFC) PFRA Branch and Statistics Canada (Saskatchewan Trends Monitor 2005). Wheat has been the dominant crop in Saskatchewan for many years but the proportion of wheat production has decreased since 2001 (Saskatchewan Trends Monitor 2005; Statistics Canada 2014).

Point source pollution from sewage treatment facilities in the study watershed were not considered in this study because of data limitations. However, from the authors' personal experience for the study watershed, point source discharges from sewage treatment facilities

usually occur twice a year during October and spring. To take into account point source discharges from sewage treatment facilities, observed data that were collected in the month of October were excluded from being used to optimize the model. On the other hand, during the spring period influence of point source discharges from sewage treatment facility were assumed to be relatively small considering the high fluxes of agricultural non-point pollution driven by the snowmelt runoff.

Observed daily streamflow (1990-1999) and sediment load (1970-1979) datasets were obtained from the Hydrometric Database (HYDAT) of Water Survey of Canada. The Kamsack gauging station (Water Survey of Canada Station Number 05MD004) is located at 51°33’53’’ N latitude and 101°54’48’’ W longitude. Nutrient datasets (phosphorous and nitrogen) were obtained from the Province of Saskatchewan. Both nitrogen and phosphorous datasets are available at monthly intervals. The water quality measurements were taken 5 km downstream of the Kamsack hydrometric station.

5.3.6 SWAT-PDLD model setup

Digital Elevation Model (DEM) data was used to delineate and discretize the study watershed into sub-watersheds using the ArcSWAT interface. A wide range of sub-watershed discretization was considered by setting different minimum threshold drainage areas ranging from 1210000 ha (corresponding to 3 sub-watersheds) to 2500 ha (corresponding to 295 sub-watersheds) during watershed delineation (Table 5–1). Following sub-watersheds discretization, the land use, soil, and slope maps were imported and overlaid to derive different HRUs. For the HRUs that were defined as agricultural HRUs, the following management scheme was adopted: the crop was planted at the end of May and harvested at the beginning of September (West Coast Seeds 2015); conventional tillage was implemented as it was the dominant tillage practice (more

than 60%) during the simulation period (Awada et al. 2014; The Encyclopedia of Saskatchewan 2015); and fertilizer was assumed to be applied during crop planting (Flaten 2013). The amount of fertilizer applied was 52.9 and 9.505 kg/ha of nitrogen and phosphorous respectively, which is the average of the lower and upper limit estimated by SWA (2010). The amount of manure added was 1363 kg/ha, which is the lower and upper limit estimated by SWA (2010). Of this total amount of manure, 55% was produced by beef cows, followed by calves (17%), heifers (9%), steers (5%), pigs (4%), bulls (3%), dairy cows (2%), poultry (1%), and others (1%). A summary of the nutrient fractions (in relation to phosphorous and nitrogen) for various types of manure is presented in Table 5–2 below, which is adapted from the SWAT fertilizer database (fert.dat). Finally, input climatic datasets of gridded daily precipitation and temperature (minimum and maximum) datasets at a grid size of 10 km were used to run the model.

Table 5–1 Sub-watershed divisions and watershed characteristics.

Number of sub-watersheds	Average sub-watershed area ($*10^4$ m^2)	Average overland slope length (m)	Average overland slope (m/m)	Average channel slope length ($*10^3$ m)	Average channel slope (m/m)
3	4035.2	111.8	0.020	65.7	0.00065
5	2421.1	115.9	0.013	56.3	0.00056
9	1345.1	122.0	0.014	40.7	0.00084
13	931.2	114.9	0.016	36.6	0.00088
15	807.0	119.9	0.007	33.4	0.00085
17	712.1	113.0	0.017	29.8	0.00087
21	576.5	119.0	0.013	25.1	0.00133
25	484.2	119.5	0.013	25.4	0.00106
31	390.5	118.0	0.014	21.9	0.00111
37	327.2	114.6	0.015	20.7	0.00104
49	247.1	117.0	0.014	19.4	0.00127
65	186.2	114.4	0.016	18.1	0.00129
81	149.5	114.6	0.015	15.6	0.00146
101	119.9	115.0	0.015	13.5	0.00168
121	100.0	114.9	0.016	12.0	0.00202
295	41.0	115.2	0.015	7.7	0.00233

Table 5–2 Summary of various types of manure in relation to phosphorous and nitrogen fractions (Source: SWAT Fertilizer Database, Arnold et al. (2009)).

Name	Mineral N	Mineral P	Organic N	Organic P	NH_3-N
Dairy	0.007	0.005	0.031	0.003	0.99
Beef	0.01	0.004	0.03	0.007	0.99
Veal	0.023	0.006	0.029	0.007	0.99
Swine	0.026	0.011	0.021	0.005	0.99
Sheep	0.014	0.003	0.024	0.005	0.99
Goat	0.013	0.003	0.022	0.005	0.99
Horse	0.006	0.001	0.014	0.003	0.99
Broiler	0.010	0.004	0.04	0.01	0.99

5.3.7 Model calibration and uncertainty analyses

Sensitivity analysis was performed with the Latin Hypercube Sampling-One factor at a time (LH-OAT: van Griensven and Meixner 2006) routine in order to identify sensitive parameters. Following identification of sensitive parameters, sequential uncertainty fitting version 2 (SUFI-2) algorithms (Abbaspour et al. 2004) was used to perform a combined calibration and uncertainty analyses.

Model calibration and validation were performed at a daily time step at the Kamsack gauging station (Station #05MD004) for streamflow and sediment, and 5 km downstream of the Kamsack hydrometric station (Station #SA05MD0002) for nitrogen and phosphorous simulations. With the limited data points for water quality variables, it was difficult to get a common window period that contained the observed datasets of all the variables (streamflow, sediment, and nutrients). Therefore, model calibration was done sequentially in the following order: (1) streamflow; (2) sediment; and (3) nutrients (phosphorous and nitrogen). A similar calibration method was used in past studies including Santhi et al. (2001), Grizzetti et al. (2003), White and Chaubey (2005), Abbaspour et al. (2007), and many others. The streamflow was calibrated first because of its influence on the other output variables and because the measurement uncertainty was likely to be smaller in streamflow data. In addition, streamflow

data has more data points (daily) than the less frequently sampled water quality datasets that were usually sampled once a month (for nutrients in particular).

The daily observed flow data in the period of 1992-1995 (1459 daily data points) and 1996-1999 (1459 daily data points) were used to calibrate and validate the SWAT-PDLD model respectively. The periods 1972 to 1975 (980 daily data points) and 1976 to 1979 (979 daily data points) were used to calibrate and validate the SWAT model for sediment yield prediction respectively. Finally, the nutrient (both phosphorous and nitrogen) component of the SWAT model was calibrated and validated at a daily time step using the observed nutrient data in the periods of 1980 to 1989 (110 data points of each) and 1990 to 1997 (88 data points of each). Sediment and nutrient calibration and validation were performed by comparing the simulated load with observations corresponding to the dates when observation data were available. In all the cases of model calibration, a warm-up period of two years prior to model calibration were used to minimize uncertainty associated with initial conditions (Bussi et al. 2014).

5.3.8 Model performance evaluation statistics

Quantitative evaluation of model performance was assessed using three statistical metrics that include the Nash & Sutcliffe efficiency index (NSE*:* Nash and Sutcliffe 1970), Percent Bias (PBIAS) (Gupta et al. 1999), and ratio of the root mean square error to the standard deviation of measured data (RSR) (Singh et al. 2005) for daily time step simulations.

To evaluate how well the simulation data versus the observed data fits a 1:1 line, the Nash & Sutcliffe efficiency index (NSE) (Nash and Sutcliffe 1970) is used:

$$\mathrm{NSE} = 1 - \frac{\sum_{i=1}^{n}\left(\hat{Q}_i - Q_i\right)^2}{\sum_{i=1}^{n}\left(\bar{Q} - Q_i\right)^2} \tag{5.8}$$

where $\hat{Q}_i$ is the simulated streamflow, Q_i is the observed streamflow at time i, n is total number of data points, and $\overline{Q}$ is the average observed streamflow.

To measure the average tendency of the predicted data set to be smaller or larger than the observed data set, the Percent Bias (PBIAS) (Gupta et al. 1999) is used. PBIAS is calculated using:

$$\text{PBIAS} = \frac{\sum_{i=1}^{n}\left(Q_i - \hat{Q}_i\right)*100}{\sum_{i=1}^{n} Q_i} \tag{5.9}$$

Finally, RSR which is a standardized version of the root mean square error is used following Singh et al. (2005). RSR is the ratio of the root mean square error (RMSE) to the standard deviation (STDEV_o) of the observed dataset (Singh et al. 2005). RSR is calculated as follows:

$$\text{RSR} = \frac{\text{RMSE}}{\text{STDEV}_o} = \frac{\sqrt{\sum_{i=1}^{n}\left(Q_i - \hat{Q}_i\right)^2}}{\sqrt{\sum_{i=1}^{n}\left(Q_i - \overline{Q}\right)^2}} \tag{5.10}$$

5.3.9 Prediction uncertainty statistics

The Sequential Uncertainty Fitting (SUFI-2) method (Abbaspour et al. 2004) was used to quantify prediction uncertainty. As reviewed by Uusitalo et al. (2015), different methods are available to evaluate model uncertainty. The SUFI-2 method has generally been recommended for large area watershed application (e.g. Yang et al. 2008; Setegn et al. 2010; Arnold et al. 2012) because of the smaller number of simulations required and the recent development of parallel processing for SUFI-2 which reduces computational time burden for large area

watershed application (Abbaspour et al. 2004). The method combines calibration and uncertainty procedures to find parameters that result in prediction uncertainties bracketing most of the measured data within the 95% prediction uncertainty band (called *P*-factor) and minimizing the average thickness of the prediction uncertainty band (called *D*-factor). It uses the Latin Hypercube Sampling method (McKay et al. 1979) to draw independent parameter sets (Abbaspour et al. 2004). Details of the SUFI-2 procedure are reported by Abbaspour et al. (2004).

Two indices were used to evaluate prediction uncertainty of the SWAT-PDLD model: (1) the width of the derived 95% uncertainty band (i.e., *D*-factor: see Equation (5.11)); and (2) percentage of the measurements bracketed by this band (i.e., *P*-factor: see Equation (5.12)).

$$D-\text{factor} = \frac{\sum_{t=1}^{n}(\mathrm{y}_{t,97.5\%} - y_{t,2.5\%})}{n\delta} \tag{5.11}$$

$$p-\text{factor} = \frac{\sum_{t=1}^{n}\mathrm{I}[\mathrm{y}_t]}{n}$$

$$\text{with } \mathrm{I}[\mathrm{y}_t] = \begin{cases} 1, \ \textit{if } \mathrm{y}_{t,2.5\%} < \mathrm{y}_t < \mathrm{y}_{t,97.5\%} \\ 0, \ \textit{otherwise} \end{cases} \tag{5.12}$$

where $y_{t,97.5\%}$ and $y_{t,2.5\%}$ are the upper and lower boundaries of the 95% prediction uncertainty, and δ is the standard deviation of observed flow.

5.3.10 Characterization of BMPs

To assess impacts of agricultural best management practices (BMPs) on sediment and nutrient export, three different scenarios were considered. The assessment was implemented by running the SWAT-PDLD model for 10 years (1990 to 1999) under the existing conditions but

with different land management scenarios. The values under the existing conditions were used as the baseline loading conditions to which the simulated loads from different management scenarios were compared. The difference in load between a management scenario and the baseline was used to indicate the load change due to implementation of the management scenario. As presented in Table 5–3 below, the three different management scenarios investigated in this study are filter strips, tillage practices, and crop cover scenarios.

In Scenario 0, also called the baseline scenario, the basin existing conditions are simulated. Scenario 1 is used to assess filter strip impacts on pollutant export. Filter strips (also called vegetative filter strips or buffer strips) were placed between water bodies and agricultural HRUs. Filter strips are mainly used to slow runoff water so that the sediment and nutrients can settle out or be trapped. The trapping efficiency of a filter strip is affected by width of the filter strip. Cho et al. (2010) and Gevaert et al. (2010) found the change in trapping efficiency of filter strip is small after a width of 30 m. In this study, four different width of filter strips were considered, which are 1, 5, 15, and 30 m, in order to assess effects of strip width on efficiency of the practice.

In Scenario 2, the impact of conservation tillage as compared to conventional tillage practice was assessed. The simulation of tillage practice was implemented through modification of the management input file, specifically the tillage operation section, of each Agricultural HRUs. This scenario is important in order to evaluate the effects that are brought by the current tillage practices in Saskatchewan, which is conservation tillage, as compared to the past conventional tillage practices. Furthermore, the tillage practice scenario is also part of Watershed Evaluation of Beneficial Management Practices (WEBs) project, which was initiated in 2004 (AAFC 2011a), by Agriculture and Agri-Food Canada (AAFC) (AAFC 2011b).

The final scenario, Scenario 3, assessed the impact of cover crop on sediment and nutrient export. Cover crops have the benefit of reducing soil erosion for the period they are providing vegetative cover. There are many different types of cover crops and various opportunities for farmers to establish cover crops depending on their cropping pattern. Among them, red clover is being assessed as cover crop by the WEBs project in the Gully Creek Watershed, Ontario, Canada (e.g., Yang et al. 2013). To represent the use of red clover in SWAT, the various land management input files were modified to simulate the seeding of red clover in early August when wheat is growing in the field and simulated to remain growing on the field after wheat harvest until late fall as recommended by Government of Saskatchewan (Government of Saskatchewan 2015).

Table 5–3 Scenario descriptions and SWAT-PDLD parameters used to represent scenarios.

Scenario no.	**Description**	**SWAT parameter used**			
		Parameter name	Input file	Initial value	Modified value
Scenario 0	Baseline	-	-	-	-
Scenario 1	Filter strip/Vegetated buffer	Filterw	.mgt	0	Implemented for Agricultural HRUs
Scenario 2	Conservation tillage	Operations	.mgt	Conventional tillage	Implemented for Agricultural HRUs
Scenario 3	Cover crop	Operations	.mgt	-	Implemented for Agricultural HRUs

5.4 Results and Discussion

The study results and discussion are presented in the following order. The sensitivity to the number of sub-watershed divisions is presented first. Model calibration, validation and uncertainty analyses of streamflow, sediment, and nutrient are presented next. Finally model

application and assessments of impacts of different agricultural management practices on water quality are presented.

5.4.1 Effects of sub-watershed divisions

The sensitivities of watershed average topographic characteristics and simulation responses are reported for increasing numbers of sub-watersheds. Nine different configurations, ranging from three sub-watersheds (coarsest level) to 295 sub-watersheds (the finest level), were investigated for the Assiniboine River watershed. Watershed simulation responses assessed include streamflow, sediment yield, nitrogen export, and phosphorous export.

5.4.2 Effect of number of sub-watershed divisions on average topographic characteristics

Figure 5–2 below shows the variation in topographic characteristics as the number of the delineated sub-watersheds increases. Average topographic characteristics, including overland slope, overland slope length, channel slope, and channel slope length, vary as the number of a sub-watershed changes (see Fig. 5–2). Topographic characteristics, however, behave differently near the coarsest and finest levels of discretization. Towards the coarsest level, the change is abrupt and unstable. Conversely, the changes are relatively insignificant and stable towards the middle and finest levels of discretization. Beyond a threshold number further changes in the number (and nominal size) of the sub-watersheds produce insignificant effect on the average topographic characteristics of the watershed. In this specific watershed, most of the topographic characteristics except average channel slope tend to change very little beyond a threshold of 65 sub-watersheds (see Fig. 5–2).

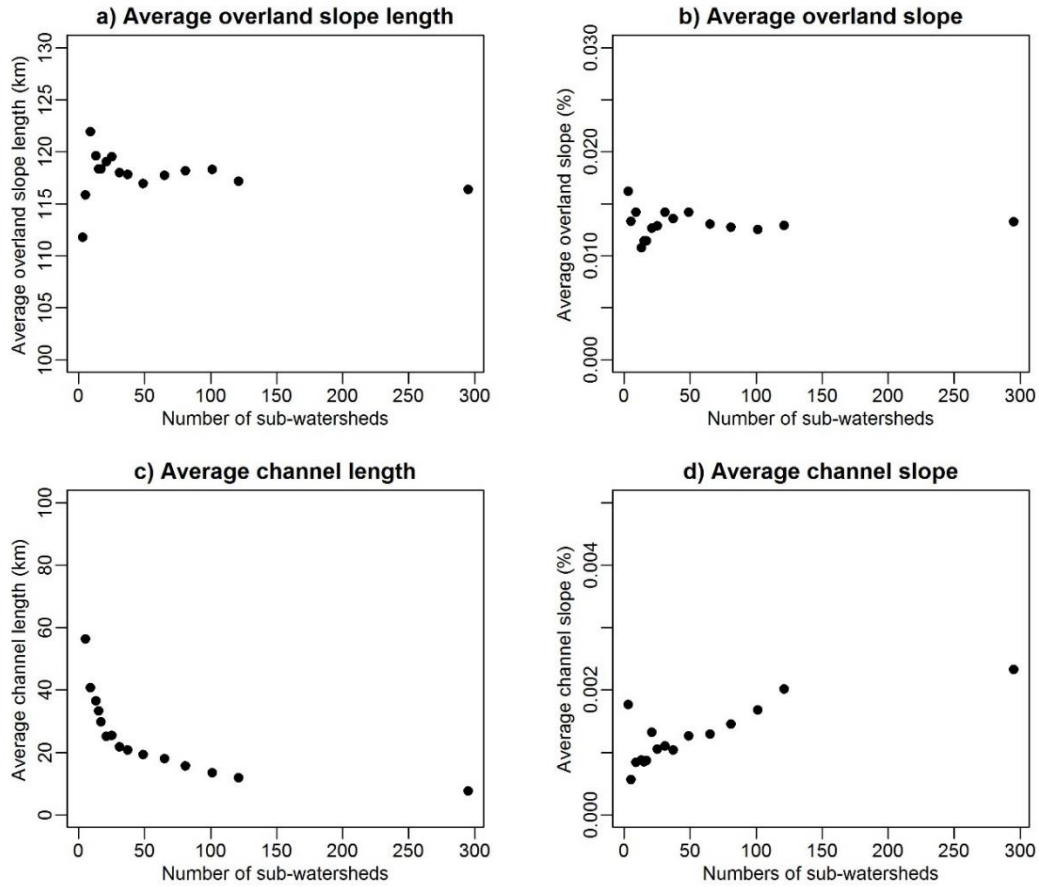

Figure 5–2 Effect of number of sub-watershed divisions on watershed characteristics: a) average overland slope length; b) average overland slope; c) average channel slope length; and d) average channel slope.

5.4.3 Effect of number of sub-watershed divisions on streamflow and water quality simulation

Figure 5–3 presents the Assiniboine River watershed responses (streamflow, sediment, total nitrogen, and total phosphorous) to the number of sub-watersheds delineated. The predicted average annual streamflow that occurred at the outlet of the Assiniboine River watershed remained nearly constant as the number of sub-watersheds increased (Fig. 5–3a). Similar results have been reported by FitzHugh and Mackay (2000) and Jha et al. (2004). In this study, a relatively lower streamflow was only observed with only 3 sub-watershed divisions. This simulation result is mainly because of the lower precipitation which is about 475 mm for 3 sub-

watersheds delineation as compared to relatively consistent and similar value of about 478 mm of precipitation for the other sub-divisions. The maximum fluctuation between the highest and lowest simulated streamflow, excluding the 3-sub-watershed delineation, was below six percent. This insensitivity of average annual streamflow is because the streamflow (surface and subsurface runoff) is generated at the HRUs level and hence the characteristics of HRUs are more important than sub-watershed size. The streamflow processes that are affected by sub-watershed size are water losses in the sub-watershed main channel, which are relatively minor compared to other processes.

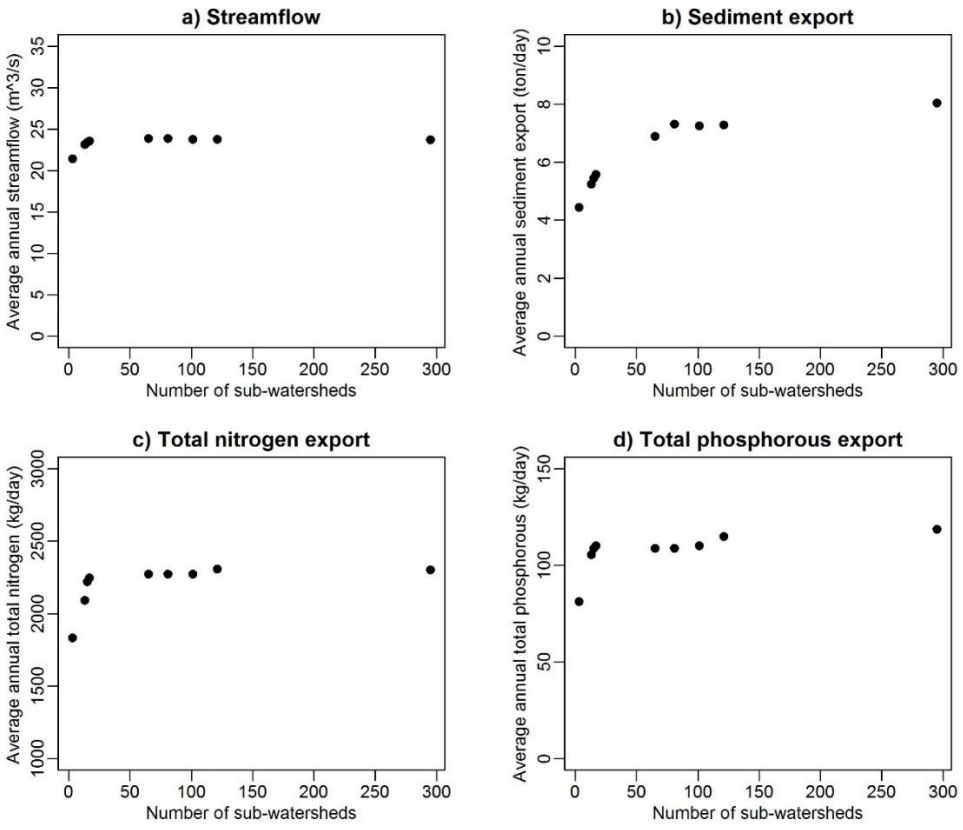

Figure 5–3 Average annual values of hydrologic and export responses at the outlet of the Assiniboine River watershed as a function of number of sub-watersheds: a) average annual streamflow; b) average sediment export; c) average annual total nitrogen export; and d) average annual total phosphorous export.

Figure 5–3b shows the trend in predicted average annual sediment export as a function of the number of sub-watersheds. In response to increasing numbers of sub-watersheds, the predicted sediment yield increased at a much greater rate as compared to the streamflow. This result is consistent with results reported by Jha et al. (2004), Arabi et al. (2006), and Setegn et al. (2010). High sensitivity of predicted sediment export to the number of sub-watershed divisions can occur for two main reasons. The first reason is that the Modified Universal Soil Loss Equation (MUSLE) (Williams and Berndt 1977) is sensitive to overland topographic parameters such as overland slope and slope length factor which are affected by sub-watershed discretization (Fig. 5–2a and Fig. 5–2b). The second reason is that the sediment routing through the channel module includes degradation and deposition (caused by settling velocity) which are affected by channel slope and other channel dimensions that are affected by the sub-watershed size (Fig. 5–2c and Fig. 5–2d). For instance, the average channel slope increases as the size of sub-watersheds decrease (Fig. 5–2d). This is because of better representation of spatial variation in elevation when smaller sub-watersheds are used. Further, Fig. 5–3b reveals that sediment yield increases at a higher rate for the coarsest sub-watershed levels as compared to the finer levels, which confirms the presence of a threshold of sub-watershed size for sediment simulation.

Figure 5–3c and Fig. 5–3d show the average annual total nitrogen and total phosphorous export respectively that occurred at the outlet of the Assiniboine River watershed in response to sub-watershed size variation. Both total nitrogen and total phosphorous export is found to be relatively sensitive to sub-watershed size. The changes in nitrogen, as well as phosphorous, were found to be large and unstable in the coarsest sub-divisions, and become insignificant and stable in middle and finer sub-division levels. This is because nutrient export at the outlet of a watershed is correlated to simulated sediment export (Arabi et al. 2006). A similar pattern of

nutrient export with sub-watershed size was observed by Arabi et al. (2006). Further changes in the size of the sub-watersheds produce very little effect on prediction of water quality variables. The sensitivity analysis confirms that continued refinement of the watershed representation, in terms of increasing numbers of sub-watersheds, may not necessarily result in improved water quality prediction. However, further increases in watershed sub-division resulted in increasing computational time and input data preparation challenges.

In general, most topographic characteristics and watershed responses showed very little change as numbers of sub-watersheds increased in the middle and finer sub-division levels. Conversely, input data preparation and computational time requirements increased as the number of sub-watershed increased. For this study, therefore, a watershed representation containing 70 sub-watersheds was selected considering the computational time and input data preparation burdens and stability of watershed responses for sub-watershed divisions.

5.4.4 Calibrated parameters

The most sensitive model parameters along with their final fitted values are listed in Table 5–4. As shown in Table 5–4, a total of 28 parameters were considered for the calibration of streamflow, sediment, phosphorous, and nitrogen loadings.

Parameter identification was performed through Pareto optimal solutions, which consider the trade-offs between the NSE and PBIAS objective functions. The two objective functions of NSE and PBIAS were utilized to identify Pareto optimal solution sets. The Pareto front is identified by setting a criteria of: NSE >=0.75 and -10 %< PBIAS<10%, NSE >=0.50 and -15 %< PBIAS<15%, NSE >=0.75 and -25 %< PBIAS<25%, and NSE >=0.75 and -25 %< PBIAS<25% respectively for streamflow, sediment, total phosphorous, and total nitrogen simulations. These Pareto front criteria were defined based on the recommendation of Moriasi et

al. (2007) rating of "very good" as much as possible or else at least "satisfactory" simulation accuracy.

Table 5–4 Sensitive SWAT parameters and their final fitted values.

	Parameter	Description	Range		Final calibrated value
			Min	Max	
Streamflow	CN2	SCS runoff curve number	-10	+10	-6.4[a]
	ESCO	Soil evaporation compensation factor	0	1	0.51[b]
	SURLAG	Surface runoff lag coefficient	0	14	0.50[b]
	ALPHA_BF	Baseflow factor for bank storage (day)	0	1	0.66[b]
	SFTMP	Snowfall temperature (°C)	-5	5	-3.02[b]
	SMTMP	Snowmelt base temperature (°C)	-5	5	-0.05[b]
	SMFMX	Maximum melt factor (mm $^{o}C^{-1}$/d)	0	7	9.43[b]
	SMFMN	Minimum melt factor (mm $^{o}C^{-1}$/d)	0	7	1.66[b]
	TIMP	Snowpack temperature lag factor	0	1	0.15[b]
	SNOCOVMX	Areal snow coverage threshold at 100% (mm)	0	500	264[b]
	SNO50COV	Areal snow coverage threshold at 50%	0	1	0.21[b]
	SMAX	Maximum storage capacity (varies)	-0.2	+0.2	+0.05[c]
	CH_N	Manning *n* for the main channel	0	0.1	0.06[b]
Sediment	PRF	Peak rate adjustment factor for sediment	0	2	0.03[b]
	SPCON	Linear parameter for maximum sediment reentrained	0.0001	0.01	0.003[b]
	SPEXP	Exponent parameter for sediment reentrained	0	1.5	0.97[b]
	USLE_P	USLE support practice	0	1.0	1.0[b]
	CH_COV1	Channel erodibility factor	0	1	0.75[b]
	CH_COV2	Channel cover factor	0	1	0.52[b]
Phosphorus	PSP	P availability index	0.01	0.7	0.65[b]
	ERORGP	Phosphorus enrichment ratio	0	5	0.123[b]
	PHOSKD	P soil partitioning coefficient	100	200	150[b]
	P_UPDIS	P update distribution parameter	0	100	65.8[b]
Nitrogen	RCN	N in rainfall (mg N/L)	0	15	0.11[b]
	NPERCO	Nitrogen percolation coefficient	0	1	0.7[b]
	ERORGN	Organic N enrichment ratio	0	5	0.27[b]
	CDN	Denitrification exponential coefficient	0	3	1.74[b]
	SDNCO	Denitrification threshold water content	0	2	1.34[b]
	N_UPDIS	N update distribution parameter	0	100	12.4[b]

Notes: [a] The given value is added to the existing parameter value. [b] The existing parameter value is replaced by the given value. [c] This indicates the existing parameter value is multiplied by (1+a given value). In general, implementation of calibration scheme [a] and [c] allows the user to make distributed parameters dependent on important influential factors such as the hydrological group, soil texture, land use, and land slope.

5.4.5 Streamflow modeling

The magnitude and temporal variation of simulated daily streamflow were well-matched with the observed values during the calibration and the validation periods (Fig. 5–4). The satisfactory performance is also supported by the magnitude of the Nash & Sutcliffe efficiency index (NSE>0.75) (Table 5–5). According to Moriasi et al. (2007), performance of a model is considered as "satisfactory" if for daily simulation the NSE is greater than or equal to 0.5, RSR is less than or equal to 0.7, and PBIAS in between -25 and +25%. In addition, a satisfactory prediction uncertainty was obtained as indicated by the values of *P*-factor and *D*-factor (Table 5–5 and Fig. 5–4). For daily streamflow simulation, the *P*-factor (percent of bracketed observed data by uncertainty band) is 77% and 69% respectively during the calibration and validation periods (Table 5–5), which generally indicate a good result. In reviewing the literature, it appears that a wider range of 95% uncertainty bands are reported by past works that range from 3.8% (Li et al. 2009) to 98.5% (Strauch et al. 2012) in terms of daily *P* -factor. The *D*-factors are also well below or around 1 in this study. Many past works reported a *D*-factor below 1(e.g. Stegn et al. 2010), though Strauch et al. (2012) reported *D*-factor of 1.9.

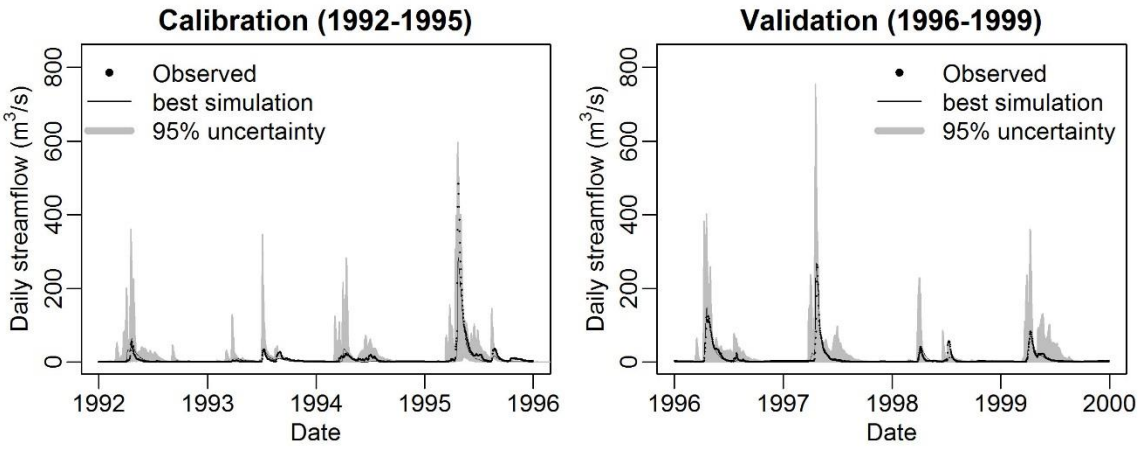

Figure 5–4 Simulated and observed daily streamflow at the watershed outlet. Right, streamflow calibration (1992–1995); and left, streamflow validation (1996–1999).

Table 5–5 Model performance statistics of streamflow modeling for the Assiniboine River watershed on a daily time step.

	Model performance parameter				
Simulation period	NSE	PBIAS (%)	RSR	*P*-factor (%)	*D*-factor
Calibration (1992-1995)	0.84	8.4	0.39	77	0.69
Validation (1996-1999)	0.77	-2.5	0.48	69	1.2

5.4.6 Sediment modeling

As shown in Fig. 5–5, satisfactorily agreement between the measured and simulated sediment export was observed, which is also indicated by the values of daily Nash & Sutcliffe efficiency index (NSE>0.6) (Table 5–6). According to Moriasi et al. (2007), sediment yield prediction performance of a model is considered as "satisfactory" if for daily load simulation the NSE is greater than or equal to 0.5, RSR is less than or equal to 0.7, and PBIAS in between -55 and +55%. In considering prediction uncertainty, the *P*-factor was found to be 25.1% and 20.8% during the calibration and validation periods respectively, while the *D*-factor was well below 1 in both periods (Fig 5 (a & b), Table 5–6). In order to assess the influence of sequential calibration, which keeps flow parameters fixed while calibrating sediment parameters, uncertainty analysis was also carried out allowing streamflow parameters to be calibrated along with sediment parameters (Fig. 5–5 (c & d), Table 5–6). As shown in Fig. 5–5 (c & d) and Table 5–6, it has been observed that the value of *P*-factor is significantly improved when streamflow parameters were allowed to be optimized during sediment optimization. Similar behavior was also reported by past works (e.g. Wellen et al. 2014).

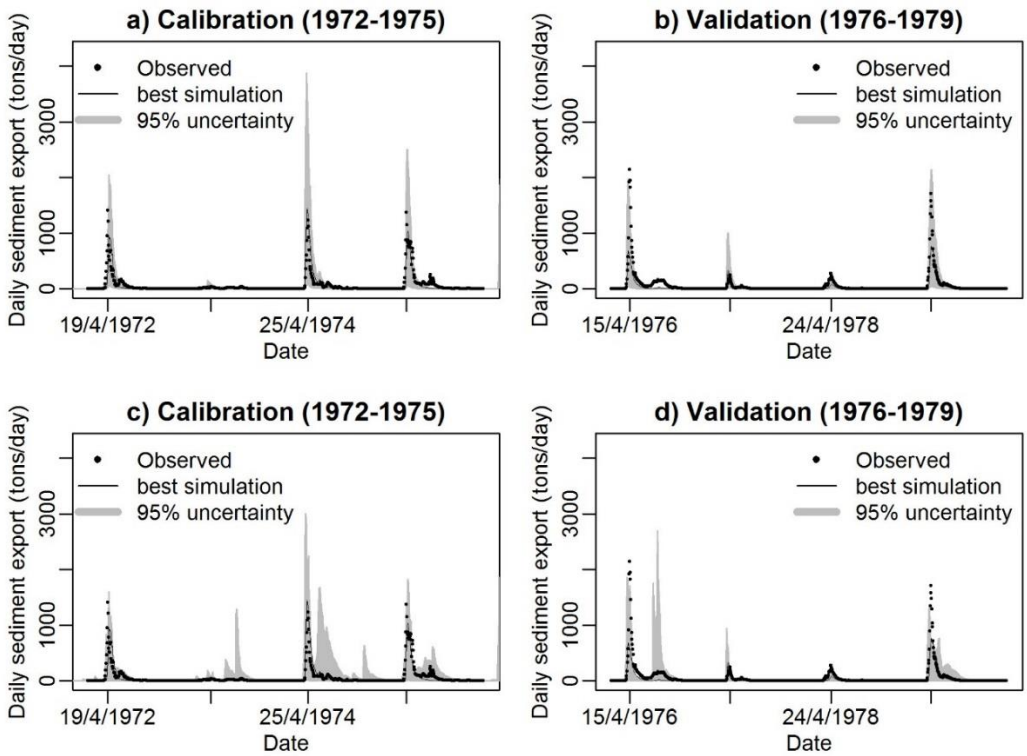

Figure 5–5 Simulated and observed daily sediment loads at the watershed outlet. Top, (a) and (b), show sediment export prediction uncertainty keeping streamflow parameters constant; Bottom, (c) and (d), show sediment export prediction uncertainty by allowing streamflow parameters to vary.

Table 5–6 Model performance statistics of sediment modeling for the Assiniboine River watershed on a daily time step.

Simulation period	**Model performance parameter**				
	NSE	PBIAS (%)	RSR	*P*-factor (%)	*D*-factor
Calibration (1972-1975)	0.63	7.9	0.61	25.1 [76.6]	0.68 [1.12]
Validation (1976-1979)	0.59	44	0.63	20.8 [52]	0.37 [0.51]

[ ] refers to uncertainty of sediment prediction uncertainty band through incorporation of streamflow parameter uncertainty.

5.4.7 Nutrient modeling

Figure 5–6 and Fig. 5–7 show temporal variation of daily simulated and observed loads of total phosphorous and total nitrogen respectively. Close agreement of the temporal pattern between the simulated and observed loads of both total nitrogen and total phosphorous export were observed. The visual observations are supported by satisfactorily values of daily Nash &

Sutcliffe efficiency index (NSE>0.6) (Table 5–7). According to Moriasi et al. (2007), model performance for nutrient simulation is considered as "satisfactory" if the NSE value is greater than or equal to 0.5, RSR is less than or equal to 0.7, and PBIAS is in between -70 and +70%. Model performance can be improved further if detailed point source data as well as the fertilizer application rate and timing information were made available. However, prediction uncertainty for nutrients is poor in terms of *P*-factor though the *D*-factor is well below 1 (Figs.5–6 (a & b) and 5–7 (a & b), Table 5–7). The lower value of *P*-factor is mainly because of the fixed streamflow parameter values during sediment and nutrient parameter optimization. As shown in Figs. 5–6 (c & d) & 5–7 (c & d) and Table 5–7, it has been observed that *P*-factor significantly improved when streamflow parameters were allowed to be optimized during nutrient optimization. The other factors that might contribute to lower *P*-factor values were the relatively scarce in-stream data points for nutrients which are often sampled only once in a month, the point source data unavailability, and uncertainty associated with the rate and timing of fertilizer applications. In fact, an improved *P*-factor has also been observed when uncertainty due to fertilizer application rate is included during nutrient optimization (see Table 5–7).

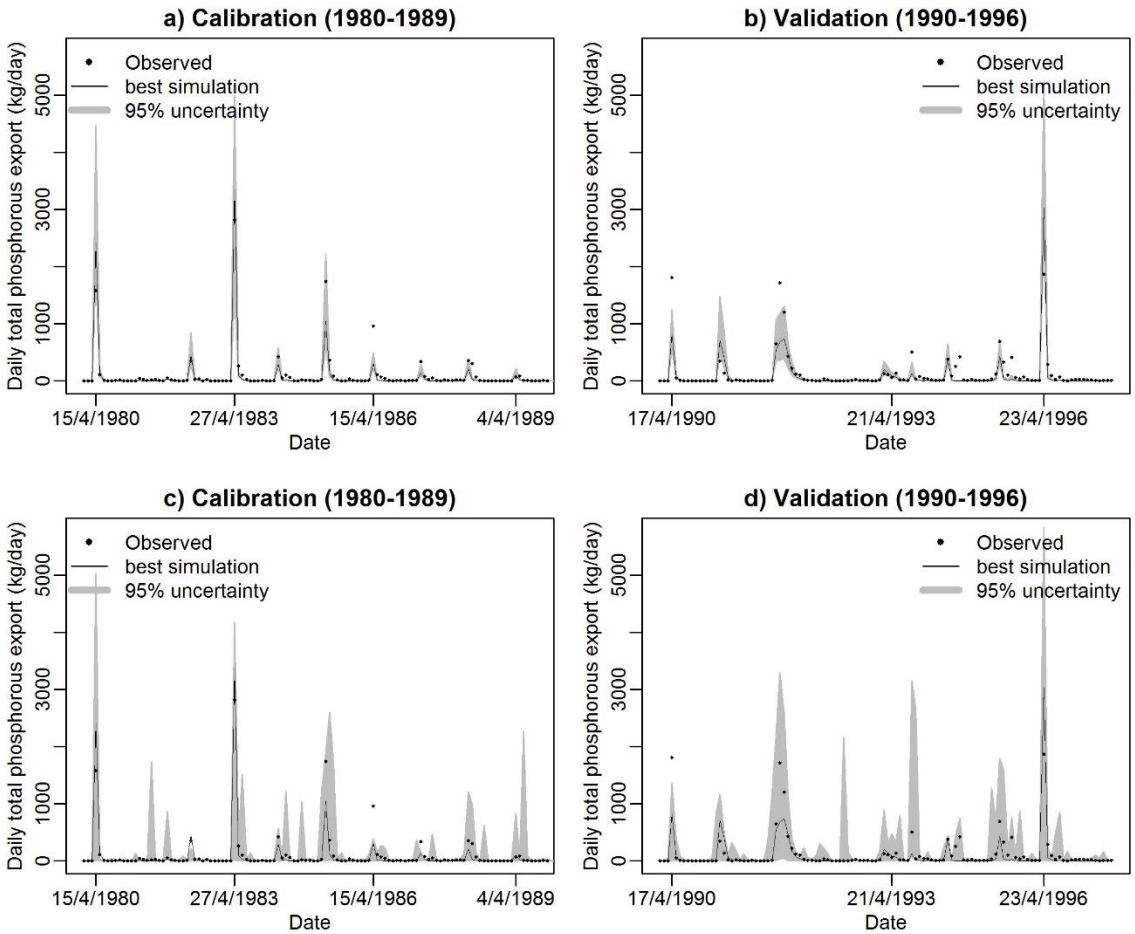

Figure 5–6 Simulated and observed daily total phosphorous export at the watershed outlet. Top, (a) and (b), show phosphorous prediction uncertainty keeping streamflow parameters constant; Bottom, (c) and (d), show phosphorous prediction uncertainty by allowing streamflow parameters to vary.

Table 5–7 Model performance statistics of nutrient modeling for the Assiniboine River watershed on a daily time step.

Process	**Simulation period**	**Model performance parameter**				
		NSE	PBIAS (%)	RSR	*P*-factor (%)	*D*-factor
Phosphorous	Calibration	0.84	19.9	0.39	11 [30.5] (61.9)	0.24 [0.86] (0.82)
	Validation	0.61	30.1	0.62	14 [35.1] (70.2)	0.28 [1.03] (1.24)
Nitrogen	Calibration	0.81	8.3	0.43	14.4 [37.3] (61)	0.34 [0.74] (0.72)
	Validation	0.70	20.6	0.58	24.6 [36.8] (60)	0.44 [1.17] (0.89)

[ ] refers to uncertainty of nutrient predictions through incorporation of nutrient input uncertainty.
( ) refers to uncertainty of nutrient predictions through incorporation of streamflow parameter uncertainty.

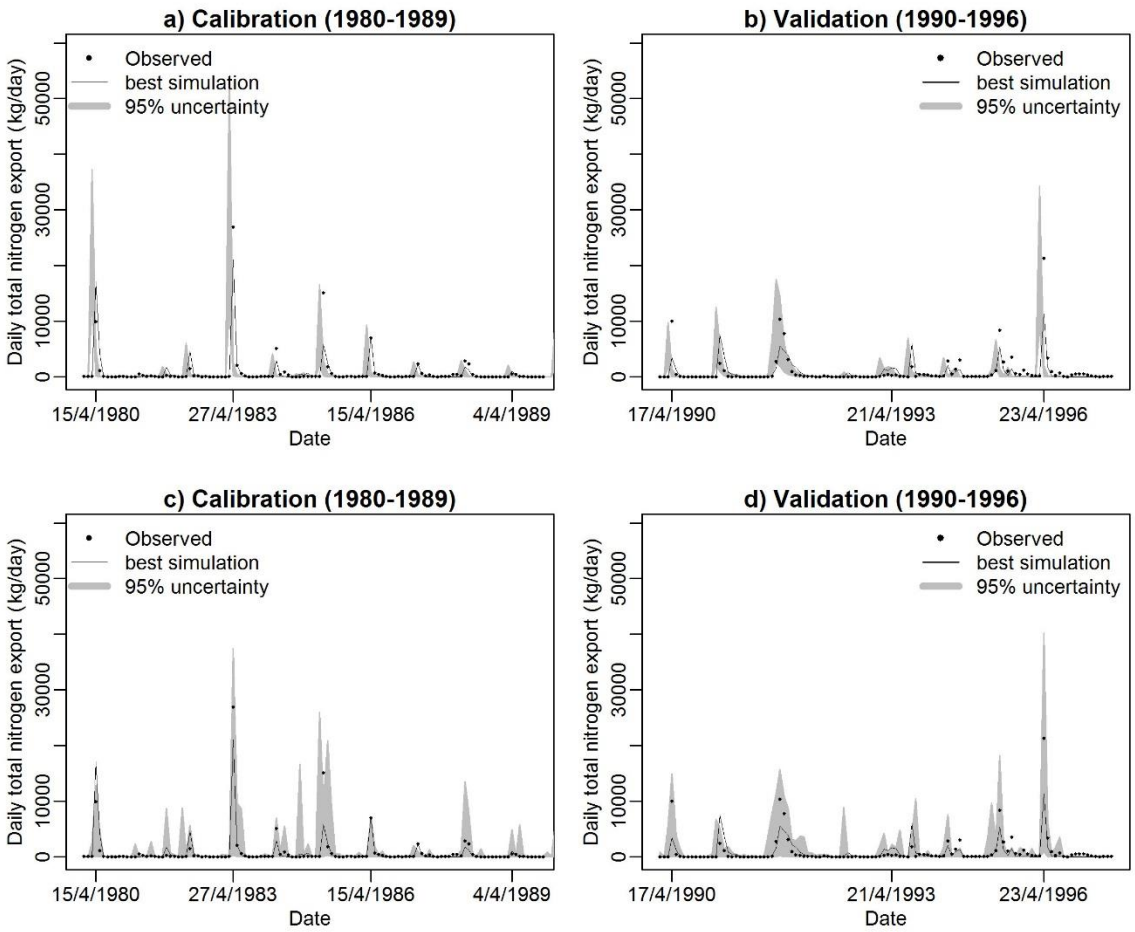

Figure 5–7 Simulated and observed daily total nitrogen export at the watershed outlet. Top, (a) and (b), show nitrogen prediction uncertainty keeping streamflow parameters constant; Bottom, (c) and (d), show to nitrogen prediction uncertainty by allowing streamflow parameters to vary.

Considering the challenges of nutrient data limitations, the model was found to be satisfactorily reliable in estimating nutrient export in the Assiniboine River watershed. Hence, it was used to evaluate impacts of different best management practices on nutrient export in the study watershed.

5.4.8 Scenario analyses

The changes from the baseline in sediment and nutrient load in response for the tested management scenarios are presented in Table 5–8. Average annual loadings for the

Table 5– 8 Annual load change (%) under different management scenarios at the outlet of the Assiniboine River watershed.

Processes		Baseline	Filter strips that varies in width				Zero tillage	Cover crop
			1m	5m	15m	30m		
Sediment	(10^2 ton/year)	50.8	46	43.2	38.3	31.1	47.2	29.9
	Change (%)	-	-9.3	-15	-25.5	-38.8	-6.9	-41
Total Phosphorous	(10^3 kg/year)	47.9	40.4	35.2	29.1	19.3	53.6	29.5
	Change (%)	-	-15.7	-26.6	-39.3	-59.7	9.6	-38.4
Total Nitrogen	(10^3 kg/year)	489	438	395	316	208	485	261
	Change (%)	-	-10.3	-19.2	-35.3	-57.4	-0.7	-46.6

scenarios and baseline simulations were calculated for sediment, total phosphorus, and total nitrogen.

As shown in Table 5–8, the filter strip scenario revealed that a significant amount of sediment, phosphorous, and nitrogen export reduction results from filter strip use. Sediment load reduction values varied between 9.3% and 38.8% as the width increased from 1 m to 30 m. Researchers have reported that use of a filter strip has produced greatly varied sediment load reduction, which range from about 0.01% and 65% (Barlund et al. 2007; Waidler et al. 2009). In considering impacts of filter strip on phosphorous export, results revealed a reduction of phosphorous export that varied between 15.7% and 59.7%, with increased reduction as the filter strip width increases. Past studies have reported different values of phosphorous with filter strip use reduction that ranges between -101% (an increase) (White and Arnold 2009) to 75% (Waidler et al. 2009). Nitrogen export reduction due to filter strip use in this study varied between 10.3% and 57.4% and increased with the width of the filter strip. Past studies have reported that use of a filter strip has produced greatly varied nitrogen load reduction, which range from about 70% nitrogen load reduction (Waidler et al. 2009) to -77% (an increase) (White and Arnold 2009).

For Scenario 2, which assessed the impact of conservation tillage, SWAT estimated that sediment and total nitrogen loads were reduced on average by 6.3% and 0.7% per year

respectively. However, total phosphorous export was 9.6% greater under conservation tillage. This result is consistent with field studies that have been carried out on the Canadian prairies (e.g., Tiessen et al. 2010; Li et al. 2011; Flaten 2013; Liu et al. 2014). The increased phosphorous export under conservation tillage is partly due to the release of nutrients from plant residue that remains on the soil surface as the soil has not been mixed during tillage (Timmons et al. 1970; Miller et al. 1994; Ulen 1997). This is especially important in cold-climate regions where freeze-thaw cycles increase cell rupture and release soluble nutrients, which are then transported to surface waters during snowmelt (Bechmann et al. 2005; Roberson et al. 2007). In addition, conservation tillage has little influence on surface runoff during the snowmelt period, which is expected be higher due to reduced infiltration of the frozen ground (Gaynor and Bissonnette 1992). Results demonstrate that although conservation tillage can effectively reduce sediment and sediment-bound nutrient export from agricultural fields, it can increase the export of dissolved phosphorous occurring during snowmelt runoff. Therefore, conservation tillage is not advisable in terms of reducing phosphorous export from the Assiniboine River watershed. These findings could apply to much of the cold-climate Canadian Prairies and may be relevant wherever snowmelt runoff dominates and dissolved phosphorous is the major form of phosphorous in runoff. In these situations, it may be appropriate to implement additional management practices (such as intermittent tillage) to reduce the accumulation of phosphorous at or near the soil surface.

For Scenario 3, which investigated the impact of the use of red clover cover crops following crop harvest in the watershed, SWAT-PDLD estimated that an average annual sediment load reduction of 41% could be achieved. Total phosphorous reduction was estimated to decline annually by 38.4%, with the majority of this decline associated with particulate

phosphorous was due to reduced soil erosion. Furthermore, cover crops also may tend to absorb surplus nutrients following crop harvest. The annual average total nitrogen reduction was estimated as 46.6%. Cover cropping as part of the cropping system across the watershed therefore would appear to have positive effects on reducing sediment, as well as both nitrogen and phosphorous. Similar findings were also observed in past model simulations in other cold-climate region (e.g., Yang et al. 2013).

5.5 Conclusion

The modified version of the SWAT model, SWAT with a Probability Distributed Landscape Depression module, together with seasonally varying soil erodibility factor was tested to simulate daily sediment and nutrient export in a cold climate prairie watershed. Both statistical measures and graphical plots show satisfactory calibration and prediction uncertainty results for sediment and nutrient export simulation for the Assiniboine River watershed upstream of Kamsack, Saskatchewan, Canada. Values of daily Nash and Sutcliffe efficiency greater than 0.5 were attained for simulation of streamflow, sediment, phosphorous, and nitrogen export. Furthermore, uncertainty analysis was estimated using Sequential Uncertainty FItting algorithm and reasonable results were attained considering unaccounted input data uncertainty (such as agricultural practices, magnitude and timing of fertilizer application, point sources, etc.).

Annual streamflow simulation was found to be relatively insensitive to sub-watershed discretization as compared to sediment and nutrient export. The rate of change or sensitivity of sediment and nutrient export, however, becomes insignificant beyond a certain threshold number of sub-watersheds. On the other hand, computational time and input data requirements keep increasing as the number of sub-watersheds increases. The appropriate number of sub-watersheds to adequately and efficiently simulate sediment and nutrient export from the

Assiniboine River watershed was found to be in the range of 65 to 100 (considering computational time requirement, and stability of watershed characteristics and responses).

According to best management scenario modeling results, future practices of both filter strip and cover crops could have positive effects on reductions of sediment, phosphorous, and nitrogen loadings in the study watershed. Conservation tillage also had a positive effect on the reduction of sediment export as well as nitrogen loadings in the study watersheds. However, phosphorous export tends to increase under conservation tillage in the study watershed. Currently, conservation tillage practices are being implemented in more than 70% of agricultural areas in Saskatchewan. It appears that it is important to also consider and implement additional management practices (such as intermittent tillage) to reduce potential increased phosphorus export due to conservation tillage practices.

5.6 Acknowledgments

The authors would like to thank the Province of Saskatchewan Go Green Fund and the Natural Sciences and Engineering Research Council of Canada (NSERC) in the form of Discovery Grants to the second authors for the financial support for this work. The authors would also like to thank Dr. Monique Dube and Dr. Nicole Nadorozny for making available the datasets (phosphorous and nitrogen) from different sources, and Dr. Dube for her initial work in the developing the broader project in which this work was part.

5.7 References

Abbaspour, K.C., Johnson, C.A., and van Genuchten, M.Th. 2004. Estimating uncertain flow and transport parameters using a Sequential Uncertainty Fitting Procedure. Vadose Zone Journal**, 3(4)**: 1340–1352.

Abbaspour, K.C., Yang, J., Maximov, I., Siber, R., Bogner, K., Mieleitner, J., Zobrist, J., and Srinivasan, R. 2007. Modelling hydrology and water quality in the pre-alpine/alpine Thur watershed using SWAT. Journal of Hydrology, **333(2-4)**: 413–430.

Abedini, M.J. 1998. On depression storage, its modelling and scale. Ph.D. thesis, Department of Water Resources Engineering, University of Guelph, Guelph, Canada.

Agriculture and Agri-Food Canada (AAFC). 2011a. "About Us." Watershed Evaluation of Beneficial Management Practices, Accessed on Sep. 25, 2015, http://www4.agr.gc.ca/AAFC-AAC/display-afficher.do?id=1296246973332&lang=eng.

AAFC. 2011b. Tillage Trade-offs in a Prairie Watershed. Accessed on Sep. 25, 2015, http://www.agr.gc.ca/eng/?id=1338581452818.

Arabi, M., Govindaraju, R.S., Hantush, M.M., and Engel, B.A. 2006. Role of watershed subdivision on modeling the effectiveness of best management practices with SWAT. Journal of the American Water Resources Association, **42(2)**: 513–528.

Arnold, J.G., Moriasi, D.N., Gassman, P.W., Abbaspour, K.C., White, M.J., Srinivasan, R., Santhi, C., Harmel, R.D., van Griensven, A., van Liew, M.W., Kannan, N., and Jha, M.K. 2012. SWAT: model use, calibration, and validation. Transactions of the ASABE, **55(4)**: 1491–1508.

Arnold, J.G., Srinivasan, R., Muttiah, R.S., and Williams, J.R. 1998. Large-area hydrologic modeling and assessment: Part I Model development. J. American Water Resour. Assoc., **34(1)**: 73–89.

Assiniboine Watershed Stewardship Association. 2000. Main report: Upper Assiniboine River Basin study. Yorkton, SK, Canada, 146pp.

Awada, L., Lindwall, C.W., and Sonntag, B. 2014. The development and adoption of conservation tillage systems on the Canadian Prairies. International Soil and Water Conservation Research, **2(1)**: 47–65.

Barlund, I., Kirkkala, T., Malve, O., and Kamari, J. 2007. Development of a simplistic vegetative filter strip model for sediment and nutrient retention at the field scale. Hydrological Processes, **23(11)**: 1602–1616.

Bechmann, M.E., Kleinman, P.J.A., Sharpley, A.N., and Saporito, L.S. 2005. Freeze–thaw eff ects on phosphorus loss in runoff from manured and catch-cropped soil. J. Environ. Qual., **34(6)**: 2301–2309.

Booty, W., and Benoy, G. 2009. Multi-criteria review of nonpoint source water quality models for nutrients, sediments, and pathogens. Water Qual. Res. J. Can., **44(4)**: 365–377.

Borah, D.K., and Bera, M. 2003. Watershed-scale hydrologic and nonpoint-source pollution models: review of mathematical bases. Transactions of the ASAE, **46(6)**: 1553–1566.

Birgand, F., Skaggs, R.W., Chescheir, G.M., and Gilliam, J.W. 2007. Nitrogen removal in streams of agricultural catchments: A literature review. Critical Reviews in Environmental Science and Technology, **37(5)**: 381–487.

Bourne, A., Armstrong, N., and Jones, G. 2002. A preliminary estimate of total nitrogen and total phosphorus loading to streams in Manitoba, Canada. Water Quality Management Section. Manitoba Conservation Report No. 2002 - 04.

Brown, L.C., and Barnwell, T.O. 1987. The enhanced stream water quality models QUAL2E and QUAL2E-UNCAS: Documentation and user manual, Report EPA/600/3/87/007, US Environmental Protection Agency, Athens, GA.

Brunet, N.N. 2011. Prairie Pothole drainage and water quality. MSc. Thesis. Department of Geography and Planning, University of Saskatchewan, Saskatoon, Saskatchewan, Canada.

Bussi, G., Francés, F., Montoya, J.J., and Julien, P.Y. 2014. Distributed sediment yield modelling: Importance of initial sediment conditions. Environmental Modelling & Software, **58**: 58–70.

Chambers, P.A., Guy, M., Roberts, E.S., Charlton, M.N., Kent, R., Gagnon, C., Grove, G., and Foster, N. 2001. Nutrients and their impact on the Canadian environment. Agriculture and Agri-Food Canada, Environment Canada, Fisheries and Oceans Canada, Health Canada and Natural Resources Canada. 241p.

Cho, J., Lowrance, R.R., Bosch, D.D, Strickland, T.C., Her, Y., and Vellidis, G. 2010. Effect of watershed subdivision and filter width on SWAT simulation of a coastal plain watershed. Journal of the American Water Resources Association, **46(3)**: 586–602.

Coote, D.R., Malcolm-McGovern, C.A., Wall, G.J., Dickinson, W.T., and Rudra, R.P. 1988. Seasonal variation of erodibility indices based on shear strength and aggregate stability in some Ontario soils. Can. J. Soil Sci., **68(2)**: 105–416.

Crumpton, W.G., and Goldsborough, L.G. 1998. Nitrogen transformation and fate in prairie wetlands. Great Plains Research, **8(1)**: 57–72.

Crumpton, W.G., Isenhart, T.M., and Fisher, S.W. 1993. Fate of nonpoint source nitrate loads in fresh-water wetlands: Results from experimental wetland mesocosms, pp. 283-291. In: Moshiri, G.A. (ed). Constructed Wetlands for Water Quality Improvement. CRC Press. Boca Raton, Florida.

Cunge, L.A., 1969. On the subject of a flood propagation method (Muskingum method). J. Hydraulic Research, ***7*(2)**: 205–230.

De, S., Bezuglov, A. 2006. Data model for a decision support in comprehensive nutrient management in the United States. Environmental Modelling & Software, **21(6)**: 852–867.

Deelstra, J., Kvaernø, S.H., Granlund, K., Sileika, A.S., Gaigalis, K., Kyllmar, K., and Vagstad, N. 2009. Runoff and nutrient losses during winter periods in cold climates–requirements to nutrient simulation models. J. Environ. Monit., **11(3)**: 602–609.

Dong, F., Liu, Y., Qian, L., Sheng, H., Yang, Y., Guo, H., and Zhao, L. 2014. Interactive decision procedure for watershed nutrient load reduction: An integrated chance-constrained programming model with risk–cost tradeoff. Environmental Modelling & Software, **61**: 166–173.

Dube, M., Nadorozny, N., and Squires, A. 2011. Development of the Healthy River Ecosystem AssessmenT System (THREATS) for integrated change assessments of water quality in Canadian watersheds. In: Lundqvist J, editor. On the water front: Selections from the 2010 World Water Week in Stockholm. Stockholm, Sweden. Stockholm International Water Institute: p 32–41.

Elshorbagy, A., and Ormsbee, L. 2006. Object-oriented modeling approach to surface water quality management. Environmental Modelling & Software, **21(5)**: 689–698,

Fang, X., and Pomeroy J.W. 2008. Drought impacts on Canadian prairie wetland snow hydrology. Hydrological Processes, **22(15)**: 2858–2873.

FitzHugh, T.W., and MacKay, D.S. 2000. Impacts of input parameter spatial aggregation on an agricultural nonpoint source pollution model. Journal of Hydrology, **236 (1-2)**: 35–53.

Flaten, D. 2013. Conservation tillage: Cure-all or problem for water quality? Saskatchewan Soil Conservation Association, 9 January 2013, Saskatoon, SK.

Gaynor, J., and Bissonnette, D. 1992. The effect of conservation tillage practices on the losses of phosphorus and herbicides in surface and subsurface drainage waters. Southwestern Ontario Agricultural Research Corporation (SWOARC), Harrow, Ontario.

GeoBase Canada. 2007. Canadian Digital Elevation Data, Level 1 Product Specifications Edition 3.0. Government of Canada, Natural Resources Canada, Centre for Topographic Information, Customer Support Group, Sherbrooke, Quebec, Canada.

GeoBase Canada. 2009. Land Cover, circa 2000-Vector Data Product Specifications: Edition 1.0. Centre for Topographic Information, Earth Sciences Sector, Natural Resources Canada, Sherbrooke (Quebec), Canada.

Gevaert, V., Van Griensven, A., Holvoet, K. Seuntjens, P., and Vanrolleghem, P.A. 2008. SWAT developments and recommendations for modelling agricultural pesticide mitigation measures in river basins, Hydrological Sciences Journal 53(5), 1075–1089.

Godwin, R.B., and Martin, F.R. 1975. Calculation of Gross and Effective Drainage Areas for the Prairie Provinces. Canadian Hydrology Symposium, (p. 5), Winnipeg.

Government of Saskatchewan 2015. Organic Crop Production: Soil Conservation Practices, cover crop. Accessed on 20 Sep. 2015.

http://www.agriculture.gov.sk.ca/Default.aspx?DN=1a2fc0cd-ddb4-47b6-8d29-91dff9dde90a

Granger, R.J., Gray, D.M., and Dyck, G.E. 1984. Snowmelt infiltration to frozen prairie soils. Canadian Journal of Earth Science, **21(6)**: 669–677.

Gray, D.M., and Landine, P.G. 1988. An energy–budget snowmelt model for the Canadian Prairies. Canadian Journal of Earth Sciences, **25(8)**: 1292–1303.

Gray, D.M., Toth, B., Zhao, L., Pomeroy, J.W., and Granger, R.J. 2001. Estimating areal snowmelt infiltration into frozen soils. Hydrological Processes, **15(16)**: 3095–3111.

Green, W.H., and Ampt, G.A. 1911. Studies on soil physics-1: The flow of air and water through soils. J. Agric. Sci., **4**: 11–24.

Grizzetti, B., Bouraoui, F., Granlund, K., Rekolainen, S., and Bidoglio, G. 2003. Modelling diffuse emission and retention of nutrients in the Vantaanjoki watershed (Finland) using the SWAT model. Ecological Modelling, **169(1)**: 25–38.

Gupta, H.V., Sorooshian, S., and Yapo, P.O. 1999. Status of automatic calibration for hydrologic models: Comparison with multilevel expert calibration. J. Hydrol. Eng., **4(2)**: 135–143.

Hall, R.I., and Leavitt, P.R. 1999. Effects of agriculture, urbanization, and climate on water quality in the northern Great Plains. Limnol. Oceanogr., 44**(3-2)**: 739–756.

Han, C.W., Xu, S.G., Liu, J.W., and Lian, J.J. 2010. Nonpoint-source nitrogen and phosphorous behaviour and modelling in cold climate: a review. Water science & Technology, **62(10)**: 2277–2285.

Hargreaves, G.L., Hargreaves, G.H., and Riley, J.P. 1985. Agricultural benefits for Senegal River Basin. J. Irrig. Drain. Eng., **111(2)**: 113–124.

Hayashi, M., van der Kamp, G., and Rudolph, D.H. 1998. Water and solute transfer between a prairie wetland and adjacent uplands: 1. Water balance. Journal of Hydrology, **207(1–2)**: 42–55.

Huel, D., Harison, T., Foster, A., and Pawana ,N. 2000. Managining Saskatchewan wetlands: A Landowner's Guide. Saskatchewan Wetland Conservation Corporation, Room 101-2022 Cornwall Street, Regina, Saskatchewan, Canada.

Hutchinson, M.F., McKenney, D.W., Lawrence, K., Pedlar, J.H., Hopkinson, R.F., Milewska, E., and Papadopol, P. 2009. Development and testing of Canada-wide interpolated spatial models of daily minimum–maximum temperature and precipitation for 1961-2003. Journal of Applied Meteorology and Climatology, **48**: 725–741

HYDAT. 2014. HYDATE database, National Water Data Archive. Water Survey of Canada.

Jha, M., Gassman, P.W., Secchi, S., Gu, R., an dArnold, J. 2004. Effect of watershed subdivision on SWAT flow, sediment, and nutrient predictions. Journal of the American Water Resources Association, **40(3)**: 811–825.

Johnston, C.A. 1991. Sediment and nutrient retention by freshwater wetlands: Effects in surface water quality. Critical Reviews in Environmental Control, **21(5, 6)**: 491–565.

Jones, G., and Armstrong, N. 2001. Long-term trends in total nitrogen and total phosphorus concentrations in Manitoba streams. Manitoba Conservation Rep. 2001-07: Water Quality Management Section, Water Branch, Manitoba Conservation, Winnipeg, Manitoba, Canada.

Labaugh W.L., Winter, T.C., and Rosenberry, D.O. 1998. Hydrologic functions of prairie wetlands. Great Plains Research, **8**: 17–37.

Lake Winnipeg Stewardship Board 2006. Reducing Nutrient Loading to Lake Winnipeg and Its Watershed Our Collective Responsibility and Commitment to Action, Report to the Minister of Water Stewardship, Manitoba, 78 pp.

Leibowitz, S.G., and Vining, K.C. 2003. Temporal connectivity in a prairie pothole complex. Wetlands, **23(1)**: 13–25.

Li, S., Elliott, J.A., Tiessen, K.H.D, Yarotski, J., Lobb, D.A, and Flaten, D.N. 2011. The effects of multiple beneficial management practices on hydrology and nutrient losses in a small watershed in the Canadian Prairies. J. Environ. Qual., **40(5)**: 1627–1642

Li, Z., Xu, Z., Shao, Q., and Yang, J. 2009. Parameter estimation and uncertainty analysis of SWAT model in upper reaches of the Heihe river basin. Hydrological Processes, **23(19)**: 2744–2753.

Liu, K., Elliott, J.A., Lobb, D.A., Flaten, D.N., and Yarotski, J. 2014. Nutrient and sediment losses in snowmelt runoff from perennial forage and annual cropland in the Canadian Prairies. Journal of Environmental Quality, **43(5)**: 1644–1655.

McConkey, B.G., Nicholaichuk, W., Steppuhn1, H., and Reimer, C.D. 1997. Sediment yield and seasonal soil erodibility for semiarid cropland in western Canada. Can. J. Soil Sci., **77(1)**: 33–40.

McKay, M.D., Beckman, R.J., and Conover, W.J. 1979. A comparison of three methods for selecting values of input variables in the analysis of output from a computer code. Technometrics, **21(2)**: 239–245.

Mekonnen, B.A., Nazemi, A., Mazurek, A.M., Elshorbagy, A., and Putz, G. 2015. Hybrid modelling approach to prairie hydrology: Fusing data-driven and process-based hydrological models. Hydrological Sciences Journal, **60(9)**: 1473–1489.

Mekonnen, B.A., Mazurek, A.M., and Putz, G. 2016a. Incorporating landscape depression heterogeneity into the Soil and Water Assessment Tool (SWAT) using a probability distribution. Hydrological Processes, DOI: 10.1002/hyp.10800

Mekonnen, B.A., Mazurek, A.M., and Putz, G., 2016b. Sediment Export Modeling in Cold Climate Prairie Watersheds. Journal of Hydrologic Engineering, DOI: 10.1061/(ASCE)HE.1943-5584.0001336

Mekonnen, M.A., Wheater, H.S., Iresona, A.M., Spence, C., Davison, B., and Pietroniro, A. 2014. Towards an improved land surface scheme for prairie landscapes. Journal of Hydrology, **511**: 105–116.

Merritt, W.S., Letcher, R.A., and Jakeman, A.J. 2003. A review of erosion and sediment transport models. Environmental Modelling & Software, **18(8–9)**: 761–799.

Miller, M.H., E.G. Beauchamp, and J.D. Lauzon. 1994. Leaching of nitrogen and phosphorus from the biomass of three cover crop species. J. Environ. Qual., **23(2)**: 267–272.

Monteith, J.L. 1965. Evaporation and the environment: In the state and movement of water in living organisms, Proc. 19th Symp. Swansea, UK, Society of Experimental Biology, Cambridge University Press.

Moraghan, J.T. 1993. Loss and assimilation of 15N-nitrate added to a North Dakota cattail marsh. Aquatic Botany, **46(3–4)**: 225–234.

Moriasi, D.N., Arnold, J.G., van Liew, M.W., Bingner, R.L., Harmel, R.D., and Veith, T.L. 2007. Model evaluation guidelines for systematic quantification of accuracy in watershed simulations. Trans. ASABE, **50(3)**: 885–900

Murkin, H.A. 1998. Freshwater functions and values of prairie wetlands. Great Plains Research, **8(1)**: 3–15.

Nash, J.E., and Sutcliffe, J.V. 1970. River flow forecasting through conceptual models. Part I: A discussion of principles. Journal of Hydrology, **10(3)**: 282–290.

Neely, R.K., and Baker, J.L. 1989. Nitrogen and phosphorous dynamics and fate of agricultural runoff, pp. 92-131. In: van der Valk, A.G. (ed.) Northern Prairie Wetlands, Iowa State University Press, Ames, Iowa.

Neitsch, S.L., Arnold, J.G. Kiniry, J.R., and Williams, J.R. 2011. Soil and Water Assessment Tool theoretical documentation: Version 2005, Grassland, Soil and Water Research Laboratory, Blackland Research Center, Temple, TX.

Newham, L.T.H., Letcher, R.A., Jakeman, A.J., and Kobayashi, T. 2004. A framework for integrated hydrologic, sediment and nutrient export modeling for catchment-scale management. Environmental Modelling and Software, **19 (11)**: 1029–1038.

Panagopoulos, Y., Makropoulos, C., and Mimikou, M. 2012. Decision support for diffuse pollution management. Environmental Modelling & Software, **30**: 57–70

Pomeroy, J.W., Gray, D.M., Brown, T., Hedstrom, N.M., Quinton, W., Granger, R.J., and Carey, S. 2007. The Cold Regions Hydrological Model, a platform for basing process representation and model structure on physical evidence. Hydrological Processes, **21(19)**: 2650–2667.

Priestley, C.H.B., and Taylor, R.J. 1972. On the assessment of surface heat flux and evaporation using large-scale parameters. Mon. Weather Rev., **100(2)**: 81–92.

Reddy, K.R., Kadlec, R.H., Flaig, E., and Gale, P.M. 1999. Phosphorous retention in streams and wetlands: A review. Critical Reviews in Environmental Science and Technology, **29(1)**: 83–146.

Ritchie, J.T. 1972. A model for predicting evaporation from a row crop with incomplete cover. Water Resources Research, **8(5)**: 1204–1213.

Roberson, T., Bundy, L.G., and Andraski, T.W. 2007. Freezing and drying effects on potential plant contributions to phosphorus in runoff. J. Environ. Qual., **36(2)**: 532–539.

Rosenberry, D.O., and Winter, T.C. 1997. Dynamics of water-table fluctuations in an upland between two prairie-pothole wetlands in North Dakota. Journal of Hydrology, **191(1–4)**: 266–289.

Salvano, E., Flatten, D.N., Rousseau, A.N., and Quilbe, R. 2009. Are current phosphorus risk indicators useful to predict the quality of surface waters in southern Manitoba, Canada. J. Environ. Qual., **38(5)**: 2096–2105.

Santhi, C., Arnold, J.G., Williams, J.R., Dugas, W.A., Srinivasan, R., and Hauck, L.M. 2001. Validation of the SWAT model on a large river basin with point and nonpoint sources. Journal of the American Water Resources Association, **37(5)**: 1169–1188.

Santhi, C., Srinivasan, R., Arnold, J.G., and Williams, J.R. 2006. A modeling approach to evaluate the impacts of water quality management plans implemented in a watershed in Texas. Environmental Modelling & Software, **21**: 1141–1157.

Saskatchewan Ministry of Agriculture. 2013. Plans and annual reports: Plan for 2014-15, Government of Saskatchewan, Regina, Saskatchewan, Canada.

Saskatchewan Watershed Authority (SWA). 2010. State of the Watershed Report: stressor indicators. Moose Jaw, SK, Canada, 138pp.

Saskatchewan Watershed Authority. 2005. Background report: Assiniboine River Watershed, Regina, Technical committee, 123 pp.

Saskatchewan Trends Monitor. 2005. What Makes Saskatchewan Tick? Primary Agriculture in the Saskatchewan Economy Detailed Statistical Report. Sask Trends Monitor, Regina, Saskatchewan, 100pp.

SCS (Soil Conservation Service). 1972. National Engineering Handbook, Section 4: Hydrology, SCS, USA.

Setegn, S.G., Srinivasan, R., Melesse, A.M., and Dargahi, B. 2010. SWAT model application and prediction uncertainty analysis in the Lake Tana Basin, Ethiopia. Hydrological Processes, **24(3)**: 357–367.

Shaw, D.A, van der Kamp G, Conly, F.M., Pietroniro, A., and Martz, L. 2011. The Fill-Spill hydrology of prairie wetland complexes during drought and deluge. Hydrological Processes, **26(13)**: 3147–3156.

Shook, K., Pomeroy, J.W., Spence, C., and Boychuk, L. 2013. Storage dynamics simulations in prairie wetland hydrology models: evaluation and parameterization. Hydrological Processes, **27(13)**: 1875–1889.

Shrestha, R.R., Dibike, Y.B., and Prowse, T.D. 2012. Modeling climate change impacts on hydrology and nutrient loading in the Upper Assiniboine Catchment. Journal of the American Water Resources Association (JAWRA), **48(1)**: 74–89.

Singh, J., Knapp, H.V., Arnold, J.G., and Demissie, M. 2005. Hydrologic modeling of the Iroquois River watershed using HSPF and SWAT. J. American Water Resources Assoc., **41(2)**: 361–375.

Soil Landscapes of Canada Working Group. 2007. Soil Landscapes of Canada v3.1.1, Agriculture and Agri-Food Canada, Digital Map and Database at 1:1 Million Scale. Accessed on 20 Mar. 2012, http://sis.agr.gc.ca/cansis/nsdb/slc/v3.1.1/intro.html.

Statistics Canada. 2014. Census of Agriculture counts 44,329 farms in Saskatchewan: highlights of Saskatchewan agriculture. Accessed on 20 Sep. 2014, http://www.statcan.gc.ca/ca-ra2006/analysis-analyses/sask-eng.htm#r1

Statistics Canada. 2011. Fertilized land area in Canada by ecozone, selected years, 1971 to 2006. Accessed 20 October 2015, http://www.statcan.gc.ca/pub/16-201-x/2009000/t235-eng.htm

Strauch, M., Bernhofer, C., Koide, S., Volk, M., Lorz, C., and Makeschin, F. 2012. Using precipitation data ensemble for uncertainty analysis in SWAT streamflow simulation. Journal of Hydrology, **414**: 413–424.

Su, M., Stolte, W.J., and van der Kamp, G. 2000. Modelling Canadian prairie wetland hydrology using a semi-distributed streamflow model. Hydrological Processes, **14(14)**: 2405–2422.

The Encyclopedia of Saskatchewan. 2015. Soil Conservation: Trends in tillage practices in Saskatchewan. Accessed on 20 Sept. 2015, http://esask.uregina.ca/entry/soil_conservation.html

Tiessen, K.H.D., Elliott, J.A., Yarotski, J., Lobb, D.A., Flaten, D.N., and Glozier, N.E. 2010. Conventional and conservation tillage: influence on seasonal runoff, sediment, and nutrient losses in the Canadian Prairies. J. Environ. Qual., **39(3)**: 964–980.

Timmons, D.R., Holt, R.F., and Latterell, J.J. 1970. Leaching of crop residues as a source of nutrient in surface runoff water. Water Resour. Res., **6(5)** : 1367–1375.

Ulen, B. 1997. Nutrient losses by surface run-off from soils with winter cover crops and spring-ploughed soils in the south of Sweden. Soil Tillage Res., **44(3–4)** : 165–177.

Uusitalo, L., Lehikoinen, A., Helle, I., and Myrberg, K. 2015. An overview of methods to evaluate uncertainty of deterministic models in decision support. Environmental Modelling & Software, **63**: 24–31.

van der Kamp, G., Hayashi, M. 2009. Groundwater-wetland ecosystem interaction in the semiarid glaciated plains of North America. Hydrogeology Journal, **17(1)**: 203–214.

van Griensven, A., and Meixner, T. 2006. Methods to quantify and identify the sources of uncertainty for river basin water quality models. Water Science and Technology, **53(1)**: 51–59.

van der Valk, A.G., and Jolly, R.W. 1992. Recommendations for research to develop guidelines for the use of wetlands to control rural NPS pollution. Ecological Engineering, **1(1–2)**: 115–34.

Waidler, D. White, M., Steglich, E., Wang, S., Williams, J., Jones, C.A., and Srinivasan, R. 2009. Conservation Practice Modeling Guide for SWAT and APEX. Accessed on 25 Nov. 2015, http://swat.tamu.edu/documentation/

Wall, G.J., Coote, D.R., Pringle, E.A., and Shelton, I.J. (editors). (2002). RUSLEFAC — Revised Universal Soil Loss Equation for application in Canada: A Handbook for estimating soil loss from water erosion in Canada. Research Branch, Agriculture and Agri-Food Canada. Ottawa. Contribution No. AAFC/AAC2244E. 117 pp.

Wall, G.J., Dickinson, W.T., Rudra, R.P., and Coote, D.R. 1988. Seasonal soil erodibility variation in southwestern Ontario. Can. J. Soil Sci., **68(2)**: 417–424.

Wellen, C., Arhonditsis, G.B., Long, T., and Boy, D. 2014. Quantifying the uncertainty of nonpoint source attribution in distributed water quality models: A Bayesian assessment of SWAT's sediment export predictions. Journal of Hydrology, **519**: 3353–3368.

Wen, L., Lin, C.A., Wu, Z., Lu, G., Pomeroy, J., and Zhu, Y. 2011. Reconstructing sixty year (1950-2009) daily soil moisture over the Canadian Prairies using the Variable Infiltration Capacity model. Canadian Water Resources Journal, **36(1)**: 84–102.

West Coast Seeds. 2015. Planting Charts across Canada: Southern Prairies. Accessed on 20 Sep. 2015, https://www.westcoastseeds.com/garden-resources/west-coast-seeds-planting-charts/

White, M.J., and Arnold, J.G. 2009. Development of a simplistic vegetative filter strip model for sediment and nutrient retention at the field scale. Hydrological Processes, **23(11)**: 1602–1616.

White, K.L., and Chaubey, I. 2005. Sensitivity analysis, calibration, and validations for a multisite and multivariable swat model. Journal of the American Water Resources Association, **41(5)**: 1077–1089.

Williams, J. R. 1969. Flood routing with variable travel time or variable storage coefficients. Trans. ASAE, **12(1)**: 100–103.

Williams, J.R., and Berndt, H.D. 1977. Sediment yield prediction based on watershed hydrology. Trans. ASAE, **20(6)**: 1100–1104.

Winter, T.C., and Woo, M.K. 1990. Hydrology of lakes and wetlands. In The Geology of North America, Vol. 0-1, Surface Water Hydrology 159–87. Boulder, CO: The Geological Society of America.

Woo, M.K., and Rowsell, R.D. 1993. Hydrology of a prairie slough. Journal of Hydrology, **146 (1–4)**: 175–207.

Yang W., Liu, Y., Simmons, J., Oginskyy, A., and McKague, K. 2013. SWAT Modelling of Agricultural BMPs and Analysis of BMP Cost Effectiveness in the Gully Creek Watershed. A research report submitted to: Ausable Bayfield Conservation Authority, Ontario Ministry of Agriculture and Food, University of Guelph, Ontario.

Yang, J, Reichert, P., Abbaspour, K.C., Xia, J., and Yang, H. 2008. Comparing uncertainty analysis techniques for a SWAT application to the Chaohe Basin in China. Journal of Hydrology, **358(1–2)**: 1–23.

Zhang, J., Jørgensen, S.E. 2005. Modelling of point and non-point nutrient loadings from a watershed. Environmental Modelling & Software, **20**: 561–574.

CHAPTER 6 INVESTIGATION OF DIFFERENT SOURCES OF UNCERTAINTY IN A SWAT-PDLD MODEL OF A CANADIAN PRAIRIE WATERSHED

This chapter is submitted as a research paper to the Hydrological Sciences Journal.

Citation: Mekonnen, B.A., Mazurek, K.A., and Putz, G. (2016). Assessment of the different sources of uncertainty of SWAT-PDLD model of a cold-climate Canadian prairie watershed. Hydrological Sciences Journal (submitted).

The document has been reformatted from the original version for inclusion in the thesis though no content has changed from the submitted version.

Contribution of the PhD candidate

The contribution of the PhD candidate in the research presented in this chapter is quantification of the different sources of modeling uncertainty for the developed model. The candidate implemented and compared different techniques of parameter uncertainty, which include GLUE, ParaSol, and SUFI-2, for the developed model. The candidate also assessed other sources of modeling uncertainty such as precipitation, observed discharge data, and model structure. The candidate drafted the manuscript while the second and third authors provided advice on various aspects of the work as well as critical review and editorial guidance of the manuscript.

Contribution of this chapter to the overall study

As part of this dissertation, which aims on developing flow and pollutants export simulation model, this section of the thesis contributes to the general theme by focusing on the research aspects of investigating the major sources of modeling uncertainty of the developed model. Quantification of the different sources of uncertainty is important in order to evaluate the reliability of the developed model before applying the model to solve water problems. Thus, this chapter is taken as the final step towards attaining the objectives of this dissertation.

6.1 Abstract

Watershed models are a simplified representation of natural systems and hence prone to different sources of uncertainty. The main objective of this study is to investigate the major sources of uncertainty in a Canadian prairie hydrologic watershed model called SWAT-PDLD, which combines the Soil and Water Assessment Tool (SWAT) and a Probability Distributed Landscape Depression (PDLD) algorithm. The uncertainty investigation was achieved by estimating parameter uncertainty in SWAT-PDLD using the GLUE, ParaSol, and SUFI-2 techniques; evaluating precipitation and discharge data uncertainty; and implementing a methodology that combines Bayesian Model Averaging (BMA) and the Shuffled Complex Evolution (SCE) to assess model structure uncertainty. Results suggest that ignoring either input error or model structure uncertainty will lead to unrealistic model simulations and incorrect uncertainty bands. The study also shows that prediction of uncertainty bands, posterior parameter distribution, and final parameter values varies significantly between uncertainty analysis methods.

6.1 Introduction

The prairie region of North America covers a vast area of the prairie provinces of Canada, and parts of North and South Dakota, Minnesota, Montana, and Iowa in the United States. This region is characterized by relatively flat terrain with millions of small depressional wetlands of glacial origin, called prairie potholes or sloughs (Woo and Rowsell 1993). The majority of these wetlands do not drain to any natural external drainage system and form internally drained closed basins that are considered non-contributing to streamflows (Leibowitz and Vining 2003). Agriculture and Agri-Food Canada (AAFC) identified a static map of non-contributing areas following Godwin and Martin (1975), who defined non-contributing areas as those that do not contribute runoff to the watershed outlet for an event of two year return period (Prairie Farm Rehabilitation Administration 1983). In reality, the extent of the non-contributing areas is dynamic and changes with the amount of water in depressional storage (Shook and Pomeroy 2011). Wetlands can connect to one another during wet conditions through the "fill and spill" mechanism and can sometimes contribute to stream flow (Shaw et al. 2011). In addition to the dynamic connectivity, memory effects of depressional storages have recently been reported by Shook and Pomeroy (2011). The response of the watershed is therefore highly dependent on the details within the landscape, including the location and the linkage among the depressional wetlands (van der Kamp and Hayashi 2003).

With increasing pressure on Canadian prairie watersheds from various types of developments since the time of European settlement, watershed management tools are needed. Consequently, substantial efforts have been made to develop watershed models and simulate the hydrological processes in prairie watersheds. These include, but are not limited to, CHRM (Cold Regions Hydrological Model, e.g., Pomeroy et al. (2007)), MESH (Modélisation Environmentale

Communautaire - Surface and Hydrology (combined CLASS and WATFLOOD), e.g., Mekonnen et al. (2014)), SLURP (Simple Lumped Reservoir Parametric, e.g., Su et al. (2000)), SWAT (Soil and Water Assessment Tool, e.g., Chanasyk et al. (2003), Yang et al. (2010), Wang et al. (2008), Rahbeh et al. (2011), Shrestha et al. (2012), Mekonnen et al. (2015, 2016a, 2016b, 2016c)), and VIC (Variable Infiltration Capacity, e.g., Wen et al. (2011)). Nevertheless of these and many other substantial efforts, modeling the hydrology of a prairie watershed remains very challenging. Recently, Mekonnen et al. (2016a) have modified the SWAT model by replacing the lumped storage module with a distributed storage using a probability distribution to help model dynamic storage in depressions. Mekonnen et al. (2016a, 2016b) tested SWAT with this probability distributed landscape depression algorithm (hereafter called SWAT-PDLD) for two large area prairie watersheds, with improved streamflow and sediment export simulation results as compared to the typical lumped approach that has often been used to represent depressional storage.

Any watershed model is a simplified representation of a natural system and therefore is subject to multiple sources of uncertainty (Beven and Binley 1992) and this must also be assessed in model development. The major sources of uncertainty while modeling the hydrological processes of a watershed include the model parameter values, the input data, and the model structure (Butts et al. 2004). Parameter uncertainty arises from measurement or estimation errors of model parameter values (Haan and Skaggs 2003). Input data uncertainty is due to measurement errors (if an input is directly measured), estimation errors (e.g. spatially interpolated rainfall input), and uncertainty associated with initial conditions (Shirmohammadi et al. 2006). Uncertainty in observed discharge data (for model calibration) arises from measurement errors such as discharge gauging errors, extrapolation of rating curves, unsteady

flow conditions, and temporal changes in channel properties (Sellami et al. 2013). Model structure uncertainty is associated with simplifications, and even missing representations, of the physical processes occurring in a watershed because of the limitations of models to describe the physical reality of a watershed (Butts et al. 2004).

Several studies of model uncertainty were devoted to developing techniques for estimation of parameter uncertainty, while input and model structure uncertainties were not addressed explicitly (Ajami et al. 2007). These techniques include the Generalized Likelihood Uncertainty Estimation (GLUE) (Beven and Binley 1992), the Parameter Solution (ParaSol) (van Griensven and Meixner 2006), and Sequential Uncertainty Fitting (SUFI-2) (Abbaspour et al. 2004). GLUE (Beven and Binley 1992) is based on the concept of equifinality. The philosophy of equifinality is that there is no single optimum parameter set that exists for the best simulation but rather it is equally well represented by a range of different parameter sets. GLUE has been extensively used for the uncertainty assessment of different hydrological models (e.g., Yang et al. 2008; Setegn et al. 2009; Shen et al. 2012). ParaSol (van Griensven and Meixner 2006) is the modified version of an optimization algorithm called the Shuffled Complex Evolution. This method has been integrated into the SWAT model and has been widely applied for optimization as well as for uncertainty assessment in SWAT (e.g., Yang et al. 2008; Setegn et al. 2010; Sellami et al. 2013). SUFI-2 (Abbaspour et al. 2004) is a step-by-step optimization and uncertainty estimation method that quantifies prediction uncertainty at the 2.5% and 97.5% levels of the cumulative distribution of output variables obtained through Latin hypercube sampling. The method also has been widely applied for the SWAT model (e.g., Yang et al. 2008; Setegn et al. 2010; Sellami et al. 2013). SUFI-2 has been seen as a good option for uncertainty

estimation in large area watershed modeling as it requires a fewer number of simulations as compared to other methods (Arnold et al. 2012).

As noted, these techniques address primarily uncertainty due errors in parameter values (Vrugt et al. 2008), although other sources of uncertainty exist for model predictions (Ajami et al. 2007). To help address these issues, new techniques to propagate confidence bands from different uncertainty sources to the model output were developed. Some of these include techniques to tackle uncertainty in input data such as the DEM resolution (Cotter et al. 2003), precipitation (Li and Xu 2014), and rating curve uncertainty for observed discharge estimation (Sellami et al. 2013), and model structure uncertainty (e.g., Strauch et al. 2012).

For estimating model structure uncertainty, techniques that combine model outputs from different model structures have been used (e.g., Raftery et al. 2005; Zhang et al. 2009; Strauch et al. 2012). This approach of ensemble modeling allows uncertainty assessment to include differences between individual member models. Weights that are used to ensemble multiple models can be equal in the simplest case (e.g. Shamseldin et al. 1997), or can be determined through regression-based approaches (e.g., Georgakakos et al. 2004), Artificial Neural Networks (e.g., See and Abrahart 2001), or Bayesian Model Averaging (Draper 1995). Bayesian Model Averaging (BMA) is a probabilistic multi-model averaging technique that has gained popularity in diverse fields (Raftery et al. 2005); the technique is increasingly being used in the hydrological community (e.g., Butts et al. 2004; Duan et al. 2007; Franz et al. 2010). More importantly, BMA has also been implemented to quantify uncertainty intervals due to model structure errors (e.g., Raftery et al. 2005; Zhang et al. 2009; Strauch et al. 2012).

The purpose of this study is to evaluate the different sources of uncertainty in a SWAT-PDLD model of a Canadian prairie watershed, the Moose Jaw watershed in the Province of

Saskatchewan. To achieve the objective, quantification of model parameter, precipitation, discharge data, and model structure uncertainties was undertaken. In estimating parameter uncertainty, three different techniques were tried (Generalized Likelihood Uncertainty Estimation (GLUE), Parameter Solution (ParaSol), and Sequential Uncertainty Fitting (SUFI-2)) and results are compared. Model structure uncertainty in the SWAT-PDLD model is estimated by implementing a framework that combines the Shuffled Complex Evaluation and Bayesian Model Averaging (called SCE-BMA).

6.2 Study Area and SWAT-PDLD Model Description

6.2.1 Watershed description

The study was conducted using data from the Moose Jaw River in the Province of Saskatchewan, Canada, the location of which is shown in Fig. 6–1. The gauging station near Burdick (Water Survey of Canada station number: 05JE006) located at 50°24’1.2” N and 105°23’52.3”W provided the daily streamflow measurements for this study. The Moose Jaw River is a major tributary of the Qu’Appelle River. The Moose Jaw River watershed has a gross drainage area of 9 230 km^2 and of this only 3 470 km^2 is considered as effective contributing area according to the Godwin and Martin (1975) definition of effective and non-contributing areas.

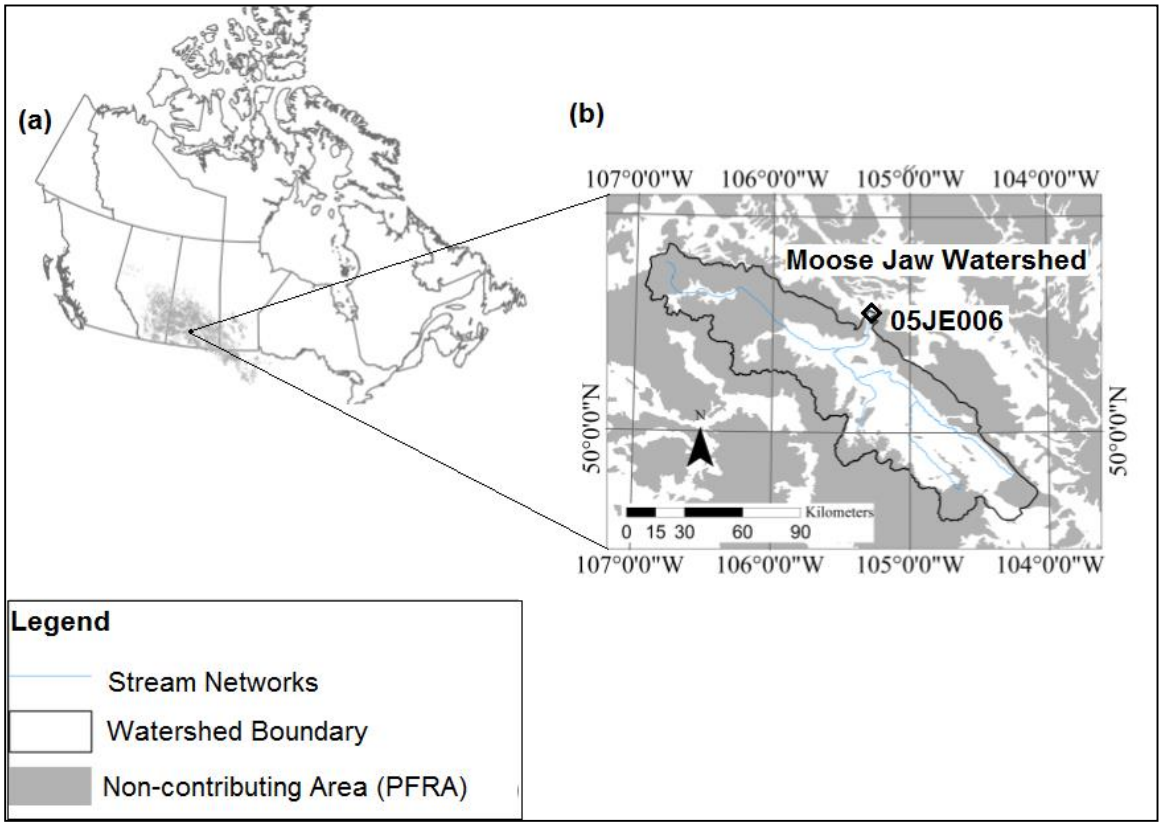

Figure 6–1 The location of the study area within the Moose Jaw River Basin in Canada: (a) Canada; and (b) Moose Jaw River Watershed.

The watershed lies within the prairie region and exhibits a cold-region hydrology characterized by long and cold winters with frozen soils and short and warm summers. The Moose Jaw River, generally, carries moderate to high flows during the period from mid-March to mid-June and its water supply is almost entirely from surface runoff like most prairie streams. The 30-year (1971-2000) mean annual precipitation at Moose Jaw is 365 mm, of which 115.5 mm occurs mostly as snow in winter. The 30-year annual average air temperature at Moose Jaw is 4°C (Environment Canada 2009). The topography of Moose Jaw watershed varies between 536.6 and 48.3 m above mean sea level and the majority of the land in this watershed is used for

agriculture (70%) and this is mainly for crop production. The watershed is located in an area of diverse soil types ranging from heavy clay soils in the East to gravelly sandy soils in the West.

6.2.2 SWAT-PDLD model description

The Soil and Water Assessment Tool (SWAT) (Arnold et al. 1998) was developed by the US Department of Agriculture-Agricultural Research Service. It is a continuous semi-distributed eco-hydrological model that simulates the various hydrological processes of a watershed at a daily or sub-daily time scale (Gassman et al. 2007; Neitsch et al. 2011). The model simulates the hydrological cycle of a watershed by partitioning a watershed into a number of sub-basins that are further grouped into Hydrological Response Units (HRUs), which are a unique combinations of land cover, soil type, and slope (Neitsch et al. 2011). In SWAT, surface runoff is computed using either the modified Curve Number Method (CN) (USDA Soil Conservation Service 1972) or Green-Ampt methods (Green and Ampt 1911). While using the CN method, the retention parameter can be estimated based on either soil profile water contents or plant evapotranspiration (Neitsch et al. 2011). Potential evapotranspiration is estimated using one of the three different methods that include Hargreaves (Hargreaves et al. 1985), Priestley-Taylor (Priestley and Taylor 1972), and Penman-Monteith (Monteith 1965). The actual evaporation from soils and plants is estimated as described by Ritchie (1972). The SWAT model also simulates impoundments such as reservoirs, wetlands, and ponds. Baseflow is modelled by partitioning groundwater into a two aquifer system (shallow and deep) (Arnold et al. 1998). Water balance computations in the SWAT model are performed at the HRU level within a sub-basin. The contributions of each HRU are then averaged out to represent water yield to the main channel within the sub-basin. The routing in SWAT is performed based on either the variable storage coefficient method (Williams 1969) or the Muskingum routing method (Cunge 1969).

In the original SWAT model, the Pond or Wetland modules, which are used to simulate depression storage, allow only a single depression per sub-basin (Neitsch et al. 2011). As a result, it has been a common modeling practice to aggregate together the numerous depressions that exist within a sub-basin and represent them by a single synthetic pond per sub-basin (e.g. Kiesel et al.2010; Almendinger et al. 2012; Mekonnen et al. 2015). This approach, however, may not be a good representation of storage in depressions for landscapes dominated by depressions (Wang et al. 2008; Mekonnen et al. 2016a, 2016b). As noted, in order to better represent the hydrological processes in a depression-dominated prairie watershed, Mekonnen et al. (2016a) modified the SWAT model by incorporating a Probability Distributed Landscape Depression algorithm, called SWAT-PDLD. The PDLD module allows some accounting for the heterogeneity in storage capacity of the numerous depressions that exist within a sub-basin. The SWAT-PDLD modeling framework was tested with data from prairie watersheds and reported an improved daily streamflow prediction performance as compared to the lumped storage approach that exists in the original SWAT model (Mekonnen et al. 2016a, 2016b).

In the SWAT-PDLD modeling approach, the water balance of a single depression is expressed as follows: the depression takes up water from precipitation and upland runoff generated from its contributing areas and loses water through evapotranspiration and seepage. The difference between these inputs and outputs either fills or empties the depression. When the net input exceeds the available storage in the depression, the depression will spill and therefore generate runoff. Over an entire sub-basin, the runoff generation principle at every depression may be similarly described, each depression differing from another only with regard to its storage capacity, which is described by a probability distribution function. The total runoff generated from the landscape depressions will be the cumulative runoff generated from the

individual depressions. Details of the SWAT-PDLD modeling framework, formulation, and integration into SWAT are available in Mekonnen et al. (2016a, 2016b).

The probability density function to be used for the study watershed was determined using DEM data analysis for the watershed. ArcGIS was used to quantify the depression geometries across the watershed. Then, the storage capacity of each depression was plotted by frequency of occurrence. A probability density function was then fitted to this data so that an expression of the variation of capacity across the watershed could be found. An exponential distribution was selected because of its relative simplicity (a one parameter function) and previous successful application by Mekonnen et al. (2016a, 2016b). An initial condition must be assumed or estimated for the amount of water stored in the landscape depressions at the beginning of a model simulation using the above described Probability Distributed Landscape Depressions (PDLD) algorithm in order for the calculations to proceed. This initial condition, used at the start of the warm up period for the model, was that during the spring snowmelt period the depressions were all at full capacity.

6.2.3 Input data availability

The basic datasets required to develop the SWAT model include topography, land use, soil, and climatic data (including precipitation and temperature). Descriptions of these datasets are given as follows:

i. Land cover data for the study watershed was obtained from the LCC200V database from GeoBase Canada [http://www.geobase.ca/]. The land cover data were prepared through vectorization of raster thematic data originating from classified Landsat 5 and Landsat 7 ortho-images with the Circular Map Accuracy Standard (CMAS) of 30 meters. The data was distributed as 1:250 000 scale National Topographic System (NTS) tiles.

ii. Topographic data for the study watershed was obtained from the GeoBase Canada database [http://www.geobase.ca/]. GeoBase provides the Canadian Digital Elevation Data (CDED) at scales of 1:50 000 and 1:250 000.

iii. Soil data at a resolution of 1:1 000 000 for the study watershed was obtained from Soil Landscapes of Canada (SLC), which is found in the Agriculture and Agri-Food Canada database (Soil Landscapes of Canada Working Group 2007).

iv. Gridded climate data sets (including precipitation, minimum temperature and maximum temperature), which were derived from the Gridded Climate Dataset for Canada (GCDC) (Hutchinson et al. 2009), were used as forcing climatic data to model the study watershed. The gridded datasets were employed instead of the relatively sparse climate observation stations data because of their more detailed spatial coverage. The suitability of such data for this region is supported by the work of Choi et al. (2009), who demonstrated that a watershed model could be suitably calibrated in a prairie environment using gridded data. The Gridded Climate Dataset for Canada (GCDC) covers for the period 1961-2003 (Hutchinson et al. 2009). The dataset is based on daily Environment Canada climate station observations interpolated at a 10 km spatial resolution using a thin-plate smoothing spline-surface fitting method.

v. Flow data was extracted from the Hydrometric Database (HYDAT) of the Water Survey of Canada. In this study, the daily weather and flow data from 1990 to 2001 was used for model development purposes including a “warm-up” period (1990 to 1991), calibration period (1992 to 1997) and validation period (1998 to 2001).

6.2.4 Model setup and calibrated parameters

The ArcSWAT interface was used to prepare input data for the SWAT-PDLD model. Several steps were followed in order to prepare the required input data. First, the DEM data was imported into the ArcSWAT interface and used to discretize the study watershed into sub-watersheds and then further divided into HRUs based on land use, soil, and slope maps. The SWAT-PDLD model input data files, both sub-watershed and HRU level input datasets, were then prepared with the help of the interface. Following model setup, the parameters that significantly affect streamflow simulation are calibrated. Table 6–1 shows the list of calibrated parameters along with their default values and recommended range of values. As seen in Table 6–1, a total of thirteen parameters were calibrated.

Table 6–1 Selected parameters for calibration and their prior likelihood ranges.

Parameter	Parameter description	Method of change	Uniform prior distribution range	
			Min	Max
CN2	SCS runoff curve number	a	-10	+10
ESCO	Soil evaporation compensation factor	b	0	1
SURLAG	Surface runoff lag coefficient	b	0	14
ALPHA_BF	Baseflow factor (Day)	b	0	1
SFTMP	Snowfall temperature (^{o}C)	b	-5	+5
SMTMP	Snowmelt base temperature (^{o}C)	b	-5	+5
SMFMX	Maximum melt factor (mm $^{o}C^{-1}$/d)	b	0	7
SMFMN	Minimum melt factor (mm $^{o}C^{-1}$/d)	b	0	7
TIMP	Snowpack temperature lag factor	b	0	1
SNOCOVMX	Areal snow coverage threshold at 100% (mm)	b	0	500
SNO50COV	Areal snow coverage threshold at 50%	b	0	1
SMAX	Maximum storage capacity (varies)	c	-0.2	+0.2
CH_N	Manning *n* for the main channel	b	0	0.10

Notes: [a] This indicates that the given value is added to the existing parameter value.
[b] This indicates that the existing parameter value is replaced by the given value.
[c] This indicates that the existing parameter value is multiplied by (1+a given value).

As shown in Table 6–1, spatial heterogeneity of parameter values during optimization can be maintained by choosing different parameter changing method. From the three schemes

used in this study, scheme ‘a’ and ‘c’ allows the user to make distributed parameters dependent on important influential factors such as: hydrological group, soil texture, land use, and slope. For instance, in this study heterogeneity of SCS Curve Number is maintained by implementing scheme ‘c’.

6.3 Uncertainty Methods

6.3.1 Parameter uncertainty

Three widely applied techniques, the Generalized Likelihood Uncertainty Estimation (GLUE) (Beven and Binley 1992), Parameter Solution (ParaSol) (van Griensven and Meixner 2006), and Sequential Uncertainty Fitting (SUFI-2) (Abbaspour et al. 2004), were investigated for parameter uncertainty estimation of SWAT-PDLD model of the Moose Jaw watershed. The investigation mainly focused on uncertainty bands, the posterior parameter distribution, and computational time.

The Generalized Likelihood Uncertainty Estimation (GLUE) (Beven and Binley 1992), which was introduced recognizing the idea of non-uniqueness (or equifinality) of parameter sets during estimation of model parameters, was implemented using a Monte Carlo based random sampling strategy. The sampled parameter sets were then divided into “behavioral” and “non-behavioral” categories based on a pre-selected threshold value of the likelihood measure. The parameter sets that were grouped as “behavioral” were used to quantify a parameter uncertainty band. This was performed by assigning a likelihood weight for “behavioral” parameter sets. Following weight assignment for every “behavioral” parameter set, prediction uncertainty was described by quantiles of the cumulative distribution realized from the weighted “behavioral” parameter sets. The following assumptions were used while implementing the GLUE method: 1) a uniform prior parameter distribution was assumed due to an absence of prior information about

parameter distribution; 2) the Nash & Sutcliffe efficiency index (NSE: Nash and Sutcliffe 1970) was used as the likelihood measure; 3) an NSE of 0.5 was used as a threshold value to divide "behavioral" and "non-behavioral" simulations (this was based on a recommendation by Gassman et al. (2007) for "satisfactory" simulations and because it has been used in previous studies e.g., Shen et al. 2012; Sellami et al. 2013); and 4) the number of Monte Carlo simulations was set to 10 000 as several other previous studies where GLUE was applied used a similar number of model runs (e.g., Yang et al. 2008; Shen et al. 2012; Sellami et al. 2013).

The Parameter Solution (ParaSol) (van Griensven and Meixner 2006), which is a modified version of the global optimization algorithm called the Shuffled Complex Evolution (SCE: Duan et al. 1993), was also used to estimate parameter uncertainty. The method was implemented using the SCE optimization algorithm, which combines the direct search method with the concept of a controlled random search, a systematic evolution of points in the direction of global improvement, competitive evolution and the concept of complex shuffling (van Griensven and Meixner 2006). The model runs obtained during optimization (using the SCE) was used to provide parameter uncertainty bands, which was done by dividing the simulations identified during optimization into 'good' and 'not good' simulations. Then, all "good" simulations were used to construct the parameter uncertainty. The following assumptions were used while implementing the ParaSol method: 1) a uniform prior distribution of parameters was assumed; 2) optimization termination criterions were set to a either a maximum number of 10 000 model runs or a convergence rate of less than 0.01percent between consecutive simulations; 3) the Nash & Sutcliffe efficiency index (NSE: Nash and Sutcliffe 1970) is used as a likelihood measure; an 4) an NSE of 0.5 is used as a threshold value to divide "behavioral" and "non-behavioral" simulations.

Sequential Uncertainty Fitting (SUFI-2) (Abbaspour et al. 2004), which is a semi-automated method that estimates uncertainties through a sequential and fitting process, was also used to estimate the parameter uncertainty. The method was implemented through step-by-step iterations for updating estimates of parameters to achieve final estimates of parameter value and uncertainty band. For every iteration stage, the Latin Hypercube Sampling method (McKay et al. 1979) was used to draw independent parameter sets. SUFI-2 was started by assuming a large parameter uncertainty (within the allowable range of prior distribution), so that most of the measured data initially fall within the 95% prediction uncertainty. Then this uncertainty was decreased in steps while keeping track of the *P*-factor, which is the percentage of measured data bracketed by the 95% prediction uncertainty bands and *R*-factor, which is the average thickness of the prediction uncertainty. Parameter ranges were updated, for subsequent iterations, by calculating the 95% confidence intervals of the parameters of best simulation. Prediction uncertainty was estimated from the percentiles of the cumulative distribution of "behavioral" simulations. For instance, the 95% prediction uncertainty is calculated by the 2.5th (lower limit) and 97.5th (upper limit) percentiles of the cumulative distribution of "behavioral" simulations. Details of the SUFI-2 procedure can be found in Abbaspour et al. (2004). The following assumption were considered while implementing SUFI-2: 1) a uniform prior distribution of parameters; 2) the Nash & Sutcliffe efficiency index (NSE: Nash and Sutcliffe 1970) was used as a likelihood measure; 3) an NSE of 0.5 was used as a threshold value to divide "behavioral" and "non-behavioral" simulations; and 4) three iterations are conducted with SUFI-2, each with 1000 model runs (giving a total of 3000 model runs), as was done in several previous studies (e.g., Yang et al. 2008; Setegn et al. 2010; Sellami et al. 2013).

6.3.2 Input uncertainty: precipitation and observed discharge data

Other sources of uncertainty assessed in this study were input data uncertainty from precipitation and discharge measurements. Precipitation uncertainty was incorporated using a multiplicative error propagation equation, which is among a range of error propagation operators listed by Refsgaard et al. (2007). A study by McMillan et al. (2011), which is validated against experimental evidence, confirms the suitability of a multiplicative error formulation for correcting precipitation with longer time steps (time step of 1 day or greater). A similar strategy of multiplicative error propagation for precipitation has also been successfully implemented into a hydrological model by Li and Xu (2014). The error propagation equation is given as:

$$P_c = cP_o \tag{6.1}$$

where P_c is the corrected precipitation depth, c is the precipitation multiplier, and P_o is the observed precipitation depth. The precipitation multiplier, c, is determined by considering it as parameter for the optimization. Recent application of similar methodology by Li and Xu (2014) recommends the multiplier *c* range between 0.9 and 1.1.

Uncertainty of observed discharge data was incorporated by estimating the upper and lower bands of error for individual measured values, as was done in past studies (e.g., Sellami et al. 2013). McMillan et al. (2012) compiled information available from the literature about uncertainty in measured discharge data. The relative error propagation method of Krueger et al. (2010), which considers total discharge uncertainty caused by gauging errors, rating curve form/extrapolation and instability of rating curves was used to estimate observed discharge error bands. The approach considers the variation of magnitude of errors in flow by implementing three different rates of error that is 100%, 10%, and 20% respectively for low, medium, and high flow conditions. Such an assumption of non-uniformity in hydrometric uncertainty with flow

magnitude is suggested for Canadian conditions (Hamilton 2008). The proposed higher error rate for low flows is suitable for Canada because low flows often occur during the winter period (Burn et al. 2008). Thus, the majority of low flows in Canadian rivers are flagged with a 'B', indicating ice condition (winter period) (Environment Canada 2007). This flag means higher error as discharge is estimated without using a valid stage-discharge relation (Hamilton 2008).

Following development of upper and lower bands of individual observed discharge, SWAT-PDLD model optimization was then performed twice by taking the lower and upper bands of observed discharge as true discharges. This procedure was done in order to estimate the possible upper and lower error limits where all the errors would fall if different samples of true observed discharge were taken from their probable range. The SWAT-PDLD model prediction uncertainty was then estimated by combining prediction uncertainty bands corresponding to the lower and upper limit of measured discharge. The combined new calculated uncertainty bound encompasses parameter and observed discharge data uncertainty.

6.3.3 Model structure uncertainty

The final source of uncertainty estimated in this study is model structure uncertainty, which was implemented using a methodology that combines the Shuffled Complex Evolution (SCE) and Bayesian Model Averaging (BMA), called SCE-BMA. The SCE-BMA framework of model structure uncertainty assessment was selected because of the following: 1) the efficient optimization scheme of the SCE in identifying the best fit parameter sets of individual model structures under consideration (e.g., Yang et al. (2008); Setegn et al. (2010)); and 2) the past successful and wider application of BMA for merging information from multiple models (e.g., Hoeting et al. 1999; Raftery et al. 2005; Refsgaard et al. 2006; and many others). The different model structures of SWAT-PDLD were identified and setup first in order to implement the SCE-

BMA framework. Each of the individual models was separately calibrated for observed flow data using the Shuffled Complex Evolution algorithm. Then, the best simulation from the optimized individual model was used to perform ensemble prediction using the Bayesian Model Averaging followed by estimation of uncertainty.

6.3.3.1 Identifying individual models

To implement the SCE-BMA framework four different SWAT-PDLD model structures were considered. The models were identified by combining soil water content and accumulated plant evapotranspiration based curve number retention parameter with the variable storage and Muskingum routing methods. The four different SWAT-PDLD model structures (Table 6–2) considered were as follows: 1) SW-VS that denotes the SWAT-PDLD with curve number retention parameter (*s*) varying accordingly the soil profile water content together with the variable storage routing; 2) SW-MK that denotes the SWAT-PDLD with *s* varying accordingly the soil profile water content together with the Muskingum flow routing; 3) ET-VS that denotes the SWAT-PDLD with *s* varying accordingly the accumulated plant evapotranspiration together with the variable storage flow routing; and 4) ET-MK that denotes the SWAT-PDLD with *s* varying accordingly the accumulated plant evapotranspiration together with the Muskingum routing.

Table 6–2 Sub-models selected for Bayesian Model Averaging analyses.

Models	**Model structure description**	
	Curve number retention parameter calculation method	Routing method
SW-VS	soil profile water content	Variable storage
SW-MK	soil profile water content	Muskingum
ET-VS	plant evapotranspiration	Variable storage
ET-MK	plant evapotranspiration	Muskingum

6.3.3.2 Bayesian Model Averaging (BMA)

The Bayesian Model Averaging (BMA) (Raftery et al. 2005), which is a post-processing statistical method for combining predictions from different sources was used to ensemble results from the different model structures. A detail description of BMA is fully presented in many past works (e.g., Duan et al. 2007; Vrugt et al. 2008; Strauch et al. 2012; and many others). The basic formulation of the Bayesian Model Averaging scheme can be described as follows: let $f = f_1,..., f_k$ denote an ensemble of predictions obtained from k different models (k =4 for this study as four different model structures are considered) and *y* be the quantity to be predicted. Using the law of total probability, which is also described by Raftery et al. (2005), the probabilistic prediction of the Bayesian Model Averaging, $P(y / f_1,..., f_4)$, is given by:

$$P(y / f_1,..., f_4) = \sum_{k=1}^{k} w_k . P_k(y / f_k) \qquad (6.2)$$

where $P(y / f_1,..., f_k)$ is the probability density function of the Bayesian Model Averaging probabilistic prediction of *y*; w_k is the posterior probability of the individual prediction f_k, which is often called weights; and $P_k(y / f_{k,})$ is the probabilistic prediction of *y* based on model f_k alone.

As described by Raftery et al. (2005), the $P_k(y / f_{k,})$ of different ensemble members can be approximated by a normal distribution, $N(a_k + b_k f_k, \sigma_k{}^2)$, with mean $a_k + b_k f_k$ and standard deviation σ_k. a_k and b_k are bias correction terms that are derived by simple regression of y on f for each of the individual ensemble members. Following Raftery et al. (2005); Ajami et al.

2007, Duan et al. 2007), the posterior mean and variance of the Bayesian Model Averaging prediction can be defined as:

$$E(y / f_1,..., f_k) = \sum_{k=1}^{K} w_k (a_k + b_k f_k) \qquad (6.3)$$

where $E(y / f_1,..., f_k)$ is the mean the Bayesian Model Averaging prediction. The variance of the BMA prediction can be expressed as follows:

$$\mathrm{Var}(y / f_1,..., f_k) = \sum_{k=1}^{K} w_k \left[(a_k + b_k f_k) - \sum_{k=1}^{K} w_k (a_k + b_k f_k) \right]^2 + \sum_{k=1}^{K} w_k \sigma_k^{\ 2} \qquad (6.4)$$

where $\mathrm{Var}(y / f_1,..., f_k)$ is the variance of the Bayesian Model Averaging prediction.

As shown in Equation (4), the uncertainty of BMA mean prediction includes the between-model error and within-model error. The BMA variance contains two components: the between model variance and the within model variance, as shown in the first and second terms of the right hand side of Equation (6.4) (Duan et al. 2007). The weights (w_k) and variance ($\sigma_k^{\ 2}$) were estimated using the iterative Expectation-Maximization (EM) procedure described by Raftery et al. (2005), Ajami et al. (2007), and Duan et al. (2007).

6.3.3.3 Quantifying uncertainty in SCE-BMA

Following estimation of weights and variances for the BMA, the probabilistic predictions of the streamflow were derived based on each individual model deterministic prediction. The procedure outlined by Duan et al. (2007), Zhang et al. (2009), and Strauch et al. (2012) was used to estimate prediction uncertainty. A brief description of the procedure is given as

I. Generate a value of *k* from the numbers {1, . . . ,K} with the probabilities (w_1, . . . ,w_k);

II. Generate a replication y from the $g(y_t / f_{k,t})$;

III. Repeat Steps I and II to obtain 1000 values that represent the distribution of y_t for each time step *t*;

IV. Derive the 95% uncertainty interval from the cumulative distribution of y_t at the 2.5th and 97.5th levels; and

V. Estimate *R*- and *P*-factors for the 95% band using Equation (6.7) and (6.8) respectively.

6.4 Evaluation Criteria

Multi-statistical measures and visual inspection of graphical plots were used to evaluate and compare the different uncertainty techniques. In particular, methods were evaluated in terms of their performance in identifying the best simulation, covering the observed discharge data with the 95% uncertainty band (called *P*-factor), the width of the 95% prediction uncertainty band (*R*-factor), and computational time requirements. The criteria are described in detail as follows:

i. Best model simulation

Quantitative evaluation of each method performance for best fit was assessed using statistical metrics that include the Nash & Sutcliffe efficiency index (NSE*:* Nash and Sutcliffe 1970) and Percent Bias (PBIAS) (Gupta et al. 1999):

$$\mathrm{NSE} = 1 - \frac{\sum_{t=1}^{n}\left(y_t - Q_t\right)^2}{\sum_{t=1}^{n}\left(\bar{Q} - Q_t\right)^2} \tag{6.5}$$

$$\mathrm{PBIAS} = \frac{\sum_{t=1}^{n}\left(Q_t - y_t\right)*100}{\sum_{t=1}^{n} Q_t} \tag{6.6}$$

where y_t = the simulated streamflow; Q_t = the observed streamflow at time t; n = total number of data points; and $\overline{Q}$ = the average observed streamflow.

ii. Model prediction uncertainty

Two indices were used to evaluate the derived 95% uncertainty band (95PPU), which includes the width of the 95PPU (i.e., *R*-factor: Equation (6.7)) and percentage of the measurements bracketed by this band (i.e., *P*-factor: Equation (6.8)).

$$r-\text{factor} = \frac{\sum_{t=1}^{n}(\mathrm{y}_{t,97.5\%} - y_{t,2.5\%})}{n\delta} \tag{6.7}$$

where $y_{t,97.5\%}$ = the upper boundaries of the 95% prediction uncertainty; $y_{t,2.5\%}$ = the lower boundaries of the 95% prediction uncertainty; n =the number of data points; and δ = the standard deviation of observed flow.

$$p-\text{factor} = \frac{\sum_{t=1}^{n}\mathrm{I}[\mathrm{y}_t]}{n}$$

$$\text{with } \mathrm{I}[\mathrm{y}_t] = \begin{cases} 1, \textit{ if } \mathrm{y}_{t,2.5\%} < \mathrm{y}_t < \mathrm{y}_{t,97.5\%} \\ 0, \textit{ otherwise} \end{cases} \tag{6.8}$$

6.5 Results and Discussion

6.5.1 Results of parameter uncertainty in SWAT-PDLD

Three different methods of parameter uncertainty analysis were tried for the SWAT-PDLD model of the Moose Jaw River watershed in Saskatchewan, Canada. The results of this assessment that include the best simulations, 95% prediction uncertainty bands, and posterior distribution of the parameters for the three techniques considered (GLUE, ParaSol, and SUFI-2) are presented below.

Daily time series plots of the observed discharge and best model simulations are plotted in Fig. 6–2. Table 6–3 presents a summary of the statistical measures that were used to evaluate performance of the model for each method.

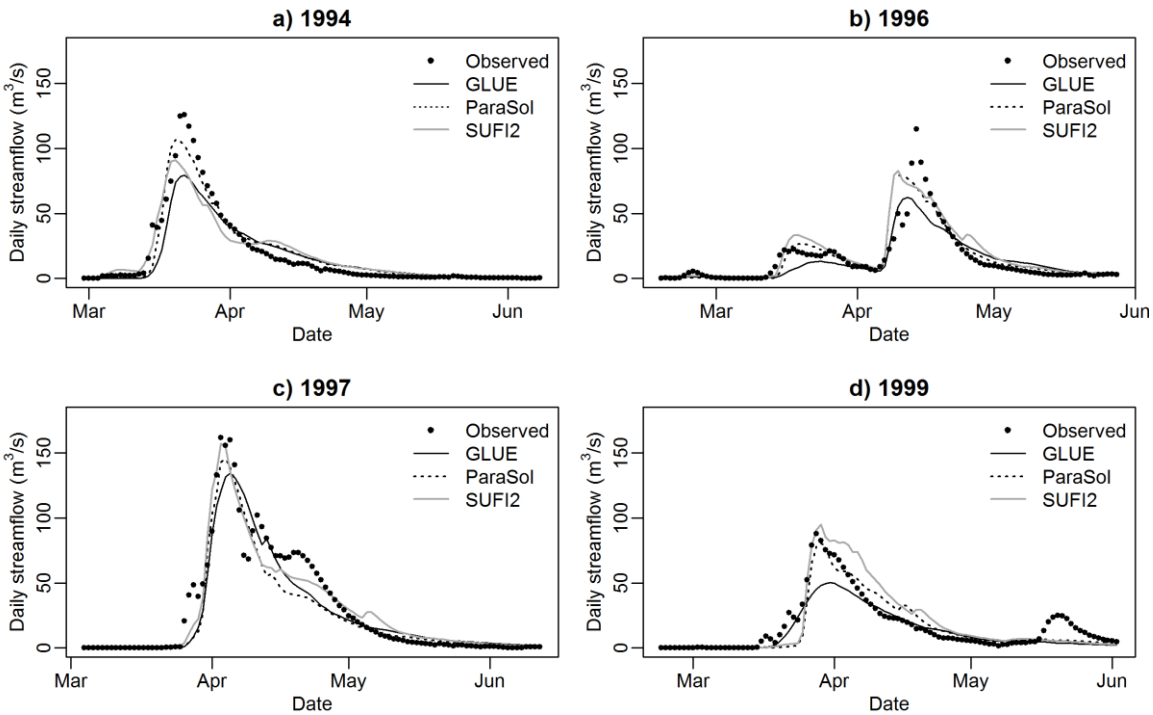

Figure 6–2 Best simulation obtained from the GLUE, ParaSol, and SUFI-2 methods during the calibration period (parts a, b, and c) and validation period (part d).

The best simulation for all three methods provide satisfactory results in terms of reproducing the temporal variation of the observed discharge. As shown in Table 6–3, the maximum NSE values for all three techniques are higher than 0.75 during the calibration period, which can be considered “very good” performance (Moriasi et al. 2007). A similar “very good” rating was also achieved by ParaSol for the validation period, while GLUE and SUFI-2 attain only a “satisfactory” rating. ParaSol is likely performing better because of its efficient searching algorithm method, which combines local and global search methods to find the optimum parameter space. GLUE and SUFI-2 use the random and Latin hypercube sampling methods

respectively. However, both similar (Yang et al. 2008; Setegn et al. 2010) and contradictory results (Sellami et al. 2013) results have been found for other watersheds.

The three methods were also used to find the 95% uncertainty bands (Fig. 6–3, Table 6–3), which were derived from the behavioral simulations, which are the simulations that give good model performance based on the NSE (NSE ≥ 0.5). The GLUE results (Table 6–3) show that 62% of the observed discharge data is bracketed by the 95% uncertainty bands with a *R*-factor of 0.56 during the calibration period, while in the 63% of the observed discharge is bracketed with a *R*-factor of 0.57 during the validation period. An *R*-factor below 1 is considered a good value, as it indicates a smaller uncertainty band. The 95% uncertainty band derived by ParaSol brackets only 13% of the observed discharge data with a *R*-factor of 0.03 during calibration period, while 14% of observed discharge data is bracketed during the validation period with a *R*-factor of 0.04. The results of SUFI-2 show that 46% of observed discharge is bracketed by the 95% uncertainty band a *R*-factor of 0.42 during the calibration period, while 37% of observed discharge data is bracketed by 95% of uncertainty band with a *R*-factor of 0.35 during the validation period. For the methods used in this study, GLUE therefore is most successful in bracketing the observed discharge data with the 95% uncertainty band, followed by SUFI-2 then ParaSol.

Table 6–3 Statistical measures of the model performance and computational time for each parameter uncertainty method.

	Calibration (1992-1997)			Validation (1998-2001)		
Criteria	GLUE	ParaSol	SUFI2	GLUE	ParaSol	SUFI2
NSE	0.87	0.89	0.86	0.66	0.78	0.69
PBIAS	-7.7	-20	-16	39	25	12
RSR	0.36	0.33	0.36	0.57	0.47	0.55
R-factor	0.56	0.03	0.42	0.57	0.04	0.35
P-factor	62	13	46	63	14	37
Simulation numbers	10000	6160	3x1000			
Computational Time (days)	16	10	4			

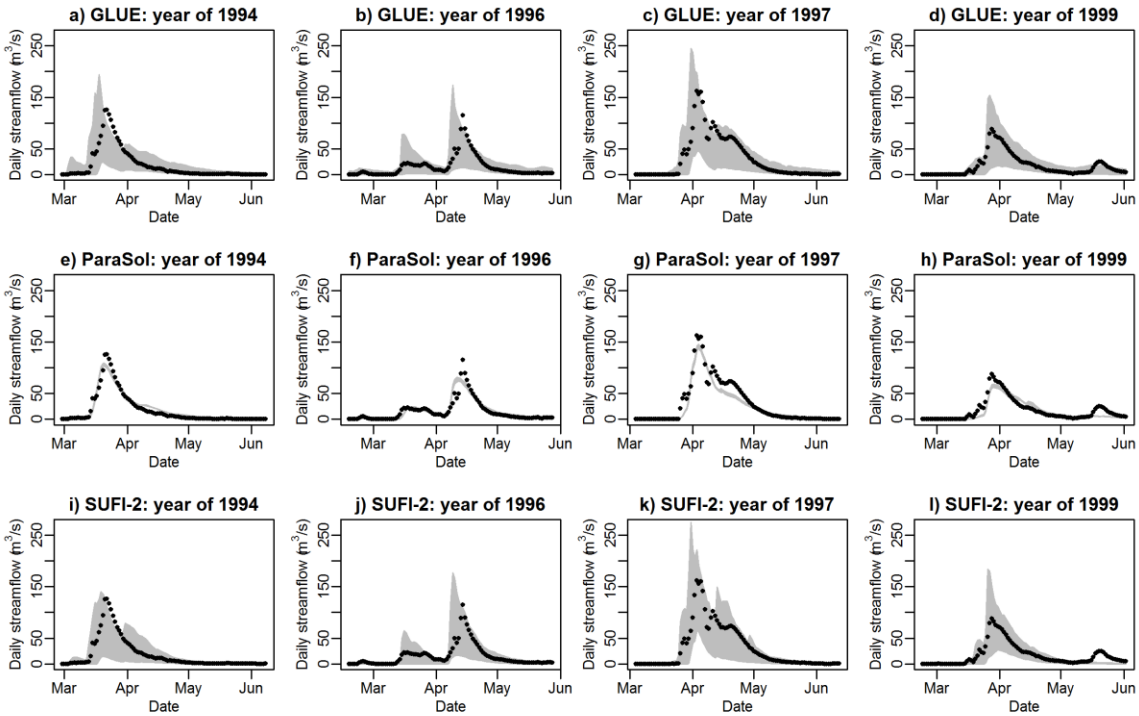

Figure 6–3 Plots of 95% prediction uncertainty (shaded area) derived by GLUE, ParaSol, and SUFI-2, methods for selected peaks; the dots correspond to the observed discharge and the solid line represents the best simulation.

The three methods were also assessed for their posterior parameter distributions in order to assess the uncertainty associated with the estimated parameter values. Figure 6–4 shows the dotty plots for the parameter values plotted against the NSE for each model run for each method. Theoretically dotty plot should not be method dependent and differences between the three methods may show incomplete sampling of the parameter space. From these plots, it is possible to assess the identifiability of the model parameters for each method. The shapes of the distributions in these figures indicate the degree of uncertainty of the estimates, which reflects parameter identifiability. Sharp and peaked distributions indicate the best performing parameters are concentrated in a small area of the feasible range (Wagener et al. 2003). Such posterior distributions are associated with well identifiable parameters. In contrast, flat distributions

indicate that parameter values associated with good model performance are distributed widely over the parameter space (Wagener et al. 2003,), which shows the problem of equifinality (Beven 2012). Methods that tend to flatten the response surface (with less identifiable parameters) has a problem of higher uncertainty in estimating parameter values.

As seen in Fig. 6–4, the posterior distributions obtained by the ParaSol method are somewhat sharper and narrower than those obtained by the GLUE method, indicating slightly better identifiable parameters and less uncertainty in parameter estimates. This is because of ParaSol's better capability of identifying optimum parameter space through combined global and local searching techniques as compared to the inefficient random sampling strategy employed by the GLUE technique. From the dotty plot (Fig. 6–4) it appears that parameter identifiability varies between methods. For instance, Curve Number (CN2) and Manning's *n* of the main channel (CH-N2) are highly identifiable in the case of ParaSol as compared to GLUE. Some parameters are similarly identifiable in all the methods. For instance, SURLAG is highly identifiable for all three methods.

The posterior parameter distributions of cumulative probability for the behavioral simulations are plotted (Fig. 6–5) to better assess parameter identifiability. As shown in Fig. 6–5, the parameter posterior cumulative probability distributions based on behavioral simulations also support the variation of parameter identifiability between methods. An abrupt change in the cumulative distribution plot shows higher identifiability of the parameter. Such "behavior" is often observed for the ParaSol method (Fig. 6–5). In contrast, a cumulative probability curve with a gentle slope shows the problem of equifinality. Such "behavior" is observed often for the GLUE method (Fig. 6–5).

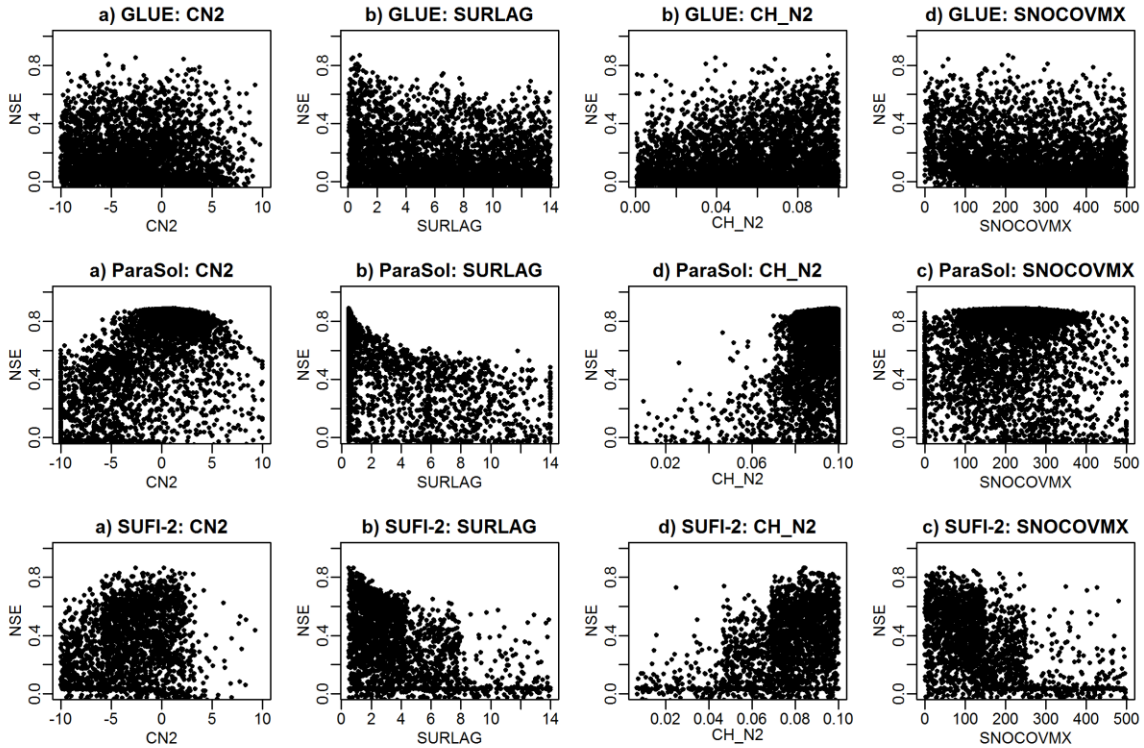

Figure 6–4 Dotty plot of NSE coefficient against SWAT model parameters conditioning with GLUE (a,b,c), ParaSol (d,e,f), and SUFI2 (g,h,i).

With respect to the computational time required to implement these methods, GLUE was found to require the longest computational time followed by ParaSol (Table 6–3). This is because of the inefficient random sampling strategy employed by the GLUE method, which needs a large number of simulations. On the other hand, SUFI-2 provides reasonable results with a relatively small number of simulations and computational time. The small number of simulations and recent integration of SUFI-2 with parallel processing make the method more suitable for large area watershed applications. Despite good results in terms of the 95% prediction uncertainty bands, application of the GLUE methods for large area watershed modeling is challenging because of the longer computational time requirements.

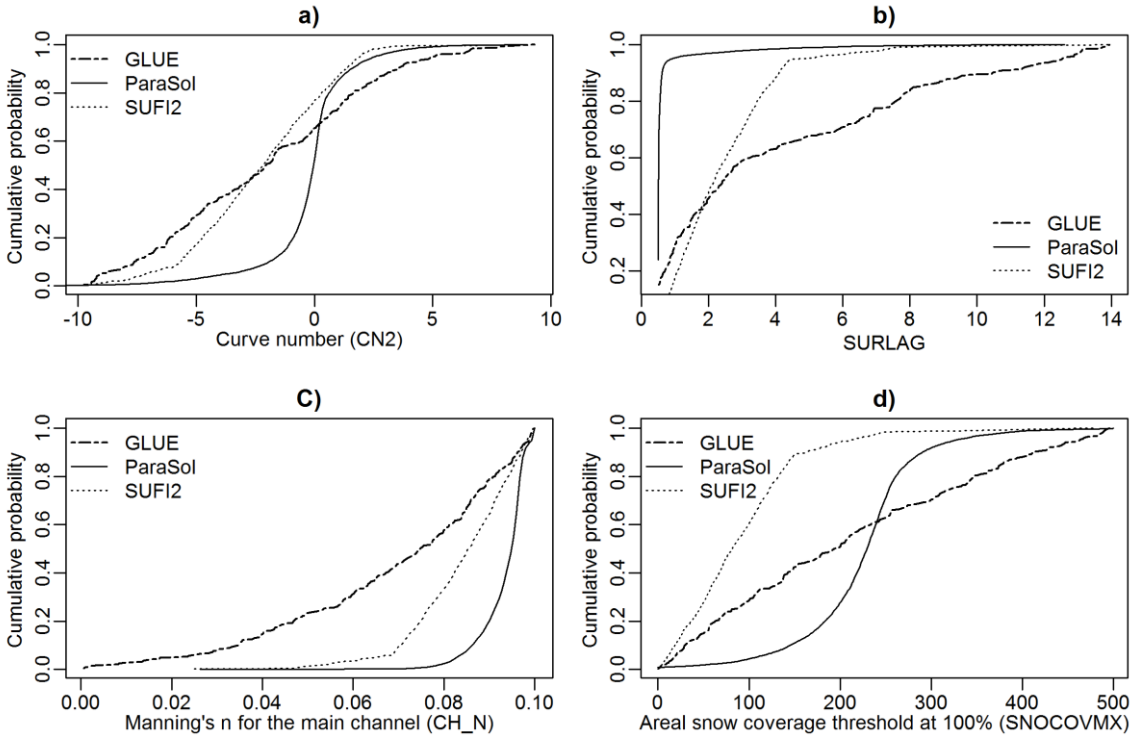

Figure 6–5 Posterior cumulative distribution function of "behavioral" parameters derived from all the methods.

6.5.2 Effect of precipitation and discharge data uncertainty

The uncertainties in the precipitation and discharge data sets were considered but not simultaneously. Figure 6–6 and Table 6–4 present the 95% prediction uncertainty when errors in precipitation data and discharge data are incorporated in comparison to the assumption of the error free precipitation and discharge datasets. To perform unbiased comparisons, the number of model simulations, the initial parameter range and distribution, and the threshold likelihood value of behavioral simulations were kept the same for all model results.

Referring to Table 6–4, about 12% and 11% of additional discharge data points are bracketed by the 95% uncertainty when uncertainty in precipitation and discharge datasets respectively are considered during the calibration period. Similarly, the observed data points bracketed by the 95% uncertainty band are improved by 10% and 8% when uncertainty in

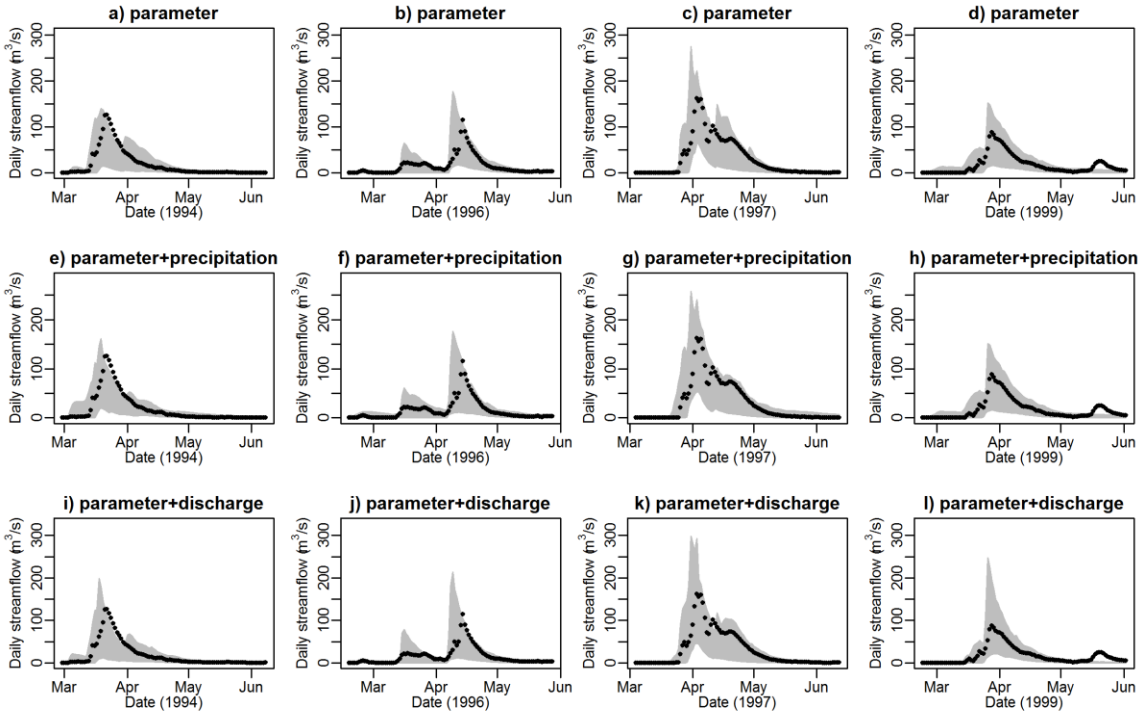

Figure 6–6 Plots of 95% prediction uncertainty (shaded area) derived by incorporating precipitation and discharge uncertainty during the years of 1994, 1996, 1997, and 1999: (a), (b), (c), and (d) refers to parameter uncertainty only; (e), (f), (g), and (h) represents parameter plus precipitation uncertainty; and (i), (j), (k), and (l) represents parameter plus observed discharge data uncertainty.

precipitation and discharge datasets respectively are considered during the validation period. An improved *P*-factor of 95% uncertainty has also been reported by previous works. For instance Ajami et al. (2007) reported an improved *P*-factor by about 10% for precipitation uncertainty incorporation. Similarly, Sellami et al. (2013) reported an improved *P*-factor by about 9% when discharge uncertainty is considered. Although consideration of uncertainty in precipitation and discharge datasets lead to an improved prediction uncertainty (*P*-factor), the uncertainty is still far from a *P*-factor of 100%. This means that parameter, precipitation, and discharge data uncertainty represents only part of the overall uncertainty and there are other sources of error. As a result, other sources of uncertainty in addition to parameter, precipitation, and discharge data

need to be incorporated. These include model structure, initial conditions, and other input datasets.

Table 6–4 Prediction uncertainty considering precipitation and observed discharge datasets uncertainty using SUFI-2.

Calibration/Validation Period	95% uncertainty bound criterions	Uncertainty considered		
		Parameter uncertainty	Parameter plus precipitation uncertainty	Parameter plus discharge uncertainty
Calibration (1992-1997)	*P*-factor (%)	46	58	57
	R-factor	0.42	0.51	0.46
Validation (1998-2001)	*P*-factor (%)	37	47	45
	R-factor	0.35	0.48	0.45

6.5.3 Effect of Model Structure Errors in SWAT-PDLD Prediction Uncertainty

As noted above, the influence of model structure uncertainty can be quantified using a framework called SCE-BMA. To implement the combined SCE-BMA prediction, four different model structures of SWAT (see Table 6–5) were setup. Each of the four models was separately calibrated for observed flow data using the Shuffled Complex Evolution algorithm. Table 6–5 below shows performance assessments of each model structure considered. Multiple statistical measures were used to evaluate the best simulations attained by each model.

Table 6–5 Model performance comparison of individual models against an ensemble using the Bayesian Model Averaging method.

	Best simulation performance					
	Calibration (1992-1997)			Validation (1998-2001)		
Model	NSE	PBIAS	RSR	NSE	PBIAS	RSR
CNS-VS	0.89	-20	0.33	0.78	25	0.47
CNS-MK	0.86	-60	0.47	0.70	19	0.14
CNET-VS	0.82	13	0.45	0.61	36	0.16
CNET-MK	0.89	-19	0.39	0.53	33	0.16
BMA	0.91	-32	0.35	0.71	22	0.12

Note: SW-VS denotes curve number retention parameter (*s*) is varying accordingly the soil profile water content together with the variable storage routing; SW-MK denotes *s* is varying accordingly the soil profile water content together with the Muskingum flow routing; ET-VS denotes *s* is varying accordingly the accumulated plant

evapotranspiration together with the variable storage flow routing; and ET-MK denotes *s* is varying accordingly the accumulated plant evapotranspiration together with the Muskingum routing.

The best simulation from the optimized individual model was used to perform ensemble prediction using the Bayesian Model Averaging. As presented in Table 6–5, the BMA prediction provides better performance during the calibration period as compared to individual model performances. As shown in Table 6–5 above, combining multiple competing sub-models using Bayesian Model Averaging improves model performance. In particular, an improved model performance is observed during the calibration period. But, the best individual model performs better than the Bayesian Model Averaging prediction during validation period. This indicates that Bayesian Model Averaging may not always guarantee an improved simulation in comparison to the best individual model. Similar findings have also been reported by Vrugt and Robinson (2007).

Figure 6–7 and Table 6–6 show the 95% uncertainty of model structure errors derived using the BMA-SCE methodology. As shown in Fig. 6–7, the 95% prediction uncertainty interval bracketed most of the observed data. More specifically, about 82% (calibration period) and 83% (validation period) of the observed data is bracketed by the 95% predictive uncertainty (Table 6–5).

Results of the current study revealed that the Bayesian Model Averaging methodology provides a good result in terms of best simulation as well as 95% prediction uncertainty band. In particular, the Bayesian Model Averaging achieves improved prediction uncertainty (see P-factor on Table 6–6) as it brackets most of the observed data compared to other methods investigated under this study. A wide range of *P*-factor values have been reported for model structure uncertainty by past works. The lowest is 76% by Ajami et al. (2007) and highest value of 96% by Zhang et al. (2009).

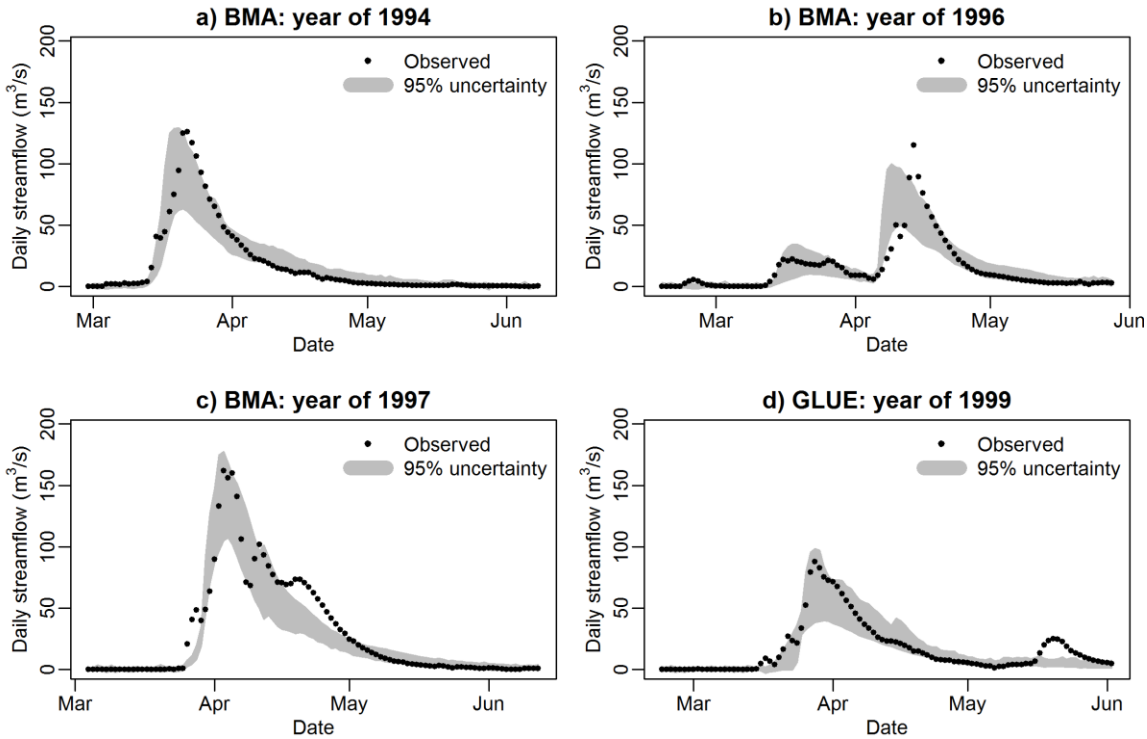

Figure 6–7 Plots of 95% prediction uncertainty (shaded area) derived by BMA_SCE method during the years of 1994, 1996, 1997, and 1999; the dots correspond to the observed discharge.

Table 6–6 95% uncertainty band derived using BMA-SCE methodology.

Period	NSE	PBIAS	RSR	*R*-factor	*P*-factor (%)
Calibration (1992-1997)	0.90	-15	0.32	0.28	82
Validation (1998-2001)	0.73	29	0.51	0.50	83

6.6 Summary and Conclusions

The conventional approach that aims to find a single best model fit is most frequently used when modeling hydrological responses of a watershed. If uncertainty is considered, the techniques generally focus on parameter uncertainty and are often implemented without explicit consideration of input, model structure, and other sources of uncertainty. In reality hydrological models are prone to multiple sources of uncertainty. Ignoring one or more sources of uncertainty may lead to an incorrect parameter identification and uncertainty estimation.

The purpose of the present study was to quantify the main sources of uncertainty for a SWAT-PDLD model of a Canadian prairie watershed. The quantification was performed by considering major sources of uncertainty including parameter, precipitation, discharge, and model structure errors using the following approach: 1) estimation of parameter uncertainty using three different methods; 2) incorporation of precipitation uncertainty into SWAT-PDLD model simulation; 3) introduction of uncertainty in observed discharge data that is used to calibrate the model; and 4) implementation of a methodology that combines SCE and BMA to quantify errors in model structure.

From parameter uncertainty analysis, the study shows that different methods of uncertainty analysis produce significant variation of uncertainty bands, posterior parameter distribution and identifiability, best model simulation, and computational efficiency. Therefore, identifying the best method of uncertainty analysis is a source of uncertainty in itself. Though comparisons among methods are site specific, the current study revealed that GLUE is better in terms of bracketing most of the observed discharge data followed by SUFI-2 and then ParaSol. SUFI-2 was found to be suitable in terms of reasonable computational time producing a reasonable result. However, the main limitation of all these three parameter uncertainty methods is that they do not account explicitly for other sources of uncertainty.

Further to parameter uncertainty, precipitation and discharge data uncertainty were also introduced to take into account errors in input data. The study demonstrated that consideration of uncertainty in precipitation and observed discharge data lead to wider model prediction uncertainty bands that are more successful at enclosing the observation discharge data points. This result suggests that parameter uncertainty alone cannot describe all modeling uncertainty sources and that input uncertainty needs to be considered for improved hydrological modeling.

Though accounting for precipitation and observed discharge data errors generated improved model uncertainty (*P*-factor) results, these results still suffer from model structure errors as only a single model is used while deriving the uncertainty.

Finally, to incorporate errors in model structure, a methodology that combines SCE and BMA was implemented. The study revealed that incorporating model structure uncertainty improves prediction uncertainty as reflected by a higher value *P*-factor. This multi-model prediction does not only improve prediction uncertainty but it does improve prediction capability as reflected by better NSE values compared to individual models.

6.7 Acknowledgments

The authors would like to thank the Province of Saskatchewan Go Green Fund for financial support for this work and the Natural Sciences and Engineering Research Council of Canada (NSERC) in terms of Discovery Grants to the second and third authors. The authors would also like to thank Dr. Monique Dube and Dr. Nicole Nadorozny for making available the datasets from different sources.

6.8 References

Abbaspour, K.C., Johnson, C.A., and van Genuchten, M.Th. 2004. Estimating Uncertain Flow and Transport Parameters Using a Sequential Uncertainty Fitting Procedure. Vadose Zone Journal, **3**(4): 1340–1352.

Ajami, N.K., Duan, Q., and Sorooshian, S. 2007. An integrated hydrologic Bayesian multimodel combination framework: Confronting input, parameter, and model structural uncertainty in hydrologic prediction. Water Resources Research, **43**(1): 1–19.

Almendinger, J.E., Murphy, M.S., Ulrich, J.S. 2012. Use of the Soil and Water Assessment Tool to scale sediment delivery from field to watershed in an agricultural landscape with topographic depressions. Journal of Environmental Quality, **43**(1): 9–17.

Arnold, J.G., Moriasi, D.N., Gassman, P.W., Abbaspour, K.C., White, M.J., Srinivasan, R., Santhi, C., Harmel, R.D., van Griensven, A., van Liew, M.W., Kannan, N., and Jha, M.K. 2012. SWAT: model use, calibration, and validation. Transactions of the ASABE, **55**(4): 1491–1508.

Arnold, J.G., Srinivasan, R., Muttiah, R.S., and Williams, J.R. 1998. Large-area hydrologic modeling and assessment: Part I Model development. J. American Water Resour. Assoc., **34**(1): 73–89.

Beven, K.J. 2012. Rainfall-runoff modelling: the primer. John Wiley & Sons.

Beven, K.J., and Binley, A.M. 1992. The future of distributed models: model calibration and uncertainty prediction. Hydrological Processes, **6**(3): 279–298.

Beven, K., and Binley, A. 2013. GLUE: 20 years on. Hydrological Processes, **28**(24): 5897–5918.

Burn, D.H., Buttle, J.M., Caissie, D., MacCulloch, G., Spence, C., and Stahl, K. 2008. The processes patterns and impacts of low flows across Canada. Canadian Water Resources Journal, **33**(2): 107–124.

Butts, M.B, Payne, J.T., Kristensen, M, and Madsen, H. 2004. An evaluation of the impact of model structure on hydrological modelling uncertainty for streamflow simulation. Journal of Hydrology, **298**(1–4): 242–266.

Chanasyk, D.S., Mapfumo, E., and Willms, W. 2003. Quantification and simulation of surface runoff from fescue grassland watersheds. Agricultural Water Management, **59**(2): 137–153.

Choi, W., Kim, S.J., Rasmussen, P.F., and Moore, A.R. 2009. Use of the North American Regional Reanalysis for Hydrological Modelling in Manitoba. Canadian Water Resources Journal, **34**(1): 17–36.

Cotter, A.S., Chaubey, I., Costello, T.A., Soerens, T.S., and Nelson, M.A. 2003. Water quality model output uncertainty as affected by spatial resolution of input data. Journal of the American Water Resources Association, **39**(4): 977–986.

Cunge, L.A. 1969. On the subject of a flood propagation method (Muskingum method). J. Hydraulic Research, **7**(2): 205–230.

Draper, D. 1995. Assessment and Propagation of Model Uncertainty: Series B (Methodological). Journal of the Royal Statistical Society, **57**(1): 45–97.

Duan, Q., Ajami, N. K., Gao, X., and Sorooshian, S. 2007. Multi-model ensemble hydrologic prediction using Bayesian model averaging. Advances in Water Resources, **30**(5): 1371–1386.

Duan, Q.Y., Gupta, V.K., and Sorooshian, S. 1993. Shuffled complex evolution approach for effective and efficient global minimization. Journal of optimization theory and applications, **76**(3): 501–521.

Environment Canada. 2009. Canadian climate normals 1971-2000(online). Available at: 573 http://www.climate.weatheroffice.ec.gc.ca/climate_normals/index_e.html. (Retrieved: 10 December 2011).

Environment Canada. 2007. Surface water and sediment data: Hydat Version 2005-2.04. Water Survey of Canada, Environment Canada.

Franz, K.J., Butcher, P., and Ajami, N.K. 2010. Addressing snow model uncertainty for hydrologic prediction. Advances in Water Resources, **33**(8): 820–832.

Gassman, P.W., Reyes, M.R., Green, C.H., and Arnold, J.G. 2007. The soil and water assessment tool: historical development, applications, and future research directions. Trans. ASABE, **50**(4): 1211–1250.

Georgakakos, K.P, Seo, Dong-Jun, Gupta, H., Schaake, J., and Butts, M.B. 2004. Towards the characterization of streamflow simulation uncertainty through multimodel ensembles. Journal of Hydrology, **298**(1–4): 222–241.

Godwin, R.B., and Martin, F.R. 1975. Calculation of Gross and Effective Drainage Areas for the Prairie Provinces. Canadian Hydrology Symposium, (p. 5): Winnipeg.

Green, W.H., and Ampt, G.A. 1911. Studies on soil physics-1: The flow of air and water through soils. J. Agric. Sci., **4**: 11–24.

van Griensven, A., and Meixner, T. 2006. Methods to quantify and identify the sources of uncertainty for river basin water quality models. Water Science and Technology, **53**(1): 51–59.

Gupta, H.V., Sorooshian, S., and Yapo, P.O. 1999. Status of automatic calibration for hydrologic models: comparison with multilevel expert calibration. Journal of Hydrologic Engineering, **4**: 135–143.

Haan, P.K., and Skaggs, R.W. 2003. Effect of parameter uncertainty on DRAINMOD Predictions: I. Hydrology and yield. Transactions of the ASABE, **46**(4): 1061–1067.

Hargreaves, G.L., Hargreaves, G.H., and Riley, J.P. 1985. Agricultural benefits for Senegal River Basin. J. Irrig. Drain. Eng., **111**(2): 113–124.

Hoeting, J.A., Madigan, D.M., Raftery, A.E., and Volinsky, C.T. 1999. Bayesian model averaging: A tutorial (with discussion). Stat. Sci., **14**: 382–401.

Hutchinson, M.F., McKenney, D.W., Lawrence, K., Pedlar, J.H., Hopkinson, R.F., Milewska, E., Papadopol, P. 2009. Development and Testing of Canada-Wide Interpolated Spatial Models of Daily Minimum–Maximum Temperature and Precipitation for 1961–2003. Journal of Applied Meteorology and Climatology, **48**: 725–741.

van der Kamp, G., Hayashi, M., and Gallen, D. 2003. Comparing the hydrology of grassed and cultivated catchments in the semi-arid Canadian prairies. Hydrological Processes, **17**: 559–575.

Kiesel, J., Fohrer, N., Schmalz, B., and White, M.J. 2010. Incorporating landscape depressions and tile drainages of a northern German lowland catchment into a semi-distributed model. Hydrological Processes, **24**: 1472–1486.

Krueger, T., Freer, J., Quinton, J.H., Macleod, C.J.A., Bilotta, G.S., Brazier, R.E., Butler, P., and Haygarth, P.M. 2010. Ensemble evaluation of hydrological model hypotheses. Water Resources Research, **46**: 7, W07516.

Leibowitz, S.G., and Vining, K.C. 2003. Temporal connectivity in a prairie pothole complex. Wetlands, **23**(1): 13–25.

Li, L., and Xu, C. 2014. The comparison of sensitivity analysis of hydrological uncertainty estimates by GLUE and Bayesian method under the impact of precipitation errors. Stochastic Environmental Research and Risk Assessment, **28**(3): 491–504.

Hamilton, S. 2008. Sources of Uncertainty in Canadian Low Flow Hydrometric Data. Canadian Water Resources Journal, **33**(2): 125–136.

McKay, M.D., Conover, W.J., and Beckman, R.J. 1979. A Comparison of Three Methods for Selecting Values of Input Variables in the Analysis of Output from a Computer Code. Technometrics, **21**: 239–245.

McMillan, H., Jackson, B., Clark, M., Kavetski, D., and Woods, R. 2011. Rainfall uncertainty in hydrological modelling: An evaluation of multiplicative error models. Journal of Hydrology, **400**: 83–94.

McMillan, H., Krueger, T., and Freer, J. 2012. Benchmarking observational uncertainties for hydrology: rainfall, river discharge and water quality. Hydrological Processes, **26**: 4078–4111.

Mekonnen, B.A, Mazurek, K.A., and Putz, G. 2016a. Incorporating landscape depression heterogeneity into the Soil and Water Assessment Tool (SWAT) using a probability distribution. Hydrological Processes. DOI: 10.1002/hyp.10800

Mekonnen, B.A, Mazurek, K.A., and Putz, G. 2016b. Sediment Export Modeling in Cold Climate Prairie Watersheds. Journal of Hydrologic Engineering. DOI: 10.1061/(ASCE)HE.1943-5584.0001336.

Mekonnen, B.A, Nazemi, A., Mazurek, K.A., Elshorbagy, A., and Putz, G. 2015. Hybrid modelling approach to prairie hydrology: fusing data-driven and process-based hydrological models. Hydrological Sciences Journal, **60**(9): 1473–1489.

Mekonnen, M.A., Wheater, H.S., Iresona, A.M., Spence, C., Davison, B., and Pietroniro, A. 2014. Towards an improved land surface scheme for prairie landscapes. Journal of Hydrology, **511**: 105–116.

Monteith, J.L. 1965. Evaporation and the environment: In The State and Movement of Water in Living Organisms, Proc. 19th Symp. Swansea, UK, Society of Experimental Biology, Cambridge University Press.

Moriasi, D.N., Arnold, J.G., van Liew, M.W., Bingner, R.L., Harmel, R.D., and Veith, T.L. 2007. Model evaluation guidelines for systematic quantification of accuracy in watershed simulations. Trans. ASABE, **50**(3): 885–900.

Nash, J.E., and Sutcliffe, J.V. 1970. River flow forecasting through conceptual models. Part I: A discussion of principles. Journal of Hydrology, **10**: 282–290.

Neitsch, S.L., Arnold, J.G., Kiniry, J.R., and Williams, J.R. 2011. Soil and Water Assessment Tool theoretical documentation: Version 2005, Grassland, Soil and Water Research Laboratory, Blackland Research Center, Temple, TX.

Pomeroy, J.W., Gray, D.M., Brown, T., Hedstrom, N.M., Quinton, W., Granger, R.J., and Carey, S. 2007. The Cold Regions Hydrological Model, a platform for basing process representation and model structure on physical evidence. Hydrological Processes, **21:**, 2650–2667.

Prairie Farm Rehabilitation Administration (PFRA), 1983. The Determination of Gross and Effective Drainage Areas in the Prairie Provinces, Hydrology Report #104 Regina: Agriculture Canada, PFRA Engineering Branch, 22pp.

Priestley, C.H.B., and Taylor, R.J. 1972. On the assessment of surface heat flux and evaporation using large-scale parameters. Mon. Weather Rev., **100**: 81–92.

Rahbeh, M., Chanasyk, D., and Miller, J. 2011. Two-Way Calibration-Validation of SWAT Model for a Small Prairie Watershed with Short Observed Record. Canadian Water Resources Journal, **36**(3): 247–270.

Raftery, A.E., Gneiting, T., Balabdaoui, E., and Polakowski, M. 2005. Using Bayesian Model Averaging to Calibrate Forecast Ensembles. Mon. Wea. Rev., **133**: 1155–1174.

Refsgaard, J.C., van der Sluijs, J.P., Brown, J., and der Keur, P. 2006. A framework for dealing with uncertainty due to model structure error. Advances in Water Resources, **29**(11): 1586–1597.

Refsgaard, J.C., van der Sluijs, J.P., Højberg, A.L., and Vanrolleghem, P.A. 2007. Uncertainty in the environmental modelling process: A framework and guidance. Environmental Modelling & Software, **22**: 1543–1556.

Ritchie, J.T. 1972. A model for predicting evaporation from a row crop with incomplete cover. Water Resources Research, **8**: 1204–1213.

SCS (Soil Conservation Service), 1972. National Engineering Handbook, Section 4: Hydrology, SCS, USA.

See, L., and Abrahart, R.J. 2001. Multi-model data fusion for hydrological forecasting. Comput. Geosci., **27**(8): 987–994.

Sellami, H., Jeunesse, I., L., Benabdallah, S., and Vanclooster, M. 2013. Parameter and rating curve uncertainty propagation analysis of the SWAT model for two small Mediterranean catchments. Hydrological Sciences Journal, **58**(8): 1635–1657.

Setegn, S.G., Srinivasan, R., Melesse, A.M., and Dargahi, B. 2010. SWAT model application and prediction uncertainty analysis in the Lake Tana Basin, Ethiopia. Hydrological Processes, **24**(3): 357–367.

Shamseldin, A.Y., O'Connor, K.M., and Liang, G.C. 1997. Methods for combining the outputs of different rainfall–runoff models. Journal of Hydrology, **197**: 203–229.

Shaw, D.A., van der Kamp, G., Conly, F.M., Pietroniro, A., and Martz, L. 2011. The Fill-Spill Hydrology of Prairie Wetland Complexes during Drought and Deluge. Hydrological Processes, 26, 3147–3156.

Shen, Z.Y., Chen, L., and Chen, T. 2012. Analysis of parameter uncertainty in hydrological and sediment modeling using GLUE method: a case study of SWAT model applied to Three Gorges Reservoir Region, China. Hydrol. Earth Syst. Sci., **16**: 121–132.

Shirmohammadi, A., Chaubey, I., Harmel, R.D., Bosch, D.D., Muñoz-Carpena, R., Dharmasri, C., Sexton, A., Arabi, M., Wolfe, M.L., Frankenberger, J., Graff, C., and Sohrabi, T.M. 2006. Uncertainty in TMDL models. Transactions of the ASABE, **49**(4): 1033–1049.

Shook, R.S., and Pomeroy, J. 2011. Memory effects of depressional storage in Northern Prairie hydrology. Hydrological Processes, **25**(25): 3890–3898.

Shrestha, R.R., Dibike, Y.B., and Prowse, T.D. 2012. Modeling Climate Change Impacts on Hydrology and Nutrient Loading in the Upper Assiniboine Catchment. J. American Water Resour. Assoc., **48**(1): 74–89.

Soil Landscapes of Canada Working Group, 2007. Soil Landscapes of Canada v3.1.1, Agriculture and Agri-Food Canada, Digital Map and Database at 1:1 Million Scale, http://sis.agr.gc.ca/cansis/nsdb/slc/v3.1.1/intro.html.

Strauch, M., Bernhofer, C., Koide, S., Volk, M., Lorz, C., and Makeschin, F. 2012. Using precipitation data ensemble for uncertainty analysis in SWAT streamflow simulation. Journal of Hydrology, **414–415**: 413–424.

Su, M., Stolte, W.J., and van der Kamp, G. 2000. Modelling Canadian prairie wetland hydrology using a semi-distributed streamflow model. Hydrological Processes, **14**(14): 2405–2422.

Vrugt, J.A., Diks, C.G.H., and Clark, M.P. 2008. Ensemble Bayesian model averaging using Markov Chain Monte Carlo sampling. Environmental Fluid Mechanics, **8**(5–6): 579–595.

Vrugt, J.A., and Robinson, B.A. 2007. Treatment of uncertainty using ensemble methods: Comparison of sequential data assimilation and Bayesian model averaging. Water Resources Research, **43**(1): W01411.

Wagener, T., McIntyre, N., Lees, M.J., Wheater, H.S., and Gupta, H.V. 2003. Towards reduced uncertainty in conceptual rainfall-runoff modelling: Dynamic identifiability analysis. Hydrological Processes, **17**(2): 455–476.

Wang, X., Yang, W., and Melesse, A.M. 2008. Using hydrologic equivalent wetland concept within SWAT to estimate streamflow in watersheds with numerous wetlands. Trans. ASAE, **51**(1): 55–72.

Wen, L., Lin, C.A., Wu, Z., Lu, G., Pomeroy, J., and Zhu, Y. 2011. Reconstructing sixty year (1950-2009) daily soil moisture over the Canadian Prairies using the Variable Infiltration Capacity model, Canadian Water Resources Journal, **36**(1): 84–102.

Williams, J.R. 1969. Flood routing with variable travel time or variable storage coefficients. Trans. ASAE, **12**(1): 100–103.

Woo, M.K., and Rowsell, R.D. 1993. Hydrology of a prairie slough. Journal of Hydrology, **146**: 175–207.

Yang, J, Reichert, P., Abbaspour, K.C., Xia, J., and Yang, H. 2008. Comparing uncertainty analysis techniques for a SWAT application to the Chaohe Basin in China. Journal of Hydrology, **358**(1–2): 1–23.

Yang, W., Wang, X., Liu, Y., Gabor, S., Boychuk, L., and Badiou, P. 2010. Simulated environmental effects of wetland restoration scenarios in a typical Canadian prairie watershed. Wetlands Ecology and Management, **18**(3): 269–279.

Zhang, X., Srinivasan, R., and Bosch, D. 2009. Calibration and uncertainty analysis of the SWAT model using Genetic Algorithms and Bayesian Model Averaging. Journal of Hydrology, **374**(3–4): 307–317.

CHAPTER 7 SUMMARY, CONCLUSIONS AND FUTURE DIRECTIONS

7.1 Summary of Research Findings

The main goal of this dissertation was to develop an improved methodology to simulate streamflow and pollutant export from Canadian prairie watersheds, which are characterized by numerous surface depressions on the landscape and a cold-climate. As an application of the research, an investigation was made using the modeling technique to assess alternative agricultural management options that can potentially mitigate the export of sediment and nutrients from a prairie watershed to downstream water resources.

Chapter 2 reviewed the available models that might be suitable for the study watersheds. Following a review of several models, the Soil and Water Assessment Tool (SWAT), a popular streamflow and pollutant export model for agricultural watersheds, was selected as a base model to be modified to address the gap in modeling capability. The SWAT model has been used extensively throughout the world, as well as for a number of studies within Canada.

The contributions of the research are documented in four papers. The first paper, which is given in Chapter 3, was developed to improve streamflow modeling capability in depression-dominated landscapes, which as noted is a typical physiographic characteristic of Canadian prairie watersheds. The storage heterogeneity of the numerous landscape depressions that exist within a Canadian prairie watershed was represented using a probability distribution. A program module called Probability Distributed Landscape Depressions (PDLD) was developed and integrated into SWAT. The modified model, called SWAT-PDLD, was then tested for two Canadian prairie watersheds (the Assiniboine and Moose Jaw River watersheds). The

performance of the newly developed model was evaluated using multiple statistical measures and graphical plots. In addition, a comparison study was performed between the newly developed methodology and the existing lumped storage approach used by the original SWAT model. The study demonstrated that the SWAT-PDLD model has better performance for streamflow simulation in depression-dominated watersheds compared to the lumped approach employed by the original SWAT model for both watershed case studies.

The second paper, which is covered in Chapter 4, builds on the approach taken in the first paper to improve sediment export modeling in Canadian prairie watersheds. The study in Chapter 4 demonstrated the need to consider seasonality of sediment export behavior when modeling sediment export in cold-climate watersheds. To explore the effects of the seasons on sediment export, a flow-sediment load relationship investigation of seasonally segmented observed data sets was performed. The investigation confirmed the existence of a variation in sediment generation between seasons. The conventional MUSLE module, which uses a constant annual soil erodibility factor that is used within the original SWAT model was then modified in order to take into account seasonal changes in soil erodibility. The modified model, SWAT-PDLD with seasonally varying soil erodibility, was then tested for two cold-climate prairie watersheds (Assiniboine and Moose Jaw River watersheds). The performance of SWAT-PDLD with seasonally varying soil erodibility factors was evaluated using both multiple statistical measures and graphical plots. Results showed that a satisfactory performance was attained using the modified methodology over both watersheds. In comparing the modified model to the original SWAT model, an improved performance was observed over both watersheds when a seasonally varying soil erodibility factor is incorporated as compared to the annual value of soil erodibility that is conventionally used.

The third paper, presented in Chapter 5, focuses on the capability of the modified model to improve simulations of nutrient export in Canadian prairie watersheds and application of the improved model for assessment of the effectiveness of agricultural management practices for mitigation of nutrient export. The study in Chapter 5 is an extension of the previous chapters. It describes an application and evaluation of the modified model SWAT-PDLD model together with seasonally varying soil erodibility for nutrient export simulations from a Canadian prairie watershed (the Assiniboine River watershed). Model performance was evaluated using multiple statistical measures and graphical plots. The study demonstrated that the model simulated both phosphorous and nitrogen export satisfactorily. Furthermore, the developed model was used to assess the impacts of different agricultural management practices on sediment and nutrient export. Three different management practices, including filter strips, conservation tillage, and red clover as a cover crop, were considered. The study revealed that both the filter strips and cover crop had a significant effect in reducing sediment, phosphorous and nitrogen export in the study watershed. Sediment and nitrogen export are also reduced for conservation tillage but the results are different for phosphorous export. Under conservation tillage the total phosphorous export increased. This is consistent with previous field studies (e.g., Tiessen et al. 2010; Li et al. 2011; Flaten, 2013; Liu et al. 2014). As a result, prairie agricultural advisory agencies should recommend other measures to reduce phosphorous export because conservation tillage practices are very popular within the region to control soil erosion.

The fourth paper, which is covered in Chapter 6, addresses the issues of estimating different categories of modeling uncertainties in application of this model. The study investigated the major sources of modeling uncertainty that include parameter, precipitation, observed flow data, and model structure uncertainty of the developed SWAT-PDLD model of

the Moose Jaw watershed. In estimating parameter uncertainty, three different techniques, GLUE, ParaSol, and SUFI-2, were implemented and compared. Precipitation uncertainty was incorporated using a multiplicative error propagation. Observed flow data uncertainty was incorporated by considering the upper and lower limits of the observed data. In addition, model structure uncertainty was estimated by implementing a methodology that combines the Shuffled Complex Evolution and Bayesian Model Averaging (SCE-BMA).

Overall, the SWAT-PDLD model together with seasonally varying soil erodibility simulates flow, sediment, and nutrient export satisfactorily for the land use systems, climate, hydrologic and physiographic conditions prevalent on the Canadian prairie watersheds.

7.2 Research Significance

The research developed an improved modeling framework for simulating flow and pollutant export, and assessing impacts of agricultural management practices under cold-climate the conditions in Canadian prairie watersheds. The main contributions of the study are conceptualization of site specific processes and modification of the existing modeling framework to suit the study area conditions. The first such contribution of this thesis is incorporation of the storage heterogeneity of the numerous landscape depressions that exist within a Canadian prairie watershed into SWAT model. The proposed modeling framework uses a probability distribution to represent the storage heterogeneity of the numerous depressions. Without applying this modeling framework, most existing conventional models including the original SWAT model that use a lumped storage approach that are not able to properly represent the numerous landscape depressions.

The other major contribution of this dissertation is incorporation of seasonality of sediment erodibility in cold-climate watersheds into SWAT-PDLD. To take into account this

behavior, a new modeling framework that considers seasonality of soil erodibility was developed. Incorporation of such behaviors into the modeling framework is important to more accurately simulate sediment export as well as other pollutants export dynamics in cold-climate watersheds. The developed method can be extended to other watersheds that exhibit a cold-climate hydrology and also to other conventional models that use an annual value of soil erodibility. The study tested the developed methodology for sediment export simulation capability over two case study watersheds. Furthermore, the developed modeling framework's capability to simulate nutrients export in cold-climate watersheds was also tested.

Further the research assessed watershed responses to various current agricultural management practices under cold-climate prairie watershed conditions. In addition, the study estimated the different sources of uncertainty of the developed model of the study watershed.

7.3 Future Directions for Application of Model

The following suggestions can be considered for future applications of the calibrated and validated model:

- Transferring the calibrated and validated parameters to other watersheds with similar characteristics on the Canadian prairies.
- Use the model to make a comprehensive assessment of effects of several other management practices on pollutant export.
- Use the model to assess impacts of future climate change on flow and pollutant export in the Canadian prairie watersheds.

7.4 Future Directions for Model Improvement

The following future research directions are recommended in order to further improve the developed modeling framework capability of streamflow and pollutant export in prairie watersheds.

- As better data sets become available (e.g., LiDAR data and additional data points of observed water quality data), the model uncertainty can be improved.
- Extend the seasonally varying soil erodibility module to include climatic variables such as temperature rather than using fixed dates in identifying each season. Season definitions based upon environmental conditions could be important as the beginning and ending date of each season varies between years.
- Improve the nutrient processes representation in the Pond module as the current version of the SWAT model does not consider nutrient transformation in ponds. Several studies have shown that transformation of nutrients occurs within potholes on the Canadian prairies, hence future research that focuses on incorporating nutrient transformation in the Pond module has potential to improve the model prediction capability.
- Extend the empirical filter strip module, in which only filter strip width is considered as a factor for trapping efficiency, to include the actual processes that occur under cold-climate prairie watershed conditions. This could be improved in future work either by replacing it with a processed based module or modifying the empirical equation for the study watershed conditions.

7.5 References

Flaten, D. 2013. Conservation tillage: Cure-all or problem for water quality? Saskatchewan Soil Conservation Association, 9 January 2013, Saskatoon, SK.

Li, S., Elliott, J.A., Tiessen, K.H.D, Yarotski, J., Lobb, D.A, Flaten, D.N. 2011. The effects of multiple beneficial management practices on hydrology and nutrient losses in a small watershed in the Canadian Prairies. J. Environ. Qual., **40(5)** : 1627–1642

Liu, K., Elliott, J.A., Lobb, D.A., Flaten, D.N., Yarotski, J. 2014. Nutrient and sediment losses in snowmelt runoff from perennial forage and annual cropland in the Canadian Prairies. Journal of Environmental Quality, **43(5)**: 1644–1655.

APPENDIX A–John Wiley and Sons License Terms and Conditions

Feb 22, 2016

This Agreement between Balew Mekonnen ("You") and John Wiley and Sons ("John Wiley and Sons") consists of your license details and the terms and conditions provided by John Wiley and Sons and Copyright Clearance Center.

License Number	3814120135449
License date	Feb 22, 2016
Licensed Content Publisher	John Wiley and Sons
Licensed Content Publication	Hydrological Processes
Licensed Content Title	Incorporating landscape depression heterogeneity into the Soil and Water Assessment Tool (SWAT) using a probability distribution
Licensed Content Author	Balew A. Mekonnen,Kerry A. Mazurek,Gordon Putz
Licensed Content Date	Jan 27, 2016
Pages	1
Type of use	Dissertation/Thesis
Requestor type	Author of this Wiley article
Format	Print and electronic
Portion	Full article
Will you be translating?	No
Title of your thesis / dissertation	Modeling and Management of Flow and Pollutant Loading in Cold-Climate Canadian Prairie Watersheds
Expected completion date	Apr 2016
Expected size (number of pages)	280
Requestor Location	Balew Mekonnen 105 cumberland ave s apt. 305204 saskatoon, SK S7N 1L7 Canada Attn: Balew Mekonnen
Billing Type	Invoice
Billing Address	Balew Mekonnen 105 cumberland ave s apt. 305204

saskatoon, SK S7N 1L7
Canada
Attn: Balew Mekonnen

Total 0.00 USD

Terms and Conditions

TERMS AND CONDITIONS

This copyrighted material is owned by or exclusively licensed to John Wiley & Sons, Inc. or one of its group companies (each a"Wiley Company") or handled on behalf of a society with which a Wiley Company has exclusive publishing rights in relation to a particular work (collectively "WILEY"). By clicking "accept" in connection with completing this licensing transaction, you agree that the following terms and conditions apply to this transaction (along with the billing and payment terms and conditions established by the Copyright Clearance Center Inc., ("CCC's Billing and Payment terms and conditions"), at the time that you opened your RightsLink account (these are available at any time at http://myaccount.copyright.com).

Terms and Conditions

- The materials you have requested permission to reproduce or reuse (the "Wiley Materials") are protected by copyright.

- You are hereby granted a personal, non-exclusive, non-sub licensable (on a stand-alone basis), non-transferable, worldwide, limited license to reproduce the Wiley Materials for the purpose specified in the licensing process. This license, **and any CONTENT (PDF or image file) purchased as part of your order,** is for a one-time use only and limited to any maximum distribution number specified in the license. The first instance of republication or reuse granted by this license must be completed within two years of the date of the grant of this license (although copies prepared before the end date may be distributed thereafter). The Wiley Materials shall not be used in any other manner or for any other purpose, beyond what is granted in the license. Permission is granted subject to an appropriate acknowledgement given to the author, title of the material/book/journal and the publisher. You shall also duplicate the copyright notice that appears in the Wiley publication in your use of the Wiley Material. Permission is also granted on the understanding that nowhere in the text is a previously published source acknowledged for all or part of this Wiley Material. Any third party content is expressly excluded from this permission.

- With respect to the Wiley Materials, all rights are reserved. Except as expressly granted by the terms of the license, no part of the Wiley Materials may be copied, modified, adapted (except for minor reformatting required by the new Publication), translated, reproduced, transferred or distributed, in any form or by any means, and no derivative works may be made based on the Wiley Materials without the prior permission of the respective copyright owner.**For STM Signatory Publishers clearing permission under the terms of the STM Permissions Guidelines only, the terms of the license are extended to include subsequent editions and for editions in other languages, provided such editions are for the work as a whole in situ and does not involve the separate exploitation of the permitted figures or**

extracts, You may not alter, remove or suppress in any manner any copyright, trademark or other notices displayed by the Wiley Materials. You may not license, rent, sell, loan, lease, pledge, offer as security, transfer or assign the Wiley Materials on a stand-alone basis, or any of the rights granted to you hereunder to any other person.

- The Wiley Materials and all of the intellectual property rights therein shall at all times remain the exclusive property of John Wiley & Sons Inc, the Wiley Companies, or their respective licensors, and your interest therein is only that of having possession of and the right to reproduce the Wiley Materials pursuant to Section 2 herein during the continuance of this Agreement. You agree that you own no right, title or interest in or to the Wiley Materials or any of the intellectual property rights therein. You shall have no rights hereunder other than the license as provided for above in Section 2. No right, license or interest to any trademark, trade name, service mark or other branding ("Marks") of WILEY or its licensors is granted hereunder, and you agree that you shall not assert any such right, license or interest with respect thereto

- NEITHER WILEY NOR ITS LICENSORS MAKES ANY WARRANTY OR REPRESENTATION OF ANY KIND TO YOU OR ANY THIRD PARTY, EXPRESS, IMPLIED OR STATUTORY, WITH RESPECT TO THE MATERIALS OR THE ACCURACY OF ANY INFORMATION CONTAINED IN THE MATERIALS, INCLUDING, WITHOUT LIMITATION, ANY IMPLIED WARRANTY OF MERCHANTABILITY, ACCURACY, SATISFACTORY QUALITY, FITNESS FOR A PARTICULAR PURPOSE, USABILITY, INTEGRATION OR NON-INFRINGEMENT AND ALL SUCH WARRANTIES ARE HEREBY EXCLUDED BY WILEY AND ITS LICENSORS AND WAIVED BY YOU.

- WILEY shall have the right to terminate this Agreement immediately upon breach of this Agreement by you.

- You shall indemnify, defend and hold harmless WILEY, its Licensors and their respective directors, officers, agents and employees, from and against any actual or threatened claims, demands, causes of action or proceedings arising from any breach of this Agreement by you.

- IN NO EVENT SHALL WILEY OR ITS LICENSORS BE LIABLE TO YOU OR ANY OTHER PARTY OR ANY OTHER PERSON OR ENTITY FOR ANY SPECIAL, CONSEQUENTIAL, INCIDENTAL, INDIRECT, EXEMPLARY OR PUNITIVE DAMAGES, HOWEVER CAUSED, ARISING OUT OF OR IN CONNECTION WITH THE DOWNLOADING, PROVISIONING, VIEWING OR USE OF THE MATERIALS REGARDLESS OF THE FORM OF ACTION, WHETHER FOR BREACH OF CONTRACT, BREACH OF WARRANTY, TORT, NEGLIGENCE, INFRINGEMENT OR OTHERWISE (INCLUDING, WITHOUT LIMITATION, DAMAGES BASED ON LOSS OF PROFITS, DATA, FILES, USE, BUSINESS OPPORTUNITY OR CLAIMS OF THIRD PARTIES), AND WHETHER OR NOT THE PARTY HAS BEEN ADVISED OF THE POSSIBILITY

OF SUCH DAMAGES. THIS LIMITATION SHALL APPLY NOTWITHSTANDING ANY FAILURE OF ESSENTIAL PURPOSE OF ANY LIMITED REMEDY PROVIDED HEREIN.

- Should any provision of this Agreement be held by a court of competent jurisdiction to be illegal, invalid, or unenforceable, that provision shall be deemed amended to achieve as nearly as possible the same economic effect as the original provision, and the legality, validity and enforceability of the remaining provisions of this Agreement shall not be affected or impaired thereby.

- The failure of either party to enforce any term or condition of this Agreement shall not constitute a waiver of either party's right to enforce each and every term and condition of this Agreement. No breach under this agreement shall be deemed waived or excused by either party unless such waiver or consent is in writing signed by the party granting such waiver or consent. The waiver by or consent of a party to a breach of any provision of this Agreement shall not operate or be construed as a waiver of or consent to any other or subsequent breach by such other party.

- This Agreement may not be assigned (including by operation of law or otherwise) by you without WILEY's prior written consent.

- Any fee required for this permission shall be non-refundable after thirty (30) days from receipt by the CCC.

- These terms and conditions together with CCC's Billing and Payment terms and conditions (which are incorporated herein) form the entire agreement between you and WILEY concerning this licensing transaction and (in the absence of fraud) supersedes all prior agreements and representations of the parties, oral or written. This Agreement may not be amended except in writing signed by both parties. This Agreement shall be binding upon and inure to the benefit of the parties' successors, legal representatives, and authorized assigns.

- In the event of any conflict between your obligations established by these terms and conditions and those established by CCC's Billing and Payment terms and conditions, these terms and conditions shall prevail.

- WILEY expressly reserves all rights not specifically granted in the combination of (i) the license details provided by you and accepted in the course of this licensing transaction, (ii) these terms and conditions and (iii) CCC's Billing and Payment terms and conditions.

- This Agreement will be void if the Type of Use, Format, Circulation, or Requestor Type was misrepresented during the licensing process.

- This Agreement shall be governed by and construed in accordance with the laws of the State of New York, USA, without regards to such state's conflict of law rules. Any legal action, suit or proceeding arising out of or relating to these Terms and

APPENDIX B–American Society of Civil Engineers License Terms and Conditions

Copyright Clearance Center RightsLink®

Home | Account Info | Help

ASCE AMERICAN SOCIETY OF CIVIL ENGINEERS

Title: Sediment Export Modeling in Cold-Climate Prairie Watersheds

Author: Balew Admas Mekonnen, Kerry Anne Mazurek, Gordon Putz

Publication: Journal of Hydrologic Engineering

Publisher: American Society of Civil Engineers

Date: 01/19/2016

Logged in as:
Balew Mekonnen
LOGOUT

Permissions Request

As an ASCE author, you are permitted to reuse you own content for another ASCE or non-ASCE publication.

Please add the full credit line "With permission from ASCE" to your source citation. Please print this page for your records.

Type of use: Dissertation/Thesis

Portion: full article

Format: print and electronic

Author of this ASCE work or ASCE will publish the new work: yes

BACK | CLOSE WINDOW

APPENDIX C–Source code of a Probability Distributed Landscape Depressions Module

```
    subroutine PDLDpond(k)

!!   ~ ~ ~ PURPOSE ~ ~ ~
!!   this subroutine routes water and sediment through ponds
!!   and computes evaporation and seepage from the ponds

!!   ~ ~ ~ INCOMING VARIABLES ~ ~ ~
!!   name        |units        |definition
!!   ~ ~ ~ ~ ~ ~ ~ ~ ~ ~ ~ ~ ~ ~ ~ ~ ~ ~ ~ ~ ~ ~ ~ ~ ~ ~ ~ ~ ~ ~ ~ ~ ~ ~ ~ ~
!!   bp1(:)      |none         |1st shape parameter for pond surface area
!!                             |equation
!!   bp2(:)      |none         |2nd shape parameter for the pond surface area
!!                             |equation
!!   chlap(:)    |none         |chlorophyll-a production coefficient for pond
!!   hru_sub(:)  |none         |subbasin in which HRU/reach is located
!!   iflod1(:)   |none         |beginning month of non-flood season
!!   iflod2(:)   |none         |ending month of non-flood season
!!   ipnd1(:)    |none         |beginning month of 2nd "season" of nutrient
!!                             |settling
!!   ipnd2(:)    |none         |ending month of 2nd "season" of nutrient
!!                             |settling
!!   i_mo        |none         |current month of simulation
!!   ndtarg(:)   |none         |number of days required to reach target
!!                             |storage from current pond storage
!!   nsetlp(1,:) |m/day        |nitrogen settling rate for 1st season
!!   nsetlp(2,:) |m/day        |nitrogen settling rate for 2nd season
!!   pet_day     |mm H2O       |potential evapotranspiration on day
!!   pnd_evol(:) |m^3 H2O      |volume of water required to fill pond
!!                             |to the emergency spillway
!!   pnd_fr(:)   |none         |fraction of HRU/subbasin area that drains
!!                             |into ponds
!!   pnd_k(:)    |mm/hr        |hydraulic conductivity through bottom of
!!                             |ponds
!!   pnd_no3(:)  |kg N         |amount of nitrate originating from surface
!!                             |runoff in pond at beginning of day
!!   pnd_no3g(:) |kg N         |amount of nitrate originating from
!!                             |groundwater in pond at beginning of day
!!   pnd_no3s(:) |kg N         |amount of nitrate originating from lateral
!!                             |flow in pond at beginning of day
!!   pnd_nsed(:) |kg/L         |normal ratio of sediment to water in pond
!!   pnd_orgn(:) |kg N         |amount of organic N originating from
!!                             |surface runoff in pond at beginning of day
```

```
!!   pnd_orgp(:) |kg P          |amount of organic P originating from
!!                             |surface runoff in pond at beginning of day
!!   pnd_psed(:) |kg P          |amount of mineral P attached to sediment
!!                             |originating from surface runoff in pond at
!!                             |beginning of day
!!   pnd_pvol(:) |m^3 H2O       |volume of water required to fill pond
!!                             |to the principal spillway
!!   pnd_sed(:)  |kg/L          |ratio of sediment to water in pond
!!   pnd_solp(:) |kg P          |amount of soluble P originating from surface
!!                             |runoff in pond at beginning of day
!!   pnd_solpg(:)|kg P          |amount of soluble P originating from
!!                             |groundwater in pond at beginning of day
!!   pnd_vol(:)  |m^3 H2O       |volume of water in pond
!!   pndflwi     |m^3 H2O       |volume of water flowing into pond on day
!!   pndsedin    |metric tons   |sediment entering pond during day
!!   psetlp(1,:) |m/day         |phosphorus settling rate for 1st season
!!   psetlp(2,:) |m/day         |phosphorus settling rate for 2nd season
!!   seccip(:)   |none          |water clarity coefficient for pond
!!   sed_stl(:)  |kg/kg         |fraction of sediment remaining suspended in
!!                             |impoundment after settling for one day
!!   sol_sumfc(:)|mm H2O        |amount of water held in the soil profile
!!                             |at field capacity
!!   sol_sw(:)   |mm H2O        |amount of water stored in the soil profile
!!                             |on any given day
!!   subp(:)     |mm H2O        |precipitation for the day in HRU
!!   ~ ~ ~ ~ ~ ~ ~ ~ ~ ~ ~ ~ ~ ~ ~ ~ ~ ~ ~ ~ ~ ~ ~ ~ ~ ~ ~ ~ ~ ~ ~ ~ ~ ~ ~ ~ ~ ~ ~

!!   ~ ~ ~ OUTGOING VARIABLES ~ ~ ~
!!   name        |units         |definition
!!   ~ ~ ~ ~ ~ ~ ~ ~ ~ ~ ~ ~ ~ ~ ~ ~ ~ ~ ~ ~ ~ ~ ~ ~ ~ ~ ~ ~ ~ ~ ~ ~ ~ ~ ~ ~ ~ ~ ~
!!   pnd_chla(:) |kg chl_a      |amount of chlorophyll-a in pond at end of day
!!   pnd_no3(:)  |kg N          |amount of nitrate originating from surface
!!                             |runoff in pond at end of day
!!   pnd_no3g(:) |kg N          |amount of nitrate originating from
!!                             |groundwater in pond at end of day
!!   pnd_no3s(:) |kg N          |amount of nitrate originating from lateral
!!                             |flow in pond at end of day
!!   pnd_orgn(:) |kg N          |amount of organic N originating from
!!                             |surface runoff in pond at end of day
!!   pnd_orgp(:) |kg P          |amount of organic P originating from
!!                             |surface runoff in pond at end of day
!!   pnd_psed(:) |kg P          |amount of mineral P attached to sediment
!!                             |originating from surface runoff in pond at
!!                             |end of day
!!   pnd_seci(:) |m             |secchi-disk depth of pond
!!   pnd_sed(:)  |kg/L          |ratio of sediment to water in pond
```

```
!!    pnd_solp(:) |kg P          |amount of soluble P originating from surface
!!                              |runoff in pond at end of day
!!    pnd_solpg(:)|kg P          |amount of soluble P originating from
!!                              |groundwater in pond at end of day
!!    pnd_vol(:)  |m^3 H2O       |volume of water in pond
!!    pndev       |m^3 H2O       |evaporation from pond on day
!!    pndflwo     |m^3 H2O       |volume of water flowing out of pond on day
!!    pndpcp      |m^3 H2O       |precipitation on pond during day
!!    pndsedc     |metric tons   |net change in sediment in pond during day
!!    pndsedo     |metric tons   |sediment leaving pond during day
!!    pndsep      |m^3 H2O       |seepage from pond on day
!!    ~ ~ ~ ~ ~ ~ ~ ~ ~ ~ ~ ~ ~ ~ ~ ~ ~ ~ ~ ~ ~ ~ ~ ~ ~ ~ ~ ~ ~ ~ ~ ~ ~ ~ ~ ~ ~ ~ ~ ~

!!    ~ ~ ~ LOCAL DEFINITIONS ~ ~ ~
!!    name        |units         |definition
!!    ~ ~ ~ ~ ~ ~ ~ ~ ~ ~ ~ ~ ~ ~ ~ ~ ~ ~ ~ ~ ~ ~ ~ ~ ~ ~ ~ ~ ~ ~ ~ ~ ~ ~ ~ ~ ~ ~ ~ ~
!!    chlaco      |ppb (ug/L)    |concentration of chlorophyll-a in pond
!!    iseas       |none          |nutrient settling rate season
!!    k           |none          |HRU or reach number
!!    nitrok      |none          |fraction of nitrogen in pond removed by
!!                              |settling
!!    phosk       |none          |fraction of phosphorus in pond removed by
!!                              |settling
!!    pndsa       |ha            |surface area of pond on current day
!!    sed         |kg/L          |sediment concentration in pond at beginning of
!!                              |day
!!    targ        |m^3 H2O       |target storage level in pond
!!    tpco        |ppb (ug/L)    |concentration of phosphorus in pond water
!!                              |on day
!!    vol         |m^3 H2O       |volume of water in pond at beginning of day
!!    xx          |none          |variable to hold intermediate calc result
!!    ~ ~ ~ ~ ~ ~ ~ ~ ~ ~ ~ ~ ~ ~ ~ ~ ~ ~ ~ ~ ~ ~ ~ ~ ~ ~ ~ ~ ~ ~ ~ ~ ~ ~ ~ ~ ~ ~ ~ ~

!!    ~ ~ ~ SUBROUTINES/FUNCTIONS CALLED ~ ~ ~
!!    Intrinsic: Min

!!    ~ ~ ~ ~ ~ ~ END SPECIFICATIONS ~ ~ ~ ~ ~ ~

      use parm

      integer, intent (in) :: k
      real :: vol, sed, pndsa, xx, targ, tpco, phosk, nitrok, chlaco
      integer :: iseas
          real :: san, sil, cla, sag, lag, inised, finsed,setsed,remsetsed

!-----------------------------------------------------------------------
```

```
!PDM BASED POND RUNOFF GENERATION USING THE EXPONENTIAL
DISTRIBUTION
!FUNCTION
!-----------------------------------------------------------------------
!REFERENCES:
!         1. MOORE, R.J., 2007. THE PDM RAINFALL-RUNOFF MODEL.
!            HYDROLOGY AND EARTH SYSTEM SCIENCES, VOL. 11, PP. 483-499

!         2. MOORE, R.J., 1985. THE PROBABILITY-DISTRIBUTED PRINCIPLE
!          AND RUNOFF PRODUCTION AT POINT AND BASIN SCALES.
!            HYDROLOGY AND EARTH SYSTEM SCIENCES, VOL. 30, PP. 273-297
!         3. MEKONNEN, B.A., MAXUREK, K.A., AND PUTZ, G. 2016.
!         INCORPORATING LANDSCAPE DEPRESSION HETEROGENEITY INTO A
!         SEMI-DISTRIBUTED HYDROLOGICAL MODEL USING A PROBABILITY
!         DISTRIBUTION. HYDROLOGICAL PROCESSES, DOI: 10.1002/HYP.10800
!-----------------------------------------------------------------------
!    DEFINITIONS
!-----------------------------------------------------------------------
!    SMAX       - MAXIMUM PONDING STORAGE
!               - PARAMETER FOR EXPONENTIAL DISTRIBUTION FUNCTION
!    CSTR       - CRITICAL PONDING DEPTH FOR A GIVEN STORAGE
!    S          - CURRENT PONDING STORAGE
!    SPRE       - PREVIOUS PONDING STORAGE
!    RNET       - NET CHANGE IN THE DEPTH OF THE PONDED WATER
!-----------------------------------------------------------------------

!    * WORKING ARRAYS - RUNOFF GENERATION
     REAL  S, SPRE, SMAX, RNET, CSTR
           SMAX = 0.0
           CSTR = 0.0
           S    = 0.0
           SPRE = 0.0
           RNET = 0.0
!-----------------------------------------------------------------------

       !! store initial values
       vol = 0.
       sed = 0.
           san = 0.
           sil = 0.
           cla = 0.
           sag = 0.
           lag = 0.
           inised = 0.
           finsed = 0.
           setsed = 0.
```

```
        remsetsed = 0.
      vol = pnd_vol(k)
      sed = pnd_sed(k)
      san = pnd_san(k)
      sil = pnd_sil(k)
      cla = pnd_cla(k)
      sag = pnd_sag(k)
      lag = pnd_lag(k)

      !! calculate water balance for day
      pndsa = 0.
      pndsa = pnd_psa(k)
      pndsa_msq=pndsa*10000.
      pnd_vol_mm(k)= 1000.*pnd_vol(k)/pndsa_msq
      pnd_pvol_mm(k)= 1000.*pnd_pvol(k)/pndsa_msq
      pndev = 10. * evpnd(k) * pet_day * pndsa
      pndev_mm=1000.*pndev/pndsa_msq
      pndsep = pnd_k(k) * pndsa * 240.
      pndsep_mm=1000.*pndsep/pndsa_msq
      pndpcp = subp(k) * pndsa * 10.
      pndpcp_mm=1000.*pndpcp/pndsa_msq
      pndflwi_mm=1000.*pndflwi/pndsa_msq


!-----------------------------------------------------------------------
!     SAVE THE PREVIOUS STORAGE AS SPRE AND
!     CALCULATE THE NET CHANGE IN THE DEPTH OF THE PONDED
!     WATER WITHIN DELTAT (BETWEEN TIME T AND T + DELTAT)
!     -------------------------------------------------------
      SPRE = pnd_vol_mm(k)
      RNET = pndpcp_mm + pndflwi_mm – pndsep_mm – pndev_mm
!-----------------------------------------------------------------------

      !! new water volume for day
      pnd_vol(k) = pnd_vol(k) - pndsep - pndev + pndpcp + pndflwi


      if (pnd_vol(k) < 0.001) then
        !! if volume deficit in pond reduce seepage
        !! so that the pond volume is zero
        pndsep = pndsep + pnd_vol(k)
        pnd_vol(k) = 0.
        !! if seepage is less than the volume deficit, take the remainder
        !! from evaporation
        if (pndsep < 0.) then
          pndev= pndev + pndsep
```

```
          pndsep = 0.
        end if
        pnd_sed(k) = 0.
        pnd_san(k) = 0.
        pnd_sil(k) = 0.
        pnd_cla(k) = 0.
        pnd_sag(k) = 0.
        pnd_lag(k) = 0.
        pnd_solp(k) = 0.
        pnd_psed(k) = 0.
        pnd_orgp(k) = 0.
        pnd_solpg(k) = 0.
        pnd_orgn(k) = 0.
        pnd_no3(k) = 0.
        pnd_no3s(k) = 0.
        pnd_no3g(k) = 0.
        pnd_chla(k) = 0.
        pnd_seci(k) = 0.

      else

        !! compute outflow
!-----------------------------------------------------------------------
!       EXPONENTIAL DISTRIBUTION FUNCTION (WITH PARAMATER SMAX).
!       pnd_pvol(k) IS EQUIVALENT TO SMAX
!       -------------------------------------------------------
        SMAX = MAX(0.0, pnd_pvol_mm(k)) !AVOID NEGATIVE MAXIMUM STORAGE


!
!       -------------------------------------------------------
        IF(RNET .GT. 0.0)THEN

!         -----------------------------------------------------
!         COMPUTE CRITICAL POND DEPTH CORRESPONDING TO SPRE
!         -----------------------------------------------------
          CSTR    = -SMAX * LOG(1.0 - SPRE/SMAX)

!         -----------------------------------------------------
!         CALCULATE THE CRITICAL POND DEPTH AT T + DELTAT AND
!         LIMIT IT TO THE MAXIMUM PONDING DEPTH
!         -----------------------------------------------------
          CSTR = MIN(SMAX, CSTR + RNET)

!         -----------------------------------------------------
!         CALCULATE THE NEW DEPTH OF THE PONDED WATER, S AT
```

```
!          T + DELTAT. THIS TAKES INTO ACCOUNT THE LOSS DUE TO
!          DIRECT RUNOFF WITHIN DELTAT (T TO T + DELTAT).
!          ---------------------------------------------------
           S = SMAX * (1.0 - EXP(-CSTR/SMAX))

!          ---------------------------------------------------
!          CALCULATE POND OUTFLOW
!          ---------------------------------------------------
           pndflwo_mm = MAX(0.0, RNET - (S - SPRE))
           pndflwo=pndflwo_mm*pndsa_msq/1000.

        ELSE
                        pndflwo = 0.0
                  ENDIF
!-----------------------------------------------------------------------

        !! compute new sediment concentration
        if (pndsedin < 1.e-6) pndsedin = 0.
             if (pndsa == 0.) pndsa = 0.001    !!MJW added line of code 040811
        velofl = (pndflwo / pndsa) / 10000.
        if (velofl > 1.e-6) then
           trappnd = velsetlp(k) / velofl
           if (trappnd > 1.) trappnd = 1.
           susp = 1. - trappnd
        else
           susp = 0.
        endif

        pnd_sed(k) = (sed * vol + susp * pndsedin) / pnd_vol(k)
        pnd_san(k) = (san * vol + pndsanin) / pnd_vol(k)
        pnd_sil(k) = (sil * vol + pndsilin) / pnd_vol(k)
        pnd_cla(k) = (cla * vol + pndclain) / pnd_vol(k)
        pnd_sag(k) = (sag * vol + pndsagin) / pnd_vol(k)
        pnd_lag(k) = (lag * vol + pndlagin) / pnd_vol(k)

        !! compute final pond volume
        pnd_vol(k) = pnd_vol(k) – pndflwo
        pnd_vol_mm(k)=1000.*pnd_vol(k)/pndsa_msq
        if (pnd_vol(k) < 0.) then
          pndflwo = pndflwo + pnd_vol(k)
          pnd_vol(k) = 0.
          pnd_vol_mm(k)=0.
        endif

        !! compute change in sediment concentration due to settling
             if (sed_stl(k) < 1.e-6) sed_stl(k) = 0.0
```

```
    if (pnd_sed(k) > pnd_nsed(k)) then
          inised = pnd_sed(k)
      pnd_sed(k) = (pnd_sed(k) - pnd_nsed(k)) * sed_stl(k) +      &
&                                                  pnd_nsed(k)
          finsed = pnd_sed(k)
          setsed = inised - finsed

        if (pnd_lag(k) >= setsed) then
          pnd_lag(k) = pnd_lag(k) - setsed
          remsetsed = 0.
        else
          remsetsed = setsed - pnd_lag(k)
          pnd_lag(k) = 0.
          if (pnd_san(k) >= remsetsed) then
            pnd_san(k) = pnd_san(k) - remsetsed
            remsetsed = 0.
          else
            remsetsed = remsetsed - pnd_san(k)
            pnd_san(k) = 0.
       if (pnd_sag(k) >= remsetsed) then
              pnd_sag(k) = pnd_sag(k) - remsetsed
              remsetsed = 0.
            else
              remsetsed = remsetsed - pnd_sag(k)
              pnd_sag(k) = 0.
        if (pnd_sil(k) >= remsetsed) then
                pnd_sil(k) = pnd_sil(k) - remsetsed
                remsetsed = 0.
              else
                remsetsed = remsetsed - pnd_sil(k)
                pnd_sil(k) = 0.
          if (pnd_cla(k) >= remsetsed) then
                  pnd_cla(k) = pnd_cla(k) - remsetsed
                  remsetsed = 0.
                else
                  remsetsed = remsetsed - pnd_cla(k)
                  pnd_cla(k) = 0.
                end if
        end if
            end if
          end if
        end if

    end if
    !! compute sediment leaving pond
    pndsedo = pnd_sed(k) * pndflwo
```

```
    pndsano = pnd_san(k) * pndflwo
    pndsilo = pnd_sil(k) * pndflwo
    pndclao = pnd_cla(k) * pndflwo
    pndsago = pnd_sag(k) * pndflwo
    pndlago = pnd_lag(k) * pndflwo

    !! net change in amount of sediment in pond for day
    pndsedc = vol * sed + pndsedin - pndsedo - pnd_sed(k) *       &
&                                          pnd_vol(k)

    !! determine settling rate
    !! part of equation 29.1.3 in SWAT manual
    if (i_mo >= ipnd1(k) .and. i_mo <= ipnd2(k)) then
      iseas = 1
    else
      iseas = 2
    endif
    phosk = 0.
    nitrok = 0.
    phosk = psetlp(iseas,k) * pndsa * 10000. / pnd_vol(k)  !setl/mean depth
    phosk = Min(phosk, 1.)
    nitrok = nsetlp(iseas,k) * pndsa * 10000. / pnd_vol(k) !setl/mean depth
    nitrok = Min(nitrok, 1.)

    !! remove nutrients by settling
    !! other part of equation 29.1.3 in SWAT manual
    pnd_solp(k) = pnd_solp(k) * (1. - phosk)
    pnd_psed(k) = pnd_psed(k) * (1. - phosk)
    pnd_orgp(k) = pnd_orgp(k) * (1. - phosk)
    pnd_solpg(k) = pnd_solpg(k) * (1. - phosk)
    pnd_orgn(k) = pnd_orgn(k) * (1. - nitrok)
    pnd_no3(k) = pnd_no3(k) * (1. - nitrok)
    pnd_no3s(k) = pnd_no3s(k) * (1. - nitrok)
    pnd_no3g(k) = pnd_no3g(k) * (1. - nitrok)

    tpco = 0.
    if (pnd_vol(k) + pndflwo > 0.1) then
    tpco = 1.e+6 * (pnd_solp(k) + pnd_orgp(k) + pnd_psed(k) +     &
&                        pnd_solpg(k)) / (pnd_vol(k) + pndflwo)
    else
      tpco = 0.
    endif
    chlaco = 0.
    pnd_chla(k) = 0.
    pnd_seci(k) = 0.
    if (tpco > 1.e-4) then
```

```
      !! equation 29.1.6 in SWAT manual
      chlaco = chlap(k) * 0.551 * (tpco**0.76)
      pnd_chla(k) = chlaco * (pnd_vol(k) + pndflwo) * 1.e-6
    endif
    if (chlaco > 1.e-4) then
      !! equation 29.1.8 in SWAT manual
      pnd_seci(k) = seccip(k) * 6.35 * (chlaco**(-0.473))
    endif
  end if

return
end
```

APPENDIX D–Curriculum Vitae

A brief bio-bibliography of the Ph.D. candidate is given below.

Name:		Balew A. **Mekonnen**
Post-secondary Education and Degrees:	2011-2016	Ph.D. candidate
		Department of Civil and Geological Engineering
		University of Saskatchewan
		Saskatoon, SK, Canada,
	2007-2008	M.Sc. (Water Resources Engineering)
		Department of Hydrology and Hydraulic Engineering
		Free University of Brussels
		Brussels, Brussels-Capital Region, Belgium
	2006-2007	Postgraduate Diploma (Water resources Engineering)
		Catholic University of Leuven
		Leuven, Flemish Brabant, Belgium
	2000-2005	B.Sc. (Agricultural Engineering)
		Department of Biosystems and Environmental Engineering Hawassa university
		Hawassa, SNNPRS, Ethiopia
Honours and Awards:	2011–2013	Department of Civil and Geological scholarship
		University of Saskatchewan
	2007–2008	De Vlaamse Interuniversitaire Raad (VLIR) Award Scholarship Catholic University of Leuven and University of Brussels
	2006–2007	De Vlaamse Interuniversitaire Raad (VLIR) Award Scholarship Catholic University of Leuven and University of Brussels
	2005	Gold medal award upon graduation for academic excellence
	2000–2005	Higher Education Scholarship of Ethiopian Ministry of Education
Related Work Experience:	2011–2016	Research and Teaching Assistant
		Department of Civil and Geological engineering
		University of Saskatchewan
		Saskatoon, SK, Canada

	2008–2010	Lecturer
		Department of Biosystems and Environmental Engineering
		Hawassa University
	2007–2008	Research Assistant
		Free University of Brussels
	2006–2007	Research Assistant
		Catholic University of Leuven
	2005–2006	Graduate Assistant II
		Hawassa University

Publications:

Published

1. **Mekonnen, B.A.**, Nazemi, A., Mazurek, K.A., Elshorbagy, A., and Putz, G. 2015. Hybrid modelling approach to prairie hydrology: Fusing data-driven and process-based hydrological models. Hydrological Sciences Journal, 60(9): 1473-1489. doi: 10.1080/02626667.2014.935778.
2. **Mekonnen, B.A**, Mazurek, K.A., and Putz, G. 2016. Incorporating landscape depression heterogeneity into a semi-distributed hydrological model using a probability distribution. Hydrological Processes, doi: 10.1002/hyp.10800.
3. **Mekonnen, B.A,** Mazurek, K.A., and Putz, G. 2016. Sediment export modeling in cold climate prairie watersheds. Journal of Hydrologic Engineering, doi: 10.1061/(ASCE)HE.1943-5584.0001336.
4. **Mekonnen, B.A**, Mazurek, K.A., and Putz, G. 2016. Nutrient export modeling and effect of management practices in cold climate prairie watersheds. Agricultural Water Management, doi: 10.1016/j.agwat.2016.06.023.

Submitted

5. **Mekonnen, B.A,** Mazurek, K.A., and Putz, G. 2016. Investigating the Different Sources of Uncertainty in a SWAT-PDLD Model of a Canadian Prairie Watershed. Hydrological Sciences Journal (submitted).

Conference Presentation

1. **Mekonnen, B.A.,** Nazemi, A., Elshorbagy, A., Mazurek, K.A., and Putz, G. 2012. Hybrid modeling approach to Prairie hydrology: Fusing data driven and process-based hydrological models, General Assembly of the European Geosciences Union, Vienna, Austria, April 22-27, Paper No. EGU2012-6562.